MODELLING AND CHARACTERISATION OF *IN VIVO* HUMAN SKIN GRAFT REJECTION FOR THE INVESTIGATION OF REGULATORY T CELL THERAPY IN VASCULARISED COMPOSITE ALLOTRANSPLANTATION

Fadi Issa

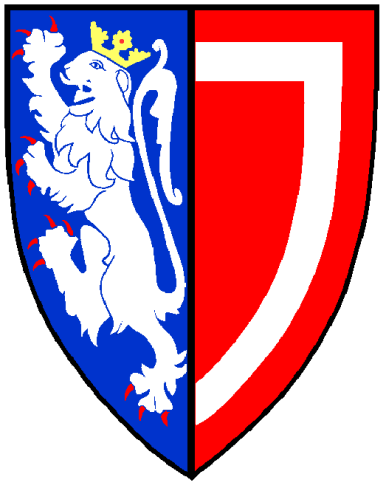

Balliol College

Nuffield Department of Surgical Sciences

University of Oxford

Thesis submitted in partial fulfilment of the requirements for the degree of Doctor of Philosophy

Supervisor: Professor Kathryn J. Wood
College Advisor: Dr. Piers C. Nye

Trinity Term 2011

ABSTRACT

Vascularised composite allograft (VCA) transplantation is revolutionising the field of plastic surgery. It reconstructs the most complex tissue defects effectively, achieving a new functional and cosmetic gold standard. However, VCA transplantation is currently limited by high rates of acute rejection and the need for patients without life-threatening conditions to be maintained on immunosuppression for life. Skin is the most problematic component of VCA transplants. It stimulates a vigorous immune response and is highly susceptible to rejection, even in the presence of potent immunosuppression. In order to expand the field of VCA transplantation and improve outcomes, the morbidity and mortality associated with immunosuppression need to be minimised or eliminated. This would require manipulation of the immune response to allow long-term survival in the absence of immunosuppression, in other words tolerance. A particular focus on the immune response directed against skin is required. Tolerance to skin allografts may be achievable with the use of regulatory T cells (Treg).

Due to relatively few clinical cases, human skin transplantation is a poorly investigated area. The studies in this thesis were therefore designed to elucidate the characteristics of human skin rejection using a novel humanised mouse model, testing the hypothesis that human Treg could prevent human skin rejection *in vivo*.

In Chapters 3 and 4 we develop a system whereby human skin rejection may be modelled effectively *in vivo*. Subsequently we investigate the unique characteristics of human skin rejection using this model. In Chapter 5 we demonstrate the capacity for Treg to prevent human skin rejection and investigate the systemic and local cellular changes resulting from Treg therapy. These changes include a reduction in the number of circulating proliferating T cells, a preservation of skin microvasculature, and a reduction in skin-infiltrating $CD8^+$ leukocytes. Treg migrate to the allograft-draining lymph node and into the skin allograft to regulate immune responses. We demonstrate the importance of expansion or activation of Treg for their suppressive activity and the requirement for these cells to be derived from the allograft recipient for efficient regulation to be achieved.

Treg cellular therapy has already been trialed clinically for the prevention of graft-versus-host disease after haematopoietic stem cell transplantation. The use of Treg in transplantation is therefore on the horizon. The unique translational data from this study bridge a critical gap between laboratory observations and the clinic. These data therefore form the basis upon which future clinical trials of Treg in skin or VCA transplantation may be performed.

ACKNOWLEDGEMENTS

First and foremost I would like to thank my supervisor, Professor Kathryn Wood, for her unfailing support, advice, and mentorship over the past three years. This thesis would not have been possible without her expert guidance and encouragement. I am immensely grateful for the opportunity Kathryn has provided me with at The Transplantation Research Immunology Group (TRIG) to develop as a clinician scientist. I would also like to express my gratitude to Dr Andrew Bushell, Dr Joanna Hester and Dr Nicholas Jones for all their support and guidance, and for all the stimulating scientific discussions over the years. I am hugely grateful to Mr Tim Goodacre for his constant support, his invaluable help with the collaborative work, and his continual enthusiasm in making the research project a reality. I am especially grateful to Joanna for her hard work and enthusiasm in our collaborative work, Dr Ryoichi Goto for his help with all the late nights transplanting skin in Wing D, Kate Milward for all her help with *in vitro* work, Dr Alex Schiopu for his mentorship during the first few months of my time in the lab and for his expert training and guidance in laboratory techniques and animal procedures, Mr Andy Pay and other members of the Plastic Surgery team for their enthusiastic assistance in providing human tissue, Radhika Chadha for her help with experimental work and for her invaluable support over the years, Dr Sebastiaan Heidt for his support and help with immunoglobulin assays, Dr Manuela Carvalho-Gaspar and Ian Toogood-Johnson for their training and support with molecular biology techniques, Monica Dolton for her expert help with funding and ethical approval paperwork, Dr Satish Nadig for his help in the initial stages of the project, Dr Linden Lyne and Professor

Alison Banham for their help with immunohistochemical staining techniques and for their kind gift of the 236A/E7 antibody, Professor Robert Fairchild for his kind gift of the RB6.8C5 hybridoma, Marinda Rye for helping me to seek out appropriate skin donors, Agnes Gwela for her assistance with qPCR assays, and Carol Webb for her help with ordering and publishing. In addition I would like to thank Alison Bradford, Renato Demetrio, Jonathon Merril, Waldemar Woznica and Natalie Cowley for their expert animal care and support with animal experimental work. I would also like to thank Dr Petter Woll for kindly gifting the NSG mice used in this thesis. Many thanks also to Gareth Plant for his smooth running of the tissue culture facility and to Roland Dunford for his help with preparing laboratory consumables. I am grateful to all members of TRIG for the scientific discussions about experimental work and presentations. Research is a team effort and none of this would have been possible without each and every one of you. I am also grateful to the Wellcome Trust, the Dunhill Medical Trust, the Royal College of Surgeons and the Oxfordshire Health Research Services Committee for their generous funding and support of this project. I would particularly like to thank Mr Martyn Coomer at the Royal College of Surgeons for his support with funding applications. I am also grateful to the BTS, TTS, BSI, IHCTAS and Balliol College for their financial support in travelling to scientific conferences. Many thanks to my college advisor Dr Piers Nye and Glynis Price for their support with my research and training over the years.

Last, but certainly not least, I would like to thank my lovely wife Ariana and my family for their faithful support over the years. I certainly could not have done this without their love, encouragement and patience. Thank you for believing!

ABBREVIATIONS

2,2'-azino-bis(3-ethylbenzothiazonline-6-sulphonic acid)	ABTS
Acute cellular rejection	ACR
Antibody-dependent cell-mediated cytotoxicity	ADCC
Adenosine monophosphate	AMP
Antibody-mediated rejection	AMR
Activator protein-1	AP-1
Antigen-presenting cell	APC
Anti-thymocyte globulin	ATG
Adenosine triphosphate	ATP
Azathioprine	AZA
BALB/c Recombination activating gene-2$^{-/-}$ common γ-chain$^{-/-}$	BALB/c-Rag2$^{-/-}$cγ$^{-/-}$ mouse
Bovine serum albumin	BSA
Central supramolecular activation cluster	c-SMAC
Complement component 4d	C4d
Chronic allograft dysfunction	CAD
CC chemokine receptor	CCR
Cluster of differentiation	CD
Carboxyfluorescein succinimidyl ester	CFSE
Current good manufacturing practice	cGMP
Cutaneous lymphocyte-associated antigen	CLA
Cytomegalovirus	CMV
Calcineurin inhibitor	CNI
Cytotoxic T lymphocytes	CTL
Cytotoxic T Lymphocyte Antigen-4	CTLA-4
Common γ-chain	cγ
Dimethylaminoazobenzene	DAB
Diacylglycerol	DAG
Damage-associated molecular patterns	DAMPs
Dendritic cell	DC
IL-10 producing dendritic cell	DC-10
Donor-specific blood transfusion	DST

Delayed-type hypersensitivity	DTH
Experimental autoimmune encephalomyelitis	EAE
Endothelial cell	EC
Enzyme-linked immunosorbent assay	ELISA
Endoplasmic reticulum	ER
Fluorescence-activated cell sorting	FACS
Fas Ligand	FasL
Fibrinogen-like protein 2	FGL2
Tacrolimus	FK-506
Forkhead box P3	FoxP3
Folate receptor 4	FR4
Granulocyte colony-stimulating factor	G-CSF
Glutamic acid/alanine rich protein	GARP
Glucocorticoid induced tumour necrosis factor receptor	GITR
Granulocyte-differentiation antigen 1	GR-1
Graft-versus-host disease	GvHD
Haematoxylin and eosin	H&E
Human leucocyte antigen	HLA
High-mobility group box 1 protein	HMGB-1
Hypoxanthine-guanine phosphoribosyltransferase	HPRT
Haematopoietic stem cells	HSC
Heat shock protein	HSP
Intercellular adhesion molecule 1	ICAM-1
Inducible T cell costimulator	ICOS
Indoleamine 2,3-dioxygenase	IDO
Interferon-γ	IFNγ
Immunoglobulin	Ig
Immunoglobulin G	IgG
Immunoglobulin M	IgM
International Hand and Composite Tissue Allotransplantation	IHTAS
Interleukin	IL
Inosine monophosphate dehydrogenase	IMPDH
Inositol triphosphate	IP_3
Immunodysregulation polyendocrinopathy enteropathy X-	IPEX
Ischaemia-reperfusion injury	IRI

Induced or adaptive regulatory T cells	iTreg
Lymphocyte-activation gene 3	Lag
Latency-associated peptide	LAP
Lymphocyte function-associated antigen-1	LFA-1
Lineage cocktail 1 (CD3, CD14, CD16, CD19, CD20, CD56)	Lin
Monoclonal antibody	mAb
Membrane attack complex	MAC
Mitogen-activated protein kinase	MAPK
Rabbit anti-murine thymocyte globulin	mATG
Median fluorescence intensity	MFI
Major histocompatibility complex	MHC
Monokine induced by interferon-γ	MIG
Minor histocompatibility	miH
Mycophenolate mofetil	MMF
Mononuclear cells	MNC
Messenger RNA	mRNA
Median survival time	MST
Mammalian target of rapamycin	mTOR
Nuclear factor of activated T cells	NFAT
Normal human serum	NHS
Natural killer cell	NK
Natural killer T cell	NKT
Non-obese diabetic	NOD
Non-obese diabetic/severe combined	NSG
Naturally-occurring regulatory T cells	nTreg
Peripheral supramolecular activation cluster	p-SMAC
Peripheral blood mononuclear cells	PBMC
Phosphate buffered saline	PBS
Phosphodiesterase 3b	PDE3b
Protein kinase-Cθ	PkCθ
Pattern recognition receptor	PRR
Quantitative real-time polymerase chain reaction	qPCR
Human rhinovirus dendritic cell	R-DC
Retinoic acid	RA
Recombination activating gene	Rag

Recombinant human	rh
Recombinant human IL-2	rhIL-2
Recombinant human IL-7	rhIL-7
Reactive oxygen species	ROS
Roswell Park Memorial Institute	RPMI
Room temperature	RT
Reconstructive transplantation	RT
Severe combined immunodeficiency	SCID
Standard deviation	SD
Standard error of the mean	SEM
Solid organ transplant	SOT
SD rat	Sprague Dawley rat
Signal transducer and activator of transcription	STAT
Superficial vascular plexus	SVP
Transplant arteriosclerosis	TA
T cell receptor	TCR
Transforming growth factor β	TGFβ
Helper T cell	Th
Toll-like receptor	TLR
Tumour necrosis factor	TNF
Tumour necrosis factor receptor	TNFR
Type 1 regulatory T cells	Tr1
Regulatory T cells	Treg
Treg-specific demethylated region	TSDR
The Transplantation Society	TTS
Umbilical cord blood	UCB
Vascularised composite allograft	VCA
Vascular cell adhesion molecule 1	VCAM-1
Xenograft-versus-host disease	XvHD

SUMMARY OF CONTENTS

CHAPTER 1

Introduction

CHAPTER 1

Materials and Methods

CHAPTER 3

Development of an *in vivo* model of human skin rejection

CHAPTER 4

Characteristics of human skin rejection and further model development

CHAPTER 5

Immunoregulation of human skin rejection

CHAPTER 6

Results summary and general discussion

PUBLICATIONS

REFERENCES

TABLE OF CONTENTS

ABSTRACT ..... **I**

ACKNOWLEDGEMENTS ..... **III**

ABBREVIATIONS ..... **V**

CHAPTER 1: INTRODUCTION **1**

1.1 Background **1**

1.2 Vascularised composite allograft transplantation **4**

1.2.1 A history 4

1.2.2 The challenges 7

1.3 Mechanisms of allograft rejection **11**

1.3.1 Overview 11

1.3.2 Initiation of rejection 13

1.3.3 Allorecognition 14

1.3.4 Costimulation 16

1.3.5 Activation 17

1.3.6 The adaptive immune response 19

1.3.6.1 $CD4^+$ T cells 20

1.3.6.2 $CD8^+$ T cells 23

1.3.6.3 B cells and antibody-mediated rejection 24

1.3.6.4 Memory cells 26

1.3.7 The innate immune response 27

1.4 Skin rejection **28**

1.4.1 Vascularisation 28

1.4.2 Dermal microvasculature 30

1.4.3 Allograft volume 32

1.4.4 Skin-specific antigens 32

1.4.5 Skin architecture and unique cellular composition 33
1.4.6 Skin alarmins....34
1.5 Immunosuppression 35
1.6 Methods of tolerance induction 40
1.6.1 Central tolerance 41
1.6.1.1 Central tolerance in VCA transplantation 43
1.6.2 Peripheral regulation: Treg....46
1.6.2.1 Experimental evidence for the use of Treg in transplantation 50
1.6.2.2 Treg in clinical tolerance 56
1.6.2.3 Immunosuppression and Treg 58
1.6.2.4 Clinical trials using Treg 61
1.6.2.5 Treg in skin and VCA transplantation....62
1.7 Humanised mouse models in transplantation research.... 64
1.7.1 The need for humanised mouse models 64
1.7.2 Humanised mouse models 67
1.8 Conclusion.... 71
1.9 Thesis aims and objectives 72
1.10 Figures and legends 73
CHAPTER 2: MATERIALS AND METHODS 84
2.1 Animals 84
2.2 Animal Procedures 85
2.2.1 Pre- and post-operative care 85
2.2.2 Procurement of human skin 86
2.2.3 Skin grafting....86
2.2.4 Adoptive transfer of human cells 87
2.2.5 HSC transplantation....87
2.2.6 Procurement of tissue from experimental mice....88
2.2.7 Mouse GR-1^{+} cellular depletion....88

2.3 Tissue typing 89

2.4 Cellular isolation for *in vivo* injection 89

2.4.1 Adult PBMC isolation 89

2.4.2 UCB MNC isolation 90

2.4.3 Cellular isolation with magnetic beads 90

2.4.4 Mouse splenocyte isolation 90

2.5 Fluorescence-activated cell sorting (FACS) and flow cytometry 91

2.6 Treg isolation and expansion 92

2.7 Carboxyfluorescein Succinimidyl Ester (CFSE) labelling 93

2.8 *In vitro* suppression tests 94

2.9 Histology and immunohistochemistry 94

2.9.1 Haematoxylin and Eosin (H&E) staining 95

2.9.2 Immunohistochemistry 95

2.10 Enzyme-linked immunosorbent assay (ELISA) 97

2.11 Quantitative real-time polymerase chain reaction (qPCR) 98

2.12 Luminex assays 99

2.13 Statistical analyses 99

2.14 Figures and legends 99

CHAPTER 3: DEVELOPMENT OF AN *IN VIVO* MODEL OF HUMAN SKIN REJECTION 103

3.1 Introduction 103

3.1.1 Chapter aim 105

3.2. Human skin rejection may be modelled *in vivo* 105

3.3. Human skin grafts require a period of healing in order to model a true alloresponse 111

3.4 Rejection kinetics of human skin allografts 114

3.5 Impact of the number of HLA mismatches on human skin rejection tempo 116

3.6 Kinetics of reconstituting human leukocytes in the humanised skin transplantation model 117

3.7 Phenotype of reconstituting human leukocytes in the humanised skin transplantation model 119

3.8 Discussion 120

3.9 Figures and legends 130

CHAPTER 4: CHARACTERISTICS OF HUMAN SKIN REJECTION AND FURTHER MODEL ENHANCEMENT..... 160

4.1 Introduction 160

4.1.1 Chapter aims.....161

4.2 Impact of resident human skin leukocytes 162

4.3 Skin allografts in the humanised mouse model display standard histopathological features of human skin rejection..... 164

4.4 A human T cell response develops against human skin allografts..... 166

4.5 The mouse innate response to human skin allografts is not functionally significant 167

4.6 NSG mice are not better hosts than BALB/c-Rag2$^{-/-}$cγ$^{-/-}$ mice in the humanised mouse skin transplantation model 169

4.7 Humanised BALB/c-Rag2$^{-/-}$cγ$^{-/-}$ mice do not produce human allospecific α-HLA immunoglobulin 170

4.8 Human HSC-transplanted BALB/c-Rag2$^{-/-}$cγ$^{-/-}$ mice achieve significant levels of peripheral human leukocytes chimerism..... 173

4.9 Human HSC transplanted BALB/c-Rag2$^{-/-}$cγ$^{-/-}$ mice produce human T and B cells..... 175

4.10 Human HSC transplanted BALB/c-Rag2$^{-/-}$cγ$^{-/-}$ mice do not reliably reject human skin allografts 178

4.11 Discussion 180

4.12 Figures and legends 189

CHAPTER 5: IMMUNOREGULATION OF HUMAN SKIN REJECTION 244

5.1 Introduction 244

5.1.1 Chapter aims.....247

5.2 Expanded human Treg maintain their phenotype and are suppressive *in vitro* 248

5.3 *Ex vivo*-expanded human Treg prevent human skin allograft rejection in a dose-dependent manner 250

5.4 Expansion or activation of human Treg is required to ensure their regulatory activity 251

5.5 Therapy with *ex vivo*-expanded Treg is associated with a reduction in the number of circulating proliferating human leukocytes 255

5.6 *Ex vivo*-expanded Treg reduce human immunoglobulin production *in vivo* 260

5.7 Therapy with *ex vivo*-expanded Treg preserves skin allograft microarchitecture and reduces the intragraft leukocytic infiltrate 262

5.8 Treg home to the skin allograft-draining lymph node and the skin allograft to regulate alloresponses 266

5.9 Autologous Treg are more effective than non-autologous Treg 270

5.10 Non-autologous Treg do not survive as well *in vivo* as autologous Treg 273

5.11 *Ex vivo*-expanded Treg are less effective when given two weeks after PBMC injection 275

5.12 Discussion 276

5.13 Figures and legends 289

CHAPTER 6: RESULTS SUMMARY AND GENERAL DISCUSSION 356

6.1 Introduction 356

6.2 Summary of experimental results 359

6.2.1 Chapter 3 359

6.2.2 Chapter 4 361

6.2.3 Chapter 5 364

6.3 Discussion 367

6.4 Future directions 377

6.5 Figures and legends 379

PUBLICATIONS 382

Papers 382

Book Chapters 383

Abstracts 383

REFERENCES 384

CHAPTER 1: INTRODUCTION

1.1 Background

Organ transplantation is the most effective treatment for end-stage organ failure and is one of the major medical success stories of the past five decades. Solid organ transplantation has become a mainstream therapy with 3740 transplants performed in the UK between 1 April 2010 and 31 March 2011[1]. The commonest of these solid organ transplants (SOTs) are renal transplants, where 1-year graft and patient survival rates are excellent at over 90%[1,2]. Such high rates of survival are largely attributable to modern immunosuppressive drugs. These effectively suppress all immune responses making acute rejection an uncommon event. However, these drugs are non-specific in nature and are associated with high levels of cardiovascular morbidity and mortality, as well as nephrotoxicity and a high rate of tumour development[3]. The end result is a steady decay in graft and patient survival rates, reaching approximately 70% at 10 years[1]. Moreover, immunosuppressive drugs are unable to address the problem of chronic allograft dysfunction (CAD), a state characterised by chronic activation of the immune system.

In recent years vascularised composite allograft (VCA) transplantation, or reconstructive transplantation (RT), has evolved as a joint field between transplantation and plastic surgery, with the aim to reconstruct the most complex tissue defects[4,5]. VCAs refer to any vascularised tissue allograft transplanted as a functional unit and comprising multiple tissues such as muscle, bone, nerves and

virtually always, skin. Results from RT are cosmetically and functionally superior to those obtained by traditional surgical techniques and in some cases, such as for limb amputations, RT is the only option for functional restoration. For these reasons RT is rapidly becoming an essential technique in the reconstructive armamentarium of plastic surgeons[6]. However, RT is limited by the same constraints of SOT, namely the need for global immunosuppression and the challenges of acute and chronic rejection[7]. Furthermore, in contrast to SOT, VCAs are particularly prone to acute rejection with over 85% of patients experiencing at least one episode in the first year alone[6].

The skin component of a VCA is almost always the first, and often the only tissue to demonstrate signs of rejection[6,8-14]. Critically, rejection of even one component of a VCA may result in dysfunction of the entire allograft, in some cases necessitating its amputation. Acute rejection is an established predictor of CAD, making this a particular risk for failure of VCAs in the future, although this is not yet apparent in the early stages of the field[6,13,15]. Although RT has shown a great deal of promise, the non-life-threatening nature of the conditions treated and the need for patients to remain on long-term toxic immunosuppression have limited its use to only the most extreme reconstructive cases.

Despite skin being notoriously susceptible to rejection, the first report of actively acquired tolerance was to a mouse skin allograft, described in a landmark paper over 50 years ago by Billingham, Brent and Medawar[16]. Achieving a tolerant state, in which there is long-term allograft acceptance in the absence of any

immunosuppressive therapy routinely in clinical transplantation, remains the 'holy grail' of transplant immunology research. Over the past three decades our understanding of the inbuilt mechanisms for self-tolerance has grown[17]. $CD4^+$ regulatory T cells (Treg) are central to this process[18]. Harnessing these immunoregulatory mechanisms to prevent transplant rejection and even achieve tolerance is an attractive prospect[19].

The global aim of this study is therefore to investigate regulatory T cell therapy as a method for the prevention of human skin allograft rejection.

1.2 Vascularised composite allograft transplantation

1.2.1 A history

Current techniques used widely in reconstructive surgery evolved from the pioneering work of Sir Harold Gillies and Sir Archibald McIndoe carried out in the first half of the twentieth century. During this period, burn and explosion injuries sustained in World Wars I and II dramatically increased the need to treat severe facial deformities[20]. While convention at the time was to cover such injuries with a facial mask, or hide the individual from public view, Gillies fought to 'normalise' the injuries and reintegrate soldiers into society. Gillies (and later McIndoe) developed procedures using autologous tissue to 'replace like with like'. Two of the principal techniques developed then and which remain in use today are skin grafting and pedicled flap reconstruction, the latter evolving along with understanding of the vascular supply of tissues. In plastic surgery, a flap is tissue which is removed from a donor site and placed in a recipient site with its blood supply intact. Many flaps contain multiple types of tissue, such as skin, fat and muscle, and are therefore termed composite. The later development of surgical techniques and microscopes to allow vascular and microvascular anastomosis (based on the original work of Alexis Carrel on renal and limb vascular anastomosis[21]) opened up another major reconstructive technique, free flap reconstruction. A free flap is a tissue which is detached completely from its donor site and re-anastomosed to recipient vessels at a distal site, in contrast to pedicled flaps where the vascular supply (the 'pedicle') is left attached and the tissue simply transposed. When composite in nature, the free flap may be termed a vascularised composite *auto*graft. Skin grafts, pedicled flaps

and free flaps now constitute the principal techniques employed by plastic and reconstructive surgeons worldwide. These techniques all employ autologous tissue, at the expense of the donor site.

Although attempts were made during Gillies' and McIndoe's time to transplant tissues (in particular, skin) between genetically disparate individuals, this resulted in only temporary graft take and eventual loss of the graft[22]. The reasons behind this were not entirely clear until Sir Peter Medawar and colleagues provided evidence that immune-dependent mechanisms were responsible[23-25]. This pioneering work marked the advent of the field of modern transplant immunology.

Around the same time, interest was growing in the possibility of renal transplantation to address renal failure. The work of Alexis Carrel had already demonstrated the feasibility of renal transplantation in dogs, and with the landmark human kidney transplant performed between genetically identical twins (i.e. an isograft, rather than an allograft) by Joseph Murray in 1954[26], interest turned towards drugs that may assist in overcoming the immunological barrier. Research soon led to the development of azathioprine (AZA), an antimetabolite immunosuppressant introduced to clinical practice by Sir Roy Calne[27]. Together with steroids, AZA became the mainstay of drug immunosuppression for at least two decades from the early 1960s onwards. These drugs facilitated the first successful cadaveric renal transplant between genetically disparate individuals, performed by Joseph Murray in Boston in 1962[26,28]. In the same year and city, the first successful replantation of an entire upper limb was performed by Ronald A. Malt[29]. With these

advances, the stage was set for the first VCA, a hand transplant, performed in Ecuador in 1964[30]. Unfortunately immunosuppressive therapy was still too crude and the transplant failed after approximately two weeks[31]. This setback along with the general thinking that skin transplantation was a 'non-starter for surgeons' (a phrase attributed to Peter Medawar) meant that another VCA was not to be performed for another three decades. Over this period, the development of modern maintenance immunosuppressive therapy peaked with the introduction of tacrolimus (FK-506) and mycophenolate mofetil (MMF). Together with steroids these drugs currently form the mainstay of SOT maintenance immunosuppression[32].

With these improvements in immunosuppression, the surgical community decided to make another attempt at VCA transplantation and in 1998 Jean-Michel Dubernard and colleagues performed the first successful human hand transplant[33]. The hand functioned very well, however various factors lead to the patient ceasing his immunosuppression, necessitating amputation of the rejecting hand in 2001[6]. Nevertheless, the transplant was hailed a success, encouraging a small number of centres worldwide to establish VCA transplantation programs.

The next landmark event in VCA transplantation took place in 2005 when Jean-Michel Dubernard together with Bernard Devauchelle performed the world's first partial face transplant[34,35]. The success of this procedure fueled further enthusiasm in RT resulting in an expansion in the numbers of centres performing the procedure worldwide, with at least eight in the US, seven in Europe and a small number in China. To date, VCA transplantation has been reported to have been performed in

98 patients: 79 upper limb transplants in 59 patients[6,9,31-33], 18 face transplant recipients[6,9,31-33], 14 abdominal wall transplant recipients[36], 6 knee transplant recipients[37,38] and 1 lower limb transplant recipient[39]. Other VCAs performed include laryngeal and tracheal transplants, although these may be categorised separately to the majority of VCAs as they do not contain skin[40].

Results from VCA transplantation have been very encouraging. The majority of recipients have regained sensation and movement and most have returned to the normal activities of daily living. Importantly, most have also returned to work.

1.2.2 The challenges

In contrast to most SOTs, VCAs have a high rate of acute rejection. At least 85% of patients experience one episode in the first year[6]. Signs of rejection are virtually always confined to the skin component of the VCA and the episodes have been largely reversible using temporary increases in the dosage of steroids or topical immunosuppression, with very few long-term sequelae[6,8-10,13]. This is also in contrast to SOT, where acute rejection may lead to loss of the transplant or graft dysfunction and where episodes of acute rejection predispose to CAD[41].

Many of the cases of acute rejection in VCA transplantation may be attributed to non-compliance with immunosuppressive therapy. While there have been eight hand transplant losses due to acute rejection (seven in China and one in France), these have all been in patients who have, for various reasons, stopped their

immunosuppressant therapy[6]. In terms of the six knee transplants performed since 1996, to date four have been removed secondary to rejection, with one of these again being a consequence of patient noncompliance with immunosuppression[38].

Two patient deaths have been reported. One was due to non-compliance with immunosuppression after face transplantation in China[42]. The second occurred in France in a patient who received simultaneous face and double hand transplants. In an operation addressing an infection of the face allograft, intraoperative cardiac complications lead to the patient's death[6]. Patient deaths reported in abdominal wall transplantation have been secondary to the primary condition rather than the transplant[36].

One knee transplant patient has had their knee transplant removed due to infection[38], and the first American double hand and face transplant patient has recently had to have her hand transplants removed secondary to complications related to infection and sepsis, although the face transplant has not been affected[43].

Other reasons for transplant loss have been secondary to vascular thrombosis associated with the microvascular anastomosis, occurring in two of the abdominal wall transplants performed. Although thrombosis has occurred in a few of the other VCAs performed, none have been lost to this complication. Complications related to vascular anastomosis are not uncommon in free flap reconstruction and limb replantation and are therefore not unique to VCA transplantation. The rates of

thrombosis in VCA transplantation are not higher than those in free flap procedures[6,44].

While acute rejection rates are high, evidence for CAD is less conclusive. Intimal hyperplasia is the hallmark lesion of CAD[45], and one hand transplant has required amputation secondary to intimal hyperplasia of the vessels supplying the hand[46]. Another hand transplant from the same centre in Louisville has developed evidence of intimal hyperplasia on high resolution ultrasound (abstract 5.4 IHCTAS 2011)[46]. In both these cases there is some debate as to the details of the surgical procedure performed, with some arguing that overaggressive stripping of the donor and recipient vessel adventitia may have been the causative factor rather than true CAD (*personal communication*, G. Brandacher and abstract 1.7 IHCTAS 2011)[46]. The longest surviving VCA recipient, the first American hand transplant patient, does not currently appear to display any signs of CAD. There have been no definitive reports of CAD developing in face transplant recipients[12].

It is important to note that rejection episodes that may lead to damage of any of the components of a VCA may also lead to permanent functional and cosmetic damage to the allograft. Furthermore, any substantial functional damage to a VCA may necessitate its removal: a poor outcome that would leave the patient with a limb stump or a requirement for urgent reconstruction of an area of facial or abdominal tissue loss. It is currently not clear whether recipient tissues would be amenable to reconstruction post-removal of a rejected VCA, or whether the recipient tissues

would be too damaged by the rejection process to allow autologous reconstruction, let alone a second VCA transplant.

The majority of complications that have arisen from RT to date have been secondary to the immunosuppressive therapy. Most recipients have developed opportunistic infections facilitated by the state of global immunosuppression and over two-thirds of patients have experienced metabolic complications secondary to the immunosuppression[6,10,12]. Such complications are not new to SOT but their presence in RT is a major challenge given the non-life-saving nature of these transplants. Indeed, experience from SOT informs us that the more serious complications, the malignancies, serious nephrotoxicity and cardiovascular morbidity, are yet to surface[47,48]. In this modern age of SOT, these complications are often the cause of death in transplant patients rather than allograft failure.

It is therefore clear that the main obstacle to RT becoming a more practical tool for the reconstruction of tissue defects is the need for life-long immunosuppression. These immunosuppressants have proven ineffective at controlling acute rejection episodes, and their side effects are poorly tolerated by patients and carry high risks of morbidity and mortality. This is highlighted by the high rate of patient noncompliance with immunosuppression[6]. Furthermore, perhaps due to the perception by surgeons that RT is not a life-saving therapy, the risks of immunosuppression have engendered a lack of enthusiasm for the procedure becoming more commonplace in plastic surgery. This is despite patients being more

prepared to accept the risks compared with surgeons, arguing that quality of life is as important as quantity of life[49-51].

In order to overcome these challenges, further insight is needed regarding the mechanisms of allograft rejection with special consideration to the factors involved in skin rejection. Ultimately, skin is the culprit tissue in VCA transplants: it is the first, and practically always, the only tissue to reject. Effectively controlling the immune response to skin with novel therapies that do not globally suppress immune responses may be the key to improved outcomes in VCA transplantation. In the next section the mechanisms of allograft rejection will be discussed, with a particular focus on skin rejection. This will be followed by a discussion of the opportunities for controlling the immune response without immunosuppression, focusing on Treg-based immunoregulatory approaches.

1.3 Mechanisms of allograft rejection

1.3.1 Overview

The immune system has evolved to clear the host of invading microorganisms, infected cells or mutated tumorigenic cells, which it recognises as 'foreign' and the molecules they express as antigens. When organs are transplanted between allogeneic individuals, the immune system recognises and reacts with the foreign antigens (alloantigens) on the transplant to cause rejection. The rejection response that ensues is the result of a complex interplay between the host innate and adaptive immune systems, leading to hyperacute, acute or chronic rejection. The

innate response is mediated by cells and molecules that include macrophages, dendritic cells (DCs), granulocytes (neutrophils, basophils and eosinophils), natural killer (NK) cells, the complement cascade as well as proinflammatory cytokines and chemokines. It represents a preformed defence that is immediately available until a specific response can be mounted by the adaptive immune system. The innate response is less specific than the adaptive response and will be induced even if an isograft has been performed, simply as a result of implanting or transplanting the cells or organ. Adaptive immunity is mediated by lymphocytes (T and B cells) and displays slower kinetics than the innate response. However, the adaptive response is specific to foreign antigens (i.e., allospecific) and is therefore not induced in isografts. Whilst the innate immune response is important for the initiation of the alloresponse and can initiate tissue damage, it cannot alone cause rejection, in other words complete destruction of the tissue. On the other hand, the adaptive immune response is more damaging and is essential to rejection. The importance of the adaptive response is reflected in the observation that animals experimentally depleted of T cells cannot reject allografts[52,53].

The next section will outline the events involved in the rejection response to transplants in general and skin allografts in particular. This is followed by a discussion of immunosuppressive therapy and strategies for the reduction of immunosuppression or induction of tolerance.

1.3.2 Initiation of rejection

The immune system is frequently exposed to harmless (and sometimes beneficial) foreign antigens that do not require an aggressive effector response, such as gut flora. The context in which foreign antigens are encountered is important in dictating the proportionality of the immune response: activation of leukocytes in inflammatory environments promotes an aggressive response. In transplantation, the inflammatory signal is provided by the surgical trauma and oxidative stress of ischaemia-reperfusion injury (IRI)[54-56] triggering elements of the innate immune system, through invariant pattern recognition receptors (PRRs) that recognise damage-associated molecular patterns (DAMPs). Chiefly, toll-like receptors (TLRs) are PRRs that recognise altered endogenous molecules on the allograft produced as a result of tissue injury by reactive oxygen species (ROS), heat shock proteins (HSP), high-mobility group box 1 protein (HMGB-1) or as a direct consequence of donor brain death[57]. Activation of innate immune cells by TLR ligation results in the production of 'danger' signals such as chemokines and preformed P-selectin (CD62P), which help recruit and direct host leukocytes into the transplant site[58,59]. Macrophages release cytokines such as tumour necrosis factor (TNF)α, interleukin (IL)-1 and IL-6 that contribute to the inflammatory environment and assist in the activation of other leukocytes. On recognition of inflammatory signals, antigen-presenting cells (APCs) in the allograft migrate to the draining lymphoid tissues where they present antigen to host T cells that orchestrate the development of the adaptive immune response[60-64].

1.3.3 Allorecognition

The recognition of genetic variation in the form of foreign antigens by naïve host (recipient) T cells (allorecognition**,** otherwise known as *signal 1*) is a principal step in activation of the adaptive immune system in the rejection process. Allorecognition in the presence of costimulation (otherwise known as *signal 2*) results in the activation and expansion of T cells that recognise the mismatched donor alloantigens (alloreactive T cells). Alloreactive T cells orchestrate the development of T cells with effector activity that can either have direct destructive activity against the transplant or promote and amplify B cell function and other elements of the innate and adaptive immune response that can damage the transplant.

Allorecognition is executed by the T cell receptor (TCR), which is associated with the CD3 molecule (the TCR-CD3 complex). The antigen targets of the recipient T cells that stimulate rejection include major histocompatibility complex (MHC) and minor histocompatibility (miH) antigens. The MHC is a gene complex present in most vertebrates that encodes cell surface molecules, known as MHC antigens, which when mismatched between donor and recipient are responsible for triggering a vigorous rejection response. In humans the MHC complex is termed the human leukocyte antigen (HLA) system. miH antigens are peptides derived from other molecules that are mismatched between the donor and recipient, and are presented by host MHC molecules to host T cells. miH antigens alone cannot cause rapid rejection. However when multiple miH antigens are mismatched, rejection can be as rapid as when MHC antigens are mismatched[65]. miH mismatches alone may be

present in transplants between siblings with identical HLA molecules, leading to slow rejection of SOTs[66].

In the normal state, antigen recognition occurs when self-MHC molecules present peptides derived from foreign antigens to host T cells, a route known as the indirect pathway of allorecognition in the context of transplantation[67,68]. Here, foreign HLA molecules are processed by APCs and presented within self-MHC molecules, with the TCR-CD3 complex recognising small specific peptide surface features (epitopes) of the foreign antigens in the context of self-MHC. An additional pathway is active in transplantation in which a large number of T cells react to intact donor HLA molecules, the direct pathway of allorecognition[69-71]. T cells that react to peptides derived from a nominal antigen are estimated to be less than 0.1% of the total T cell repertoire, whereas a much higher frequency (about 10%) of T cells react to an MHC mismatched transplant. This discrepancy can be resolved if direct allorecognition, which is only active in transplantation, is taken into account[72]. In direct allorecognition, host T cells interact with donor-derived 'passenger' APCs present in the transplant, including DCs, which migrate out of the transplant into the draining lymphoid tissue. Absence of these donor-derived APCs in experimental models may prolong transplant survival and prevent acute rejection[73], whereas their reintroduction restores the normal acute rejection response[74]. With time after transplantation, the direct pathway becomes of decreasing importance as passenger APCs are lost. In contrast, the indirect pathway of allorecognition is maintained and remains active for as long as the transplant is present[75-79]. The direct pathway is therefore theoretically more active during the early phase of the immune response

post-transplantation and is often linked to acute allograft rejection, with the indirect pathway becoming more important in chronic allograft rejection[80].

A third pathway may also be involved in allorecognition in which intact donor HLA molecules that have been transferred to recipient APC are recognised by host T cells, the semi-direct pathway of allorecognition[81]**.** In this mechanism, recipient APC acquire intact HLA molecules from exosomes secreted by donor APC or through cell-to-cell contact[82,83]. The relative contribution of this pathway to allograft rejection is not clear. ***Figure 1.1*** illustrates the pathways of allorecognition and subsequent effector mechanisms.

1.3.4 Costimulation

Allorecognition alone is insufficient to promote T cell activation. The second essential signal, costimulation, is provided by the interaction of pairs of cell surface molecules present on T cells and APCs. Absence or blockade of costimulatory signals typically results in T cell unresponsiveness or 'anergy'. These molecules can be divided into two families: the B7 family of which the prototype receptor-ligand pair are CD28 (on the T cell) and CD80/86 (B7.1/B7.2, on the APC), and the TNF and TNF receptor (TNFR) family best characterised by CD40 (on the APC) and CD154 (CD40L, on the T cell). Other costimulatory T cell/APC pairs include CD27/CD70, inducible T cell costimulator (ICOS or CD278)/ICOS ligand, 4-1BB/4-1BB ligand, OX40/OX40 ligand and CD279/CD274. Signalling via CD28 lowers the threshold for T cell activation and increases the expression of the T cell growth factor (leukocytotrophic)

IL-2 by stabilising the messenger RNA (mRNA) species, thereby promoting T cell proliferation and resistance to apoptosis. During an immune response, activated T cells also upregulate expression of CTLA-4 (cytotoxic T-lymphocyte antigen 4, CD152), a molecule that has close homology to CD28 but has an inhibitory effect on T cell activation. CTLA-4 has a higher affinity for CD28 than CD80/86 and is able to attenuate immune responses by competing for CD28. CD28 signalling also upregulates expression of other costimulatory molecules such as CD154 (CD40 ligand) which on ligation with CD40 activates APCs, leading to increased expression of B7 family molecules and therefore a greater ability to activate further T cells. The balance of positive and negative signals through these molecules to the T cell ultimately determines whether the T cell will be activated or become anergic.

1.3.5 Activation

The interface of a T cell with an APC in which both the TCR-MHC and costimulatory molecule interaction occurs is termed the 'immunological synapse'. This immunological synapse forms a "bull's eye" structure with a central supramolecular activation cluster (c-SMAC) containing the TCR-MHC complex, surrounded by a peripheral SMAC (p-SMAC) ring containing adhesion molecules, such as LFA-1 (leukocyte function-associated antigen 1) on the T cell bound to ICAM-1 (intercellular adhesion molecule 1, CD54) on the APC.

Within the cell membrane phospholipid bilayer are cholesterol-rich regions termed lipid rafts. Certain membrane bound molecules are preferentially associated with

lipid rafts, in particular those with lipophilic attachments to the cell membrane. In resting T cells the TCR-CD3 complex is not usually associated with lipid rafts and is therefore unable to interact with other signal transduction molecules found within them. During the formation of an immunological synapse, clustering of signalling and adhesion molecules occurs as a result of multiple TCRs binding to MHC-peptide complexes on the surface of the APC. A reorganisation of the cell membrane subsequently takes place, allowing TCR-CD3 complexes to integrate into lipid rafts. This facilitates downstream signalling by placing the TCR-CD3 complex in close proximity to signal transduction molecules, which are then activated by phosphorylation. The end result is the activation of the intracellular Ras- and Rac-mitogen-activated protein kinase (MAPK) pathways and hydrolysis of membrane phosphatidylinositol 4,5-biphosphate to generate the secondary messengers inositol triphosphate (IP_3) and diacylglycerol (DAG). IP_3 leads to the release of stored calcium from the endoplasmic reticulum (ER) and activation of phosphatase calcineurin, which dephosphorylates the transcription factor NFAT (nuclear factor of activated T cells), allowing it to translocate to the nucleus. Generation of DAG results in the activation of the transcription factor nuclear factor-κB (NF-κB). The MAPK cascade also leads to the generation of the transcription factor activator protein 1 (AP-1). The action of these transcription factors alters the expression of many genes, and in particular leads to upregulation of IL-2 and the high affinity IL-2 receptor (IL-2R) α-chain (CD25) required for T cell growth. Large amounts of IL-2 and other leukocytotrophic cytokines are produced and act to provide further signalling to promote cell cycle progression, clonal expansion and differentiation of activated T cells.

Activated lymphocytes upregulate chemokine receptor expression, allowing them to activate further leukocytes and subsequently infiltrate the allograft. The process by which leukocytes migrate into the graft is termed leukocyte recruitment. Leukocyte recruitment is enhanced by vasodilation to slow cells down in the vicinity of the transplant and endothelial activation in the vicinity of the transplant. Chemokines that have been released from the allograft become tethered to the activated endothelium, providing a signal gradient recognised by passing leukocytes. When leukocytes bind to activated endothelium, further adhesions are made between integrin molecules on the leukocyte and endothelial adhesion molecules such as ICAM-1, which bring about arrest of the leukocyte and extravasation into the transplant.

1.3.6 The adaptive immune response

Two types of T cells identified by the cell surface markers CD4 and CD8 are active in rejection. $CD4^+$ T cells are activated by MHC (HLA) class II molecules, which have two transmembrane domains and are expressed by APCs. Functionally, $CD4^+$ T cells are usually helper T cells (Th) and are therefore often referred to as Th cells. $CD4^+$ Th cells can differentiate into several subtypes including Th1, Th2 or Th17 (***Figure 1.1***). $CD8^+$ T cells are activated by MHC (HLA) class I molecules which differ structurally to MHC class II, having only one transmembrane domain. $CD8^+$ T cells often have cytotoxic activity and are therefore known as cytotoxic T lymphocytes (CTLs). Class I MHC is expressed, albeit at varying levels, by all nucleated cells. As discussed earlier, alloreactive T cells are activated only after an immunological synapse is formed with

an APC that provides the appropriate MHC with costimulation. APCs that are able to provide these signals are termed 'immunostimulatory' or 'professional', and constitutively express MHC class II (e.g. DCs, macrophages and B cells). TLR ligation on DCs induces upregulation of costimulatory molecules and MHC class II, enhancing their ability to activate T cells. So-called non-professional APCs express MHC class II only on stimulation with a cytokine, such as interferon-γ (IFNγ, e.g. fibroblasts and epithelial cells).

1.3.6.1 $CD4^+$ T cells

$CD4^+$ Th cells are critical to allograft destruction. The type of Th response is determined by the cytokine microenvironment in which APC and T cell interactions take place. Both cell-mediated immunity, driven by Th1 cells, and humoral immunity, driven by Th2 cells are capable of causing allograft destruction independently[84,85]. IL-17-producing Th17 cells have also recently been implicated in allograft rejection[86,87]. Notably, although $CD4^+$ activity is triggered in an antigen-specific manner, the effector mechanisms of allograft destruction are non-specific.

1.3.6.1a Th1 cells

Th1 cells produce IFNγ and IL-2, which result in the activation of $CD8^+$ cytotoxicity, macrophage-dependent delayed-type hypersensitivity (DTH) and the synthesis of complement-activating immunoglobulin (Ig)G2a by B-cells, all of which have been associated with allograft rejection. Furthermore, Th1 cells may express Fas ligand (FasL or CD95L) themselves, enabling them to exhibit cytotoxic activity. The Th1 DTH

response is a non-specific effector mechanism that induces the production of mediators such as nitric oxide, ROS and inflammatory arachidonic acid derivatives such as prostaglandin E2, thromboxane and leukotrienes from macrophages. Th1-mediated effects have been shown to directly affect graft physiology by altering cell permeability and vascular smooth muscle tone and are implicated in the early stages of rejection, otherwise known as acute cellular rejection (ACR).

The role of IFNγ, a principal Th1 cytokine, is not straightforward. IFNγ mRNA is increased in acutely rejecting murine allografts[88,89] and urinary protein levels of the IFNγ-induced chemokine MIG (monokine induced by IFNγ) are elevated during episodes of acute human kidney rejection[90]. However, IFNγ knockout mice receiving heart and kidney allografts develop accelerated rejection compared to their wild-type counterparts[91,92]. In renal transplant patients who have not experienced a rejection episode, levels of IFNγ in the serum are significantly raised 24 months following surgery[93]. In addition, a great deal of evidence is emerging that attributes a regulatory capability to IFNγ[94-97]. This effect may be due to the ability of IFNγ to promote Treg development and inhibit Th17 cell development[94,97]. In further support of this theory, a recent study using *Tbet* deficient mice lacking Th1 cells has shown that rejection is accelerated due to an increased activity of Th17 cells[98].

1.3.6.1b Th2 cells

Th2 cells express the transcription factor GATA-3 and secrete IL-4, IL-5, IL-9, IL-10 and IL-13, which activate B cells (inducing immunoglobulin class-switching) and

eosinophils to promote graft rejection primarily through the humoral immune response. In rejecting mouse cardiac allografts, an increase in Th2 cytokine gene expression is present which is associated with intragraft eosinophil accumulation[99]. Furthermore, in human renal and liver transplant rejection there is an association between intragraft Th2 cytokines and graft eosinophil infiltration[100-102]. In an adoptive transfer model, *ex vivo* polarised Th2 cells are able to reject mouse cardiac or islet allografts with kinetics similar to polarised Th1 cells[103,104]. An IL-9 and IL-10 producing population of effector T cells has also recently been described[105,106]. These cells appear distinct from Th2 cells as they do not produce the other Th2 cytokines and do not express the Th2-specific transcription factor, GATA3. IL-9 is known to contribute to allergic disease but its role in transplantation is not clear[107].

1.3.6.1c Th17 cells

The role of Th17 cells in allograft rejection is not yet fully elucidated but experimental evidence is mounting. Th17 cells express the transcription factor RORγt and produce IL-17, IL-21 and IL-22, which act alone and synergistically with other cytokines to promote neutrophil recruitment to the site of rejection[108]. In rat renal and mouse corneal transplant models, IL-17 mRNA expression was shown to increase in the early post-transplant period[109,110]. Furthermore, in the corneal transplant model, levels of the Th17 transcription factor *RORγt* were increased in the allograft-draining lymph nodes[109]. In humans, IL-17 protein levels have been found to be elevated in borderline rejecting renal allograft biopsies by immunofluorescent staining together with detectable IL-17 mRNA in the urinary mononuclear cell (MNC)

sediment[110,111] and increased levels have also been detected in the broncheoalveolar lavage of acutely rejecting lung allografts[112]. In a human vessel allograft model, graft derived IL-1 has been shown to promote IL-17 production from alloreactive T cells, enhancing the production of the proinflammatory cytokines IL-6, CXCL8 and CCL20[113]. In mouse models, the neutralisation of IL-17 can reduce the features of vascular acute rejection of aortic allografts and also significantly extend the survival of cardiac allografts[114,115]. In these studies IL-17 neutralisation also reduces the intragraft production of inflammatory cytokines. The majority of these experimental studies have found IL-17 levels to be higher in acute rather than chronic rejection indicating a role for Th17 cells in the early post-transplant period[116].

1.3.6.2 $CD8^+$ T cells

$CD8^+$ T cells are involved in transplant destruction via cytotoxic activity leading to cell target death. Activated $CD8^+$ CTLs migrate to the graft site where they are able to identify their target cells in the graft by recognition of allogeneic class I MHC molecules. Once a target cell is located, CTLs release granules containing cytotoxic molecules such as perforin and granzyme B. In addition, CTLs are able to upregulate cell surface expression of FasL and secrete soluble mediators such as TNFα. Perforins polymerise and insert into the target cell membrane, forming a pore that facilitates the entry of granzyme B and other compounds into the cell. Granzyme B is a protease that is able to initiate apoptosis by several mechanisms including activation of caspase cascades. Binding of FasL to Fas on the target cell surface is also able to trigger apoptosis by activating caspases. In kidney transplant rejection,

$CD4^+$ and $CD8^+$ T cells permeate the interstitial space around tubules[117] and contain perforin and granzyme A and B or FasL and are thus pro-apoptotic[118]. Gene expression studies have shown an increase in the mRNA for the cytolytic-associated transcripts of granzyme B, perforin and FasL in rejecting tissues[119-122]. Furthermore, the lack of a functional Fas molecule is sufficient to prolong survival of allogeneic skin transplants[123]. Moreover, $CD8^+$ T cell activity is a significant barrier to the induction of transplantation tolerance[124-126].

1.3.6.3 B cells and antibody-mediated rejection

Although the great majority of episodes of graft rejection are initiated by alloreactive T cells, antibody-mediated rejection (AMR) is increasingly seen as problematic in clinical transplantation[127]. B cells utilise surface Ig as an antigen receptor, internalising alloantigens that are processed and presented in conjunction with class II MHC molecules. Antigen-specific recognition and costimulatory signalling from activated $CD4^+$ T cells is required for the activation and differentiation of B cells, resulting in plasma cell generation and the production of alloantibodies.

Antibodies may be directed against donor HLA molecules, ABO blood group antigens or endothelial cell (EC) antigens. These are usually generated during the immune response to the allograft, although in the case of antibodies to ECs, may be pre-existing at the time of time of transplantation. AMR may be subdivided into hyperacute, acute and chronic. Hyperacute AMR is a rare event, occurring when recipients have pre-formed antibody directed against allogeneic MHC molecules or

ABO-isoagglutinins expressed on the graft endothelium. It is defined by rejection occurring within 24 hours of reperfusion and is characterised by immediate or near immediate loss of graft function secondary to complement-mediated thrombosis within the allograft vascular supply. Modern cross-matching techniques have made hyperacute rejection extremely rare whereas acute and chronic AMR remain problematic. Acute AMR occurs around the same time as ACR and is likely due to a recall response of B cells that have been sensitised by previous antigen-encounter during pregnancy, a blood transfusion or a previous transplant. AMR appears to be active in 20-30% of acute transplant rejection episodes[128].

In cardiac transplants, the presence of donor-reactive immunoglobulin G (IgG) responses increases the risk of acute rejection[129,130]. Moreover, patients with detectable α-HLA antibodies at the time of transplantation have significantly worse graft survival than patients that are not sensitised, and the development of α-HLA antibodies in previously non-sensitised patients following transplantation is highly predictive of early graft failure[131]. AMR is also active in chronic rejection, with evidence for anti-donor antibodies in up to 60% of CAD cases and an association with late loss of kidney, heart, lung and liver transplants[131-135].

The hallmark of AMR is the activation of complement and membrane attack complex (MAC) formation, leading to target cell lysis. Positive histological staining for complement component 4d (C4d) in biopsies is indicative of AMR. In endomyocardial biopsies, C4d staining of capillaries correlates well with the presence of circulating anti-donor antibodies and AMR[136,137]. Cell killing by antibody

may also occur via a mechanism termed antibody-dependent cell-mediated cytotoxicity (ADCC) in which NK cells or macrophages recognise and kill target cells that have been coated in antibody.

1.3.6.4 Memory cells

Following the clearance of a pathogen by naïve cells of the adaptive immune system (*the primary response*), a small number of antigen-specific T and B cells survive as memory cells that are able to mount a rapid response in the event of reintroduction of the same pathogen (*the secondary* or *memory response*). The immune response to a transplanted organ results from the stimulus of both naïve and memory alloreactive T cells. Unlike naïve T cells, memory T cells can survive in the absence of antigen and can be activated in the absence of costimulatory molecules essential for naïve T cells[138]. Memory T cells may be present due to prior exposure to alloantigen during pregnancy, from a previous transplant, or from a blood transfusion[139]. However, memory cells capable of responding to alloantigen may also be present in individuals even without prior exposure to that antigen. This occurs through the operation of three mechanisms: cross-reactivity through molecular mimicry from prior infectious agents[140], bystander proliferation following lymphopaenia[141], or heterologous immunity[142]. Properties of memory cells not only include more rapid and efficient responses to previously encountered antigen, but also a resistance to apoptosis due to the upregulation of anti-apoptotic molecules such as Bcl-2 and Mcl-1[143]. Furthermore, there is evidence that rejection mediated by memory T cells is

resistant to some immunosuppressants and immunoregulation[124,144,145]. These characteristics give memory cells an especially detrimental role in rejection[146,147].

1.3.7 The innate immune response

Due to the intimate relationship of the adaptive and innate immune responses, many of the aspects of the innate immune response have already been discussed, such as the role of DCs, the complement cascade, NK cells, macrophages and granulocytes such as neutrophils and eosinophils. A few points on the mechanisms of action of two innate immune system components that have not been fully covered, the complement cascade and NK cells, will now be discussed.

The complement cascade is a proteolytic cascade that generates a range of effector molecules: complement components C5a and C3a are chemoattractant molecules that assist leukocytes in migrating towards the allograft; C3b, C4b and their fragments act to opsonise cells (thus targeting them for destruction by phagocytes such as macrophages and neutrophils) as well as facilitating antigen presentation and T cell activation[148-151]. The terminal components of the cascade, C5b-9, result in the formation of the MAC in the target cell membrane, inducing cell lysis[152]. Apart from being activated by immunoglobulin, complement can be activated as a result of IRI, cytomegalovirus (CMV) infection and anti-lymphocyte antibody treatment.

NK cells kill target cells in an identical manner to CTLs but do not possess antigen-specific TCRs or require activation. NK cells express a variety of inhibitory and

activating receptors that regulate their activity. Self-cells are able to deliver an inhibitory signal to NK cells, whereas infected or malignant cells cannot deliver this signal and are subsequently killed. Theoretically, allogeneic cells are also unable to deliver an inhibitory signal to NK cells, but in reality NK cells do not appear to contribute significantly to solid organ rejection, although a role for NK cells in bone marrow transplantation has been reported[153]. Interestingly, NK cells have been shown to kill donor-derived APCs, in theory reducing the relative contribution of direct allorecognition to rejection[154].

1.4 Skin rejection

While the mechanisms of rejection discussed are applicable to all transplants including VCAs, the presence of skin in VCAs presents a unique immunological challenge. It has long been known that skin is more susceptible to rejection than any other tissue[155-157]. Skin is virtually always the first and usually the only tissue to reject in VCA transplants, and a higher level of immunosuppression is required for VCAs that contain skin compared to those that do not[158]. The reasons why the character of the immune response to skin is altered will now be discussed.

1.4.1 Vascularisation

Although VCAs contain skin that is immediately vascularised (i.e. primarily vascularised), the majority of experimental studies in the literature have utilised non-vascularised skin grafts (i.e. secondarily vascularised), which undergo a period of relative ischaemia lasting 2 to 3 days, before receiving a blood supply through

vascular inosculation. In contrast, the skin in VCAs receives a blood supply immediately on anastomosis of the donor and recipient vessels. While there is evidence that vascularised skin allografts have a survival advantage over non-vascularised skin allografts[159], the skin component of a VCA is still more susceptible than any other component to rejection and it is therefore unlikely that the state of vascularisation is the critical factor in the susceptibility of skin grafts to rejection[160]. For example, in an MHC-matched miniature swine model of transplantation of primarily or secondarily vascularised skin, both types of grafts were rejected, even though the musculoskeletal component of the primarily vascularised graft was accepted[161-163]. In a rat model of an immediately vascularised skin graft compared with a secondarily vascularised skin graft, rejection kinetics were also found to be similar[160].

Nevertheless, as the assays performed in the studies in this thesis utilise skin that undergoes an initial period of ischaemia, there are certain issues to take into consideration. Importantly, the period of ischaemia may induce cell death within the graft, promoting the release of immune mediators. These mediators would then initiate the immune response via leukocytic recruitment and migration of donor APCs through the lymphatics and into the peripheral lymphoid tissue, where they are well placed to present antigen[64,164,165]. While migration of APCs from primarily vascularised skin is also likely to occur due to the release of inflammatory mediators induced by the surgical trauma (albeit to a lesser degree), these APCs will take a different route through the peripheral blood, ending up in the spleen[166-168]. The character of the resulting immune response is therefore likely to be partly a function

of the degree of release of immune mediators, the route of APC migration, and the final destination of the APCs to an area where they may efficiently present antigen and activate recipient T cells. There is also evidence that the character of the cellular infiltrate differs between primarily and secondarily vascularised skin allografts, with the former infiltrated with a greater density of cells, and the presence of recipient-derived APCs in the skin of only primarily vascularised allografts, an observation that may be related to the rapid accessibility of recipient leukocytes to the primarily vascularised skin allograft[169]. Finally, there is a greater likelihood of mixed chimerism developing in primarily vascularised skin compared to secondarily vascularised skin[170], a state beneficial to allograft survival (see *section 1.6.1*).

1.4.2 Dermal microvasculature

The microvasculature of the dermis is unique in that the ECs have a central role in immunity. ECs express MHC Class I and II as well as costimulatory molecules and receptors for T cell homing molecules, therefore leading to the recruitment and activation of circulating T cells[171,172]. Furthermore, dermal capillaries are narrower than the width of a T cell, forcing cells passing through to come into contact with ECs and the molecules they express. Resting memory T cells that come into contact with peptide-MHC complexes on ECs respond by proliferating and producing inflammatory cytokines. In contrast, other tissue cells such as fibroblasts and epithelial cells, even if expressing MHC molecules cannot activate resting memory T cells[173,174]. Indeed, cultured ECs alone are sufficient to present antigen to T cells *in vitro*.

In terms of costimulatory power, human ECs are more capable of costimulation of T cells than monocytes or even professional APCs[172]. ECs also induce the early expression of CD40L on $CD4^+$ T cells, 24 hours before APCs are able to induce the same expression levels[175,176]. Memory T cells that recognise EC-expressed peptide-MHC complexes rapidly initiate integrin-mediated adhesion to ECs, leading to their recruitment into the skin. Naïve T cells are deficient in integrin expression and therefore fail to adhere or be recruited. Antigen presentation by ECs therefore increases the likelihood of allorecognition by memory T cells. In contrast, in most other SOTs, memory T cells may only come into contact with APCs bearing their cognate peptide-MHC complex in the peripheral lymphoid tissue.

Many more T cells are recruited to skin allografts than only the small percentage of alloreactive cells[177]. This appears to be due to activation of ECs by inflammatory mediators released after keratinocyte damage, for example after transplantation. Such activation of ECs causes them to display or release multiple leukocyte-activating chemokines, leukocyte adhesion molecules (such as VCAM-1, ICAM-1 and E-selectin) or vasodilatory mediators (such as nitric oxide, prostacyclin, endothelium-derived hyperpolarising factor and bradykinin)[172,178-180]. This leads to the extravasation of T cells directly into the skin. Such T cells may not necessarily be alloreactive but may contribute to allograft destruction through non-specific effector mechanisms and inflammatory cytokine release.

1.4.3 Allograft volume

Large volume allografts are less prone to rejection than smaller allografts, a possible causative factor for the susceptibility of skin grafts, which are of low overall volume, to rejection[181,182]. Interestingly, heart allografts have been shown to stimulate the activation and proliferation of more T cells than skin allografts, yet skin allografts are rejected more acutely than heart allografts[157]. Skin allografts therefore appear to require a smaller number of effector T cells for destruction, a function of the small amount of tissue available to be destroyed. The relatively large volume of non-skin tissues being transplanted as part of VCA allografts may explain their relative protection from rejection compared to the overall low-volume skin component of the VCA.

1.4.4 Skin-specific antigens

The observation that skin, and in particular, the epidermis, is the only tissue that is rejected in both MHC-matched transplant models as well as chimeric models of tolerance[161-163,183,184], has given rise to the possibility that certain skin-specific antigens exist that are distinct from MHC antigens[185,186]. As further evidence, in a rat model of skin transplantation, marginally prolonged survival of skin allografts was observed in mice that received injections of epidermal cells together with bone marrow cells from the donor as neonates, compared with those that received bone marrow cells alone, suggesting the presence of unique antigens on the epidermal cells[187].

Skn-1, Skn-2 and Epa-1 are epidermis-specific antigens that may be relevant in this regard, however evidence for their involvement is inconclusive. Skn antigens have been defined in both the mouse epidermis and neural cells[188,189], and while α-Skn antibodies have been demonstrated, these do not appear to be sufficient for skin rejection in chimeric models, likely because the antigens do not induce a T cell response of the necessary proportion[190,191]. There is therefore doubt over whether these antigens are truly transplantation antigens[192]. The Epa-1 antigen has been defined on mouse epidermal cells and may have a human counterpart[185]. While Epa-1^+ skin allografts do appear to be rejected faster than Epa-1^- skin allografts[185], the Epa-1 antigen has been defined on various other tissues that do not share the same susceptibility to rejection as skin, such as the heart[193].

1.4.5 Skin architecture and unique cellular composition

There is evidence that the very features that give skin its unique immunological barrier properties also play a role in its susceptibility to rejection. Other tissues with barrier functions, such as the intestine, are also particularly susceptible to rejection[194]. The extracellular scaffold matrix of skin contains a high density of lymphocyte adhesion molecules, such as the ligands for cutaneous lymphocyte-associated antigen (CLA), that attract memory T cells[195]. Furthermore, the microarchitecture of the skin extracellular matrix positions T cells ideally for activation and effector function, and the high vascularity of the dermis allows rapid infiltration with leukocytes. Resident T cells in skin may also kill damaged keratinocytes (for example, ischaemic keratinocytes), compounding the destructive

process occurring with skin graft rejection. Furthermore, skin contains a high number of resident leukocytes which include T cells and skin DCs, with a particularly high density of specialised Langerhans cells in the epidermis[196].

Human keratinocytes and ECs of the dermal vessels are also able to express MHC Class II, providing multiple opportunities for antigen exposure both via the direct and indirect allorecognition routes[172,197]. Nevertheless, mouse skin allografts from MHC Class II knockouts are rejected with similar kinetics to wild type skin allografts[198]. While this may appear to contradict evidence that EC-expressed MHC Class II is important in the alloresponse to skin, it in fact highlights an important species difference. Human ECs express HLA Class II both constitutively and upon stimulation with IFNγ, and are able to present antigen to memory T cells, whereas mouse ECs do not express MHC Class II on their ECs and cannot present antigen to T cells[172,199-201]. In fact, the expression of HLA on human ECs appears to be important for the development of memory alloresponses to skin[172].

1.4.6 Skin alarmins

The role of DAMPs generated by the trauma of transplantation and IRI in initiating the immune response against a transplant was discussed in *section 1.3.2*. The endogenous molecules that act as DAMPs are known as *alarmins*, a term coined by Joost Oppenheim in 2006[202,203]. These molecules initiate host defence in response to injury by acting as chemoattractants as well as by activating receptors on host APCs. Importantly, both keratinocytes and resident skin leukocytes may produce alarmins

following nonprogrammed cell death or through active secretion in response to trauma, allergen exposure, UV radiation or IRI. Important alarmins include HMBG1[204], HSPs[205], S100 proteins[206], IL-1α[207] and uric acid[208]. A recent addition to both the IL-1 and alarmin families is IL-33, which is secreted by both human ECs and keratinocytes[209]. IL-33 appears to have a role in the pathogenesis of atopic dermatitis and psoriasis and acts to activate mast cells and neutrophil chemotaxis[210,211]. The majority of alarmins engage TLRs, the IL-1 receptor, or ST2 receptor, leading to NF-κB activation and the subsequent transcription of cytokines and chemokines such as IL-1β, IL-6 and TNFα that attract and activate elements of both the innate and adaptive immune systems[212]. Another putative alarmin, IL-25, may be relevant in the skin. IL-25 transcripts have been detected in keratinocytes and dermal DCs, and may act to expand a Th2 response in the skin and promote the expression of IL-9[213-216]. The unique susceptibility of skin to rejection may therefore at least in part be related to the rapid activation of the immune system by alarmins released in response to the trauma of surgery and ischaemia.

1.5 Immunosuppression

Before discussing the experimental techniques in development for tolerance induction, it is important to discuss briefly current immunosuppressants that are in clinical use. Any new tolerance inducing or immunoregulatory therapy to be introduced clinically will be compared against the 'gold standard' of these immunosuppressive drugs. Furthermore, given the excellent short-term survival rates for most SOT and VCA transplants, any new therapy will initially be used

alongside current traditional immunosuppression in an effort to reduce the dosages and thus the toxicity of current immunosuppressive drugs without endangering allograft survival.

The most common clinical immunosuppressive strategy is for recipients to receive strong induction immunosuppression during the first three months post-transplantation when the risk of acute rejection is highest, then for immunosuppression to be gradually reduced to a maintenance dose. Broadly speaking, immunosuppressants can be divided into those that act on intracellular targets affecting signal initiation (such as antimetabolites and macrolides) or signal reception (such as mammalian target of rapamycin (mTOR) inhibitors), and those acting on extracellular targets (such as antibodies and fusion proteins). Corticosteroids cannot be placed into one of these classes, as their effects are widespread and dose-dependent.

In the early 1960s, the introduction of protocols containing combinations of prednisolone (a corticosteroid) and AZA (an antimetabolite or antiproliferative agent) was responsible for moving transplantation from an experimental therapy to a clinical one[27,28]. The introduction of cyclosporine, a macrolide with selective T cell inhibitory action in the 1980s was responsible for another leap forward in transplant immunosuppression. Subsequently, various refinements have been made with the introduction of other targeted immunosuppressants. ***Figure 1.2*** summarises the mechanisms of action of common immunosuppressive drugs currently in clinical use.

Corticosteroids act by binding to cytoplasmic glucocorticoid receptors, altering the expression of multiple cytokines and inflammatory mediators by targeting the transcription factors NF-κB and AP-1. Molecules affected include IL-1, IL-2, IL-3, IL-6, TNF-α, IFN-γ, leukotrienes and prostaglandins as well as several chemokines. Corticosteroids therefore possess both immunosuppressive and anti-inflammatory effects. Side effects of corticosteroid therapy include weight gain, hyperlipidaemia, osteoporosis and glucose intolerance.

Antimetabolites such as AZA and MMF interfere with DNA synthesis and cell cycle progression, therefore impairing the clonal expansion of T cells. MMF is a more lymphocyte-specific drug than AZA, which also has bone marrow suppressive effects. AZA is metabolised in the liver into 6-mercaptopurine which is then incorporated into DNA, inhibiting purine nucleotide synthesis with widespread effects on gene transcription and cell cycle progression. MMF is metabolised in the liver into mycophenolic acid, a non-competitive reversible inhibitor of inosine monophosphate dehydrogenase (IMPDH), an enzyme required for purine generation. IMPDH inhibition has downstream effects on DNA and RNA synthesis. Side effects of antimetabolites include bone marrow suppression, hepatotoxicity, macrocytosis and diarrhoea.

Calcineurin inhibitors (CNIs) are a subset of the macrolide compounds (so called because their activity depends on the structural presence of a macrolide ring), and include cyclosporine and tacrolimus. Both drugs bind cytoplasmic immunophilins to form complexes that inhibit calcineurin, a phosphatase enzyme in the T cell signal

transduction pathway. Inhibition of calcineurin prevents the translocation of NFAT to the nucleus. Effects include inhibition of the production of the cytokines IL-2, IL-4, TNF-α and IFN-γ as well as the down-regulation of costimulatory molecules such as CD154. Side effects of CNIs include nephrotoxicity, hypertension, glucose intolerance, gingival hyperplasia and hyperlipidaemia.

mTOR inhibitors include sirolimus (rapamycin) and everolimus. These drugs act by binding and inhibiting mTOR, which has a critical role in cytokine receptor signal transduction, specifically in relation to IL-2, IL-4 and IL-15. These cytokines act through mTOR to induce the production of proteins that are necessary for progression from the growth phase to the DNA synthesis phase of the cell cycle, and are therefore critical for T cell clonal expansion. Side effects of mTOR inhibitors include abdominal pain, hyperlipidaemia, thrombocytopaenia, mouth ulcers and pneumonitis.

Antibodies can be polyclonal, such as antithymocyte globulin (ATG) directed against multiple epitopes of antigens on human lymphocytes, or monoclonal, such as OKT3 directed against human CD3ε. Both these antibodies can cause lymphocyte depletion that does not fully recover for over a year and are therefore useful for induction immunosuppression or for treatment of severe rejection episodes. Both antibodies can initially activate lymphocytes, inducing the release of cytokines and leading to a 'cytokine release syndrome'. This may manifest as a rare severe systemic inflammatory response with hypotension, rigors and pulmonary oedema.

Newer monoclonal antibodies (mAbs) include alemtuzumab, rituximab, basiliximab and daclizumab. Alemtuzumab is a humanised mAb against human CD52, present on most mature nucleated bone marrow derived cells. Alemtuzumab therefore depletes T and B cells, monocytes, macrophages and some granulocytes. Recovery of these cells to normal levels can take years after administration of alemtuzumab, and it is therefore reserved for special circumstances in a select group of transplant recipients for induction immunosuppression or for the treatment of rejection episodes. Rituximab is directed against CD20, which is present on most mature B cells and is useful for the treatment of AMR. Basiliximab and daclizumab are humanised mAbs directed against CD25, which is present on activated T and B cells. Basiliximab and daclizumab are generally used as induction immunosuppression.

Fusion proteins include abatacept and belatacept, which are molecules that are composed of the non-binding portion of IgG fused to the extracellular domain of CTLA-4. As mentioned earlier, CTLA-4 has a high affinity for CD80/86 and therefore prevents the CD80/86-CD28 interaction required for costimulation, raising the threshold for activation of T cells.

The majority of VCA transplant recipients have received immunosuppression similar to that given to most straightforward cases of SOT, taking into account data from the Symphony Trial which recommended maintenance on low-dose tacrolimus, MMF and steroids[6,10,32]. A few patients have received alternative regimens that include rapamycin, although it is not clear whether this has provided any benefit over

standard therapy. Induction immunosuppression has varied, using basiliximab, ATG or alemtuzumab.

1.6 Methods of tolerance induction

The immunosuppressive regimens discussed above are less than ideal: they are nonspecific, require lifelong use, favour the development of opportunistic infections and tumours, directly damage transplanted organs and significantly increase cardiovascular morbidity and mortality[3,48]. Their use is limiting the field of VCA transplantation as only the most severe reconstructive problems are being considered. There is therefore a critical need for strategies that may allow a reduction or complete withdrawal of immunosuppression. Long-term graft acceptance with normal function in the complete absence of immunosuppression with otherwise normal immune responses is known as tolerance, the hallmark of which is donor-specific immune hyporesponsiveness. The achievement of this state would remove the need for immunosuppression and improve long-term outcomes in terms of both graft function and patient morbidity and mortality.

The quest for transplantation tolerance began in earnest with the landmark paper by Billingham, Brent and Medawar in 1953, in which tolerance was induced to a mouse skin allograft by injection of the recipient mouse with donor-derived cells as a neonate[16]. Current experimental and early clinical strategies to induce tolerance centre on the induction of central tolerance techniques, most commonly the

induction of chimerism, or on peripheral tolerance techniques most commonly the induction or use of Treg.

1.6.1 Central tolerance

During T cell development in the thymus, T cells that are strongly reactive to host MHC molecules are deleted by a process termed negative selection (i.e. central deletion). This physiological process has been harnessed experimentally for the induction of tolerance to foreign antigens.

Haematopoietic complete chimerism through myeloablative therapy and donor-derived bone marrow transplantation results in the repopulation of the host thymus with donor-type DCs that delete donor-reactive T cells. Complete chimerism is the replacement of all host haematopoietic cells with donor-derived stem cells such as haematopoietic stem cells (HSCs). Because such donor-derived stem cells have the ability to replicate perpetually, they theoretically continue to provide donor-type DCs indefinitely.

A number of successful clinical cases in SOT have been reported whereby patients with haematological indications for bone marrow ablation who also require renal transplantation have received a bone marrow transplant and a kidney transplant from the same donor, resulting in long-term donor-specific tolerance[217-219]. Nevertheless, the morbidity and mortality of myeloablative therapy and risk of graft-versus-host disease (GvHD) in most transplant patients makes this mode of therapy

unacceptable to those without a haematological indication for bone marrow ablation. On the other hand, mixed chimerism, where donor cells represent a varying proportion (but not 100%) of the total haematopoietic pool is a more promising area of research[220]. Mixed chimerism can be established using non-myeloablative conditioning regimens, therefore maintaining immunocompetence and reducing the risk of GvHD.

Two promising clinical trials for SOT utilising mixed chimerism for the induction of tolerance have been performed. An initial trial enrolled 6 patients with renal failure consequent to multiple myeloma, a haematological malignancy[218]. Patients received non-myeloablative bone marrow transplants and renal transplants from an HLA-identical sibling followed by a donor leukocyte infusion as treatment for both the multiple myeloma and renal failure. These patients successfully accepted their renal transplants long-term without any immunosuppression. Following this study, a similar approach was piloted in 5 patients *without* a haematological malignancy[221,222]. Patients received an HLA-mismatched haploidentical bone marrow transplant along with a renal transplant from the same donor. Four patients in the trial currently maintain graft function after weaning from their initial immunosuppression (follow up 2-5 years post-weaning). However, one kidney transplant was lost due to acute AMR, leading to a modification in the trial protocol to include B cell depletion with rituximab.

1.6.1.1 Central tolerance in VCA transplantation

The method used by Medawar to achieve tolerance to skin allografts over 60 years ago was in a fortunate strain combination with only a class I MHC mismatch[16]. More recently, similar methods have been used to achieve 'central deletion' in fully MHC-mismatched models of skin or VCA transplantation. In a rat model of vascularised musculoskeletal transplantation, infusion of bone marrow cells into neonates achieved prolonged survival of allografts[223]. Similar work with fully MHC-mismatched skin transplants in rodent models has been less fruitful[187,224]. In a miniature swine model using prenatal injection of bone marrow, skin grafts only attained moderately prolonged survival, whereas renal transplants in the same model were accepted long-term[225]. In a rhesus monkey model, only very modest prolongation of survival of vascularised skin allografts was achieved with intravenous or intrathymic injections of allogeneic donor cells, although the mode of action here may be secondary to induction of Treg (see next section)[226]. Clearly, such strategies are neither consistently successful nor easily translatable to the clinic.

Induction of mixed chimerism by non-myeloablative therapy with or without subsequent stem cell infusion has been trialled in skin and VCA transplantation. Non-myeloablative therapy with a HSC transplant has achieved prolonged allograft survival in both mouse and dog models of skin transplantation[227-229]. However in miniature swine models of skin and cardiac transplantation where mixed chimerism was attained, tolerance could only be reliably achieved to the heart transplant[162]. There is evidence that in models using T cell depletion in conjunction with non-myeloablative therapy such as irradiation, peripheral regulation with Treg is an

important contributor to the tolerant state[230]. Other methods have trialled T cell depleting antibodies with immunosuppression in the absence of irradiation in an effort to facilitate mixed chimerism. For example, in a rat hindlimb transplantation model using T cell depletion and immunosuppression with a bone marrow transplant to achieve chimerism, long-term donor-specific hindlimb allograft survival was attained across a full MHC mismatch barrier[231,232]. In a mouse model of skin transplantation using non-depleting α-$CD4^+$ and α-$CD8^+$ antibody in association with a bone marrow transplant, tolerance was attained across a class I MHC mismatch barrier[233]. This particular method induced anergy of peripheral T cells, again suggesting peripheral regulation with Treg and not solely central deletional mechanisms. Others have since shown that costimulatory blockade rather than irradiation or T cell depletion in conjunction with HSC transplantation may successfully induce skin graft tolerance in various mouse models[234-237]. Again, in these models peripheral regulation was a prominent feature of the effect. In larger animal models results have not been as promising. In a miniature swine model of VCA transplantation using HSC transplantation together with a T cell depleting antibody, tolerance could only be achieved to the musculoskeletal element of the VCA, with skin (and in particular, the epidermis) eventually being rejected[163].

Clinically, bone marrow transplantation has been trialled in a few VCA transplantation cases. The first face transplant performed in France used a post-transplant donor-derived bone marrow infusion, although it does not appear that this approach accorded any clear benefit in terms of a reduction in episodes of rejection[238]. Furthermore, microchimerism was only detectable at a single point 2

months post-operatively and not thereafter[238]. Since then, five VCA transplants performed in Pittsburgh have used the 'Pittsburgh Protocol' in which a bone marrow infusion is given within 15 days of VCA transplantation[239]. Early reports indicate that patients treated in this manner have been maintained successfully on single drug immunosuppression with tacrolimus (IHCTAS, Atlanta, 2011)[46].

The presence of vascularised bone marrow in many VCA transplants has raised the possibility that chimerism may develop by nature of the simultaneous transplantation of HSCs within the VCA. To this end, various rat models of hindlimb transplantation using T cell depleting antibody along with immunosuppression have achieved long-term allograft survival[240-245], although mixed chimerism is not always readily detectable[246]. In these models, the bone marrow component of the VCA transplant is critical to the attainment of mixed chimerism and long-term allograft survival[247,248]. Moreover, increased levels of chimerism are detectable with larger sized VCA allografts in rats, indicating the role of the transplant in providing donor cells[249]. In a rat model of facial allograft transplantation, mixed macrochimerism has been observed with the use of only cyclosporine monotherapy[250,251]. Mixed chimerism has also been achieved using non-depleting $CD4^+$ blockade and depleting $CD8^+$ antibody in conjunction with rapamycin and α-CD154 costimulatory blockade, without a bone marrow transplant, relying on bone marrow in a mouse hindlimb VCA to provide donor cells for chimerism[252]. There is also some experimental evidence of 'reverse' chimerism, with donor bone marrow cells replaced with recipient-type bone marrow cells post-transplantation[253], although no evidence for this has been seen clinically[254].

In general, clinical data has not been particularly encouraging with no evidence for the development of chimerism, possibly due to the fact that only small amounts of bone marrow are transferred, and which in the adult may have limited functionality[14,255]. Moreover, there is experimental evidence that the recipient thymus is necessary for peripheral chimerism to develop with a bone marrow-containing VCA transplant[256]. In humans the thymus involutes and becomes atrophic after puberty and is therefore less likely to support the development of chimerism.

It is important to note that in theory chimerism is a double-edged sword, whereby the greater the likelihood of chimerism, the greater the overall antigenic load, and therefore the more pronounced the alloresponse[257]. This in theory would lead to a greater risk of GvHD, which is an unacceptable risk in VCA recipients.

1.6.2 Peripheral regulation: Treg

While the methods described above relate to exploiting the immune system's mechanisms ensuring self-tolerance through central mechanisms, several peripheral regulatory mechanisms also exist to ensure self-tolerance and to prevent an overshoot of the normal immune response. As mentioned, most autoreactive cells are deleted centrally in the thymus. However some autoreactive T cells escape this process and therefore require peripheral regulation to prevent autoimmunity. $CD4^+$ Treg are central to these mechanisms: 'scurfy mice' lacking the Treg-specific transcription factor Forkhead box P3 (FoxP3) develop a lymphoproliferative disorder[258] and humans with mutations in FoxP3 can develop IPEX

(immunodysregulation, polyendocrinopathy and enteropathy, X-linked)[259]. FoxP3 is closely linked to suppressive activity and its sustained expression is required for the maintenance of regulatory activity[260].

Treg can be divided into thymic-derived naturally-occurring $CD4^+CD25^{hi}FoxP3^+$ Treg (nTreg)[261] and induced or adaptive $CD4^+$ Treg (iTreg), which upregulate FoxP3 in the periphery under conditions of antigen-exposure and transforming growth factor β (TGFβ) stimulation[262-264]. nTreg represent 5-10% of the peripheral $CD4^+$ pool and constitutively express high levels of surface CD25 (the α-chain of the IL-2 receptor) although this is not a reliable marker due to its upregulation on activated non-regulatory T cells. It is unclear how much of the peripheral $CD4^+$ population iTreg represent, but given that these cells are induced in specific inflammatory environments it is likely that the percentage is location and time-dependent. Interestingly, although CD25 appears on recently activated $CD4^+$ T cells, some of these are true proliferating Treg. For example, during the secondary antigenic response that develops after human tuberculin purified protein derivative is injected into skin, $CD4^+CD25^+$ cells proliferate within the skin. However, many of these proliferating cells are in fact $FoxP3^+$ and display functional and phenotypic characteristics of Treg[265].

Other described regulatory $CD4^+$ T cells include 'type 1 Treg' (Tr1) cells which employ a FoxP3-independent suppression mechanism mediated via secretion of IL-10 and TGFβ[266]. Tr1 cells can be generated by stimulation with IL-10 or CD46-engagement. These cells induce suppression by bystander regulation of effector T cells

irrespective of the antigen specificity of the target cells[266,267]. Bystander regulation, in which cells are suppressed in a non-specific manner, is also an important mechanism of suppression employed by activated FoxP3$^+$ Treg[264].

In humans, FoxP3 is upregulated on non-suppressive recently activated CD4$^+$ T cells, making it a less useful marker than for mouse Treg[268,269]. Despite this, epigenetic studies have identified differences in the methylation status of the Treg-specific demethylated region (TSDR) site within the FoxP3 locus in different CD4$^+$ T cells. In naïve and activated CD4$^+$ T cells the TSDR is heavily methylated, whereas in iTreg it is partially demethylated and in nTreg is completely demethylated[270,271]. Analysis of Treg based on quantitative methylation of the TSDR site is a useful adjunct to the phenotyping of Treg for clinical use[272].

Differentiation of iTreg and nTreg may also be possible with the use of the transcription factor Helios, a member of the Ikaros transcription factor family. In a study by Thornton and colleagues[273], Helios was found to be expressed on all thymically-derived FoxP3$^+$ cells, but not on iTreg. Interestingly, 70% of peripheral Treg in this study were Helios positive, indicating that up to 30% of Treg in the periphery may be iTreg.

Both nTreg and iTreg require TCR engagement for activation and induction of suppression *in vivo*. Once activated, Treg suppress immune responses at multiple levels by direct inhibition of both CD4$^+$ and CD8$^+$ T cell activation and proliferation as well as through prevention of T cell activation by modulation of APC function[274].

Other described targets of Treg include B cells, NK cells, natural killer T (NKT) cells and mast cells[274-277]. The molecular mechanisms involved in Treg suppressive activity are summarised in ***Figure 1.3***[263,278-291].

Treg suppressive activity may be inhibited by ligation of their surface glucocorticoid-induced TNF receptor (GITR)[292,293]. Another member of the TNF receptor superfamily, OX40 (CD134), which is constitutively expressed on the surface of Treg, appears to have a more complex role. OX40 stimulation has been shown to reduce FoxP3 expression and Treg-mediated anti-tumour suppressive activity *in vivo*[294]. Furthermore, OX40-OX40 ligand interaction between Treg and mast cells is important for suppression of degranulation and allergic responses[295]. However in the additional presence of IL-6, mast cells can force Treg to differentiate into IL-17-producing proinflammatory cells[296]. OX40 is also required for the accumulation of Treg in the colon to prevent T cell-induced colitis and the lack of OX40 co-stimulation after Treg activation may lead to activation-induced cell death (AICD)[297]. An insight into these distinct effects on Treg is gained from a recent study of OX40 in experimental autoimmune encephalomyelitis (EAE), in which the local cytokine milieu at the time of ligation was important: OX40 ligation early in the response (during antigen priming) expanded Treg and reduced the severity of EAE; OX40 ligation later (when effector T cells had already infiltrated the central nervous system) caused an enhancement of effector T cell responses and promoted the development of EAE[298].

Treg may not remain suppressive throughout their lifetime. In a recent study it was demonstrated that some cells that lose FoxP3 (exFoxP3 cells) develop an activated memory-type phenotype and are pathogenic *in vivo*[299]. The loss of FoxP3 appears linked to a proinflammatory microenvironment. Under such conditions Treg can acquire an effector T cell phenotype, secreting IL-17 and interferon γ (IFNγ)[86,300-303], a phenomenon likely related to the ability of inflammatory cytokines such as IL-6 to methylate the FoxP3 TSDR site[271]. This conversion is physiologically relevant and not simply an artefact of *in vitro* conditions, as it occurs in the chronic inflammatory environment of psoriasis in humans[304]. Importantly, Treg may not be particularly effective at suppressing IL-17 producing T cells[86,87,305]. Stability of Treg is important to consider in transplantation as there is evidence that Treg transfer into lymphopaenic mice can result in the loss of FoxP3 expression in up to 50% of the adoptively transferred cells[306]. This is a particularly important point to consider if Treg cellular therapy is to be used in patients who are lymphopaenic post-immunosuppressive induction therapy.

1.6.2.1 Experimental evidence for the use of Treg in transplantation

Studies assessing the potential of nTreg, iTreg and Tr1 cells to promote allograft survival in experimental transplantation have yielded promising results to date. In these studies Treg may be induced *in vivo* by employing lymphocyte depletion around the time of transplantation in conjunction with a donor-specific antigen challenge, such as a donor-specific blood transfusion (DST). Alternatively nTreg may

be expanded *ex vivo* or converted from non-Treg cell types to iTreg. ***Figure 1.4*** illustrates the common methods for experimental generation of Treg[264,266,307-328].

1.6.2.1a Mouse Treg

Treg may be generated *in vivo* or *ex vivo* for later adoptive transfer. *In vivo* approaches are based on increasing the frequency or potency Treg by exposure to antigen, inducing an expansion of nTreg or converting non-regulatory T cells to iTreg[329,330]. Treg may be generated *in vivo* by pre-treating mice with a donor alloantigen (in the form of a DST) along with a non-depleting α-CD4 mAb. Mice treated in this manner develop Treg capable of preventing allograft rejection *in vivo,* including the prevention of skin rejection[263,264,307,308,331-337]. While this tolerance appears to be antigen-specific in nature, another 'boosting' blood transfusion allows tolerance to develop to a third party allograft[264]. The tolerant state that develops is dependent on the generation of $CD4^{+}CD25^{+}$ Treg, which may be further isolated from tolerant animals to prevent allograft rejection in naïve mice by adoptive transfer[282,338]. These Treg are able to prevent skin graft rejection initiated by both $CD4^{+}$[282,339] and $CD8^{+}$[340,341] T cells. Furthermore, Treg produced in this manner have been shown to express increased levels of alpha-1,2-mannosidase, an enzyme involved in the synthesis and processing of N-linked glycoproteins. The resultant altered N-glycosylation of Treg cell surface proteins is necessary for Treg migration to lymph nodes where they may regulate priming[342]. Interestingly, nTreg isolated from naïve animals may even prevent skin rejection, although 10-fold more such Treg are required to attain long-term allograft survival compared to Treg isolated

from tolerant mice[343]. The folate receptor 4 (FR4) allows the identification of these alloantigen-stimulated Treg[344]. Alloantigen-stimulated $FR4^{high}$ Treg are significantly more effective at prolonging mouse skin allograft survival compared to $FR4^{intermediate}$ Treg.

Another method for *in vivo* generation involves injection of IL-2-IL-2 mAb complexes into mice, resulting in an over ten-fold expansion of Treg *in vivo*. Animals treated by this method are resistant to EAE induction and display tolerance to islet allografts[345]. Injection of IL-2-IL-2 mAb complexes together with recombinant granulocyte-colony stimulating factor (G-CSF) induces expansion of Treg and myeloid-derived suppressor cells *in vivo*, promoting mouse skin allograft survival in MHC Class II-mismatched models[346].

Treg may be generated by similar principles *in vitro*, by culturing $CD4^+$ T cells with alloantigen and α-CD4 antibody[347]. These cells, when enriched for the $CD62L^+$ expressing compartment, achieve long-term skin transplant survival in an immunodeficient mouse adoptive transfer model. Mouse Treg may also be expanded *ex vivo* with IL-2 and either αCD3/αCD28 microbeads or DCs for TCR and costimulatory molecule stimulation[318,348,349]. The use of IL-2-IL-2 mAb complexes together with depleting α-CD4 and α-CD8 antibodies and an adoptive transfer of *ex vivo*-expanded mouse Treg (expanded with the use of donor DCs for stimulation) significantly prolongs mouse skin allograft survival but does not maintain robust long-term survival[350].

Treg may also be generated *in vitro* by the conditioning of non-regulatory $CD4^+$ cells with alloantigen in the presence of IFNγ, which helps convert these cells into Treg and induces preferential AICD in the non-Treg population[97,311]. IFNγ-conditioned Treg have been shown to prevent the rejection of skin and islet allografts *in vivo*[311]. Furthermore, these cells can inhibit transplant-associated vasculopathy[351], a phenomenon current immunosuppressive drugs have failed to influence. In the latter study the infiltration of vessel allografts with allogeneic T cells was markedly reduced by regulatory mechanisms that included reduced priming and proliferation of $CD4^+$ effectors. Interestingly, Treg isolated from tolerant animals produce IFNγ transiently after activation, which acts in an autocrine manner to activate the signal transducer and activator of transcription (STAT)-1 intracellular signalling pathway necessary for regulation[352].

The alloreactivity of Treg is important in determining their ability to prevent rejection. Treg that are both directly and indirectly alloreactive display more potent effects than those that are only directly alloreactive[353,354]. In a study by Joffre and colleagues[353], mouse Treg stimulated *in vitro* with alloantigen and specific for directly presented donor antigens could only prevent the acute rejection of skin and cardiac allografts. By contrast, Treg specific for both directly and indirectly presented alloantigens were capable of preventing both acute and chronic rejection. This may be related to the observation that indirect allorecognition outlasts direct allorecognition after the loss of donor-derived passenger APC and is therefore theoretically more active in CAD[355].

1.6.2.1b Human Treg

Human Treg for therapy are generally produced by isolation of cells from peripheral or umbilical cord blood (UCB) and subsequent *ex vivo* expansion or direct use. In order to isolate Treg efficiently and to a high purity, reliable markers of identification are required. Given the non-specificity of CD25 and FoxP3 expression, a number of other markers have been explored. Of these markers, CD127 (the IL-7 receptor α-chain), CD49b (the α-chain of the integrin VLA-4 – a4b1), CD45RA, and latency-associated peptide (LAP) are currently the most useful. Another surface marker, GARP (glutamic acid/alanine rich protein, LRRC32), is linked to the expression of FoxP3 and associated with Treg suppressive activity but its role in efficiently distinguishing Treg requires further investigation[356]. Other Treg markers include CTLA-4, GITR, CD69 and CD44 but these are less useful as they may also be expressed in almost identical patterns on non-regulatory activated T cells.

CD127 is a promising marker to assist in defining Treg populations. In a humanised mouse model of vessel allograft rejection in which allogeneic human leukocytes induce a neointimal expansion similar to that developing with transplant arteriosclerosis (TA), human *ex vivo-expanded* $CD25^{+}CD4^{+}$ or $CD127^{lo}CD25^{+}CD4^{+}$ nTreg were used to modulate immune responses *in vivo* to reduce neointimal expansion. Treg expressing low levels of CD127 were found to be 5 times more potent at this ability, in line with previous studies demonstrating enhanced suppressive qualities of $CD127^{lo}$ Treg[357-359]. The absence of CD49b is another useful marker for Treg identification[360]. The benefit of CD127 and CD49b is that a

population of Treg can be isolated by negative selection alone without the need for CD25.

CD45RA allows cells to be divided into $CD25^{+}CD45RA^{+}FoxP3^{lo}$ (resting naïve Treg), $CD25^{hi}CD45RA^{-}FoxP3^{hi}$ (activated Treg) and $CD25^{+}CD45RA^{-}FoxP3^{lo}$ (non-suppressive T cells) populations[361]. Resting naïve and activated Treg are both suppressive *in vitro*, whilst only resting naïve Treg proliferate *in vivo* and evolve into suppressive $CD45RA^{-}$ Treg. UCB contains a high number of naïve $CD45RA^{+}$ cells, and is therefore an attractive source of resting naïve Treg[362]. However UCB Treg are low in frequency and require either *in vitro* culture or pooling of multiple blood units. Furthermore, UCB Treg are "third-party" (allogeneic to both the donor and recipient) and thus subject to an alloresponse. Theoretically however, given the increase in the frequency of UCB banking in recent years it may one day be possible to infuse autologous UCB Treg into a patient. Treg may be $CD45RA^{+}$ (naïve) or $CD45RO^{+}$ (memory) but very rarely both. Interestingly, there is an increase in $CD45RO^{+}$ Treg with age with a concomitant decrease in $CD45RA^{+}$ Treg. Although $CD45RA^{+}$ Treg have enhanced proliferative abilities, $CD45RO^{+}$ Treg preferentially migrate to skin, by virtue of an increase in their expression of CLA and CC chemokine receptor 4 (CCR4)[363,364]. $CD45RO^{+}$ Treg that express skin homing receptors are therefore theoretically more effective at regulating responses in skin despite $CD45RA^{+}$ Treg displaying enhanced proliferation *in vivo*.

LAP has also recently been shown to define a population of Treg which express high levels of FoxP3, secrete the immunosuppressive cytokine TGFβ, and exhibit

enhanced *in vivo* regulatory activity[365]. LAP itself has also been shown to have regulatory activity independent of TGFβ[366]. Importantly, in Treg expansion cultures, the expression of LAP allows the distinction and selection of activated Treg from activated non-Treg cell types[367].

Ex vivo expansion of isolated Treg is generally performed by stimulation with αCD3/αCD28 microbeads in the presence of recombinant human (rh) IL-2[368,369]. The non-specific TCR stimulation in this system leads to the production of a polyclonally-reactive population of Treg. Nevertheless, both mouse and human donor alloantigen-reactive Treg have been shown to be more potent suppressors *in vitro* and *in vivo,* and their specific reactivity implies that they are safer for *in vivo* use than polyclonally-reactive Treg[339,370]. Current methods for the production of alloantigen-reactive Treg include culture with allogeneic stimulators rather than αCD3/αCD28 microbeads[371,372] or retroviral vector transduction of Treg with genes that encode for TCRs with known antigen specificities[373]. Selection of alloantigen-stimulated Treg from a culture where allogeneic stimulators are used may be possible by enrichment of Treg that co-express the activation markers CD69 and CD71[370].

1.6.2.2 Treg in clinical tolerance

Thus far the focus has been on the role of Treg as a modulating cellular therapy. However, equally important is an appreciation of the role of endogenous Treg in

preventing rejection and maintaining operational tolerance in a select number of clinical cases.

There are multiple reports of clinical operational tolerance, or long-term functioning allograft survival in the absence of any immunosuppression. This has most commonly been observed in liver transplantation[374] but has also been reported in a small number of renal transplant recipients[375]. In these patients there is some evidence that Treg may be involved in maintaining the tolerant state. For example, there is an increase in $FoxP3^+$ Treg in the graft and periphery in tolerant liver transplant recipients[376-379]. Sagoo and colleagues[380] recently analysed the immune profile of tolerant renal transplant recipients. In this study they observed a diminished direct T cell response and donor-specific hyporesponsiveness of $CD4^+$ T cells, suggesting a heightened role for Treg in promoting tolerance, as well as a high ratio of FoxP3 to alpha-1,2-mannosidase gene expression. However, in this study the most striking feature was a bias towards a differential expression of B cell-related genes and an expansion of peripheral blood B cells in tolerant patients. This latter observation raises the interesting possibility that regulatory B cells may be playing a role. In another study, lower numbers and percentages of $CD4^+CD25^+FoxP3^+$ cells were detected in the peripheral blood of patients with chronically rejecting or stable renal allografts compared to those that were operationally tolerant[381].

While there is a trend for an increase in the number of $FoxP3^+$ cells in long-term operationally tolerant patients there is also an increase in patients undergoing acute

rejection. For example, increased *FOXP3* mRNA levels have been detected in rejecting cardiac[382] and renal allografts[383], as well as in the urine of patients with rejecting renal transplants[384]. Higher peripheral FoxP3$^+$ cell numbers also predict a higher risk of development of cutaneous squamous cell carcinoma in renal transplant patients[385]. The increase in FoxP3$^+$ cells in acute rejection may be related to its upregulation on activated effector T cells, or an increase in Treg in response to high donor-activated effector T cell activity.

1.6.2.3 Immunosuppression and Treg

As discussed earlier, Treg adoptive cellular therapy in SOT is likely to be initially introduced in conjunction with conventional immunosuppression. In light of this, it is important to delineate the effects immunosuppression may have on Treg activity and proliferation[386].

Treg and effector T cells preferentially employ different intracellular activation pathways: Treg utilise IL-2-dependent STAT-5[387,388], whereas effector T cells utilise the phosphoinositide 3-kinase/Akt/mTOR pathway[389]. Immunosuppression with rapamycin, an mTOR inhibitor, takes advantage of this distinction. The beneficial effects of rapamycin on Treg survival and proliferation have been demonstrated *in vitro* and *in vivo*[314,325,390-393]. Experimental work in mouse allograft models has shown that rapamycin inhibits chronic cardiac allograft rejection and that this effect is potentiated when used in combination with an α-CCR5 antibody[394]. In this study, an increase in intragraft numbers of CD4$^+$CD25$^+$FoxP3$^+$ Treg was observed. A similar

effect has also been observed clinically, with rapamycin increasing the frequency of $CD62L^{high}$ Treg in the peripheral blood of lung transplant recipients[395]. Experimentally, the adoptive transfer of a small number of alloantigen-specific Treg along with low dose of rapamycin has been shown to induce long-term survival of cardiac allografts in mice[396]. Importantly for VCA transplantation, alloantigen-pulsed rapamycin-conditioned DCs have been shown to promote long-term engraftment of vascularised skin allografts in rats with an associated expansion of $CD4^{+}FoxP3^{+}$ Treg[397]. Likewise low dose tacrolimus has been shown to induce and expand Treg in both the periphery and allograft[398,399].

Rabbit anti-murine thymocyte globulin (mATG), a T cell depleting polyclonal antibody generated in the same manner to thymoglobulin has also shown promise. When combined with CTLA4-Ig and rapamycin, mATG has been shown to shift the effector memory T cell – Treg balance in favour of Treg, allowing prolongation of skin allograft survival in a fully MHC-mismatched mouse model[400].

Interestingly, glucocorticoids have recently been demonstrated to act on human Langerhans cells to promote a phenotype that favours the induction of Treg[401]. In this study, glucocorticoid-treated Langerhans cells promoted the development of Treg in an *in vitro* culture, and had an increased expression of the receptor activator for NF-κB and TGFβ. Moreover, patients treated with glucocorticoids had increased numbers of dermal $FoxP3^{+}CD25^{+}$ Treg as well as increased numbers of epidermal Langerhans cells that displayed upregulated expression of TGFβ mRNA.

Alemtuzumab may also favour Treg survival, with evidence from one study demonstrating a higher proportional depletion of T effector cells than Treg[402]. However, data in this study may be confounded by the introduction of rapamycin in patients early after transplantation. Indeed, in a separate study Treg numbers in alemtuzumab-treated patients remained low until the late introduction of rapamycin[403].

In a study of immunosuppression in renal transplant recipients with both belatacept and basiliximab compared with CNIs, there was no significant difference in circulating Treg numbers[404]. Nevertheless, CNIs such as cyclosporine have a detrimental effect on Treg[405,406], confounding this observation. Interestingly, in this same study patients receiving belatacept displayed higher levels of intragraft $FoxP3^+$ T cells during acute rejection[404]. The effects of α-CD25 mAb on Treg are not entirely clear. In the former study, basiliximab was shown to deplete all CD25-bearing cells, including Treg. However in another study examining daclizumab (a humanised α-CD25 mAb) in cardiac transplant patients, Treg generation in the periphery was not affected[407]. Despite the detrimental effects of CNI inhibition on Treg, in a study examining topical CNI-inhibition for atopic dermatitis using tacrolimus there was a significant reduction in intralesional $CD25^+$ but not $FoxP3^+$ cells[408].

In a recent study investigating a novel CD28 antagonist for use in transplantation, there was an increase in the number and activity of Treg in a non-human primate renal transplantation model[409]. The benefit of this co-stimulatory blockade, unlike CTLA-4-Ig, is that it does not affect physiological CD80/86-CTLA-4 interaction,

therefore allowing normal immune regulation through this important pathway to continue[287].

1.6.2.4 Clinical trials using Treg

At the time of writing there are no ongoing clinical trials testing the efficacy of Treg in VCA or SOT. However, there have been several studies investigating Treg for the treatment of GvHD post-HSC transplantation. It is important to discuss these studies as they are paving the way for Treg therapy in SOT and VCA transplantation. Trzonkowski and colleagues were first to report the use of *ex vivo*-expanded recipient-derived Treg in two patients: in one case of chronic GvHD a significant alleviation of symptoms and a reduction of required immunosuppression was achieved, whereas in one case of severe grade IV acute GvHD only a transient improvement in symptoms and signs was reported[410].

More importantly, two major trials have been carried out at the University of Minnesota and in Italy. In Minnesota, a clinical trial evaluated the safety profile of human UCB-derived partially HLA-matched *ex vivo*-expanded Treg. The study was designed as a Phase I dose-escalation trial and reported a reduced incidence of grades II-IV acute GvHD in the test group of 23 patients compared to 108 identically-treated historical controls not receiving Treg therapy[411]. The Italian study was performed to assess the safety and efficacy of human Treg in prevention of GvHD in 28 patients with high-risk acute leukaemias undergoing HLA-haploidentical HSC and conventional T cell transplants. Treg were derived from the same HLA-haploidentical

donor by apheresis followed by large scale CliniMACS® $CD4^+CD25^+$ magnetic bead selection. GvHD did not develop in 25 out of 29 patients. Furthermore, patients in this trial displayed overall faster post-transplant immune reconstitution as well as a reduction in the risk of CMV reactivation[412].

Other ongoing trials not yet published include one being conducted by Matthias Edinger at the University Hospital in Regensburg using $CD25^{hi}$ magnetically-isolated non-expanded Treg infused into post-HSCT recipients[413] (M. Edinger, *personal communication*). At the time of writing nine patients have been treated with no adverse effects. Trials using Tr1 cells for GvHD are also ongoing at the San Raffaele Hospital in Milan (M.G. Roncarolo, *personal communication*). Early results have been promising with no adverse side effects, although the beneficial effects on GvHD are not yet clear[413,414].

1.6.2.5 Treg in skin and VCA transplantation

As discussed, there is clear evidence for the efficacy of Treg generated *in vitro* or *in vivo* for the prevention of skin rejection in mouse models. In all these models non-vascularised skin was used as the challenge allograft. Treg have not been directly used as a cellular therapy in experimental models of VCA transplantation. Nevertheless, a role for Treg has been demonstrated indirectly in promoting VCA survival in the various rat models where the primary aim was induction of mixed chimerism (*section 1.6.1.1*), or the use of Treg-facilitating immunosuppression such as rapamycin[230,233-237,397]. In all these studies, peripheral regulation was a significant

feature of the effect, demonstrating the importance of Treg even in techniques that rely on central tolerance.

Other experimental studies have also demonstrated an association of Treg with improved VCA survival. For example, in a study which utilised mesenchymal stem cells together with cyclosporine and a bone marrow transplant to achieve long-term engraftment of a hindlimb allograft in a swine model, an increase in the numbers of peripheral blood and intragraft $CD4^+CD25^+$ cells was detected compared to controls[415]. $CD4^+FoxP3^+$ infiltrates have also been detected in higher numbers in the skin of tolerant rat hindlimb transplants where tacrolimus together with lymphodepletion, irradiation and a donor bone marrow transplant were performed[230]. Finally, in a rat model of vascularised skin allograft transplantation where treatment with rapamycin-conditioned DCs promoted long-term allograft survival, there was an increase in $CD4^+FoxP3^+$ Treg numbers in recipients' spleens, graft-draining lymph nodes and the graft itself[397].

Clinically, functional $CD4^+CD25^+FoxP3^+$ cells have been detected in and isolated from the skin of a hand transplant, in a patient who was stably maintained on immunosuppression six years post-transplantation[416]. FoxP3 mRNA levels were significantly higher in the skin of the transplanted hand compared to the contralateral native leg. The significance of these cells in a patient maintained on conventional immunosuppression is unclear.

Given that the need for immunosuppressive drug therapy and the susceptibility of skin to rejection are the major barriers to widespread implementation of VCA transplantation, achieving tolerance to a skin transplant would be an ideal solution. There are no convincing reports of clinical tolerance developing to human skin allografts, with only dated anecdotal reports[417,418]. The only experimental evidence of tolerance to skin allografts derives from the rodent models discussed above. In larger animal models, such as swine, data has been less encouraging and tolerance has generally only been achievable to the non-skin component of a VCA transplant[161,163]. There is therefore a need to determine whether human skin allograft rejection may be prevented using Treg as a cellular therapy. To address this, systems are required in which human skin rejection is modelled and in which cellular therapies such as Treg may be examined. In recent years, humanised mouse models have emerged as useful tools for such studies.

1.7 Humanised mouse models in transplantation research

1.7.1 The need for humanised mouse models

Translation of cellular therapies such as Treg to the clinic requires a system whereby human Treg may be tested on human targets. The necessity for such a system is evident by the difficulty in translating therapies between small and large animals, and even between non-human primates and humans. In some cases, molecules that were proven effective in large animal models have had disastrous effects in humans[419,420].

The immune systems of rodents and humans are dissimilar on multiple levels[199]. Some of the important points to consider are:

- MHC Class II is inducible on the vascular endothelium of rodents, whereas in humans and large animals it is constitutively expressed[421,422]. Similarly, human T cells express MHC Class II and may present antigens, whereas mouse T cells do not[423-425].
- ECs may activate human $CD4^+$ resting memory cells, whereas mouse $CD4^+$ cells cannot be similarly activated[172,200].
- Mice lack the LFA-3 gene. LFA-3 is an important molecule expressed by ECs that provides a costimulatory signal to T cells through CD2[426].
- Only human ECs express the T cell costimulatory molecule CD40[176,427].
- Resident T cells in the skin and mucosa of mice largely express the γ/δ TCR whereas in humans the majority of resident T cells express the α/β TCR[199,428].
- Human skin Langerhans cells express the CD1 isoform CD1a, which may present various self- and microbial lipid antigens to T cells[429-431]. Mice have deleted the *CD1A* gene and therefore mouse Langerhans cells do not express CD1a[432,433].
- The mouse is a poor model for human T cell homing as mice lack IL-8, the predominant neutrophil chemokine in humans. Furthermore, P-selectin is constitutively expressed on human ECs, whereas it is only inducible in the mouse[172].
- Humans are exposed to a variety of antigenic stimuli and therefore form a significant pool of memory T cells which may react with the allograft through

heterologous immunity[146]. Mice kept in individually ventilated cages in specific pathogen-free conditions will lack a similar pool of memory T cells.

- Importantly for skin transplantation, various structural differences exist between mouse and human skin:
    - Mouse skin contains a higher density of hair follicles than human skin. As skin adnexae are a known target of allogeneic leukocytes during skin rejection this is a particularly important point[434]. Furthermore, the hair cycle in mice is approximately 3 weeks whereas in humans it is highly variable and region-dependent[435].
    - Human skin is thicker than mouse skin and may therefore present a greater antigen load during transplantation.
    - The majority of mouse epithelium does not contain rete ridges, whereas in human skin rete ridges are present[436].
    - Mouse skin is generally compliant and loose, as well as being mobile due to the presence of the panniculus carnosus. In humans, skin is relatively stiffer and generally adherent to underlying tissues with no similar underlying subcutaneous muscle layer apart from platysma in the neck[437].
    - The major method of wound healing in mice is via contraction, whereas in humans it is through granulation tissue formation and re-epithelialisation[437].

Whether these differences are responsible for the failure to translate many tolerance-inducing therapies from mouse to larger animal models is not clear. What

is clear is that models are required that emulate the human response to a human allograft.

1.7.2 Humanised mouse models

Various mouse models have developed over the past two decades which incorporate elements of a human immune system in order to study transplant immunology, infection, tumour immunology and autoimmune diseases[438]. These models have utilised human foetal liver or thymus, or human $CD34^+$ HSCs or peripheral blood mononuclear cells (PBMC), to engraft functional human leukocytes within immunodeficient mice, creating mouse-human chimeras, or humanised mice.

A key requirement for these mice is for them to lack an adaptive immune response with reduced innate immunity and defective NK responses, in order to allow engraftment of human leukocytes. The first humanised mice harboured only mutations that caused defective T and B cell development, such as the severe combined immunodeficiency (SCID) mutation[439]. However, spontaneous rearrangement of T and B cell receptors ('leakiness') in these mice meant that they would eventually produce functional mouse lymphocytes capable of mounting a response against human leukocytes.

Subsequently, mice lacking the recombination-activating gene-1 (Rag1) and Rag2 were developed[440,441]. The Rag genes encode enzymes necessary for the rearrangement and recombination of TCRs and immunoglobulin receptors during

somatic recombination. These mice are not 'leaky' and therefore have a more sustained and profound lack of mouse lymphocytes. However, the presence of mouse NK cells in these models remained a barrier to successful and lasting human leukocyte engraftment. For this reason, non-obese diabetic (NOD) mice[442] and mice lacking the common cytokine-receptor γ-chain locus (cγ or IL-2-R-γ-chain)[443-445] were crossed with mice that had defective lymphocyte development. These crosses produced the current common immunodeficient mouse strains in use, which include the BALB/c-Rag2$^{-/-}$cγ$^{-/-}$ mouse (homozygous deficiencies of both Rag-2 and cγ on a BALB/c (H2^{d}) background), the NOD-SCID mouse, and the NOD-SCID-cγ$^{-/-}$ (NSG) mouse (***Figure 1.5a***)**.** Lack of the cγ chain results in defective signaling in IL-2, IL-4, IL-7, IL-9, and IL-15 and hence severe innate and adaptive immune deficiencies. Another mouse in use is the SCID-bg mouse which together with the SCID mutation harbours a homozygous beige/beige mutation leading to severe impairment of NK cell activity[446].

Each of these mice has a specific phenotype, with the NSG and BALB/c-Rag2$^{-/-}$cγ$^{-/-}$ mice exhibiting the most profound immunodeficiencies (***Figure 1.5b***). These two mouse strains are the most advantageous as they require the least amount of human tissue or leukocytes for successful human leukocyte engraftment and subsequent chimerism[438].

Models of human allograft rejection using humanised mice include human skin, vessel and islet rejection models. Vessel and islet models have used robust outcome measures to determine the degree of rejection of the allograft. Humanised mouse

models of vessel rejection have used the development of luminal narrowing within the vessel allograft as a simulation of TA development[447-450]. Humanised mouse models of islet rejection have used blood glucose monitoring in mice where native islets have been destroyed chemically to evaluate engraftment of human islets[451-454].

In contrast, humanised mouse models of human skin allograft rejection have relied on the histological appearance and degree of infiltration with human leukocytes of skin to quantify the degree of rejection and the benefit of any therapy[447,455]. For example, in a humanised NOD-SCID mouse model of human skin allograft rejection, human myeloid DCs transduced with an adenoviral vector to express human IL-10 were effective at reducing the skin mononuclear cell infiltrate and dermo-epidermal junctional damage, compared with DCs transduced with a control vector[456]. In another humanised NOD-SCID mouse model using human foetal skin transplants, a humanised α-CD2 antibody was shown to reduce the infiltration of skin grafts with human T cells and the microvascular injury occurring within the graft through an NK cell dependent ADCC-mediated mechanism[457]. In another model using SCID-bg mice engrafted with cadaveric human skin, FK734, a humanised mouse α-human CD28 antibody, reduced EC destruction and T cell infiltration of human skin allografts[458]. At the time of writing, a recently published study has examined the efficacy of human Treg therapy in a humanised mouse model. In this study, NSG or BALB/c-Rag2$^{-/-}$cγ$^{-/-}$ mice were engrafted with only human CD4^{+} cells and the degree of rejection determined by quantifying the amount of cell death and microvascular destruction histologically[370].

However none of the models in the above mentioned studies have achieved complete macroscopic human skin destruction. Models using human neonatal foreskin as a challenge allograft have been marred by the replacement of human vessels by mouse vessels, even in the absence of an alloresponse, removing a large target of the response against the allograft[447]. Studies using foetal skin are weakened due to the lack of expression of human HLA Class II on skin ECs and keratinocytes[459]. The use of cadaveric skin in the majority of studies is also less than ideal as the overall time of ischaemia of these grafts is substantially increased. Many models have necessitated the injection of massive amounts of human cells to produce measurable levels of chimerism, an impractical requirement when attempting to control assays using one human leukocyte donor per set of experimental groups. Moreover, some studies reconstituted mice with only particular T cell populations and are therefore not representative of the full adaptive immune response towards a skin transplant[370]. None of these studies have examined the role of human immunoglobulin in the alloresponse against the skin allograft. Finally, models utilising NSG mice have necessitated depletion of GR-1^{+} cells from the host mice as these innate mouse cells caused significant damage to the human skin graft[455].

1.8 Conclusion

The need for VCA recipients to be on life-long toxic immunosuppression is a major challenge. Reducing the risk of skin rejection in VCA transplantation would tip the risk-benefit balance of the technique to allow it to become considered in a wider variety of clinical cases. In addition, given that the functional and cosmetic results are superior, therapies that induce tolerance to a VCA would make the technique accessible to the majority of reconstructive cases where free flap surgery would normally be considered. The number of patients requiring tissue reconstruction far outstrips those requiring a SOT. If a tolerance induction technique were successfully developed, VCA transplantation would be revolutionised becoming a much larger field than SOT is today. Even if complete tolerance is not achieved, any therapy that significantly reduces the need for immunosuppression without reducing graft survival or function is worth pursuing and will have a major impact on patient morbidity and mortality.

The experimental techniques that have achieved tolerance to skin in rodents have been unsuccessful in large animal models. This is particularly true for techniques employing mixed chimerism and is likely to be due to major differences in the immunobiology of rodents and large animals. On the other hand, cellular therapy with Treg is proving to be efficacious in various models of transplantation, including murine models of skin rejection and clinical studies of bone marrow transplantation. However, because of the challenges in translation of cellular therapies from mouse to human it is not clear whether human Treg will also be active in the prevention of human skin rejection. This is a particular problem when assessing cellular therapies,

which are by nature species-specific. The cells developed for use in the rodent are significantly different in both function and phenotype to those used in the human, notwithstanding the methods for production, which also differ (*section 1.6.2.1*).

There is therefore a need to develop an experimental model where human Treg may be assessed in the context of a human skin transplant without incurring direct patient risk. A system whereby human skin rejection is modelled would also allow a thorough examination of the characteristics of the immune response towards human skin, which to this point have only been examined sporadically and opportunistically in the few clinical cases of VCA that have been performed.

1.9 Thesis aims and objectives

The aims of this thesis are:

- To develop a robust humanised mouse model of human skin rejection through which human skin rejection may be examined and characterised (***Chapters 3 and 4***), and;
- To develop a translational therapeutic strategy based on Treg cellular therapy to prevent human skin rejection (***Chapter 5***).

1.10 Figures and legends

Figure 1.1 Allorecognition and initiation of the adaptive immune response.

Direct allorecognition is the recognition of intact MHC molecules on donor-derived passenger leukocytes by host TCRs. Indirect recognition occurs when host TCRs recognise donor MHC molecules that have been processed and presented as peptides on self-MHC. In semi-direct allorecognition, intact donor MHC molecules are transferred either by direct cell-to-cell contact or via membrane fusion to recipient APCs. These intact MHC molecules are then recognised by recipient TCRs. Cells activated by the different allorecognition pathways may interact to activate each other. Both indirect and semi-direct allorecognition may theoretically occur on a single APC.

The effector response develops after allorecognition and T cell activation in the presence of cytokines secreted by professional APCs, T cells or in some cases parenchymal cells. $CD4^+$ T cells recognising MHC class II will be activated and polarised to a Th1, Th2 or Th17 response depending on the local cytokine environment. $CD8^+$ T cells recognising MHC Class I molecules receive help from activated $CD4^+$ T cells and in turn produce IFNγ. Both activated Th1 and activated $CD8^+$ T cells have the potential to be cytotoxic. $CD8^+$ T cells preferentially use the perforin/granzyme pathway whereas $CD4^+$ T cells use the Fas/FasL pathway. Th1 cells also produce IFNγ and promote a DTH response that drives the production of toxic molecules such as nitric oxide, TNFα and ROS from macrophages. Th2 cells interact with alloreactive B cells to produce alloantibodies that may subsequently activate complement or promote antibody-dependent cell-mediated cytotoxicity. Th17 cells cause damage through the production of various cytokines, but mainly IL-17 which acts to recruit neutrophils to the site of allograft rejection.

Figure 1.2 Molecular targets of immunosuppressant drugs.

The major immunosuppressants in current clinical use are shown along with their molecular targets. Apart from rituximab and alemtuzumab, the immunosuppressants illustrated target T cells. Rituximab targets B cells and alemtuzumab targets most nucleated bone marrow-derived cells.

PI3K: phosphoinositide 3-kinase; PkCθ: protein kinase-Cθ.

Figure 1.3 Molecular mechanisms of action of Treg.

Treg employ a multitude of redundant and non-redundant mechanisms to suppress immune responses[278].

1) Treg can cause direct cytolysis of target cells through perforin-dependent and –independent granzyme B mechanisms[279,280].

2) Galectin-1 expressed on the surface of Treg binds target cells to induce cell cycle arrest and apoptosis[281].

3) Suppressive secreted cytokines such as IL-10, transforming growth factor β (TGFβ) and IL-35 induce bystander regulation of T cells[263,282-284].

4) Treg inhibit the induction of IL-2 mRNA in target T cells[285].

5) Surface CD25 on Treg consumes IL-2 in the surrounding environment, depriving cells of this growth factor[286].

6) CTLA-4 interacts with CD80/CD86 on the surface of APCs to prevent their binding to CD28, therefore indirectly inhibiting the activation of T cells[263,287].

7) The interaction of CTLA-4 and CD80/86 induces the expression of indoleamine 2,3-dioxygenase (IDO) from DCs, which inhibits T cell activation by depleting tryptophan from the extracellular milieu[288].

8) Lymphocyte-activation gene 3 (Lag, CD223) on the surface of Treg binds MHC Class II to inhibit DC maturation[289].

9) Fibrinogen-like protein 2 (FGL2) on the surface of Treg binds FcγRIIB on the surface of DC to prevent their maturation[290].

10) CD39 on the surface of Treg hydrolyses adenosine triphosphate (ATP) to adenosine monophosphate (AMP), reducing the availability of ATP-triggered proinflammatory signals[291].

Figure 1.4 Common methods for experimental generation or expansion of Treg.

In mice, **(a)** Treg may be generated *in vivo* by administration of an alloantigen challenge, for example in the form of a DST under the cover of α-CD4 antibody[264,307,308]. **(b)** Treg may also be generated *in vivo* by administration of IL-2/IL-2 complexes[309]. **(c)** $CD4^+CD25^-$ mouse cells may be converted into functional $FoxP3^+$ Treg by culturing *in vitro* using an IFNγ-conditioning protocol[310,311].

In humans, **(d)** nTreg may expanded *in vitro* to produce large numbers of Treg[312,313]. **(e)** Administration of rapamycin to patients has been shown to expand numbers of $FoxP3^+$ Treg *in vivo*[314].

In both mice and humans, **(f)** activation of $CD4^+$ cells with αCD3/αCD28 microbeads or antibody, or activation with DCs, may convert non-regulatory cell types to $FoxP3^+$ cells, a process that is more efficient and reliable if performed in the presence of TGFβ with or without retinoic acid (RA) (mouse[315-318]; human[319-321]). **(g)** Non-regulatory cell types may be transduced to express FoxP3 using retroviruses or lentiviruses, producing functional Treg (which are more stable in humans if produced by lentiviral transduction)[322-324]. **(h)** Rapamycin selectively expands and converts activated non-regulatory $CD4^+$ T cells *in vitro*, also inhibiting the proliferation of effector T cells[314,325]. **(i)** Culture of $CD4^+CD25^-$ cells in the presence of a phosphodiesterase 3b (PDE3b) inhibitor and APCs produces functional Treg which prevent allograft rejection *in vivo*[326]. In both mouse and humans, two regulatory cell types have also been described which do not express FoxP3 and exert their regulatory activity via the production of suppressive cytokines. **(j)** The iT_R35 cells are induced from $CD4^+$ T cells in the presence of IL-35 or DCs activated by human rhinoviruses (R-DC)[327,328]. **(k)** Tr1 cells are produced from cells conditioned by exogeneous IL-10 or IL-10 producing DCs (DC-10)[266].

Figure 1.5 Common immunodeficient mouse strains in use in humanised models.

Common immunodeficient mouse strains include the BALB/c-Rag2$^{-/-}$cγ$^{-/-}$ mouse, the NOD-SCID mouse, the NOD-SCID-cγ$^{-/-}$ (NSG) mouse and the SCID/beige mouse**.** The NOD-Rag1/2$^{-/-}$ is not in common use. The original mutations and crosses used to create the first three of these strains are shown in **(a)**. The immunophenotype of each of these mouse stains is detailed in **(b)**[438]**.**

CHAPTER 2: MATERIALS AND METHODS

2.1 Animals

BALB/c-Rag2$^{-/-}$cγ$^{-/-}$ (C.Cg-Rag2^{tm1Fwa} Il2rg^{tm1Sug}/Jic, H2^{d}) and NOD-SCID-cγ$^{-/-}$ (NSG, NOD.Cg-*Prkdc*^{scid} *Il2rg*^{tm1Wjl}/SzJ, H2^{g7}) mice were obtained from Charles River Laboratories and The Jackson Laboratory and housed under specific pathogen-free conditions in the Biomedical Services Unit of the John Radcliffe Hospital (Oxford, UK). Mice were housed in individually ventilated cages and handled with gloves. All experiments were performed using protocols approved by the Committee on Animal Care and Ethical Review at the University of Oxford and in accordance with the UK Animals (Scientific Procedures) Act 1986, under project license PPL 30/2550 and personal license 30/8305. Mice between the ages of 6 and 12 weeks at the time of the first experimental procedure were used.

The late development of human anti-mouse responses manifesting as xenograft-versus-host disease (XvHD) has long been recognised in human PBMC engrafted immunodeficient mice[460]. We have observed this phenomenon in our PBMC engrafted BALB/c-Rag2$^{-/-}$cγ$^{-/-}$ mice, however without exception this occurs at a point after skin graft rejection if mice receive the inoculation of PBMC between 3 days and 5 weeks after skin grafting. Importantly, in an assay where BALB/c-Rag2$^{-/-}$cγ$^{-/-}$ mice (n=3) received an intraperitoneal injection of 5x10^{6} PBMC followed four weeks later by a human skin allograft, signs of XvHD developed before any macroscopic signs of human skin graft rejection. This precluded the use of such a strategy in this model,

although it may be possible to reduce the time between the initial injection of PBMC and human skin grafting in an effort to avoid early XvHD development. This would require further investigation. Importantly, mice treated with Treg therapy in our study displayed a lower incidence of XvHD, in line with many experimental and clinical studies[410,461]. Any mice developing signs of XvHD or weight loss of >20% from starting weight were euthanised according to local animal welfare regulations.

2.2 Animal Procedures

2.2.1 Pre- and post-operative care

Stock concentrations of medetomidine hydrochloride (Domitor®, Pfizer Pharmaceutical Ltd.) were diluted with normal saline to provide a working concentration of 100μg/ml. This solution was then mixed with a 7.6μg/ml solution of ketamine hydrochloride (Ketaset®, Fort Dodge Animal Health Ltd.). Recipient mice received a subcutaneous injection of 200μl of this solution along with 200μl of 10μg/ml buprenorphine hydrochloride (Vetergesic®, Reckitt Benckiser Healthcare Ltd.) to provide general anaesthesia during surgical procedures. For terminal anaesthesia, mice received 500μl of Domitor/Ketaset solution. Postoperatively, mice received 200μl of 100μg/ml atipamezol hydrochloride (Antisedan®, Pfizer Pharmaceutical Ltd.) as anaesthetic reversal. Mice were then placed in a warm recovery cabinet for 2 hours.

2.2.2 Procurement of human skin

Split-thickness human skin at between 8-10/1000 inches thick was harvested with the use of an air-driven dermatome from the lateral thigh of live donors undergoing plastic surgery procedures in the Department of Plastic and Reconstructive Surgery of the John Radcliffe Hospital. Only skin that appeared macroscopically normal was used in the study. Donors on immunosuppressive medication or with a primary inflammatory skin condition were excluded. Donor age ranged from 31 to 98 years (mean 67.25, median 69.5). Skin was procured with the assistance of Mr Tim Goodacre, Plastic Surgery Consultant and other members of the Plastic Surgery team. Tissue was stored in Roswell Park Memorial Institute (RPMI)-1640 medium (PAA Laboratories, UK) on ice and transplanted within 12 hours of procurement. Unused skin was destroyed. Tissue was obtained with full patient consent and ethical approval from the Oxfordshire Research Ethics Committee, study number 07/H0605/130. Blood samples were obtained with consent from skin donors for HLA-typing and autologous leukocyte isolation.

2.2.3 Skin grafting

Skin grafting procedures were performed with full sterile precautions. Mice were placed prone and a 1x1cm piece of skin removed from the left dorsal thorax over the costal margin. A 1x1cm piece of human skin was then fashioned and its edges sutured to the mouse recipient skin with a non-absorbable 8-0 PROLENE* suture (Ethicon, UK). Grafts were fenestrated and covered with a povidone-iodine mesh and pressure dressing which was secured with circumferential tape. Bandages were

left in place for 7-10 days then removed under general anaesthetic. Skin grafts were monitored every 1-2 day until complete loss.

2.2.4 Adoptive transfer of human cells

Cells were suspended in RPMI-1640 medium or human serum and injected intraperitoneally (500µl suspension) or intravenously via the lateral tail veins (200µl suspension). When no adoptive transfer of human cells was performed as a control, RPMI-1640 medium was injected alone. Mice receiving PBMC that did not achieve levels of human leukocyte chimerism of >1% in the spleen or >0.1% in the peripheral blood at the time of sacrifice were excluded from survival analyses. Adoptive transfer of mouse splenocytes was performed similarly, with cells suspended in RPMI-1640 medium.

2.2.5 HSC transplantation

Neonatal BALB/c-Rag2$^{-/-}$c$\gamma^{-/-}$ mice received 2 doses of 2 Gy total body irradiation 4 hours apart within 24 hours of birth. Irradiation was carried out using a chambered carousel. 4-6 hours later, mice were placed on ice for anaesthesia before receiving thawed preparations of 5x10^6 7AAD$^-$CD45$^-$CD34$^+$Lin$^-$-enriched cells suspended in 50µl of RPMI-1640 medium and delivered intrahepatically using a BD Microfine 30G syringe (BD, UK).

2.2.6 Procurement of tissue from experimental mice

Mice were sacrificed at the stated time points. Animals received terminal doses of anaesthetic for tissue procurement. Skin was excised and divided into two pieces for future histological and mRNA analyses. For histological analysis, skin was placed in OCT-compound (Raymond Lamb, UK) and snap-frozen in liquid nitrogen. For molecular biology techniques a section of skin was placed into a screw-cap microcentrifuge container and snap-frozen in liquid nitrogen. Specimens were transferred to a -80°C freezer for long-term storage before analysis. A midline abdominal incision was then performed and a 26-gauge needle used for inferior vena caval puncture with up to 1ml of blood harvested. Serum was obtained after centrifugation and stored at -80°C. The remaining cell pellet was used for immediate flow cytometry analysis. After blood was obtained a splenectomy and lymph node harvest was performed. For monitoring of peripheral blood over time, serial tail bleeds were performed. Total blood volume obtained did not exceed 10% of the total blood volume on any one occasion or 15% over 28 days.

2.2.7 Mouse GR-1^{+} cellular depletion

For depletion of mouse GR-1^{+} cells, BALB/c-Rag2$^{-/-}$c$\gamma^{-/-}$ mice were injected intraperitoneally with 200µg α-mouse GR-1^{+} mAb (RB6.8C5 hybridoma, a kind gift from Professor Robert Fairchild) every 3-4 days. Depletion was confirmed by FACS and histological analysis.

2.3 Tissue typing

5ml of whole blood was obtained from skin donors and stored from each buffy coat or UCB unit for later analysis. These samples were analysed by the Oxford Transplant Centre Histocompatibility and Genetics Laboratory. A full tissue typing was performed for HLA-A, -B, -Cw, -DR and –DQ. When necessary DNA was extracted from samples using a QIAamp DNA Blood Midi Kit according to manufacturer's protocols (Qiagen, UK).

2.4 Cellular isolation for *in vivo* injection

All cellular isolation techniques were performed with aseptic precautions in a laminar flow cabinet.

2.4.1 Adult PBMC isolation

Fresh adult buffy coats were obtained from the National Blood Bank (UK) and PBMC isolated using a standard Ficoll separation technique. Whole blood was carefully layered above Ficoll solution and then centrifuged for 20 minutes at 2000RPM at 20°C. Isolated PBMC were pelleted and red cells lysed with PharmLyse™ buffer (BD Pharmigen, UK). PBMC were then washed, filtered and enumerated, then frozen for later use or resuspended in RPMI-1640 medium for injection into mice. PBMC were obtained from random donors and the data pooled. For autologous PBMC isolation, Ficoll separation was performed on blood obtained from the respective skin donor.

2.4.2 UCB MNC isolation

Fresh UCB units were provided by the Oxford NHS Blood and Transplant Centre (John Radcliffe Hospital, Oxford, UK) within 12 hours of procurement. MNCs were isolated from UCB units in an identical manner to PBMC from buffy coats. Ethical approval for research using UCB was obtained from the Oxfordshire Research Ethics Committee, study number 07/H0605/130.

2.4.3 Cellular isolation with magnetic beads

For isolation of human HSCs, $CD34^+$ cells were positively selected from UCB-derived MNCs using a human $CD34^+$ MACS® kit (Miltenyi, UK) according to manufacturer's guidelines. Post-isolation cells were assessed for purity of $7AAD^-CD34^+Lin^-$ by flow cytometry (*section 2.5*). Ethical approval for research using HSCs was obtained from the Oxfordshire Research Ethics Committee, study number 07/H0605/130.

For $CD4^+$ cellular depletion from PBMC, $CD4^+$ cells were positively selected using a human $CD4^+$ MACS® kit (Miltenyi, UK) according to manufacturer's guidelines and the $CD4^-$ flow-through collected for use. Purity of depletion was assessed by flow cytometry.

2.4.4 Mouse splenocyte isolation

Mouse splenocytes used for *in vivo* injection were isolated from fresh spleens. Cells were obtained by morsalisation through a 70μm cell strainer followed by washing,

red blood cell lysis and filtration. Cells were then enumerated and resuspended in RPMI-1640 medium for injection within 4 hours of splenic harvest.

2.5 Fluorescence-activated cell sorting (FACS) and flow cytometry

Cells from human peripheral blood were obtained by Ficoll separation (see *section 2.4*) followed red blood cell lysis using PharmLyse (BD Pharmigen, UK) and filtration. Cells from mouse peripheral blood were obtained by red blood cell lysis followed by filtration. Cells from mouse spleens and lymph nodes were obtained by morsalisation through a 70μm cell strainer followed by washing, red blood cell lysis and filtration. Fluorochrome coupled mAbs were then incubated with processed and enumerated cells for 30-45 minutes at 4°C in the dark. Fluorochrome-coupled antibodies specific for 7-AAD (eBioscience), CD45 (BD), CD3 (eBioscience), CD4 (Beckman Coulter), CD8 (BD), CD19 (BD), CD25 (BD), CD127 (BD), FoxP3 (eBioscience), CD27 (BD), CCR4 (BD), CCR7 (BD), CD62L (Invitrogen), CD34 (BD), HLA-DR (BD), HLA-A11 (Abcam), HLA-B8 (Abcam), and lineage cocktail 1 (Lin, BD) were used to phenotypically profile cells. Flow cytometric data were acquired using a FACSAria or BD Canto II (BD Biosciences, UK) and analysed using FACSDiva software (BD Biosciences, UK). Mice were considered adequately reconstituted if the percentage of live human leukocytes (human $7AAD^{-}CD45^{+}$ cells) as a proportion of total live mononuclear cells was >1% in the spleen or >0.1% in the peripheral blood. Mononuclear cells were gated on a standard FSC/SSC flow cytometry dotplot. This percentage is termed the human leukocyte chimerism level (i.e. human macrochimerism level). Data from our laboratory using the humanised mouse vessel

transplant system have demonstrated that a level of human leukocyte chimerism of >1% in the spleen is sufficient to induce intimal proliferation in transplanted allogeneic human vessels. A phenotypic FACS analysis was also performed on PBMC isolated from buffy coats and *ex vivo*-expanded Treg prior to injection into mice. The following table details the antibodies used and their originating clones.

Specificity	Reactivity	Conjugation	Clone	Species of origin	Isotype
7-AAD	N/A	PerCP	N/A	N/A	N/A
B220	Mouse	PE	RA3-6B2	Rat	IgG_{2a} κ
CD3	Human	eFluor® 450	OKT3	Mouse	IgG_{2a} κ
CD4	Human	PE/Texas Red®	L3T4	Mouse	IgG_{2a} κ
CD8	Human	PE	HIT8a	Mouse	IgG_1 κ
CD8	Human	APC-Cy7	SK1	Mouse	IgG_1 κ
CD19	Human	APC-Cy7	SJ25C1	Mouse	IgG_1 κ
CD25	Human	PE	M-A251	Mouse	IgG_1 κ
CD25	Human	FITC	M-A251	Mouse	IgG_1 κ
CD34	Human	PE	563	Mouse	IgG_1 κ
CD45	Human	APC	HI30	Mouse	IgG_1 κ
CD127	Human	PE	hIL-7R-M21	Mouse	IgG_1 κ
CCR4	Human	PE-Cy7	1G1	Mouse	IgG_1 κ
CCR7	Human	PE	150503	Mouse	IgG_{2a} κ
FoxP3	Human	FITC	236A/E7	Mouse	IgG_1 κ
FoxP3	Human	PE	236A/E7	Mouse	IgG_1 κ
HLA-DR	Human	PE-Cy7	L243 (G46-6)	Mouse	IgG_{2a} κ
HLA-B8	Human	Biotin	8.L.215	Mouse	IgG_{2b} κ
HLA-A11	Human	Biotin	8.L.170	Mouse	IgM κ
IgG-Fc	Human	PE	G18-145	Mouse	IgG_1 κ
Lineage cocktail 1 (CD3, CD14, CD16, CD19, CD20, CD56)	Human	FITC	NCAM16.2, MϕP9, L27, SJ25C1, 3G8, SK7	Mouse	IgG_{2b} κ, IgG_1 κ
TCRβ	Mouse	APC	H57-597	Hamster	IgG κ

2.6 Treg isolation and expansion

Treg isolation and expansion was performed in collaboration with Dr Joanna Hester according to established protocols[312,448]. PBMC were isolated from buffy coats

obtained from healthy blood donors (National Blood Service, UK) by Ficoll separation (see *section 2.4.1*). $CD4^+$ cells were then enriched from PBMC using a $CD4^+$ T cell isolation kit II (Miltenyi Biotech, UK). $CD127^{lo}CD25^+CD4^+$ cells were sorted using a BD FACSAria cell sorter (BD Biosciences, UK), using CD127 PE, CD25 APC and CD4 PerCP antibodies (see *section 2.5*). Cells were sorted to over 94% purity and subsequently expanded *in vitro* with 1000U/ml of rhIL-2 (Chiron, UK) and αCD3/αCD28 microbeads (Invitrogen, UK) in a 1:2 cell to bead ratio over two 7-day rounds of expansion, followed by 2 days of silencing in a reduced amount of IL-2 (200U/ml) with no αCD3/αCD28 microbeads. Cells were cultured in RPMI-1640 medium supplemented with L-glutamine, penicillin-streptomycin (both PAA Laboratories, UK), sodium pyruvate (Gibco, UK) and 10% human AB pooled serum (National Blood Service, UK). After expansion, *in vitro* suppressive capacity and expression of Treg phenotypic markers were assessed before *in vivo* use. Expanded cells were cryopreserved for later use.

2.7 Carboxyfluorescein Succinimidyl Ester (CFSE) labelling

CFSE is membrane-permeable and binds to cytoplasmic amino acids, where it becomes cleaved and membrane impermeable. With each cell division, the amount of fluorescence emitted by CFSE is halved. Cells were labelled with CFSE using a Cell Trace CFSE Proliferation Kit (Invitrogen, UK). $1x10^6$ cells were suspended in 1ml pre-warmed phosphate-buffered saline (PBS). CFSE was diluted in pre-warmed PBS to a working concentration of 2μM. 100μl of the 2μM CFSE solution was then added to

the 1ml of cells and incubated at 37°C for 15 minutes. Labelling was confirmed by flow cytometry.

2.8 *In vitro* suppression tests

In vitro suppression assays were performed in collaboration with Dr Joanna Hester. Treg *in vitro* suppressive activity was assessed by measuring inhibition of proliferation of autologous PBMC stimulated with alloantigen or polyclonally stimulated with αCD3/αCD28 microbeads. In the allostimulation assay, PBMC ($1x10^5$) were incubated with irradiated allogeneic PBMC ($1x10^5$) and varying numbers of Treg. In the polyclonal stimulation assay, PBMC ($2x10^4$) were incubated with αCD3/αCD28 microbeads ($2x10^3$) and varying numbers of Treg. Incubations were performed at 37°C and 5% CO_2. In both assays, proliferation was measured after 7 days by addition of ^{3}H-thymidine (0.5Ci per well, Perkin Elmer) for the last 16 hours of culture. 18-24 hours later, plates were harvested with a Skatron cell harvester onto labelled filter paper. Filter paper was allowed to dry before being placed into a laminated cover and ^{3}H-thymidine incorporation into proliferating cells determined with a β-scintillation counter (BD). For assays using CFSE labelled cells, PBMC were labelled using a Cell Trace CFSE Proliferation Kit as above (Invitrogen, UK) and labelling confirmed by flow cytometry.

2.9 Histology and immunohistochemistry

Snap frozen skin samples were cross-sectioned using a Bright*® 5040 cryostat at a thickness of 6µm for Haematoxylin & Eosin (H&E) staining and 10µm for

immunohistochemistry. Sections were air-dried at room temperature for 1-2 hours and then stored at -80° C for later analysis.

2.9.1 Haematoxylin and Eosin (H&E) staining

Frozen sections were defrosted at room temperature for 20 minutes, fixed and subsequently stained with Haematoxylin (20 seconds) and Eosin (10 seconds) (Raymond Lamb, UK).

2.9.2 Immunohistochemistry

Frozen sections were defrosted at room temperature then fixed in ice-cold acetone for 15 minutes and allowed to dry. Sections were then rehydrated in PBS before incubation with 0.1% hydrogen peroxide in PBS for 5 minutes to neutralise endogenous peroxidase. After washing in PBS, sections were incubated with 10% mouse serum in PBS for 30 minutes at room temperature (RT) to block non-specific binding sites. Samples were once again washed in PBS then incubated with biotinylated antibodies (anti-mouse: Ly-6G, CD31; anti-human: HLA-B8, CD3, CD4, CD8, CD45, CD31) or unconjugated antibodies (anti-human CD3, CD4, CD8, CD45, BD Biosciences, Oxford, UK) diluted in DAKO® antibody diluent (DAKO Cytomation) at RT- for 1 hour. After three further PBS washes, samples stained with biotinylated primary antibodies were incubated with a VECTASTAIN® Elite ABC Kit (Vector® Laboratories). Sections stained with unconjugated primary antibodies were incubated with polyclonal rabbit α-mouse immunoglobulins/HRP (DAKO® Cytomation) for 45 minutes at RT. All sections were then washed and incubated

with dimethylaminoazobenzene (DAB, Sigma®, St. Louis, Missouri), then counterstained with haematoxylin for 20 seconds. Samples were air-dried for 1 hour before mounting in DPX or Aqueous Mounting Medium (both Sigma, UK) for analysis.

For human FoxP3 staining, mouse α-human 236A/E7 clone antibody was kindly gifted by Dr Alison Banham, who developed the antibody clone. This antibody has been previously shown to identify reliably $FoxP3^+$ cells with good specificity[462]. Staining was carried out in a similar fashion to that performed using primary unconjugated antibodies, however secondary staining and amplification was performed with a Histofine® kit (Nichirei, Japan) or DAKOEnvision® kit both according to manufacturer's protocols, before incubation with DAB substrate as usual. ***Figure 2.1*** shows a photomicrographic section of human tonsil where α-human FoxP3 236A/E7 antibody was used as a positive control for human $FoxP3^+$ cells given that 5-10% of $CD4^+$ cells present in human tonsil are normally $FoxP3^+$[463]. For double staining of FoxP3 and CD4, the staining protocol was repeated for each antigen, with DAB as the substrate for FoxP3 and VECTOR® Blue used for CD4 (Vector laboratories).

For all human-specific antibodies used for immunohistochemical staining, a sample of mouse skin was stained to ensure that there was no cross-reactivity (n=6 stained sections for each antibody type). None of the antibodies showed any positivity on mouse tissue.

For each set of sections and antibody stain, a control section was included using an isotype control antibody or no antibody if an isotype control was not available. For infiltrating cell quantification, positive cells were counted at 400x magnification in 3 random fields of each of 4 separate sections for each antibody stain. The table below details the antibodies used for immunohistochemical analysis.

Specificity	Reactivity	Conjugation	Clone	Species of origin	Isotype
CD3	Human	Primary	HIT3a	Mouse	IgG_{2a} κ
CD3	Human	Biotin	OKT3	Mouse	IgG_{2a} κ
CD4	Human	Primary	RPA-T4	Mouse	IgG_1 κ
CD4	Human	Biotin	OKT4	Mouse	IgG_{2b} κ
CD8	Human	Primary	HIT8a	Mouse	IgG_1 κ
CD8	Human	Biotin	HIT8a	Mouse	IgG_1 κ
CD31 (PECAM-1)	Human	Biotin	WM-59	Mouse	IgG_1 κ
CD31 (PECAM-1)	Mouse	Biotin	390	Rat	IgG_{2a} κ
CD45	Human	Primary	HI30	Mouse	IgG_1 κ
CD45	Human	Biotin	HI30	Mouse	IgG_1 κ
GR-1	Mouse	Biotin	RB6-8C5	Rat	IgG_{2b} κ
HLA-B8	Human	Biotin	8.L.215	Mouse	IgG_{2b} κ

2.10 Enzyme-linked immunosorbent assay (ELISA)

ELISA was performed to determine serum concentration levels of human IgG and immunoglobulin M (IgM) in humanised mice. Nunc® multiwall plates were coated with goat α-human IgG (GαHuIgG) or goat α-human IgM (GαHuIgM) antibody overnight. Between all incubation steps plates were washed thoroughly with an automatic plate washer (Skatron Skanwasher®, UK). Plates were then blocked with 2% bovine serum albumin (BSA) solution and incubated for 30 minutes at 37°C. Normal human serum (NHS) standards at halving dilutions in duplicate, unknown samples at 3 concentrations in duplicate, and buffer only negative controls in

quadruplicate were then incubated in plates for 1 hour at 37°C. Plates were then incubated with biotin-labelled GαHuIgG or biotin-labelled GαHuIgM, followed by incubation with streptavidin-HRP conjugate, each for 1 hour at 37°C. 2,2'-azino-bis(3-ethylbenzothiazoline-6-sulphonic acid) (ABTS) was then used as substrate and stopped with 250mM oxalic acid. Plates were analysed with a spectrophotometer at 450nm and unknown values determined by relating to a standard curve plotted with values from the NHS standards.

2.11 Quantitative real-time polymerase chain reaction (qPCR)

Human skin samples were broken down using a tissue homogeniser. RNA was subsequently extracted using the Absolutely RNA Miniprep Kit (Stratagene, UK), according to manufacturer's instructions. RNA concentration was determined using a NanoDrop Spectrophotometer (ThermoScientific, UK). An RNA agarose gel was performed to ensure that there was no genomic DNA contamination or RNA degradation. Reverse transcription reactions to produce cDNA were performed as previously described, using between 1 to 5µg of RNA per reaction[464]. For qPCR, a mastermix was created using forward and reverse primers for the human genes *FOXP3* (FoxP3), *IFNG* (IFNγ), or *CD3* at specific concentrations, Taq Polymerase (Bioline, UK), dNTPs, $MgCl_2$, and 10x reaction buffer. 1µl of cDNA was added to each qPCR tube containing 49µl of mastermix. Duplicate samples were amplified using the following cycle conditions: 50°C for 2 minutes, 95°C for 10 minutes, followed by 45 cycles of 95°C for 15 seconds and 60°C for 1 minute. PCR products were measured using a Stratagene Mx3000P QPCR System (Agilent Technologies). The

quantity of the target gene was normalised to the housekeeping gene hypoxanthine-guanine phosphoribosyltransferase (*HPRT*) and evaluated using the calculation $2^{-\Delta Ct}$, where ΔCt (delta-cycle threshold) is the difference between the Ct of the target gene and *HPRT*[465]. Mouse splenocytes from n=3 BALB/c mice were also analysed in the same manner to ensure that the primers used were human-specific. For the three genes measured, no signal was detectable for any of the mouse splenocyte samples.

2.12 Luminex assays

Luminex® multiplexed and single antigen bead assays were performed for human immunoglobulin specificity identification according to manufacturers' guidelines. Samples were analysed by the Oxford Transplant Centre Histocompatibility and Genetics Laboratory with the kind assistance of Dr Susan Fuggle.

2.13 Statistical analyses

Survival data were only analysed from mice that achieved human leukocyte chimerism levels of >1% in the spleen or >0.1% in the peripheral blood. PBMC. Nonparametric Mann-Whitney U tests, Student's t tests or two-way ANOVA tests were applied on data as appropriate apart from survival data in which Log-rank tests were applied, all using Graphpad Prism software. *p* values under 0.05 were taken as significant.

2.14 Figures and legends

Figure 2.1. The 236A/E7 α-human FoxP3 antibody clone reliably identifies FoxP3$^+$ cells.

Representative photomicrograph of a healthy human tonsil stained by immunohistochemistry for FoxP3$^+$ cells. The histology shown is representative of 6 stained sections from n=2 different tonsils. Sections were fixed in acetone then incubated with mouse α-human FoxP3 236A/E7 clone antibody. Cells were then visualized using a DAKO EnVision™ kit and substrate reagent as per manufacturer's guidelines, followed by counterstaining with haematoxylin and mounting with aqueous mounting solution. Clear staining restricted to the cellular nucleus is demonstrated.

CHAPTER 3: DEVELOPMENT OF AN *IN VIVO* MODEL OF HUMAN SKIN REJECTION

3.1 Introduction

The lack of any significant clinical activity involving skin transplantation is responsible for a relative paucity of data on the immunobiology of human skin rejection. There is a therefore a need to develop a system whereby human skin rejection may be modelled and studied *in vivo* without any direct risk to patients. The benefits of such a model would be twofold. Firstly, the cellular and histological characteristics of rejecting human skin and the mechanisms of the unique alloresponse to skin may be studied. Secondly, the model may serve as a preclinical system in which a range of human therapies that are specific for human targets may be evaluated, including cellular therapies. Together with relevant *in vitro* mechanistic data, such a model would provide efficacy and limited safety data to form the basis for direct translation of novel therapies to clinical trials.

Humanised mouse models have proven very useful for the evaluation of both human vessel and islet allograft rejection. However, data on human skin is still limited with the majority of humanised models relating to the study of dermatological conditions such as psoriasis[180,466], or humanised skin transplantation models where there is incomplete skin rejection and destruction[370,447,455]. Some of these studies have only examined the alloresponse of a single T cell subpopulation towards the allograft[370]. Moreover, the majority utilise either cadaveric skin with its inherent problem of a

long ischaemia time[447,458], neonatal skin where human vasculature is replaced with mouse vasculature[447], or foetal skin where there is no expression of HLA Class II in the skin[459]. There are currently no humanised mouse models that emulate complete adult human skin destruction secondary to rejection.

NSG and BALB/c-Rag2$^{-/-}$cγ$^{-/-}$ mice are the two most efficacious strains for the reconstitution of functional human leukocytes with the lowest cell dose (*section 1.7.2*). However, NSG mice mount a significant mouse innate response against human skin and are therefore less than ideal for the purposes of this study[455]. While the transplantation of a vascularised human skin allograft would more closely mimic the transplantation of skin within a VCA, such a strategy is not currently feasible. In this chapter, we therefore opt for the transplantation of a partial thickness human skin graft procured intraoperatively from live adult donors undergoing plastic surgery procedures.

Firstly, we hypothesise that BALB/c-Rag2$^{-/-}$cγ$^{-/-}$ mice may be engrafted successfully with human PBMC and that these cells may subsequently induce the rejection of a human skin graft derived from a live adult donor. Secondly, we hypothesise that mice engrafted with human PBMC derived from the same donor as the skin graft would not cause rejection of the autologous skin graft, confirming the allospecific nature of the response. Finally we investigate the phenotype of the human cells that engraft in the model in order to determine the nature of the predominant response against the skin allograft.

3.1.1 Chapter aim

The aim of this chapter is to develop a robust humanised mouse model of human skin allograft rejection. This model will then be used to examine the mechanisms and characteristics of human skin rejection *in vivo* (***Chapter 4***) and then as a system to investigate methods for the immunoregulation of skin rejection using Treg cellular therapy (***Chapter 5***).

3.2. Human skin rejection may be modelled *in vivo*

Intraperitoneal and intravenous injections of between $10x10^6$ and $300x10^6$ PBMC have been used to reconstitute the adaptive immune system of an immunodeficient mouse in order to allow it to mount a human alloresponse against a human allograft, with skin models being on the higher end of this cell dose spectrum[370,447,448,467]. In many of these studies PBMC were isolated and cryopreserved for later use once mice were ready for the adoptive cellular transfer. Cryopreservation has not been found to be detrimental to PBMC reconstitution efficacy[448], and for logistical reasons we adopted cryopreservation of human cells in this study unless indicated otherwise. The commonly accepted definition of a successful level of human leukocyte reconstitution is the attainment of human leukocyte chimerism levels of >0.5-1% in the mouse spleen and >0.1% in the mouse peripheral blood[370,447,448,468,469]. For the purposes of this study the higher threshold of >1% splenic human leukocyte chimerism was accepted. To calculate the human leukocyte chimerism level, the proportion of live human $7AAD^-CD45^+$ cells is

determined as a percentage of total live mononuclear cells by FACS analysis (*section 2.5*).

In order to attain an adequate statistical power for *in vivo* assays, we aimed for at least n=4 mice per experimental group for survival assays. The lower the number of PBMC used to reconstitute a mouse, the larger the number of mice that could be reconstituted per PBMC donor. This is especially important when aiming to keep the PBMC donor constant across multiple experimental groups in the same assay. The lowest reconstituting dose of PBMC that induces rejection of a human vessel allograft in BALB/c-Rag2$^{-/-}$cγ$^{-/-}$ mice is 10x10^6 PBMC per mouse, suspended in RPMI-1640 medium and injected intraperitoneally[448]. Previous work in our laboratory has suggested that the intraperitoneal route may be the most reliable for successful reconstitution, although the intravenous route may allow for lower cell numbers if injected cells are suspended in human serum rather than RPMI-1640 medium (*unpublished observations*, S. Nadig and S. Luo).

We therefore asked whether 5x10^6 or 2x10^6 PBMC injected intraperitoneally or intravenously would successfully reconstitute a BALB/c-Rag2$^{-/-}$cγ$^{-/-}$ mouse. Furthermore, we hypothesised that the resuspension of cells in human serum derived from the PBMC donor would improve the engraftment of PBMC given through the intravenous route. BALB/c-Rag2$^{-/-}$cγ$^{-/-}$ mice received intraperitoneal injections of 5x10^6 or 2x10^6 PBMC suspended in RPMI-1640 medium, or intravenous injections of 5x10^6 or 2x10^6 PBMC suspended in RPMI-1640 medium or human serum. Four weeks post-adoptive cellular transfer, human leukocyte chimerism

levels were measured in the mouse spleens. Human leukocyte chimerism levels of >1% in the spleen were only attained with $2x10^6$ or $5x10^6$ PBMC injected intraperitoneally, or $5x10^6$ PBMC suspended in human serum and injected intravenously (***Figure 3.1***). While the addition of human serum did allow mice that received $5x10^6$ cells via the intravenous route to achieve human leukocyte chimerism levels of >1%, the highest levels of chimerism were nonetheless attained with injections via the intraperitonal route, irrespective of cell dose. We therefore concluded that intraperitoneal injection of PBMC at doses as low as $2x10^6$ cells may successfully achieve adequate reconstitution. In all future assays in this thesis cells were suspended in RPMI-1640 medium and injected intraperitoneally. For control mice receiving no cells, RPMI-1640 medium was injected alone.

We next aimed to determine whether human split-thickness skin transplants derived from live adult donors would successfully engraft and revascularise on BALB/c-$Rag2^{-/-}c\gamma^{-/-}$ mice and whether these skin grafts would then be destroyed in mice reconstituted with human PBMC from a donor allogeneic to the skin graft donor. With the knowledge that between $2x10^6$ and $10x10^6$ human PBMC injected intraperitoneally may successfully reconstitute a BALB/c-$Rag2^{-/-}c\gamma^{-/-}$ mouse, we aimed to determine the lowest dose possible that may lead to rejection of the skin allograft. BALB/c-$Rag2^{-/-}c\gamma^{-/-}$ mice therefore received a human skin graft of 1x1cm onto the left flank and 3 days later were injected with $2x10^6$, $5x10^6$, or $10x10^6$ human PBMC from a donor allogeneic to the skin graft donor, or no cells (***Figure 3.2a***).

In mice receiving no cells, skin engrafted successfully and all grafts appeared macroscopically normal at 4 weeks post-transplantation with features expected from a human skin graft with 'good take' (***Figure 3.2b***). Skin grafts appeared to have a healthy tone without erythema, and when lifted from the graft bed appeared revascularised as inferred from the presence of blood vessels entering the graft (***Figure 3.2c***). In addition, immunohistochemical staining for human $CD31^+$ (platelet endothelial cell adhesion molecule 1, PECAM-1) cellular rings in human skin grafts revealed the presence of human microvessels in the papillary layer of the human dermis pre-transplantation, that then proliferate into the deeper layers of the skin and into the mouse hypodermis post-transplantation (***Figure 3.3a***). Mouse $CD31^+$ cellular rings are also present within the human skin dermis post-transplantation (***Figure 3.3b***), indicating that as the skin graft 'takes' there is revascularisation with both mouse and human vessels. Others have demonstrated that anastomosis of mouse vessels with human vessels takes place to allow perfusion of the skin graft[447].

Mice receiving PBMC but not achieving human leukocyte chimerism levels of >1% in the spleen were excluded from the survival analysis. In mice not receiving an adoptive transfer of PBMC, human skin grafts survived long-term (>100 days, ***Figures 3.4a and b***). In these mice, skin grafts appeared normal and were soft and pliable with no erythema, swelling or thickening (***Figure 3.4c***). In contrast, in mice receiving $2x10^6$, $5x10^6$ or $10x10^6$ allogeneic PBMC, skin grafts were lost with median survival times (MSTs) of 36, 32 and 33 days respectively (***Figures 3.4a and b***). Human skin grafts on these mice became swollen, thickened and erythematous, with an occasional exudate or an eschar, before shrinking and becoming hard and crusty.

Eventually they were completely lost, leaving an erythematous bed of granulation tissue that was then replaced with pale white scar tissue (***Figure 3.4d*** shows the typical appearance of a rejecting skin graft). Importantly, although MSTs were similar between the three groups receiving human cells, one mouse receiving $2x10^6$ allogeneic PBMC did not fully reject the skin graft (***Figure 3.4a and b***). The allograft on this particular mouse appeared inflamed and swollen, yet destruction was incomplete.

We then asked whether the difference in rejection tempo between mice receiving $2x10^6$ PBMC compared with $5x10^6$ or $10x10^6$ PBMC (p=0.030) was secondary to reduced human leukocyte chimerism levels. We therefore examined both the levels of human leukocyte chimerism and rates of successful reconstitution in mice receiving the three different doses of PBMC. At the point of skin graft loss mice were sacrificed and spleens examined for the percentage human leukocyte chimerism and number of human leukocytes present per spleen. When mice that had failed to reconstitute (i.e. achieve >1% human leukocyte chimerism in the spleen) were excluded, there was no significant difference in the levels of human leukocyte chimerism (***Figure 3.5a***) or total numbers of human leukocytes in the spleen (***Figure 3.5b***) between the three different cell dosage groups. However, examination of the overall rate of reconstitution in all mice revealed a high rate of failure of reconstitution (i.e. under 1% human leukocyte chimerism in the spleen) in mice receiving $2x10^6$ cells (33%) compared with $5x10^6$ cells (17%) and $10x10^6$ cells (0%) (***Figure 3.5c***). In addition, in the single mouse receiving $2x10^6$ PBMC that successfully reconstituted but did not fully reject the skin allograft, the level of

reconstitution was the lowest of all mice receiving $2x10^6$ cells (3.43% *cf.* mean of 32.55% with a standard deviation (SD) of ±15.71 for all mice receiving $2x10^6$ cells).

Over the time course of the survival assay, mice were also monitored for signs of human anti-mouse xenograft-versus-host disease (XvHD) through weight loss (>20% loss from initial weight), hair loss, decreased activity, hunching, and ear pallor (as a sign of anaemia). For mice achieving human leukocyte chimerism levels of >1% in the spleen, rates of XvHD development were determined. Very high rates of XvHD developed in mice receiving $10x10^6$ PBMC (50%) compared with mice receiving $5x10^6$ (20%) or $2x10^6$ (12.5%) PBMC (***Figure 3.5d***). No mice developed XvHD before skin rejection, suggesting that human alloresponses predominate over human anti-mouse xenoresponses. The development of XvHD in humanised mice is a recognised phenomenon and secondary to a predominantly T cell based human anti-mouse response[460].

We concluded that an intraperitoneal injection of $5x10^6$ PBMC is the most reliable number of cells to induce rejection with the most acceptable balance of risk in terms of rates of both XvHD development and reconstitution failure. This currently represents the lowest reported dose of human PBMC required to mount an immune response against skin that leads to its complete destruction in a humanised mouse model[370,447,455,467].

3.3. Human skin grafts require a period of healing in order to model a true alloresponse

In order to confirm that the destruction of human skin grafts by allogeneic PBMC in BALB/c-Rag2$^{-/-}$cγ$^{-/-}$ mice was a true alloresponse, a survival assay was carried out using PBMC derived from the skin graft donor (i.e. autologous PBMC). Mice therefore received a human skin graft and 3 days later an injection of 5x10^{6} autologous or allogeneic PBMC (the optimal dose determined above in ***Figures 3.4 and 3.5***). Mice not achieving human leukocyte chimerism levels of >1% in the spleen or >0.1% in the peripheral blood were excluded from the survival analysis. Unexpectedly, autologous skin grafts were destroyed over the same time period as allogeneic skin grafts (autologous MST 28 days, allogeneic MST 30.5 days, ***Figures 3.6a and b***). The destruction of autologous skin grafts in this case is not related to a mouse anti-human immune response, as human skin grafts transplanted onto BALB/c-Rag2$^{-/-}$cγ$^{-/-}$ mice not receiving any human cells survive indefinitely (***Figures 3.4a and b***). In addition, these human skin autografts were infiltrated with human leukocytes, suggesting that a human immune response against the skin graft is taking place (***Figure 3.6c***). Nevertheless, infiltration of mouse skin grafts with syngeneic leukocytes has been reported by others and is suggested to be a poor indicator of an alloresponse, being rather an indicator of a non-specific inflammatory response[177].

To confirm that the destruction of the autologous human skin graft was a characteristic unique to human PBMC engrafting in BALB/c-Rag2$^{-/-}$cγ$^{-/-}$ mice and not related to a peculiarity of the mouse strain, BALB/c-Rag2$^{-/-}$cγ$^{-/-}$ mice were engrafted

with a BALB/c wild-type skin transplant and 3 days later injected intraperitoneally with either $5x10^6$ syngeneic BALB/c wild-type mouse splenocytes or no cells. Here, skin grafts survived long-term (***Figure 3.6d***) with all mice achieving reconstitution levels of >10% mouse T cells in the spleen. In a previously developed humanised mouse model of human vessel rejection in use in our laboratory, autologous human vessels did not display any signs of rejection[448]. We therefore inferred that the destruction of autologous human skin grafts was a phenomenon restricted to human PBMC and human skin.

Autoreactivity is known to develop as a result of the homeostatic expansion of leukocytes[470,471] and in response to lymphopaenia (termed 'spontaneous proliferation')[472-474]. Some investigators promote a 'two-hit' model whereby lymphopaenia and another inflammatory insult are required in order to promote the proliferation of autoreactive T cells[473]. The presence of 'danger signals' from surgical inflammation may also independently induce autoreactivity[475]. We therefore hypothesised that reducing the impact of the surgical trauma would prevent the destruction of human skin grafts by autologous PBMC. To achieve this, human skin grafts were allowed to heal for a period of 5 weeks in an effort to reduce the effects of trauma-associated inflammation, before adoptive transfer of $5x10^6$ autologous or allogeneic human PBMC (***Figure 3.7***). Interestingly, most other research groups allow human skin to heal before adoptive transfer of cells[447,467,468,476]. Survival time for skin grafts was measured from the point of adoptive cellular transfer and mice not achieving human leukocyte chimerism levels of >1% in the spleen or >0.1% in the peripheral blood were excluded from the survival analysis. As expected, mice

receiving $5x10^6$ allogeneic PBMC rejected the human skin grafts with a MST of 39 days (***Figures 3.8a and b***). By contrast, in mice receiving $5x10^6$ autologous PBMC, skin grafts survived long-term (MST >100 days, ***Figures 3.8a and b***) with no macroscopic signs of rejection. Unfortunately, two mice injected with autologous PBMC required euthanasia at days 72 and 76 post-adoptive cellular transfer due to the development of XvHD, indicating that while there is no significant human anti-human response with autologous PBMC, the human anti-mouse response remains intact. Notably, these 'healed in' human skin autografts were not infiltrated with human leukocytes to the same degree as autografts that were not allowed to heal (***Figure 3.6c***, no healing *cf.* ***Figure 3.8c***, with healing, both shown at the same time point of 28 days post-adoptive transfer of PBMC).

In order to confirm that the survival of autologous human skin grafts was not secondary to a reduced level of human leukocyte engraftment, the number of human $CD45^+$ leukocytes was determined in the spleens of mice receiving autologous or allogeneic PBMC that were included in the survival analysis. As shown in ***Figure 3.8d***, levels were similar between these two groups. However, enumeration of human $CD45^+$ leukocytes in the skin-draining and contralateral axillary lymph nodes demonstrated a higher number of cells in the skin-draining (but not contralateral) lymph nodes of mice receiving allogeneic PBMC compared with the number of cells in the skin-draining axillary lymph nodes of mice receiving autologous PBMC (***Figure 3.8e***). This suggests a preferential aggregation of alloantigen-responding human cells at the site of the alloantigen source.

Together these data indicated that a true human alloresponse to skin may be modelled *in vivo* using human skin grafts that are allowed to heal for 5 weeks.

3.4 Rejection kinetics of human skin allografts

We noted that the MST of skin grafts that were allowed 5 weeks healing before adoptive transfer of $5x10^6$ allogeneic PBMC in the survival assay in ***Figure 3.8b*** was slightly longer than the MST of human skin grafts that are not allowed to heal before the adoptive transfer of $5x10^6$ allogeneic PBMC (***Figure 3.4b***). Given the role played by the surgical trauma in the initiation of the immune response (as discussed in *section 1.3.1*), a reduction in the surgery-associated inflammation with time may indeed lead to dampening down of the alloresponse. We therefore asked whether allowing skin grafts to heal prolongs their survival time. Data were pooled from all survival assays performed in this thesis comparing the survival of human skin grafts from mice receiving $5x10^6$ allogeneic human PBMC 5 weeks post-skin grafting (i.e. with healing) with mice receiving $5x10^6$ allogeneic human PBMC 3 days post-skin grafting (i.e. without prolonged healing). Mice not achieving human leukocyte chimerism levels of >1% in the spleen or >0.1% in the blood were excluded from the survival analysis. In this analysis, healed human skin allografts on humanised mice had marginally longer survival times (MST no healing 28 days *cf.* MST healing 35 days, $p<0.0001$, ***Figures 3.9a and b***). Importantly however, all healed skin allografts reliably rejected. Mice receiving allogeneic PBMC 5 weeks post-skin grafting rejected their allografts with similar macroscopic features to those receiving PBMC 3 days post-skin grafting (***Figure 3.9d***). For reference, ***Figure 3.9e*** demonstrates the

typical macroscopic appearances of human skin grafts undergoing destruction mediated by $5x10^6$ allogeneic human PBMC.

Although inflammation is known to be important for the initiation of rejection (see *section 1.3.2*), the observation that rejection still occurs in the absence of these inflammatory signals has been demonstrated in the mouse, where vigorous and consistent rejection of mouse healed skin allografts takes place[477]. Non-specific inflammation may therefore enhance the immune response against the transplant, but the absence of inflammation does not prevent rejection. Finally, mice that did not receive PBMC all engrafted skin transplants long-term (***Figures 3.9a and b***). These grafts appeared macroscopically normal with no gross evidence of inflammation (***Figure 3.9c***), indicating that there is no significant mouse immune response that may lead to destruction of the human skin graft.

The survival of autologous human skin grafts using 'healed in' skin implies a more faithful model of human skin transplantation. Furthermore, allowing skin grafts to heal and revascularise before cellular injection, to a certain extent converts these transplants into 'vascularised' allografts, creating a more authentic representation of VCA transplantation. For these reasons all *in vivo* assays performed in this thesis from this point onwards utilise the 'healed in' skin model (***Figure 3.7***).

3.5 Impact of the number of HLA mismatches on human skin rejection tempo

In SOT, the greater the number of HLA mismatches between donor and recipient, the higher the risk of rejection. Clinically, mismatches in HLA-A, HLA-B, HLA-DR and HLA-DQ are routinely measured. We therefore asked whether the number of HLA mismatches between PBMC and skin donor impacted the MST of human skin allografts in our model. This is important given that donors are chosen randomly, leading to an inter-experimental variation in the degree of HLA mismatch between skin and PBMC donors. Data were therefore pooled from all survival assays performed in this thesis in order to confirm that any inferences are not secondary to differences in the number of HLA mismatches between assays. In all these survival assays BALB/c-Rag2$^{-/-}$cγ$^{-/-}$ mice received a human skin transplant and 5 weeks later an adoptive transfer of 5x10^{6} PBMC from a donor allogeneic to the skin graft donor. 19 separate groups of mice were transplanted using a distinct skin and PBMC donor combination for each group of mice. The MST for each group of mice was calculated and categorised according to the number of mismatches within the HLA-A (***Figure 3.10a***), HLA-B (***Figure 3.10b***), HLA-DR (***Figure 3.10c***) and HLA-DQ (***Figure 3.10d***) loci as well as the total mismatches across all of these loci (**Figure 3.10e**). The maximum number of possible mismatches per locus is two, and the minimum number of possible mismatches is zero. The number of total mismatches ranged from 4 to 8 with a median mismatch of 7. Importantly, in this range of total HLA mismatches, there was no significant association between the MST and the number of mismatches. There was also no significant association between the MST and the number of mismatches in any particular HLA locus. This indicates that when large

differences in survival time are observed between assays, these are not due to differences in the degree of HLA mismatch between the donors in the different survival assays. Moreover, this implies that data may be pooled from survival assays using different donors where the same variables are being evaluated, without the risk of skewing results secondary to variations in the degree of HLA mismatch between donors.

3.6 Kinetics of reconstituting human leukocytes in the humanised skin transplantation model

Overall, human skin grafts appeared to take a much longer time to reject in our model compared with what is observed in wild type fully MHC-mismatched mouse models of skin rejection, where skin is normally lost 8-12 days after transplantation. We therefore hypothesised that this may be due to a need for a certain threshold of human leukocyte chimerism to be reached before enough human cells are present to respond to the allograft. Therefore, in order to further characterise the model, the percentage of human leukocyte chimerism was monitored in the peripheral blood of human skin-transplanted BALB/c-Rag2$^{-/-}$cγ$^{-/-}$ mice receiving 5x10^{6} allogeneic PBMC 5 weeks post-transplantation (***Figure 3.11a***). Human cells were only detectable at levels of over 0.1% from two weeks post-adoptive transfer onwards. The level of human leukocyte chimerism steadily increased and then plateaued from 5 weeks onwards. The peak of human leukocyte chimerism observed appeared to coincide with the mean time at which human skin grafts rejected (i.e. MST of 35 days, ***Figure 3.9b***). The delay of two weeks before reaching significantly detectable

levels of human leukocytes in the peripheral blood may partly explain the longer rejection time observed in comparison to mouse models of skin rejection.

Human leukocytes were detectable in the peripheral blood as well as the spleen, axillary skin-draining and contralateral lymph nodes, indicating the proliferation and seeding of human cells throughout the peripheral lymphoid tissues of mice receiving human skin allografts (***Figure 3.11b*** and representative FACS plot from spleen in ***Figure 3.13c***). We next asked whether there was variation in the rate of splenic reconstitution of $5x10^6$ PBMC between several different human PBMC donors. Interestingly, there were slight (although not statistically significant) differences in both the percentage (***Figure 3.11c***) and number (***Figure 3.11d***) of human cells in the spleens of mice receiving PBMC from different donors (here represented by a separate B-number code for each donor). Importantly however, for all donors the mean percentage of human leukocyte chimerism in the spleen was above the required threshold of 1% (mean across all donors 35.12% SD±25.21). In addition, although the lowest percentage of chimerism detected for any one mouse was 1.1%, skin allografts were still rejected at this level.

There appeared to be no association pattern between the level of human chimerism and the MST of human skin allografts (***Figure 3.11e***). For example, donor B137 produced the shortest MST but had only a moderate level of human leukocyte chimerism, and importantly this short MST was not due to a high level of HLA mismatching between the skin and PBMC donor in this assay (***Figure 3.11e***). As a further example, the lowest level of chimerism was detected with donor B131,

however the MST for the group of mice reconstituted with this donor was average at 35.5 days (***Figure 3.11e***). Taken together, these data indicate that although there may be slight variation between the levels of human leukocyte chimerism (***Figure 3.11c***) and degree of HLA mismatch (***Figure 3.10e***) between different donors, these factors do not impact significantly the MST of human skin grafts destroyed by allogeneic PBMC. Furthermore, mice receiving $5x10^6$ PBMC that achieve the defined threshold level of human leukocyte chimerism of >1% in the spleen will invariably reject their human skin allografts. Again, these observations imply that data may be pooled from multiple assays when necessary.

3.7 Phenotype of reconstituting human leukocytes in the humanised skin transplantation model

In order to further characterise the nature of the human alloresponse developing in the mouse, we analysed the phenotype of reconstituting cells in the standard 'healed in' model. Pre-injection, PBMC mainly consisted of T cells (human $CD3^+$, mean 64.3% SD±11.3) with some B cells (human $CD19^+$, mean 6.9% SD±1.1), NK cells, NKT cells and DCs. However post-reconstitution the majority of human $CD45^+$ cells in the spleen were T cells (mean 98.2% SD±1.7) with very few B cells (mean 0.1% SD±0.1) (***Figure 3.12a*** and representative FACS plots in ***Figures 3.13a and d***) and there were no detectable NK cells, NKT cells or DCs. The phenotype of T cells in PBMC pre-injection consisted of approximately two-thirds $CD4^+$ cells (mean 53.7% SD±16.7) and one-third $CD8^+$ cells (mean 30.8% SD±13.4), while post-reconstitution the T cell split was approximately half $CD4^+$ cells (mean 44.8% SD±15.6) and half

$CD8^+$ cells (mean 44.8% SD±16.6) (***Figure 3.12b*** and representative FACS plots in ***Figures 3.13b and e***).

The majority of $CD3^+$ cells post-reconstitution acquired a memory phenotype with the expression of CD45RO (***Figure 3.12c***). This acquisition a memory phenotype is consistent with previous studies and has been shown to be necessary for the engrafted human cells to effect allograft damage[458,478]. Finally, we asked whether there was a predominance of either $CD4^+$ or $CD8^+$ T cells in the peripheral blood of humanised mice that are actively rejecting human skin allografts that would suggest a relative importance of one T cell type in the rejection process. We therefore monitored the peripheral blood of mice for the proportion of human T cells that were $CD4^+$ or $CD8^+$ over time post-reconstitution (***Figure 3.12d***). Interestingly, $CD8^+$ T cells significantly increased in proportion, plateauing at the point at which most human skin grafts are destroyed (i.e. the MST of 35 days, ***Figure 3.9b***), whereas the relative proportion of $CD4^+$ cells decreased. For a histological profile of infiltrating cells please refer to *section 4.3*.

3.8 Discussion

In this chapter we have optimised a clinically relevant system for modelling human skin transplant rejection *in vivo*. This is the first model in which complete human skin allograft destruction is induced in a humanised mouse *in vivo* (***Figure 3.9***).

Although data from clinical studies show that the number of HLA mismatches impact the risk of rejection[479-481], this observation is not apparent in the humanised mouse model given that a high degree of HLA mismatching exists overall due to random selection of skin and PBMC donors (***Figure 3.10***). Our model is predominantly a T cell-mediated model of skin rejection (***Figure 3.12***). The domination by T cells with engrafting PBMC in immunodeficient mice is a recognised phenomenon[447]. The peaking of the $CD8^+$ T cell subset at a time coincidental with skin rejection (***Figure 3.12***) may reflect their importance in mediating the destruction of the allografts[341,482], or related to the apparent ability of these cells to proliferate more readily compared with $CD4^+$ T cells (*in vitro* observations, Dr J Hester). The relative deficiency in human B cells may be secondary to the lack of specific niches required for B cell proliferation, or the lower propensity of these cells to homeostatically proliferate compared with T cells. Models in which more complete human leukocyte engraftment may be achieved are addressed in *Chapter 4*.

Our findings are in agreement with others, who have demonstrated the efficacy of BALB/c-$Rag2^{-/-}c\gamma^{-/-}$ mice as hosts for the engraftment of human leukocytes through the intraperitoneal route[326,448] (***Figure 3.1***). Previous work in our laboratory as well as work by others using immunodeficient mice has shown that intraperitoneally injected human cells proliferate in the peritoneal cavity of immunodeficient mice from day 10 and that human cells are only consistently detectable in the spleen, liver and peripheral blood by day 14 post-injection[483]. The relatively long survival time of allografts in our model may be secondary to the delay while cells expand in the peritoneum before seeding into the circulation[483]. Within the peritoneal cavity,

production of growth factors such as IL-2 by human cells would assist in the proliferation of cells before their seeding into mouse tissues.

Some have also suggested that a mouse inflammatory response to the intraperitoneal injection would result in the production of mouse cytokines that cross-react to provide proliferation signals to the human cells[483,484], although whether such a mechanism is relevant in mice lacking cytokine-producing T, B and NK cells is unclear. Mice receiving intravenous injections of human cells may not develop a similar inflammatory response with the resultant cytokine production, thus explaining the reduced human leukocyte chimerism levels attained with intravenous injections. Alternatively, circulating human cells may not proliferate as successfully as cells that are static within the pseudo-culture conditions of the intraperitoneal cavity. Providing human cells with human serum and thereby the various cytokines and growth factors that are present within human serum improves engraftment of cells by the intravenous route, supporting this hypothesis (***Figure 3.1***). There does not appear to be a particular need to provide human serum to cells injected by the intraperitoneal route given the high levels of human leukocyte chimerism attained via this route. Nevertheless, this may be a tactic to be considered in the future if necessary.

For the purposes of the studies in this thesis, reconstitution of mice with $5x10^6$ PBMC is adequate. This dose induced skin allograft rejection in a reliable fashion. Injection of $2x10^6$ cells unfortunately did not induce reliable rejection within a reasonably tight time frame in all mice (***Figure 3.4b***). Moreover, injection of $2x10^6$

PBMC was associated with a high rate of reconstitution failure (***Figure 3.5c***). While doses of $10x10^6$ PBMC did reliably induce skin allograft rejection (***Figure 3.4b***), this dose was associated with high rates of XvHD development (***Figure 3.5d***).

From these particular assays, there appears to be a relationship between the levels of human leukocyte chimerism attained and skin graft rejection. The majority of mice that rejected their skin grafts within 40 days in any group attained levels of human leukocyte chimerism of over 10% in the spleen. Such levels of chimerism have also been observed to be important in other humanised models[448]. However, achieving this level of human leukocyte chimerism is not alone sufficient to cause skin rejection, as there are other factors at play such as the phenotype of reconstituting cells and the balance of effector and regulatory mechanisms active[448]. Cases in which splenic levels of human leukocyte chimerism are still above this level and yet skin grafts are not rejected are discussed in subsequent chapters. Given that both the number and chimerism level of human leukocytes were similar in mice receiving $2x10^6$, $5x10^6$ or $10x10^6$ PBMC (***Figure 3.5a and b***), it is possible that the differences in MST between mice receiving $2x10^6$ PBMC and $5x10^6$ or $10x10^6$ PBMC (***Figure 3.4a***) is rather due to a varying tempo of reconstitution. In other words, mice receiving $5x10^6$ PBMC may reach a certain level of human leukocyte chimerism faster than mice receiving $2x10^6$ PBMC.

The development of XvHD in immunodeficient mice inoculated with human PBMC is a recognised phenomenon[484,485] (***Figure 3.5***). We and others have found that a large proportion of human leukocytes engrafting in immunodeficient mice acquire a

memory phenotype (***Figure 3.12***)[447,454,486]. Previous work in our laboratory has also shown that these cells are virtually all CD62L$^-$, making them effector memory in phenotype (*unpublished data*, P. Dhaliwal). These cells are unlikely to respond to mouse MHC directly as human HLA is too divergent. There is also no indirect allorecognition active due to the lack of adoptively transferred human APCs in the system. The effector memory phenotype observed is likely to be secondary to homeostatic expansion[471]. XvHD in our model develops late, always a few weeks after skin rejection, implying that human anti-mouse xenoresponses are less potent than human anti-human alloresponses. XvHD in our model is therefore unlikely to be due to any rapid xenoantigen-specific expansion. In another model developed in our laboratory using human vessel transplants, human anti-mouse xenoresponses were absent against mouse vessels and XvHD was again a late observation (S. Nadig, *unpublished observations*).

While the principal human vessels visible in human skin pre-transplantation are those of the superficial vascular plexus (SVP) in the papillary dermis (***Figure 3.3a, left panel***)[487], post-transplantation human vessels may be seen throughout the deeper layers, even extending into native mouse tissue in the hypodermis (***Figure 3.3a, right panel***). Importantly, after transplantation skin grafts are sufficiently vascularised and human vessels preserved despite incorporation of mouse vessels (***Figure 3.3b, right panel***). Others have demonstrated that anastomosis of mouse vessels with human vessels takes place to allow perfusion of the skin graft[447]. The preservation of human vasculature is of particular importance given the central role the vascular endothelium plays in facilitating the immune response against the allograft (*section*

1.4.2). The presence of human microvessels is necessary to ensure the development of a DTH response by human memory T cells, which are only able to interact with human ICAM-1 expressed on human ECs in order for them to be recruited into the skin. This is due to species differences that prevent human LFA-1 on human memory T cells from recognising mouse ICAM-1 on mouse ECs[172,447]. In models utilising human neonatal skin, human microvessels are replaced by mouse microvessels[447], and in models using human foetal skin, skin ECs do not express MHC Class II[459], eliminating a central facet of the alloresponse and reducing the power of these models. For an analysis of the changes in skin microvasculature that occur with rejection please refer to *section 5.7* and ***Figure 5.13***.

Allowing human skin grafts to heal (***Figure 3.7***) before injection of human PBMC adds a further dimension to the model, by converting secondarily vascularised skin grafts into grafts that are theoretically closer to primarily vascularised ones and thus more relevant in the context of VCA transplantation. Irrespective of this, whether grafts are primarily or secondarily vascularised they still undergo vigorous rejection and the state of vascularisation is not the defining factor in the susceptibility of skin to rejection (*section 1.4.1*).

The effects of skin ischaemia that may lead to non-specific inflammatory signal production are likely to be important in this model. Development of the adaptive effector response requires the presence of chemokine and cytokine signals that direct and recruit host T cells into the allograft (*section 1.3.2*)[58,475,488]. These signals originate from innate responses following the surgical stress and IRI post-

transplantation and may include the secretion of alarmins[54,55,57]. A healed and revascularised skin graft (***Figures 3.3 and 3.7***) would display fewer inflammatory signals and this may reduce the rapidity of the effector response, prolonging graft survival. However, data from this study and from studies by other groups show that rejection still occurs after healing (albeit at a marginally slower rate) in a state in which these inflammatory signals are reduced[477] (***Figure 3.9***). The importance of healing of skin grafts in the current model is related to the differentiation of true alloresponses from apparent autoimmune responses. Healing of human skin allografts prevents their destruction by autologous human leukocytes (***Figures 3.6 and 3.8***). It is not clear how long the period of healing needs to be in order to achieve this and it is possible that periods of healing shorter than 5 weeks are effective. It is also possible that the number of weeks that the skin autograft is allowed to heal for results in proportional increases in survival time, until the attainment of long-term survival at 5 weeks. This would require further investigation.

Autoreactivity is known to develop as a result of homeostatic expansion[470,471] and in response to lymphopaenia (termed 'spontaneous proliferation')[472-474]. The presence of 'danger signals' from inflammation may also independently induce autoreactivity[475]. A similar observation where human skin is infiltrated and damaged by autologous leukocytes has been reported in a humanised SCID mouse model[489]. In this model, reconstitution with PBMC but not T cells alone lead to infiltration of the autologous skin graft with T cells, implying that another element within PBMC promotes the activation of T cells. The authors propose that B cells within PBMC

may provide an activation signal to T cells, however further work is required to confirm this[489]. Apart from this report and the assays described in this thesis, no other studies have reconstituted humanised mice with leukocytes that are autologous to the transplanted human skin graft. It is therefore unclear whether this is a widespread phenomenon.

In terms of causative factors for the development of autoreactivity, in the 'two-hit' model a state of lymphopaenia and another insult are required to promote autoreactive T cell proliferation[473,490,491]. Inflammation and IRI are two such 'second hits', both of which are present in our model where grafts are not allowed to heal in. However, the observation of graft destruction by autologous leukocytes appears to be confined to skin, as it is not observed in a humanised model of human vessel rejection[448]. The unique characteristics of skin that alter the resulting immune response are discussed in *section 1.4*. One of these characteristics include the observation that only a small fraction of T cells that infiltrate human skin are alloantigen specific, with the majority being nonspecifically recruited to the site of rejection[177,492] through release of inflammatory mediators by activated ECs and keratinocytes[172,178,179,202,203]. In fact, some have shown that the number of infiltrating leukocytes in mouse syngeneic skin grafts is only slightly less than allogeneic mouse grafts[177,493]. Such T cells may not necessarily be antigen specific, but may, in a state of overall inflammatory activation, contribute to destruction of the skin through non-specific effector mechanisms[492]. It is therefore possible that nonspecific inflammatory signals from keratinocytes and ECs in skin grafts that are not healed for an extended time result in the recruitment of human T cells to the

skin graft, which promote its destruction through non-specific effector mechanisms. The infiltration of autologous skin grafts in our model with human leukocytes may represent this non-specific inflammation-induced infiltration, which is significant in 'unhealed' autologous skin grafts (***Figure 3.6c***) but sparse and presumably inconsequential in 'healed in' autologous skin grafts (***Figure 3.8c***).

However, this does not explain why autologous human skin grafts in clinical practice are not destroyed. It is possible that the lymphopaenic environment in which human cells proliferate is also important in promoting their autoreactivity[490]. One argument is that proliferating cells in a lymphopaenic inflammatory environment that happen to have affinity for the HLA molecules present will have a survival and proliferation advantage over those that are not reactive to the HLA molecules. Such a situation would preferentially expand T cells reactive to the HLA molecules over those that do not react to it. In a scenario where the only HLA molecules present are derived from self and in which there an inflammatory environment is present, such as the model using 'unhealed' autologous skin grafts, there will be a preferential expansion of autoreactive T cells. Such a mechanism may explain the higher incidence of autoimmune disease in transplant patients in whom a relative state of lymphopaenia exists[490]. The expression of HLA Class II and costimulatory molecules on skin vascular ECs facilitates the activation and migration of memory T cells into the graft[172,174,478]. Given that the majority of T cells are phenotypically memory-type after homeostatic proliferation in the current mouse model (***Figure 3.12c***), autoreactive memory T cells will efficiently destroy the autologous skin graft with a

low threshold requirement for costimulatory signals. However, in a model where the graft is 'healed in' and inflammatory signals are reduced, this may not occur.

Together, these data indicate that the optimum model for human skin allograft rejection *in vivo* requires $5x10^6$ PBMC injected intraperitoneally 5 weeks after skin transplantation. This is therefore the model utilised for the remaining studies in this thesis.

Having developed a working system of *in vivo* human skin rejection in *Chapter 3*, in *Chapter 4* we proceed to evaluate the characteristics and mechanisms of skin rejection in the humanised model as related to information from clinical skin rejection. We then evaluate techniques whereby the model may be further improved to encompass a wider spectrum of reconstituting human leukocytes.

3.9 Figures and legends

Figure 3.1. PBMC doses of $2x10^6$ or $5x10^6$ administered via intraperitoneal injection reliably reconstitute BALB/c-Rag2$^{-/-}$cγ$^{-/-}$ mice.

Engraftment analysis of human PBMC injected into BALB/c-Rag2$^{-/-}$cγ$^{-/-}$ mice. BALB/c-Rag2$^{-/-}$cγ$^{-/-}$ mice were injected intraperitoneally or intravenously with $2x10^6$ or $5x10^6$ human PBMC. In mice receiving intraperitoneal injections, cells were suspended in 200µl RPMI-1640 medium. For those receiving cells intravenously, PBMC were either suspended in 200µl of human serum derived from the PBMC donor or 200µl RPMI-1640 medium. All mice received cells from the same PBMC donor with n=3 mice per group. Mice were sacrificed 4 weeks post-injection of PBMC and spleens analysed by FACS for the presence of live human 7AAD$^-$CD45$^+$ cells as a percentage of total live mononuclear cells (%huCD45$^+$). Mice achieving %huCD45$^+$ levels of >1% were considered to be adequately reconstituted (dotted line). Data are represented as mean ±SD.

Figure 3.2. The humanised mouse skin transplantation model.

(a) Schematic representation of the model. BALB/c-Rag2$^{-/-}$cγ$^{-/-}$ mice receive a human skin graft measuring 1x1cm, followed by an intraperitoneal injection of human PBMC 3 days later to reconstitute their immune systems to levels of >1% human leukocyte chimerism in the spleen or >0.1% in the peripheral blood. Human skin grafts are monitored for survival and mice are optionally tail-bled for time-course analysis of peripheral human cellular reconstitution. Mice may be sacrificed at specific time-points for particular analyses. **(b)** Macroscopic appearance of human skin grafts 4 weeks post-transplantation in the absence of PBMC injection. **(c)** At two weeks post-transplantation, human skin grafts are revascularised as demonstrated by the ingrowth of vessels on the underside of the graft.

Figure 3.3. Revascularisation of human skin grafts on BALB/c-Rag2$^{-/-}$cγ$^{-/-}$ mice.

Representative photomicrographs of human skin graft sections. BALB/c-Rag2$^{-/-}$cγ$^{-/-}$ mice received a human skin graft without an injection of PBMC. Skin was analysed pre-transplantation and 100 days post-transplantation. Sections were stained for specific antigens by immunohistochemistry and counterstained with haematoxylin. **(a)** Human CD31^{+} cells in human skin grafts pre-transplantation and 100 days post-transplantation. Arrows indicate cross-sections of complete vessels seen as rings. **(b)** Mouse CD31^{+} cells in human skin grafts pre-transplantation and day 100 post-transplantation. Arrows indicate cross-sections of complete vessels seen as rings. The histology shown is representative of 6 stained sections for each stain type from each of n=4 mice from n=2 different skin donors, for each time point.

Figure 3.4. Intraperitoneal injection of $5x10^6$ or $10x10^6$ allogeneic PBMC reliably induces human skin graft rejection in BALB/c-Rag2$^{-/-}$cγ$^{-/-}$ mice.

(a) and (b) Survival analysis of BALB/c-Rag2$^{-/-}$cγ$^{-/-}$ mice reconstituted with allogeneic human PBMC. BALB/c-Rag2$^{-/-}$cγ$^{-/-}$ mice received a human skin graft and 3 days later were injected intraperitoneally with $2x10^6$ (n=8 mice), $5x10^6$ (n=10 mice) or $10x10^6$ (n=10 mice) human PBMC allogeneic to the skin graft donor. A further group did not receive any cells (n=5 mice). Skin grafts were monitored until rejection or long-term survival, specified as survival over 100 days. Mice receiving PBMC that did not achieve human leukocyte chimerism levels of >1% in the spleen were excluded from the analysis. Data are pooled from n=4 separate assays using a different PBMC and skin donor combination for each assays. The MST was calculated for each group. **(c)** Representative photograph of a human skin graft from a mouse not receiving cells at day 100 post-transplantation. **(d)** Representative photograph of a human skin graft from a mouse receiving $5x10^6$ PBMC, taken at the point of rejection, 35 days after transplantation.

Figure 3.5. Reconstitution levels and rates in BALB/c-Rag2$^{-/-}$cγ$^{-/-}$ mice receiving human PBMC.

BALB/c-Rag2$^{-/-}$cγ$^{-/-}$ mice received a human skin transplant and were then injected with 2x10^6 (n=12 mice), 5x10^6 (n=12 mice) or 10x10^6 (n=12 mice) human PBMC allogeneic to the skin graft donor. Mice were harvested at rejection or long-term survival if rejection was not observed, and spleens analysed for the presence of human cells. For figures (a), (b) and (d), mice not achieving human leukocyte chimerism levels of >1% in the spleen were considered to have failed to reconstitute and were excluded from the analysis. **(a)** The percentage of live human 7AAD$^-$CD45$^+$ cells as a fraction of total live mononuclear cells (%huCD45$^+$) was determined in mouse spleens by FACS. **(b)** The total number of live human 7AAD$^-$CD45$^+$ cells in the spleen was determined by FACS. Data for (a) and (b) are represented as mean ±SD. 2x10^6 cells: n=8 mice, 5x10^6 cells: n=10 mice, 10x10^6 cells: n=12 mice. **(c)** Rate of failure of reconstitution. Mice not achieving human leukocyte chimerism (%huCD45$^+$) rates of >1% in the spleen were considered to have failed to reconstitute. **(d)** Animals were monitored for weight loss (>20% initial weight), hair loss, decreased activity, hunching and pallor (as a sign of anaemia) to determine the rate of development of XvHD per cell dose used.

Figure 3.6. Humanised BALB/c-Rag2$^{-/-}$cγ$^{-/-}$ mice reject human skin autografts with similar kinetics to human skin allografts.

(a) and (b) BALB/c-Rag2$^{-/-}$cγ$^{-/-}$ mice received a human skin graft and 3 days later were injected with 5x10^{6} autologous (i.e. derived from the same skin graft donor, n=5 mice) or allogeneic (n=6 mice) human PBMC. Skin grafts were monitored for rejection and the MST for each group calculated. **(c)** Representative photomicrograph of a human skin autograft harvested 28 days post-transplantation and stained by immunohistochemistry for human CD45^{+} cells and counterstained with haematoxylin. The histology shown is representative of 6 stained sections from each of n=4 mice from n=2 independent assays. **(d)** BALB/c-Rag2$^{-/-}$cγ$^{-/-}$ mice received a skin graft from a BALB/c mouse and 3 days later received an intraperitoneal injection of 5x10^{6} BALB/c splenocytes (n=3 mice) or no cells (n=3 mice). Skin grafts were monitored for rejection.

Figure 3.7. Schematic for the humanised mouse model of 'healed in' human skin rejection.

Model for assays that follow in this thesis. BALB/c-Rag2$^{-/-}$cγ$^{-/-}$ mice receive a human skin graft measuring 1x1cm, followed 5 weeks later by an intraperitoneal injection of 5x10^{6} human PBMC to reconstitute their immune systems to levels of human leukocyte chimerism of >1% in the spleen or >0.1% in the peripheral blood. Human skin grafts are monitored for survival and mice are optionally tail-bled for time-course analysis of peripheral human cellular reconstitution. Mice are sacrificed for analysis at the point of skin graft rejection (to avoid the later development of xenograft-versus-host disease), or at 100 days (termed long-term survival). Optionally mice may be sacrificed at a time point prior to skin graft rejection for a specific analysis.

Figure 3.8. Humanised BALB/c-Rag2$^{-/-}$cγ$^{-/-}$ mice do not reject skin autografts if the skin graft is allowed to heal for a period of 5 weeks before cellular adoptive transfer.

(a) and (b) BALB/c-Rag2$^{-/-}$cγ$^{-/-}$ mice received a skin transplant and 5 weeks later were injected with 5x10^6 autologous (i.e. derived from the skin graft donor, n=7 mice) or allogeneic (n=9 mice) human PBMC. Skin grafts were monitored for rejection and the MST for each group calculated. Two mice required euthanasia at days 72 and 76 due to the development of XvHD although skin grafts were not rejected. **(c)** Representative photomicrograph of a human skin autograft allowed to heal for 5 weeks before adoptive transfer of PBMC, harvested 28 days post-adoptive transfer and stained by immunohistochemistry for human CD45$^+$ cells and counterstained with haematoxylin. The histology shown is representative of 6 stained sections from each of n=4 skin grafts from n=2 different donors. **(d)** Mice from the survival assay were analysed further. At the point of rejection (for mice reconstituted with allogeneic PBMC, n=4 mice) or long-term survival (for mice reconstituted with autologous PBMC, n=4 mice), spleens were harvested and the number of live human 7AAD$^-$CD45$^+$ cells per spleen assessed by FACS. There was no significant difference in cell numbers between the two groups (p=0.5163). Data are represented as mean ±SD, p=0.5163. **(e)** BALB/c-Rag2$^{-/-}$cγ$^{-/-}$ mice received a human skin transplant and 5 weeks later were reconstituted with 5x10^6 autologous (n=3 mice) or allogeneic (n=4 mice) PBMC. At day 21 post-cellular adoptive transfer, mice were sacrificed and skin graft-draining axillary and contralateral axillary lymph nodes harvested for quantification of live human 7AAD$^-$CD45$^+$ (huCD45$^+$) cells by FACS. There were significantly more huCD45$^+$ cells in the skin graft-draining compared with the contralateral lymph nodes in mice receiving allogeneic PBMC (p=0.0418) but not those receiving autologous PBMC (p=0.9383). Data are represented as mean ±SD.

Figure 3.9. Human skin allografts that are allowed to heal for 5 weeks reject with slower kinetics than those that are allowed to heal for 3 days.

(a) and (b) Pooled data from multiple skin survival assays presented in this study using 18 distinct skin and PBMC donor combinations. BALB/c-Rag2$^{-/-}$cγ$^{-/-}$ mice received a skin transplant and 3 days later ('no healing', n=40 mice) or 5 weeks later ('with healing', n=55 mice) were injected with 5x10^{6} allogeneic human PBMC. HLA-A, HLA-B, HLA-DR and HLA-DQ mismatches between skin and PBMC donors in each assay ranged from a total of 4 mismatches to 8 mismatches, with a median of 7 mismatches and mean of 6.26 mismatches. A further group of mice received a skin graft that was allowed to heal for 5 weeks followed by an injection of RPMI-1640 medium only ('no cells', n=10 mice). Time is calculated from the point at which mice received the injection of cells or medium. Skin grafts were monitored for rejection and the MST for each group calculated. Healed skin allografts survived for significantly longer than unhealed skin allografts, p<0.0001. **(c)** Representative photograph of a skin graft from a mouse that did not receive any cells, taken at day 135 post-transplantation. **(d)** and **(e)** Representative photographs of skin grafts from mice that received a skin graft that was allowed to heal for 5 weeks before adoptive cellular transfer of 5x10^{6} allogeneic PBMC. Photographs are taken at the point of rejection showing changes including erythema, swelling, shrinking and loss of human skin allografts.

Figure 3.10. The degree of HLA mismatch between skin and PBMC donor does not significantly alter the kinetics of rejection.

Pooled data are presented from multiple assays performed in this thesis. BALB/c-Rag2$^{-/-}$cγ$^{-/-}$ mice received a human skin transplant and 5 weeks later an adoptive transfer of 5x10^{6} PBMC from a donor allogeneic to the skin graft donor. 19 separate groups of mice (minimum n=3 mice per group) were transplanted using a distinct skin and PBMC donor combination for each group of mice. The MST for each group of mice was calculated. PBMC and skin graft donors were tissue typed and the number of HLA mismatches between PBMC donor and skin graft donor calculated for each group across the HLA loci of HLA-A, HLA-B, HLA-DR and HLA-DQ. The number of HLA mismatches is shown plotted against the MST for that particular group for: **(a)** mismatches in the HLA-A locus; **(b)** mismatches in the HLA-B locus; **(c)** mismatches in the HLA-DR locus; **(d)** mismatches in the HLA-DQ locus; and **(e)** total mismatches across HLA-A, HLA-B, HLA-DR and HLA-DQ. There was no significant reduction in MST with increased total HLA mismatches (p=0.5703, with total mismatches ranging from 4 to 8 and a median of 7 HLA mismatches) or with increased mismatches in any one particular locus (HLA-A: p=0.1043, HLA-B: p=0.7853, HLA-DR: p=0.6823, HLA-DQ: p=0.2877, with 1 or 2 mismatches in each locus apart from HLA-A where mismatches ranged from 0 to 2).

Figure 3.11. Reconstitution analysis of BALB/c-Rag2$^{-/-}$cγ$^{-/-}$ mice receiving a human skin graft and 5x10^{6} allogeneic PBMC.

BALB/c-Rag2$^{-/-}$cγ$^{-/-}$ mice received a human skin transplant and 5 weeks later were reconstituted with 5x10^{6} allogeneic PBMC. **(a)** Peripheral blood of mice was monitored for the percentage of live human 7AAD^{-}CD45^{+} cells as a fraction of the total live mononuclear cell population (%huCD45^{+}) over time (n=36 mice). Data are represented as mean ±SD and are pooled from n=9 assays with a distinct skin and PBMC donor combination for each assay. **(b)** At the point of skin graft rejection %huCD45^{+} was measured in the spleen, peripheral blood, and skin graft-draining and contralateral axillary lymph nodes (n=4 mice). Data are represented as mean ±SD. **(c)** %huCD45^{+} and **(d)** total human CD45^{+} cell numbers from cellular preparation of spleens taken at the point of skin graft rejection from BALB/c-Rag2$^{-/-}$cγ$^{-/-}$ mice which had received a human skin graft and 5x10^{6} allogeneic PBMC 5 weeks later. Each B-number represents a separate skin rejection assay where a particular skin and PBMC donor was used (minimum n=3 mice per group). Also shown are pooled data from all of these assays combined (n=29 mice). Data are represented as mean ±SD. **(e)** The number of HLA mismatches (across HLA-A, B, DR and DQ) between skin and PBMC donors and the respective MST is shown for each group of mice.

Figure 3.12. Phenotypic changes of human leukocytes post-engraftment in BALB/c-Rag2$^{-/-}$cγ$^{-/-}$ mice.

Human PBMC preparations (n=12 separate donors) were phenotyped before injection of 5x10^6 cells into BALB/c-Rag2$^{-/-}$cγ$^{-/-}$ mice that had received an allogeneic skin transplant 5 weeks prior. At the point of skin graft rejection, mice were sacrificed and human cells in cellular preparations from spleens or peripheral blood phenotyped (n=22 spleens from 6 separate skin and PBMC donor combinations). **(a)** The mean proportion of human CD3$^+$ and CD19$^+$ cells of total live human 7AAD$^-$ CD45$^+$ pre-injection and in mouse spleens at the point of rejection. **(b)** The mean proportion of human CD4$^+$ and CD8$^+$ cells of total live human 7AAD$^-$CD45$^+$CD3$^+$ cells in PBMC pre-injection and in mouse spleens at the point of rejection. **(c)** The proportion of 7AAD$^-$CD45$^+$CD3$^+$ human cells that express CD45RO pre-injection and in the peripheral blood of mice at the point of rejection. Data are represented as mean ±SD. ****:p<0.0001 **(d)** BALB/c-Rag2$^{-/-}$cγ$^{-/-}$ mice received a human skin transplant and 5 weeks later were reconstituted with 5x10^6 allogeneic PBMC (n=20 mice from 5 separate skin and PBMC donor combinations). Peripheral blood was monitored for 8 weeks post adoptive transfer for the proportions of human CD4$^+$ and CD8$^+$ cells of human 7AAD$^-$CD45$^+$CD3$^+$ cells. Data are represented as mean ±SEM. **:p=0.0067 (two-way ANOVA).

Figure 3.13. Phenotypic changes of human leukocytes post-engraftment in BALB/c-Rag2$^{-/-}$cγ$^{-/-}$ mice.

Representative FACS dotplots. Human PBMC was phenotyped before injection of 5x10^{6} cells into BALB/c-Rag2$^{-/-}$cγ$^{-/-}$ mice that had received an allogeneic skin transplant 5 weeks prior. At the point of skin graft rejection, mice were sacrificed and human cells in cellular preparations from spleens phenotyped. **(a)** Pre-injection human CD3^{+} and CD19^{+} cells as proportions of all live lymphocytes. **(b)** Pre-injection CD4^{+} and CD8^{+} cells as proportions of human 7AAD^{-}CD45^{+}CD3^{+} cells. Dotplots are representative of data from n=12 different PBMC donors. **(c)-(e)** Cellular preparations from mouse spleens at the point of rejection showing live human 7AAD^{-}CD45^{+} cells as a percentage of all live mononuclear cells; human CD3^{+} and CD19^{+} proportions of live human 7AAD^{-}CD45^{+} cells; and human CD4^{+} and CD8^{+} cells as proportions of human 7AAD^{-}CD45^{+}CD3^{+} cells. Dotplots are representative of data from n=22 spleens from n=6 independent assays.

CHAPTER 4: CHARACTERISTICS OF HUMAN SKIN REJECTION AND FURTHER MODEL ENHANCEMENT

4.1 Introduction

In contrast to SOTs, data relating to the histological changes in human skin rejection are limited. There are only a few case reports of the changes that occur in the rejection of skin in VCA transplants and a Banff classification has been published, although the classification is still evolving[8,9,12,434,494]. The most recent Banff meeting took place in April 2011, however the consensus from this meeting is still not publically available. The current Banff 2007 classification is reproduced with permission below[434]:

Table 1: The Banff 2007 working classification of skin-containing composite tissue allograft pathology

Grade 0. No or rare inflammatory infiltrates.
Grade I. Mild. Mild perivascular infiltration. No involvement of the overlying epidermis.
Grade II. Moderate. Moderate-to-severe perivascular inflammation with or without mild epidermal and/or adnexal involvement (limited to spongiosis and exocytosis). No epidermal dyskeratosis or apoptosis.
Grade III. Severe. Dense inflammation and epidermal involvement with epithelial apoptosis, dyskeratosis and/or keratinolysis.
Grade IV. Necrotizing acute rejection. Frank necrosis of epidermis or other skin structures.

1398 *American Journal of Transplantation* 2008; 8: 1396–1400

Clearly, many of these changes are non-specific and may have a wide range of differential diagnoses[494]. Additionally, the role of antibody in skin graft rejection is unclear. While significant levels of C4d deposits have not been identified in VCA transplants[6,495], a few cases of neointimal hyperplasia have been reported (*section 1.2.2*), although whether these are true cases of CAD is still up for debate. Given the rarity of VCA transplantation, there is a particular need for an experimental model in which skin rejection may be examined without direct patient participation.

In the previous chapter we developed a reliable model of human skin rejection. This model now provides a unique opportunity to characterise in more depth the histological changes that occur during rejection as well as to examine the elements of the alloresponse that develop against skin.

Firstly, we hypothesise that passenger leukocytes within the skin graft contribute to its immunogenicity. Secondly, we examine whether skin cells in our model express HLA Class II that may facilitate direct allorecognition. We then examine the histological profile of skin rejection in terms of microarchitectural changes and the character of the cellular infiltrates in order to assess whether changes are consistent with clinical observations in VCA transplantation. Finally, we investigate the role of human antibody in the model, subsequently evaluating alternative humanised models that may provide more efficient engraftment of human B cells together with higher levels of immunoglobulin production.

4.1.1 Chapter aims

There are two principal aims to this chapter. The first is to characterise the histological changes, cellular responses and antibody responses to the human skin allograft in the model developed in *Chapter 3*. The second is to develop the model further to improve the engraftment and function of human B cells.

4.2 Impact of resident human skin leukocytes

Human skin contains a high density of resident leukocytes[195,212]. Moreover, these potential APCs migrate out of the graft after only a few hours post-transplantation in an alloantigen-independent manner[64]. These 'passenger leukocytes' present antigen via the direct pathway and are therefore important in the alloresponse as demonstrated by the delayed rejection of APC-depleted rat renal allografts[73,74].

We therefore looked to establish whether the human skin transplanted in our model contains leukocytes, and whether these cells may then leave the skin and survive in the mouse to subsequently provide a source for direct allorecognition. Human skin grafts were therefore stained by immunohistochemistry for the presence of human $CD45^+$ cells, which were found to be present throughout the epidermis and dermis (***Figure 4.1a***). We then looked to ascertain whether these cells could migrate from the skin graft after transplantation and engraft within an immunodeficient BALB/c-$Rag2^{-/-}c\gamma^{-/-}$ mouse. Two groups of mice were transplanted with a human skin allograft, and 5 weeks later one group received $5x10^6$ PBMC while the other group did not receive cells (RPMI-1640 medium only). Although human leukocytes were detectable in the spleens of mice not receiving any PBMC, the percentage chimerism achieved was low when compared to the levels achieved with an adoptive transfer of PBMC (36.9% SD±23.1 for PBMC compared with 0.3% SD±0.2 for no cells, p=0.0194 ***Figure 4.1b***).

Nevertheless, these resident leukocytes may still play a role in T cell activation despite their low number. This will only be the case if they survive in humanised

mice where there is a possibility of cell killing by the allogeneic reconstituting PBMC. In an effort to determine whether this is the case we tracked skin passenger leukocytes in an assay where the skin donor was HLA-B8^{+} but the PBMC donor HLA-B8^{-}. Here, all skin cells expressed HLA-B8 (***Figure 4.2a***) and therefore any HLA-B8^{+} cells detected within the peripheral blood or spleen would have originated from the skin allograft. Two groups of mice therefore received a skin allograft from an HLA-B8^{+} donor and 5 weeks later one group received 5x10^{6} PBMC from an HLA-B8^{-} donor. As predicted, the proportion of human CD45^{+} cells that were HLA-B8^{+} in both the peripheral blood and spleen of mice receiving PBMC was much lower than the proportion in mice receiving no cells, where the only human cells present would necessarily be HLA-B8^{+} (***Figure 4.2b***). However, in terms of absolute numbers of CD45^{+}HLA-B8^{+} cells, there were similar numbers in both groups of mice, both in the peripheral blood and spleen (***Figure 4.2c***). This indicated that skin passenger leukocytes survive in the mouse even in the presence of allogeneic PBMC and may therefore act to present antigen by the direct pathway.

In rodent renal allograft rejection models, renal transplants that are depleted of passenger APC by 'parking' in an immunodeficient animal have markedly reduced immunogenicity and are not rejected promptly when retransplanted into a new animal[73,74]. We therefore hypothesised that skin grafts depleted of passenger leukocytes in the same manner would not reject, or reject at slower rates than skin grafts that are not depleted of passenger APC. BALB/c-Rag2$^{-/-}$cγ$^{-/-}$ mice received a fresh human skin graft and 5 weeks later an adoptive transfer of 5x10^{6} PBMC allogeneic to the skin graft donor (control 'non-depleted allografts'). Another set of

BALB/c-Rag2$^{-/-}$cγ$^{-/-}$ mice received human skin grafts from the same donor as the first group of mice, but which had been parked in a BALB/c-Rag2$^{-/-}$cγ$^{-/-}$ mouse for 100 days. Five weeks later this new set of mice received 5x10^{6} PBMC allogeneic to the skin graft donor, derived from the same PBMC donor as that used in the first group of mice ('depleted allografts'). Four 'depleted' human skin allografts analysed by immunohistochemistry for the presence of human CD45^{+} cells displayed very few remaining positive cells (***Figure 4.2d***). Mice not achieving human leukocyte chimerism levels of >1% in the spleen were excluded from the analysis. Surprisingly, skin grafts from both sets of mice rejected at similar tempos and MSTs (p=0.0953, ***Figures 4.2e and f***). These data suggest that passenger leukocytes are not significant contributors to the rejection response elicited following skin transplantation in this model.

4.3 Skin allografts in the humanised mouse model display standard histopathological features of human skin rejection

As discussed in *section 1.4*, skin ECs and epidermal cells are capable of expressing MHC Class II, thereby providing another opportunity for antigen exposure via direct allorecognition. We therefore asked whether human skin allografts in our model express HLA Class II post-transplantation, hence providing further alloantigens for direct allorecognition. We stained human skin grafts pre-transplantation for the presence of HLA-DR expressing cells, which were present in the epidermis and dermis (***Figures 4.3a and b***). Here the expression was restricted to a few interspersed cells, some of which are likely to be passenger leukocytes which migrate out of the graft after transplantation (***Figures 4.1 and 4.2***). However, post-

transplantation onto BALB/c-Rag2$^{-/-}$cγ$^{-/-}$ mice and in the absence of any PBMC, an increase in the expression of HLA-DR throughout the epidermis was observed (***Figure 4.3c***). Furthermore, many epidermal cells displayed surface HLA-DR (***Figure 4.3c*** enlarged box). In mice reconstituted with PBMC, skin HLA-DR expression in the epidermis was similar to that in mice receiving no adoptive transfer of cells (***Figure 4.3d***). However, in mice receiving PBMC, clusters of HLA-DR^{+} cells were visible in the dermis (***Figure 4.3d*** arrow). These cells are likely to be infiltrating leukocytes from reconstituting PBMC (***Figure 4.5***).

The histopathological evaluation of human skin rejection is a field that is still in its infancy. We therefore sought to determine what histopathological changes occur in human skin allograft rejection in our standard model. While it is important that any changes correlate with what has been observed clinically, the model may also serve to study the histopathological features of rejection in further depth. In skin harvested from mice 40 days post-adoptive transfer of PBMC, a standard H&E stain revealed clear microarchitectural changes. These included a marked thickening and dyskeratosis of the stratum spinosum of the epidermis and sloughing off of the most superficial layers of the epidermis, as well as a dense dermal cellular infiltrate with some aggregation around microvessels (***Figure 4.4a***). At higher magnification marked thinning of the strata corneum and lucidum was observed (***Figure 4.4b***). Evidence of apoptosis with vacuolation of cells was also observed in some allografts, together with dermo-epidermal junctional destruction and a saw-tooth appearance of the dermo-epidermal junction (***Figure 5.12a***). Together these changes are indicative of Grade III/IV Banff 2007 rejection and are consistent with changes

observed in human skin rejection[8,9,12,434,456,467,494]. For an analysis of the changes in skin microvasculature that occur with rejection please refer to *section 5.7* and ***Figure 5.13***.

4.4 A human T cell response develops against human skin allografts

The character and phenotype of the cellular infiltrate initially noted in ***Figure 4.4a*** was then analysed. At 40 days post-adoptive transfer of allogeneic PBMC, a very dense human leukocytic infiltrate was present in human skin transplants, generally confined to the dermis but in some cases extending into the dermo-epidermal junction and epidermis (***Figure 4.5a*** with PBMC *cf.* ***Figure 4.5d*** with no PBMC). This is consistent with previous observations in human skin rejection, where infiltrates were generally confined to the dermis, extending to the dermo-epidermal junction and epidermis in more severe cases[434,494]. The number of $CD45^+$ cells in skin grafts from mice receiving PBMC was over 10 times the number of resident $CD45^+$ cells present in skin grafts from mice not receiving PBMC ($p<0.0001$, ***Figure 4.5e***). The majority of these infiltrating cells were in the dermis, with occasional clustering around dermal vessels and some interface dermatitis leading to epidermal infiltrates.

As expected, these cells were exclusively $CD3^+$ given that the vast majority of reconstituting cells in our humanised mice are T cells. This is consistent with findings from other humanised mouse studies[447,457,458,494]. No B cells ($CD19^+$) or macrophages ($CD68^+$) cells were detected within the skin grafts. Skin grafts were infiltrated with

both $CD4^+$ (***Figure 4.5b***) and $CD8^+$ (***Figure 4.5c***) cells. On quantification roughly half of the infiltrating human leukocytes were $CD4^+$ and half $CD8^+$ (***Figure 4.5e***), despite $CD8^+$ cells predominating in the peripheral blood (***Figure 3.12d***). However $CD4^+$ cells were generally confined to the dermis, with only $CD8^+$ cells entering the epidermis (***Figures 4.5b and c***).

With the knowledge that the MST of these skin grafts is 35 days (***Figure 3.9b***), and that the peak of human leukocyte chimerism occurs at the same time (***Figure 3.11a***), it was not surprising that intragraft human *CD3* mRNA levels increased significantly between days 21 and 40 post-adoptive transfer of PBMC ($p<0.05$, ***Figure 4.5f***). In contrast intragraft *CD3* mRNA levels in skin grafts from mice not receiving PBMC or skin grafts pre-transplantation were low (***Figure 4.5f***). Interestingly however, human *IFNG* (the gene encoding IFNγ) mRNA was detectable as early as day 21, increasing significantly by day 40 in comparison to mRNA levels in skin from mice receiving no cells, or skin pre-transplantation (***Figure 4.5g***). IFNγ is a key $CD4^+$ Th1 and $CD8^+$ cell cytokine involved in the alloresponse (as discussed in *section 1.3.6.1a*), and these data suggest that the effector response begins long before the peak in the cellular infiltrate.

4.5 The mouse innate response to human skin allografts is not functionally significant

BALB/c-$Rag2^{-/-}c\gamma^{-/-}$ mice are lacking in T, B and NK cells and are therefore receptive hosts for the engraftment of human cells (see *section 1.7*). However, despite major

immunodeficiencies, these mice still produce granulocytes which may have an impact on the human skin graft in our model. In a recent humanised mouse study utilising NSG mice, a substantial mouse GR-1$^+$ (granulocyte differentiation antigen-1) granulocytic infiltrate was observed in human skin grafts from mice that had not been reconstituted with human cells, and this infiltrate was active in the destruction of the human skin grafts[455]. We therefore looked to determine whether a similar intragraft infiltrate is present in our model and if so, whether it impacts the rejection of the skin grafts. We analysed human skin grafts for the presence of mouse GR-1$^+$ cells, 40 days post adoptive transfer in mice that received either 5x10^6 allogeneic PBMC or no cells (RPMI-1640 medium only). Mice receiving PBMC that did not achieve human leukocyte chimerism levels of >1% in the spleen or >0.1% in the peripheral blood were excluded from the analysis. In contrast to the reported study in NSG mice, a substantial mouse GR-1$^+$ infiltrate was only observed in skin grafts from mice that received PBMC and not in mice that did not receive human cells (***Figure 4.6a***). In skin from mice receiving PBMC, the mouse GR-1$^+$ cellular infiltrate was confined to the dermis and hypodermis (***Figure 4.6b and c***).

We then asked what impact the granulocytic infiltrate exerted on the survival of human skin grafts in mice reconstituted with allogeneic human PBMC. Mice transplanted with human skin allografts received α-mouse GR-1 mAb (RB6.8C5 clone) or isotype control antibody (rat IgG) every 3-4 days (as previously described[341,455]), and 5 weeks later received an adoptive transfer of 5x10^6 allogeneic PBMC. A control group was included where mice received neither cells nor antibody. Mice receiving PBMC but not achieving human leukocyte chimerism levels

of >1% in the spleen were excluded from the survival analysis. In mice receiving α-mouse GR-1 antibody, depletion of mouse GR-1^+ cells was confirmed by flow cytometry (***Figures 4.7a and b***). 21 days after adoptive transfer of PBMC, a reduction of intragraft mouse GR-1^+ cells was observed in mice receiving the α-mouse GR-1 antibody (***Figure 4.7c***). Most importantly, there was no significant difference between the MST of human skin grafts on mice that had received α-mouse GR-1 antibody and mice that had received control antibody (***Figures 4.7d and e***), indicating that the intragraft mouse GR-1^+ cellular infiltrate is inconsequential in comparison to the human alloresponse. Furthermore, routine depletion of mouse GR-1^+ cells is not necessary in this model.

4.6 NSG mice are not better hosts than BALB/c-Rag2$^{-/-}$cγ$^{-/-}$ mice in the humanised mouse skin transplantation model

Despite the requirement for GR-1^+ cell depletion in NSG mice, there have been reports that this strain is a more efficient host for human cellular engraftment[468]. In order to optimise further the humanised mouse skin transplantation model, we asked whether a lower number of PBMC might be used to induce human skin allograft rejection in NSG mice. Three groups of NSG mice therefore received a human skin transplant, with one group receiving $5x10^6$ allogeneic PBMC, another $2.5x10^6$ allogeneic PBMC, and the third group not receiving an adoptive transfer of cells. All mice receiving PBMC attained levels of human chimerism of >1% in the spleen and were therefore included in the survival analysis. While $5x10^6$ PBMC led to reliable destruction of the skin allografts, $2.5x10^6$ cells induced rejection in only 3

out of 4 skin grafts (***Figures 4.8a and b***). This echoes observations in BALB/c-Rag2$^{-/-}$cγ$^{-/-}$ mice where although 2x10^{6} PBMC may achieve adequate human leukocyte chimerism levels, rejection is not reliably observed (***Figure 3.4a***). In mice receiving 5x10^{6} PBMC, a marked dermal and hypodermal mouse GR-1^{+} infiltrate was noted (***Figure 4.8c***) as well as a pronounced human CD4^{+} and CD8^{+} T cell infiltrate (***Figure 4.8d***). NSG mice therefore appear to be equivalent to BALB/c-Rag2$^{-/-}$cγ$^{-/-}$ mice in terms of the number of PBMC required to induce skin rejection reliably, with both models requiring 5x10^{6} PBMC in order to achieve reliable rejection (***Figure 4.8a*** for NSG mice and ***Figure 3.4a*** for BALB/c-Rag2$^{-/-}$cγ$^{-/-}$ mice). Nevertheless, in mice receiving no cells, one skin graft was lost (***Figure 4.8a and b***), and on histological examination of this skin graft a marked mouse GR-1^{+} infiltrate was seen (***Figure 4.8c***). This observation echoes that of Racki and colleagues[455], where in contrast to BALB/c-Rag2$^{-/-}$cγ$^{-/-}$ mice, NSG mice develop a damaging and occasionally destructive mouse anti-human skin granulocytic response. BALB/c-Rag2$^{-/-}$cγ$^{-/-}$ mice therefore represent the best option at present for the modeling of human skin transplant rejection.

4.7 Humanised BALB/c-Rag2$^{-/-}$cγ$^{-/-}$ mice do not produce human allospecific α-HLA immunoglobulin

The bulk of reconstituting human leukocytes in our model are T cells (***Figure 3.12a***) and the only skin-infiltrating cells are CD3^{+}, indicating that the principal response to the skin allograft is T cell based in the humanised BALB/c-Rag2$^{-/-}$cγ$^{-/-}$ mouse model. Nevertheless, we looked to ascertain whether the very small percentage of

engrafting B cells in mice reconstituted with PBMC (0.1% SD±0.1%, ***Figure 3.12a***) were producing human IgM or IgG. Serum from mice reconstituted with $5x10^6$ PBMC that had rejected a human skin allograft and control serum from mice that did receive human cells was analysed for the presence of human IgG and IgM. Surprisingly, significant amounts of human IgG and IgM were detectable in mice receiving PBMC at levels of approximately 10% of that normally found in healthy human adults[496] (***Figure 4.9a***).

We then asked whether this human immunoglobulin was significant in terms of the alloresponse generated towards the human skin graft. In order to be relevant to the alloresponse, human IgG produced would need to be allospecific for HLA molecules expressed by the skin graft. As a primary screen, a Luminex® assay using multiplexed beads was performed to determine whether any immunoglobulin was specific for a range of HLA molecules[497]. Luminex® assays were performed in collaboration with Dr Susan Fuggle at the Oxford Transplant Centre Histocompatibility and Genetics Laboratory. The assay used 18 separate serum samples containing significant levels of human IgG confirmed by ELISA, from humanised mice that had rejected a human skin allograft. None of the samples achieved a level of fluorescence indicative of positivity for either α-human HLA Class I (***Figure 4.9b***) or α-human HLA Class II (***Figure 4.9c***). The role of antibody in promoting rejection in skin transplantation is not clear. C4d deposition has not been detected in skin from VCA transplants[495] and no well-defined cases of AMR have been reported[6].

Given that the human immunoglobulin was not specific for HLA molecules, we hypothesised that the antibody was developing as part of the anti-mouse xenoresponse. We therefore devised a flow cytometry based assay where cells with target antigen were incubated with serum from humanised mice, which were subsequently incubated with an α-human IgG Fc-fragment PE fluorochrome-coupled antibody to detect cells with bound human IgG immunoglobulin. To confirm that the assay would provide adequate specificity, monoclonal human antibodies against human HLA-A1 or HLA-B12 were incubated with HLA-A1 expressing human PBMC followed by the α-human IgG Fc-fragment fluorescent antibody. In this assay, only cells incubated with the α-human HLA-A1 antibody were positive by flow cytometry (***Figures 4.10a and b***), confirming the specificity of the assay.

Splenocytes from BALB/c-Rag2$^{-/-}$cγ$^{-/-}$ mice, human PBMC or splenocytes from Sprague Dawley rats (SD rats) were then each incubated with serum from humanised mice containing 5, 25, or 125μg human IgG (as measured by specific ELISA). Human PBMC used in the assay were obtained from a donor allogeneic to the skin in order to act as a negative control. SD rat splenocytes were used in order to confirm that any positivity detected in the assay was specifically directed against BALB/c-Rag2$^{-/-}$ cγ$^{-/-}$ antigens and not a non-specific xenoresponse. Interestingly, a significant degree of positivity was detected with BALB/c-Rag2$^{-/-}$cγ$^{-/-}$ splenocytes, with only a small level of positivity with SD rat splenocytes and no positivity with human PBMC (***Figures 4.10c and d***). These data indicate that a specific human antibody-mediated anti-BALB/c-Rag2$^{-/-}$cγ$^{-/-}$ mouse xenoresponse develops. However the bulk of human immunoglobulin produced in these humanised mice is neither specific for human nor

mouse antigens, and may therefore represent the normal production of a baseline amount of immunoglobulin by human B cells.

4.8 Human HSC-transplanted BALB/c-Rag2$^{-/-}$cγ$^{-/-}$ mice achieve significant levels of peripheral human leukocytes chimerism

Given the singular bias towards a T cell response in our model, we looked to develop the humanised mouse skin transplantation model to improve the reconstitution levels of B cells, and consequently the human antibody rejection response. Reports have suggested that immunodeficient mice engrafted with human HSCs display improved reconstitution of B cells (with production of functional human IgM and IgG), macrophages, DCs, NK, and NKT cells[468,476,498,499]. Furthermore, there is a theoretical advantage that T cells developing from HSCs in the mouse will be negatively selected against mouse MHC in the thymus, therefore reducing the risk of XvHD development. CD34 is a reliable marker for the isolation of HSCs from human UCB[499,500].

Based on protocols from previous studies, BALB/c-Rag2$^{-/-}$cγ$^{-/-}$ mice received 4 Gy myeloablative total body irradiation within 24 hours of birth to provide a niche for human HSC seeding[468,501,502]. This was followed by an intrahepatic injection of 5x10^4 CD34$^+$CD45$^-$Lin$^-$-enriched putative HSCs, a dose previously shown to be adequate for human leukocyte development *in vivo*[468,503]. CD34$^+$ cells were derived from human UCB from a single donor by magnetic bead isolation, to a purity of over 92%. Post-transplantation into mice, human CD34$^+$ cells seeded into the correct niche, with the

majority detectable in the bone marrow (***Figures 4.11a and b***). Four weeks post-HSC transplantation, peripheral blood was monitored for the number of human leukocytes (***Figure 4.11c***) as well as the percentage human leukocyte chimerism (***Figure 4.11d***). Chimerism was only detectable from week 6 post-HSC transplantation onwards and increased over time. However, overall chimerism levels were low in comparison to levels achieved using PBMC in the standard model (***Figure 3.11a***).

Given the low levels of human leukocyte chimerism, we hypothesised that the presence of a human skin graft allogeneic to the HSC donor, or the addition of $CD45^{+}CD34^{-}$ mononuclear cells (MNCs) derived from the same UCB unit from which the HSCs were derived would improve reconstitution levels. These approaches may improve reconstitution by providing antigen for activation and proliferation, or by providing mature cytokine-producing leukocytes to enhance HSC differentiation and proliferation, respectively. BALB/c-$Rag2^{-/-}c\gamma^{-/-}$ mice received 4 Gy myeloablative total body irradiation and an intrahepatic injection of $5x10^{4}$ $CD34^{+}CD45^{-}Lin^{-}$-enriched putative HSCs as above. Six weeks later mice received an allogeneic human skin graft. One group received no further cells and another group received an intraperitoneal injection of $5x10^{6}$ MNCs derived from the same UCB donor 5 weeks after skin transplantation, to allow for skin healing. Peripheral blood was then monitored from 9 weeks post-HSC engraftment onwards for the development of human leukocytes. ***Figure 4.12*** shows a schematic of the experimental plan. In the two groups of mice receiving a human skin graft, both the percentage human leukocyte chimerism (***Figure 4.13a***) and number of peripheral blood human

leukocytes (***Figure 4.13b***) peaked at week 15, and were still detectable at significant levels by week 19 (representative FACS plot, ***Figure 4.13c*** and ***Figure 4.13b***). Mice receiving a human skin graft or a human skin graft with MNCs had significantly higher human leukocyte numbers and chimerism levels at week 10 compared with mice without a skin allograft (***Figures 4.13d and e***). However in mice receiving a human skin allograft, the addition of MNCs was not associated with an additional improvement in either the numbers of human leukocytes or human leukocyte chimerism levels (***Figures 4.13d and e***, p=0.56 and p=0.91 respectively). The levels of human chimerism generated in these assays are higher than those attained in similar models using the same mouse strain but where no skin allograft was present[468], suggesting that the presence of the skin allograft is important in terms of human leukocyte development. Over the 19-week time period none of the mice developed XvHD, indicating that the developing leukocytes were either non-functional or negatively selected against mouse MHC during development.

4.9 Human HSC transplanted BALB/c-Rag2$^{-/-}$cγ$^{-/-}$ mice produce human T and B cells

Given the encouraging levels of human leukocyte chimerism attained in HSC-engrafted mice, we looked to determine whether these were developing into mature lymphocytes. In particular, we asked whether there was improved engraftment of B cells and whether these were functional in producing specific α-HLA antibody. The phenotype of reconstituting leukocytes was therefore analysed in the peripheral blood of the mice that received HSCs and a skin graft with or without

MNCs. Until week 15, the percentage and number of human leukocytes that were T cells remained low, after which a substantial increase was observed (***Figures 4.14a and b***). This late development of T cells has been observed in similar studies using NSG mice[503]. Moreover, in mice receiving MNCs, T cells eventually became the dominant engrafting leukocyte type. At week 19 the percentage of leukocytes that were T cells was significantly higher in mice receiving skin with MNCs compared with those receiving skin alone (p<0.0001, ***Figure 4.14a***), although there was no difference in overall numbers (***Figure 4.14b***). Interestingly, T cells developing in these mice ranged from double negative ($CD4^-CD8^-$) to double positive ($CD4^+CD8^+$) through to single positive ($CD4^+CD8^-$ or $CD4^-CD8^+$), as shown in the representative FACS plot in ***Figure 4.14c***, indicating that T cells were present at all three stages of development.

Importantly, B cell development in the HSC model was substantially improved compared with the PBMC humanised model. In mice receiving skin grafts with or without MNCs, approximately 80% of developing cells were B cells, although there was a decline after week 15 which coincided with the increase in T cell development (***Figures 4.15a and b***). Significantly more B cells by number (but not percentage) developed in mice receiving HSCs only, compared with those receiving HSCs with MNCs (p<0.05, ***Figure 4.15b***). Therefore, while the addition of MNCs improves the development of human T cells, this is at the relative expense of B cells. NK cells, NKT cells and DCs were not detectable in the mice, although a small number of peripheral blood $CD14^+$ human monocytes were detectable (range 0.1-1.1%; mean 0.4%, ***Figure 4.15c***).

We then asked whether the high level of B cell engraftment is accompanied with improved human IgG and IgM production *in vivo*. Serum from these mice was analysed by ELISA over a similar time period. Human IgG and IgM were only detectable at low concentrations from week 11 post-HSC transplantation onwards (***Figures 4.16a and b***). From week 15 onwards, there was a small increase in both IgG and IgM levels in mice receiving HSCs only, whereas in mice receiving HSCs with MNCs, a substantial increase in the production of human IgG, and to a lesser extent, IgM, was detected. Interestingly, the increases in serum immunoglobulin from week 15 onwards in both groups coincided with the appearance of T cells (***Figure 4.14a***).

The IgG immunoglobulin being produced in this system was analysed to determine its specificity for skin HLA antigens. Serum from mice in both groups underwent a Luminex® multiplexed bead assay with multiple antigen beads as a primary screen to determine whether any α-HLA antibody was present before progressing to single antigen bead testing based on the HLA type of the skin graft donor. In this assay, the only positive sample was from a mouse that received HSCs with MNCs. This sample displayed fluorescence with the HLA Class I bearing beads 7, 8, 69, 86, and 89 (***Figure 4.17***). The positivity of these beads indicated that the likely antibody present was against HLA-A9 (A23 and A24) as these antigens were present on all the positive beads. This was confirmed with a Luminex® single antigen bead assay. However the skin donor haplotype in our assay did not include HLA-A9, indicating that the α-HLA antibody present in this mouse was not specific for the skin allograft, and therefore most likely present due to a prior sensitisation such as a blood transfusion or

pregnancy. Therefore, despite enhanced engraftment of B cells in the HSC model, allospecific antibody is not generated.

4.10 Human HSC transplanted BALB/c-Rag2$^{-/-}$cγ$^{-/-}$ mice do not reliably reject human skin allografts

The ultimate test of *in vivo* function of the lymphocytes that had developed in our HSC model was whether they were capable of rejecting an allogeneic human skin allograft. Skin grafts were therefore monitored in the two groups of mice described above, i.e. those receiving HSCs alone or HSCs with MNCs, and the MST for each group calculated from the time of skin transplantation (***Figures 4.18a and b***). Mice that did not achieve human leukocyte chimerism levels of >1% in the spleen were excluded from the survival analysis. The MSTs for both groups of mice were longer than the MST of humanised mice receiving PBMC (***Figure 3.9b***). For the group receiving HSCs alone, rejection times were spread widely from 40 days to 81 days. More problematic was the fact that two skin grafts survived long term in mice receiving HSCs with MNCs. In a separate assay where mice received a skin graft and 5 weeks later were reconstituted with 5x10^6 UCB-derived MNCs alone without a HSC transplant, skin graft rejection was again not consistently observed over a narrow time frame (***Figure 4.18c***), despite achieving human leukocyte chimerism levels of >1% in the spleen. This suggests that MNCs lack the functional ability to induce skin graft rejection to the same degree as PBMC.

The majority of skin grafts in these HSC-engrafted mice were lost around week 15, the point at which there is a marked increase in both human T cell levels and human immunoglobulin levels (***Figures 4.14 and 4.16***). Whether these increases are a cause or a consequence of rejection is not clear. In order to help determine whether an alloresponse is developing, skin grafts from both groups of mice were analysed for the presence of a human skin infiltrate. Interestingly, in skin grafts from all mice, including those that were not ultimately rejected, there was a marked human leukocytic infiltrate. A representative photomicrograph of a rejected skin graft from a mouse not receiving MNCs shown is in ***Figure 4.18d***. In addition, the phenotype of these cells included T cells, B cells, $CD4^+$ cells, $CD8^+$ cells, as well as macrophages (***Figure 4.18e***). The HSC humanised mouse model therefore recreates a more complete picture of the human immune system, with T and B cells as well and blood monocytes and tissue macrophages. However, the functionality of these cells is not clear.

There is concern that T cells developing in these mice are mouse MHC restricted and therefore ineffective in a human alloresponse. Given their infiltration into human skin allografts and macroscopic appearances of rejection in some (but not all) skin grafts, they may still retain some limited functionality, but this is not reliable enough for our planned studies. As mice are already 'reconstituted' with human leukocytes from birth, there is no opportunity for skin grafts to heal before engraftment of human leukocytes. Inflammatory mediators from the unhealed skin graft may therefore recruit human leukocytes to the skin graft to cause damage through non-specific effector mechanisms rather than alloreactive mechanisms. B cells in

particular do not appear to be functional in the alloresponse, as the immunoglobulin produced is not directed against HLA antigens. For these reasons the remaining studies in this thesis were carried out using the standard PBMC model where the alloresponse is robust and reliable.

4.11 Discussion

The humanised system developed in this thesis is a model of T cell-mediated human skin rejection. Together, the data indicate that the predominant mechanism of antigen allorecognition is direct allorecognition of antigens on the skin graft. Human skin grafts express HLA Class II, which is increased post-transplantation (***Figure 4.3***), thus providing peptide-HLA complexes for direct allorecognition. These HLA molecules are present not only on ECs, but also on epidermal cells themselves. It is also possible that direct allorecognition of passenger APCs that escape the graft and appear in mouse tissues takes place, although rejection kinetics are not significantly altered when this mechanism is eliminated (***Figure 4.2e and f***). However, we cannot exclude the possibility that a few passenger leukocytes remain in the passenger leukocyte-'depleted' skin grafts, even after 100 days of parking, that are still able to stimulate T cells to the same degree. No human recipient-type DCs engraft in this model, implying that indirect allorecognition of HLA-peptide on professional APCs is not a significant element of the alloresponse. However, we also cannot exclude the possibility that engrafting recipient-type B cells, or even T cells, process antigen for presentation to T cells via the indirect pathway.

ECs are known to express HLA Class I and II as well as some T cell costimulatory molecules[171,172]. The majority of human T cells post-engraftment in the mouse acquire a memory phenotype[172,478,486] (***Figure 3.12c***). If primed via heterologous immunity, when these cells come into contact with ECs expressing their cognate antigen, they will respond by proliferating and producing inflammatory cytokines, eventually infiltrating the skin graft[172]. Naïve T cells may also receive the same signals from ECs expressing their cognate antigen. However, naïve T cells lack the integrins required for adhesion to ECs to allow their local recruitment[504]. Furthermore, ECs do not necessarily have the correct costimulatory molecules to provide naïve cells with a second signal, a requirement that may not be necessary for memory T cell activation. Memory T cells adhering to ECs after allorecognition of the peptide-HLA complex will be recruited into the tissue, whereas naïve T cells will not[172,200,201]. The deficiency of integrins on naïve cells indicates that they are only activated in secondary lymphoid tissues after interacting with professional APCs. In contrast, memory T cell responses are less controlled and allow for a prompt response against the allograft[172,504].

While naïve T cells may not respond in the same manner as memory T cells, they may be recruited to the skin graft through non-specific inflammatory mechanisms. In other humanised mouse models, human memory T cells have been shown to be the principal effector population, with naïve cells being ineffective at causing allograft damage[478]. Plausibly, this phenomenon stems from the requirement of engrafting T cells to recognise antigen directly on skin graft cells and subsequently for them to be activated without the assistance of signals from professional APCs.

Only memory T cells are able to do this. While passenger APCs from the graft may activate naïve cells, it appears that this mechanism is not significant in the current model. Alternatively, the mechanism may be active but swamped by the faster, more potent memory T cell response. A large number of cells are recruited to the allograft which may not all be alloreactive, and it is conceivable that some of these are recruited through non-specific mechanisms. This non-specific T cell recruitment may also be partly responsible for the infiltration and destruction of 'unhealed' human skin grafts by autologous PBMC (***Figure 3.6***).

The histological appearance of rejecting human skin allografts is consistent with what has been observed clinically (***Figure 4.4***). This is encouraging as it helps to confirm the clinical relevance of the model and provides a measure for quantification of damage to the allograft using the Banff 2007 system[434]. In *Chapter 5*, where immunoregulatory therapies are evaluated, the degree of protection of the allograft may be evaluated by histological means. Quantification of the degree of damage to the human skin graft microvasculature is another method employed in the next chapter.

Skin grafts are heavily infiltrated with human T cells, of both $CD4^+$ and $CD8^+$ phenotype at a ratio of approximately 1:1 (***Figure 4.5***). These figures are consistent with what has been reported in the literature for human skin rejection[505]. Skin grafts were progressively infiltrated with increasing numbers of cells with time, peaking around day 40, the time at which skin grafts are normally rejected. Beyond this point it is not possible to assess the level of infiltration of skin grafts with cells as

they become necrotic and unexaminable. However, although the peak of reconstitution and infiltration occurs around day 40, the presence of *IFNG* mRNA and low levels of *CD3* mRNA within the allograft at day 21 indicates that the alloresponse is already in progress earlier, at a time when reconstitution levels are still relatively low (***Figures 3.11 and 4.5***). A threshold level of reconstitution may be necessary to ensure complete allograft destruction. Once this is attained by 5-6 weeks, maximal infiltration levels are reached within the skin graft and reconstitution levels begin to plateau, as there is no more drive for T cell proliferation beyond homeostatic proliferation.

The granulocytic mouse innate response against the human skin allograft is inconsequential (***Figure 4.7***). This is a particularly important characteristic of our model, as the mouse innate response causes significant damage in NSG mice[455] (***Figure 4.8***). This difference may be due to different levels of residual mouse innate immunity between the two mouse strains. Differences in the innate immune activity of the various immunodeficient mouse strains used in humanised models is well recognised[506]. Moreover, a mouse GR-1^{+} infiltrate is only seen in BALB/c-Rag2$^{-/-}$cγ$^{-/-}$ mice reconstituted with PBMC, whereas in NSG mice the GR-1^{+} infiltrate is present even in the absence of PBMC. This may indicate that GR-1^{+} cells are more functional in NSG mice, whereas in BALB/c-Rag2$^{-/-}$cγ$^{-/-}$ mice human cytokines secreted by infiltrating T cells recruit mouse GR-1^{+} granulocyte to the skin graft. Many chemokines are conserved across species, making this a possibility[507]. We concluded from these data that BALB/c-Rag2$^{-/-}$cγ$^{-/-}$ mice remain the strain of choice for humanisation for the modeling of human skin graft rejection.

A specific antibody-mediated response towards human skin was not present in either the PBMC or HSC humanised models (***Figures 4.9 and 4.17***). Some antibody was xenoreactive against mouse antigens (***Figure 4.10***), indicating that the xenoresponse is not only T cell mediated as previously thought[483,484]. There was no advantage to immunoglobulin production levels using HSC instead of PBMC, despite the higher levels of B cell engraftment (***Figure 4.15***). In fact, mice receiving HSC alone had significantly lower levels of human IgG and IgM production compared to those receiving PBMC in the standard model (***Figure 4.9*** *cf.* ***Figure 4.16***). The addition of MNCs to HSC-engrafted mice resulted in the production of human IgG and IgM at levels similar to that produced in PBMC engrafted mice (***Figure 4.16*** *cf.* ***Figure 4.9***). Engrafting T cells in these mice that provide B cell help may be responsible for this effect, as the rise in human immunoglobulin concentration coincided with the increase in human T cell numbers (***Figure 4.14***). T cells from MNCs may be more mature than those developing from HSCs, therefore providing improved help to B cells and resulting in higher levels of immunoglobulin in these mice (***Figure 4.16***). The relative lack of human T cell development in mice receiving HSC alone may also explain the low levels of human immunoglobulin production in these mice.

In similar studies using HSC to produce functional human leukocytes in NSG mice, B cells were found to be present in functionally immature forms despite the production of IgG and IgM antibody[502,503]. Importantly, no donor-specific human antibody was detected in these studies or our model (***Figure 4.17***). While this may indicate a deficiency of proper B cell niches in immunodeficient mice for the

development of antigen-specific B cells, it is possible that antibody is simply not relevant in human skin rejection. Removal of B cells from the PBMC inoculate in a humanised SCID mouse model of skin transplantation such that human immunoglobulin does not develop does not alter the pattern of skin damage that takes place[508]. Clinically, there is no convincing evidence of CAD in VCA transplantation and there is no consistent evidence for the development of donor-specific antibody in patients[6,495].

Although the model using HSCs alone was not advantageous overall in terms of producing a reliable model of skin rejection (***Figure 4.18***), it may act as a framework for further model development. The presence of human leukocytes within skin grafts that are not ultimately rejected suggests that a response develops (***Figure 4.18***), although it is not powerful enough to cause significant skin damage. Alternatively, there may be a non-specific recruitment of cells to the graft but no true destructive alloresponse. Considering the higher levels of engraftment of B cells and monocytes together with infiltration of skin grafts with B cells and macrophages (***Figures 4.15 and 4.18***), this model may provide a foundation for the development of a humanised model where there is a more complete spectrum of reconstituting human leukocytes. Achieving this may require the *in vitro* maturation of UCB-derived MNCs to a phenotype closer to adult PBMC before injection, the injection of rhIL-7 *in vivo* to improve lymphocyte function[509], or the provision of human niches such as human foetal liver or thymus to allow improved progenitor development[498,510]. The role of such tissues would be to provide human HLA molecules for correct self-restriction of lymphocytes during development. Another

method may be the use of immunodeficient mice with transgenic expression of human HLA genes[511]. Expression of human HLA molecules in the mouse thymus would allow HLA-restriction of developing thymocytes.

However, in the current HSC-humanised model, developing lymphocytes may be selected against mouse MHC in the mouse thymus, essentially producing human cells that are 'xenoreactive' against human HLA. This would make them ineffective at the allorecognition of HLA on human skin. This absence of the correct niche for progenitor development may also be responsible for the lack of significant human T cell development (***Figure 4.14***), which only occurs late post-transplantation. The improved development of human leukocytes in HSC-humanised mice engrafted with human skin compared with those not receiving a human skin graft may indicate that the presence of HLA molecules on skin grafts provides signals to assist in the activation and proliferation of human cells (***Figures 4.13d and e***). Alternatively, the improved levels may be related to the quality of the particular HSCs used in this assay, given that the comparison made between mice receiving skin and those not receiving skin also used different HSC donors. Using the same HSC donor for all assays is not possible as not enough cells are isolated per UCB unit. Therefore in order to confirm the findings, the assay would need to be repeated and data pooled from multiple HSC donors. The late appearance of T cells in HSC-engrafted mice is a recognised phenomenon, although the cause is unclear[503].

Interestingly, skin grafts were rejected at late time points with a wide variation in the graft loss times between individual mice in each group. Skin grafts were rejected

over a much longer time period than in mice engrafted with PBMC, and the overall responses appeared less vigorous macroscopically (*personal observation*). The appearance of T cells coincided with the rejection of skin grafts (***Figures 4.14 and 4.18***), suggesting that the effector response is mainly T cell-mediated, albeit weak and inconsistent. The theoretical lack of HLA-restricted T cells may explain their ineffectiveness at inducing skin rejection, even though they reach significant levels after week 15 post-HSC injection. Other studies have also noted a reduced functionality of human lymphocytes in HSC-engrafted mice[503]. Given the late development of T cells, this model may be more useful if skin grafting is delayed to week 15 after HSC inoculation, although this would require further investigation.

Interestingly, the inoculation of HSC-engrafted mice with UCB-derived MNCs did not improve chimerism levels, possibly indicating a 'saturation' point for human leukocyte development in the model (***Figure 4.13***). In addition, MNCs alone did not reliably induce the rejection of human skin grafts *in vivo* (***Figure 4.18***). These data suggest that MNCs may contain or produce cells that are consistently functional in an alloresponse. Reasons may include the lack of a threshold of cells of a certain precursor frequency that may respond to alloantigen. Alternatively, this may be due to a defect in the development of cells into functionally mature leukocytes, secondary to a deficiency in the necessary human lymphoid development niches[438]. Alternatively, it is possible that many cells develop into a regulatory population. Human cord blood contains a high percentage of $CD4^{+}FoxP3^{+}$ cells that are naïve in phenotype ($CD45RA^{+}$)[411]. Treg bearing this naïve phenotype have been shown to proliferate more rapidly than those that are $CD45RA^{-}$[361]. $CD45RA^{+}$ have also been

shown to be more suppressive both *in vitro* and *in vivo* than cells that are $CD45RA^-$ (Issa and Hester, *unpublished observations* and other studies[361]). Although the HSC model with or without MNCs exhibits features that are improvements on the standard PBMC model, it is ultimately unreliable in terms of producing robust human skin reject in its current form. For this reason, the remaining studies in this thesis utilise the standard PBMC model with 'healed in' skin.

Having developed a model of human skin graft rejection with clinically relevant features, and defined parameters that assist in the quantification of the destruction caused by the alloresponse, in the next chapter we focus on immunoregulatory therapies using human Treg to prevent the rejection of human skin grafts.

4.12 Figures and legends

Figure 4.1. Resident human leukocytes are present in human skin pre-transplantation but do not engraft in large numbers in BALB/c-Rag2$^{-/-}$cγ$^{-/-}$ mice in comparison with intraperitoneal injections of 5x10^{6} PBMC.

(a) Representative photomicrograph of a section of human skin stained pre-transplantation for human CD45^{+} cells by immunohistochemistry. Sections were counterstained with haematoxylin. The histology shown is representative of 6 stained sections from each of n=4 different mice from n=2 independent assays. **(b)** BALB/c-Rag2$^{-/-}$cγ$^{-/-}$ mice received a human skin graft and 5 weeks later an intraperitoneal injection of 5x10^{6} allogeneic PBMC (PBMC, n=4 mice) or no cells (No cells, n=4 mice). 40 days post-injection of cells, mice were sacrificed and spleens assessed for the presence of live human 7AAD^{-}CD45^{+} cells as a percentage of total live mononuclear cells (%huCD45^{+}). Data are represented as mean ±SD. *:*p*=0.0194.

Figure 4.2. Resident human leukocytes migrate from the human skin graft and survive in the host mouse in the presence of allogeneic PBMC.

(a) Representative photomicrographs of sections of human skin from an HLA-B8 positive donor and an HLA-B8 negative donor stained by immunohistochemistry for HLA-B8+ cells and counterstained with haematoxylin. The histology shown is representative of n=6 separate sections from each donor. Skin from an HLA-B8+ human donor was transplanted onto BALB/c-Rag2$^{-/-}$cγ$^{-/-}$ mice, which were injected 5 weeks later with 5x10^{6} allogeneic HLA-B8- PBMC (n=4 mice) or no cells (n=4 mice). 40 days later, mice were sacrificed and peripheral blood and spleens analysed for the presence of human CD45^{+}HLA-B8+ cells. **(b)** Percentage of HLA-B8+ cells of total human 7AAD^{-}CD45^{+} cells, and total number of human 7AAD^{-}CD45^{+}HLA-B8+ cells in the peripheral blood. **(c)** Percentage of HLA-B8+ cells of total human 7AAD^{-}CD45^{+} cells and total number of human 7AAD^{-}CD45^{+}HLA-B8+ cells in the spleen. Data are represented as mean ±SD. **(d)** BALB/c-Rag2$^{-/-}$cγ$^{-/-}$ mice received a human skin graft and no adoptive transfer of cells. 100 days later the human skin allografts were analysed for the presence of human CD45^{+} cells by immunohistochemistry. Sections were counterstained with haematoxylin. The histology shown is representative of 6 stained sections from each of n=4 mice from n=2 different donors. **(e)** BALB/c-Rag2$^{-/-}$cγ$^{-/-}$ mice received a human skin graft and 5 weeks later an adoptive transfer of 5x10^{6} allogeneic PBMC ('Non-depleted allografts'). Another set of BALB/c-Rag2$^{-/-}$cγ$^{-/-}$ mice received a human skin graft from the same donor as the other group of mice, but no adoptive transfer of human cells. 100 days later, the long-term surviving human skin grafts were removed from the mice and retransplanted on a fresh set of mice that 5 weeks later received 5x10^{6} allogeneic PBMC, derived from the same PBMC donor as that used in the first group of mice ('Depleted allografts'). Mice not achieving human leukocyte chimerism levels of >1% in the spleen were excluded from the survival analysis. Skin graft survival time was measured from the point of the adoptive transfer of cells for each respective group and **(f)** the MST calculated.

Figure 4.3. HLA Class II expression in human skin grafts transplanted onto BALB/c-Rag2$^{-/-}$cγ$^{-/-}$ mice.

Representative photomicrographs of human skin graft sections stained by immunohistochemistry for HLA-DR^{+} cells. **(a)** Pre-transplantation, HLA-DR^{+} cells are visible throughout the epidermis and dermis of human skin. **(b)** Skin section pre-transplantation incubated with an isotype control antibody. The histology shown is representative of 6 stained sections from each of n=4 mice from n=2 different skin donors.

BALB/c-Rag2$^{-/-}$cγ$^{-/-}$ mice received a human skin graft which was allowed to heal for 5 weeks before injection of mice with 5x10^{6} allogeneic PBMC or no cells (i.e. RPMI-1640 medium only). 21 days after the injections, skin grafts were harvested from both groups of mice and stained by immunohistochemistry for HLA-DR^{+} cells. Sections were counterstained with haematoxylin. **(c)** Skin from mice receiving RPMI-1640 medium only. **(d)** Skin from mice receiving 5x10^{6} allogeneic PBMC. A cluster of dermal HLA-DR^{+} cells is indicated with the arrow. The histology shown is representative of 6 stained sections from each of n=4 mice in each group, from n=2 different skin donors.

Figure 4.4. Microarchitectural changes of rejecting human skin in the humanised mouse model.

Representative photomicrographs of human skin graft sections stained with H&E. BALB/c-Rag2$^{-/-}$cγ$^{-/-}$ mice received a human skin graft which was allowed to heal for 5 weeks before adoptive transfer of 5x10^{6} allogeneic PBMC, or no cells. Skin grafts were harvested for analysis 40 days post-adoptive transfer of cells. The histology shown is representative of 8 stained sections from each of n=5 mice per group. **(a)** Low magnification, demonstrating thickening of the stratum spinosum layer of the epidermis (indicated by brackets) as well as dense dermal infiltrates and aggregates (indicated by left arrow). An area of cross-cut dermis is indicated with the right arrow. **(b)** High magnification, demonstrating thinning of the superficial layers of the epidermis, i.e. the strata corneum and lucidum (indicated by brackets).

Figure 4.5. Character of infiltrating human cells in rejecting human skin allografts.

(a)-(c) Representative photomicrographs of human skin graft sections stained by immunohistochemistry. BALB/c-Rag2$^{-/-}$cγ$^{-/-}$ mice received a human skin graft which was allowed to heal for 5 weeks before adoptive transfer of 5x10^6 allogeneic PBMC or no cells (RPMI-1640 medium only). The histology shown is representative of 6 sections for each type of stain for each of n=7 mice (or n=3 mice for those not receiving PBMC) from n=2 independent assays. Analysis was performed on skin grafts harvested from mice 40 days post-adoptive transfer of cells. Sections were counterstained with haematoxylin. **(a)** Human CD45$^+$ cellular infiltrate (huCD45) in mice receiving PBMC. **(b)** Human CD4$^+$ cellular infiltrate (huCD4) in mice receiving PBMC. **(c)** Human CD8$^+$ cellular infiltrate (huCD8) in mice receiving PBMC. **(d)** Human CD45$^+$ cells (huCD45) in human skin grafts at the same time point in mice not receiving an adoptive transfer of PBMC. **(e)** The number of graft infiltrating human CD45$^+$ (huCD45$^+$), CD4$^+$ (huCD4$^+$) and CD8$^+$ (huCD8$^+$) cells was quantified in skin grafts from mice receiving 5x10^6 PBMC (n=7 mice, at the point of rejection c. day 40) or no cells (n=3 mice, at day 100) by immunohistochemistry. Cells were counted in 3 random fields at 400X magnification in each of 4 separate sections for each skin graft, and the mean taken for each data point. Data are represented as mean ±SD. ****:p<0.0001. **(f)** At days 21 (n=4 mice) and 40 (n=5 mice) post-adoptive transfer of 5x10^6 PBMC, human skin grafts were analysed for the presence of human *CD3* mRNA by qPCR. Also shown is skin from a mouse receiving no cellular adoptive transfer, at day 40 (n=1 mouse). *:p<0.05. **(g)** At days 21 (n=6 mice) and 40 (n=8 mice) post-adoptive transfer of 5x10^6 PBMC, human skin grafts were analysed for the presence of human *IFNG* (IFNγ) mRNA by real-time quantitative PCR. Also shown is skin from a mouse receiving no cellular adoptive transfer, at day 40 (n=1 mouse). *:p<0.05. Target gene transcripts are normalised to the reference housekeeping gene *HPRT* (mRNA/*HPRT*). Data are represented individual data points and calculated means.

Figure 4.6. Rejecting human skin grafts are infiltrated with mouse GR-1$^+$ cells, which enter the dermis and hypodermis.

(a) BALB/c-Rag2$^{-/-}$cγ$^{-/-}$ mice received a human skin graft which was allowed to heal for 5 weeks before adoptive transfer of 5x10^6 allogeneic PBMC (n=5 mice) or no cells (RPMI-1640 medium only, n=3 mice). Analysis was performed on skin grafts harvested from mice 40 days later. Mouse GR-1$^+$ cells were quantified in 3 random fields at 400X magnification for each of 4 separate sections for each skin graft, and the mean taken for each data point. Data are represented as mean ±SD. ****:p<0.0001.

Also shown are representative photomicrographs taken at the same time point, stained for mouse GR-1$^+$ cells and counterstained with haematoxylin from mice **(b)** not receiving an adoptive transfer of cells and **(c)** mice receiving 5x10^6 PBMC allogeneic to the skin graft donor. The histology shown is representative of 6 stained sections from each of n=7 mice from n=2 independent assays.

Figure 4.7. Mouse GR-1$^+$ cells do not contribute significantly to the rejection of human skin grafts in the humanised BALB/c-Rag2$^{-/-}$cγ$^{-/-}$ mouse model.

BALB/c-Rag2$^{-/-}$cγ$^{-/-}$ mice received a human skin graft followed by intraperitoneal injections of α-mouse GR-1 antibody (RB-6 clone) or isotype control antibody (rat IgG) every 3-4 days. 5 weeks later mice received an intraperitoneal injection of 5x10^6 PBMC from a donor allogeneic to the skin graft donor. A further group of mice did not receive cells or antibody. **(a)** Representative FACS dotplot demonstrating the presence of mouse CD45$^+$GR-1$^+$CD11b$^+$ cells in the peripheral blood of BALB/c-Rag2$^{-/-}$cγ$^{-/-}$ mice receiving isotype control antibody, the day before the next injection of isotype control antibody (i.e. trough levels). **(b)** Representative FACS dotplot demonstrating absence of mouse CD45$^+$GR-1$^+$CD11b$^+$ cells in the peripheral blood of BALB/c-Rag2$^{-/-}$cγ$^{-/-}$ mice receiving α-mouse GR-1 antibody, the day before the next injection of α-mouse GR-1 antibody (i.e. at trough levels). The FACS data shown are representative of n=4 mice per group.

(c) At day 21 post-adoptive transfer of PBMC, the number of mouse GR-1$^+$ cells was quantified in human skin grafts from mice receiving 5x10^6 PBMC and α-mouse GR-1 antibody (n=3 mice) or 5x10^6 PBMC and isotype control antibody (n=4 mice), as well as mice not receiving PBMC or antibody (n=2 mice). Positive cells were counted in 3 random fields at 400X magnification for each of 4 separate sections for each skin graft, and the mean taken for each data point. **(d) and (e)** Human skin graft survival analysis. Mice receiving cells that did not achieve human leukocyte chimerism levels of >1% in the spleen were excluded from the survival analysis. The MST was calculated for mice receiving 5x10^6 PBMC with α-mouse GR-1 antibody (n=5 mice) or isotype control antibody (n=3 mice), as well as mice not receiving PBMC or antibody (n=2 mice). MSTs were not significantly different between mice receiving α-mouse GR-1 antibody or isotype control antibody (p=0.1460).

Figure 4.8. NSG mice do not reliably reject human skin allografts.

(a) and (b) Human skin graft survival analysis. NSG mice received a human skin graft and 5 weeks later an intraperitoneal injection of $5x10^6$ (n=4 mice) or $2.5x10^6$ (n=4 mice) allogeneic PBMC. A further group did not receive cells (RPMI-1640 medium only, n=2 mice). Mice receiving cells that did not achieve human leukocyte chimerism levels of >1% in the spleen were excluded from the survival analysis. The MST for each group was calculated. **(c)** Representative photomicrographs. Human skin grafts harvested from NSG mice receiving $5x10^6$ PBMC (taken at the point of rejection) or no cells (taken at the point of rejection) stained for mouse $GR1^+$ cells by immunohistochemistry and counterstained with haematoxylin. The histology shown is representative of 6 stained sections from n=4 mice (PBMC) or n=1 mouse (no cells). **(d)** Representative photomicrographs of human skin grafts harvested from NSG mice receiving $5x10^6$ PBMC (harvested at the point of rejection) or no cells (not rejected and harvested at day 100). Sections were stained by immunohistochemistry for human $CD45^+$ cells (huCD45), human $CD3^+$ cells (huCD3), human $CD4^+$ cells (huCD4) or human $CD8^+$ cells (huCD8) and counterstained with haematoxylin. The histology shown is representative of 6 stained sections for each stain type from each of n=4 mice (PBMC) or n=1 mouse (no cells).

Figure 4.9. BALB/c-Rag2$^{-/-}$cγ$^{-/-}$ mice receiving a human skin graft and 5x10^6 allogeneic PBMC produce non-HLA specific human antibodies.

BALB/c-Rag2$^{-/-}$cγ$^{-/-}$ mice received a human skin graft followed by 5x10^6 allogeneic PBMC (n=9 mice) or no cells (n=3 mice) 5 weeks later. At the point of skin graft rejection (for those receiving PBMC) or long-term survival (>100 days, for those not receiving cells), mice were sacrificed and serum levels of human IgG and human IgM determined by ELISA. All mice receiving 5x10^6 PBMC achieved human leukocyte chimerism levels of >1% in the spleen. Data are represented as mean ±SD. **(b)** and **(c)** Serum samples from 18 mice (numbered 1 to 18, from 6 separate survival assays using different PBMC and skin donor combinations) that had received a human skin graft and 5x10^6 allogeneic PBMC 5 weeks later were assessed using a multiplexed microbead array assay (Luminex™) for the presence of antibodies to **(b)** HLA Class I antigens and **(c)** HLA Class II antigens. The mean fluorescence intensity (MFI) was calculated for each microbead (each of which is reactive to a range of HLA Class I or II antigens). All MFI values generated for the range of microbeads for each of HLA Class I or Class II antigens were averaged to produce an aggregate mean MFI for each sample. Data are represented as this mean value ±SD. A positive control sample is also shown for each class of HLA antigens.

Figure 4.10. Humanised BALB/c-Rag2$^{-/-}$cγ$^{-/-}$ mice produce human antibody with some specificity against BALB/c-Rag2$^{-/-}$cγ$^{-/-}$ mouse antigens.

(a) Human HLA-A1+ HLA-B12- PBMC were incubated with a monoclonal human IgG α-HLA-A1 antibody or a monoclonal human IgG α-HLA-B12 antibody followed by a fluorochrome coupled α-human IgG-Fc and the percentage of positive cells determined by FACS. **(b)** Representative FACS histograms. mAb: monoclonal antibody. A single assay was performed. **(c)** Human PBMC, BALB/c mouse splenocytes or Sprague Dawley rat (SD rat) splenocytes were incubated with pooled serum harvested at the point of skin graft rejection from BALB/c-Rag2$^{-/-}$cγ$^{-/-}$ mice that had received a human skin graft and 5x10^{6} PBMC 5 weeks later (n=4 mice). After incubation with 3 different concentrations of this pooled serum (5µg, 25µg or 125µg human IgG, measured by ELISA), cells were incubated with a fluorochrome-coupled α-human IgG-Fc and the percentage of positive cells determined by FACS. **(d)** Representative FACS histograms from a single assay using pooled serum from n=4 mice as described.

Figure 4.11. BALB/c-Rag2$^{-/-}$cγ$^{-/-}$ mice engrafted with human UCB-derived HSCs develop human leukocytes.

BALB/c-Rag2$^{-/-}$cγ$^{-/-}$ mice received 4 Gy total body irradiation within 24 hours of birth, followed shortly by an intrahepatic injection of 5x10^4 CD34$^+$CD45$^-$Lin$^-$-enriched cells (derived from human UCB by magnetic bead isolation to a purity of over 92%). **(a)** At 10 weeks, the number of live human 7AAD$^-$CD34$^+$Lin$^-$ cells was determined in the bone marrow (from one tibia), spleen, blood and thymus of mice. Data are represented as mean ±SD (n=6 mice from two separate HSC donors). **(b)** Representative FACS plot from the bone marrow of one mouse at week 10, showing human 7AAD$^-$CD34$^+$Lin$^-$ cells (huCD34$^+$; huLin$^-$). Dotplot is representative of staining from n=6 mice from n=2 different HSC donors.

Four weeks post-HSC transplantation, mice were tail bled fortnightly for monitoring of peripheral blood levels of live human 7AAD$^-$CD45$^+$ cells (huCD45$^+$). Cells were only detectable in significant numbers from 6 weeks onwards. **(c)** Number of huCD45$^+$ cells per 100µl peripheral blood. **(d)** Percentage of huCD45$^+$ cells as a proportion of total live mononuclear cells in peripheral blood. Data shown are pooled from two separate assays using a different human UCB donor for each (n=5 mice per HSC donor, n=10 mice total) and are represented as mean ±SEM.

Figure 4.12. Schematic of experimental plan for HSC engraftment of BALB/c-Rag2$^{-/-}$cγ$^{-/-}$ mice.

BALB/c-Rag2$^{-/-}$cγ$^{-/-}$ mice received 4 Gy total body irradiation within 24 hours of birth, followed shortly by an intrahepatic injection of 5x10^4 CD34$^+$CD45$^-$Lin$^-$-enriched cells derived from human UCB by magnetic bead isolation, to a purity of over 92%. Six weeks later mice received a human skin graft from a donor allogeneic to the HSC donor. One group received no further cells (n=5 mice) and another group received an intraperitoneal injection of 5x10^6 MNCs derived from the same UCB donor 5 weeks post-skin transplantation (n=4 mice). All mice received HSCs from the same UCB donor. Peripheral blood was monitored from 9 weeks onwards for the development of human CD45$^+$ leukocytes, human CD19$^-$CD3$^+$CD45$^+$ leukocytes, human CD19$^+$CD3$^-$CD45$^+$ leukocytes and human IgG and IgM.

Figure 4.13. Long-term kinetics of human leukocyte development in human HSC-engrafted BALB/c-Rag2$^{-/-}$cγ$^{-/-}$ mice receiving a human skin allograft.

BALB/c-Rag2$^{-/-}$cγ$^{-/-}$ mice received 4 Gy total body irradiation within 24 hours of birth, followed shortly by an intrahepatic injection of 5x10^4 CD34$^+$CD45$^-$Lin$^-$-enriched cells (derived from human UCB by magnetic bead isolation, to a purity of over 92%). Six weeks later mice received a human skin graft from a donor allogeneic to the HSC donor. One group received no further cells (n=5 mice) and another group received an intraperitoneal injection of 5x10^6 MNCs derived from the same UCB donor 5 weeks post-skin transplantation (n=4 mice). All mice received HSCs from the same UCB donor. Peripheral blood was monitored from 9 weeks onwards for the development of live human 7AAD$^-$CD45$^+$ (huCD45$^+$) leukocytes. **(a)** Percentage huCD45$^+$ as a proportion of total live mononuclear cells in the peripheral blood. **(b)** Number of huCD45$^+$ cells in 100µl of peripheral blood. Data are represented as mean ±SD. **(c)** Representative FACS dotplot of live human 7AAD$^-$CD45$^+$ cells in the peripheral blood, gated on mononuclear cells, in a mouse receiving HSCs only at week 19 post-HSC transplantation. Plot is representative of staining from n=5 mice.

Figure 4.14. Development of human T cells in human HSC-engrafted BALB/c-Rag2$^{-/-}$cγ$^{-/-}$ mice receiving a human skin transplant.

BALB/c-Rag2$^{-/-}$cγ$^{-/-}$ mice received 4 Gy total body irradiation within 24 hours of birth, followed shortly by an intrahepatic injection of 5x10^4 CD34$^+$CD45$^-$Lin$^-$-enriched cells (derived from human UCB by magnetic bead isolation, to a purity of over 92%). Six weeks later mice received a human skin graft from a donor allogeneic to the HSC donor. One group received no further cells (n=5 mice) and another group received an intraperitoneal injection of 5x10^6 MNCs derived from the same UCB donor 5 weeks post-skin transplantation (n=4 mice). All mice received HSCs from the same UCB donor. Peripheral blood was monitored from 9 weeks onwards for the development of live human 7AAD$^-$CD45$^+$CD3$^+$ (huCD3$^+$) leukocytes. **(a)** Percentage huCD3$^+$ as a proportion of total live human 7AAD$^-$CD45$^+$ cells. ****:p<0.0001, two-way ANOVA. **(b)** Number of huCD3$^+$ cells in 100µl of peripheral blood. Data are represented as mean ±SD. **(c)** Representative FACS dotplot of live human 7AAD$^-$CD45$^+$CD3$^+$ cells phenotyped for human CD4 (huCD4) and CD8 (huCD8) expression in a mouse receiving HSCs only, at week 19 post-HSC transplantation. Plot is representative of staining in n=5 mice.

Figure 4.15. Development of human B cells and monocytes in human HSC-engrafted BALB/c-Rag2$^{-/-}$cγ$^{-/-}$ mice receiving a human skin transplant.

BALB/c-Rag2$^{-/-}$cγ$^{-/-}$ mice received 4 Gy total body irradiation within 24 hours of birth, followed shortly by an intrahepatic injection of 5x10^4 CD34$^+$CD45$^-$Lin$^-$-enriched cells (derived from human UCB by magnetic bead isolation, to a purity of over 92%). Six weeks later mice received a human skin graft from a donor allogeneic to the HSC donor. One group received no further cells (n=5 mice) and another group received an intraperitoneal injection of 5x10^6 MNCs derived from the same UCB donor 5 weeks post-skin transplantation (n=4 mice). All mice received HSCs from the same UCB donor. Peripheral blood was monitored from 9 weeks onwards for the development of live human 7AAD$^-$CD45$^+$CD19$^+$ (huCD19$^+$) leukocytes. **(a)** Percentage huCD19$^+$ as a proportion of total live human 7AAD$^-$CD45$^+$ cells. **(b)** Number of huCD19$^+$ cells in 100µl of peripheral blood. Data are represented as mean ±SD. *:p<0.05, two-way ANOVA. **(c)** Representative FACS dotplot of human CD14$^+$ (huCD14) cells, gated on live human 7AAD$^-$CD45$^+$ cells from a mouse receiving HSCs only, at week 19 post-transplantation. Plot is representative of staining in n=5 mice.

Figure 4.16. Development of human immunoglobulin in human HSC-engrafted BALB/c-Rag2$^{-/-}$cγ$^{-/-}$ mice receiving a human skin transplant.

BALB/c-Rag2$^{-/-}$cγ$^{-/-}$ mice received 4 Gy total body irradiation within 24 hours of birth, followed shortly by an intrahepatic injection of 5x10^4 CD34$^+$CD45$^-$Lin$^-$-enriched cells (derived from human UCB by magnetic bead isolation, to a purity of over 92%). Six weeks later mice received a human skin graft from a donor allogeneic to the HSC donor. One group received no further cells (n=5 mice) and another group received an intraperitoneal injection of 5x10^6 MNCs derived from the same UCB donor 5 weeks post-skin transplantation (n=4 mice). All mice received HSCs from the same UCB donor. Serum from peripheral blood was monitored from 9 weeks onwards for the development of human IgG and IgM, measured by specific ELISA. Immunoglobulin was only detectable from week 11 onwards. **(a)** Serum concentration of human IgM over time. **(b)** Serum concentration of human IgG over time. Data are represented as mean ±SD.

Figure 4.17. Human α-HLA antibody production in HSC-engrafted BALB/c-Rag2$^{-/-}$cγ$^{-/-}$ mice receiving a human skin graft.

BALB/c-Rag2$^{-/-}$cγ$^{-/-}$ mice received 4 Gy total body irradiation within 24 hours of birth, followed shortly by an intrahepatic injection of 5x10^4 CD34$^+$CD45$^-$Lin$^-$-enriched cells (derived from human UCB by magnetic bead isolation, to a purity of over 92%). Six weeks later mice received a human skin graft from a donor allogeneic to the HSC donor. One group received no further cells (n=5 mice) and another group received an intraperitoneal injection of 5x10^6 MNCs derived from the same UCB donor 5 weeks post-skin transplantation (n=4 mice). All mice received HSCs from the same UCB donor. Despite mice developing significant amounts of human IgG and IgM antibody (***Figure 4.16***), only one mouse developed α-HLA antibody. **(a)** Multiplexed microbead array assay (Luminex™) showing α-HLA Class I antibody reactive to beads 7, 8, 69, 86, 89. On further single antigen bead analysis, this antibody was identified to be specific against HLA-A9.

Figure 4.18. Human skin allograft survival in human HSC-engrafted BALB/c-Rag2$^{-/-}$ cγ$^{-/-}$ mice.

BALB/c-Rag2$^{-/-}$cγ$^{-/-}$ mice received 4 Gy total body irradiation within 24 hours of birth, followed shortly by an intrahepatic injection of 5x10^4 CD34$^+$CD45$^-$Lin$^-$-enriched cells (derived from human UCB by magnetic bead isolation, to a purity of over 92%). Six weeks later mice received a human skin graft from a donor allogeneic to the HSC donor. One group received no further cells ('HSCs only' n=4 mice) and another group received an intraperitoneal injection of 5x10^6 MNCs derived from the same UCB donor 5 weeks post-skin transplantation ('HSCs + 5x10^6 MNC' n=4 mice). All mice received HSCs from the same UCB donor. All mice achieved human leukocyte chimerism levels of >1% in the spleen. **(a) and (b)** Human skin graft survival in HSC-engrafted mice. The MST was calculated for each group.

(c) In a separate assay, mice received a human skin graft and 5 weeks later received an injection of 5x10^6 MNCs derived from a human UCB donor allogeneic to the skin graft donor. Mice did not receive a HSC transplant. Survival times were monitored from the time of cellular injection. Only mice achieving human leukocyte chimerism levels >1% in the spleen are shown (n=5 mice).

(d) Representative photomicrograph of a human skin graft harvested at the point of rejection from a mouse receiving HSCs only, stained by immunohistochemistry for human CD45$^+$ (huCD45) cells and counterstained with haematoxylin. **(e)** Representative photomicrographs of human skin grafts harvested at the point of rejection from a mouse receiving HSCs only, stained by immunohistochemistry for human CD3$^+$, CD19$^+$, CD4$^+$, CD8$^+$, or CD68$^+$ cells, and counterstained with haematoxylin. The histology shown is representative of 6 stained sections for each stain type from each of n=5 mice.

CHAPTER 5: IMMUNOREGULATION OF HUMAN SKIN REJECTION

5.1 Introduction

VCA transplantation is severely limited in both availability and scope due to the risks associated with immunosuppression and the susceptibility of skin to rejection[6,512,513]. Consequently, there is a clear need to translate tolerance induction therapies, many of which have shown some promise in animal models, to the clinic. Studies examining tolerance induction techniques for skin or VCA transplantation have generally been based on rodent models with only a few swine or non-human primate models. As described in *section 1.6*, the majority of the approaches have evaluated mixed chimerism as a technique for tolerance induction. While these data are invaluable, results may not always translate to the production of an effective therapy for humans, especially as the techniques are less effective in larger animal models and in particular in respect to skin (*section 1.6.1.1*)[161,163,415]. Indeed, therapies that have shown promise in rodents have failed in larger animals, and even therapies that have been effective in non-human primates have failed in humans[419,420]. This is particularly the case for molecules and cellular therapies developed with unique specificity for human targets, as the predictability of work carried out in animal models is diminished.

As discussed in *section 1.6.2.1a*, studies exist in rodent models where Treg as a cellular therapy has proven successful for skin transplantation[307]. However, there

are no studies assessing Treg as a direct cellular therapy for VCA or skin transplantation in larger animals, and currently no studies in humans. That being said, Treg therapies are currently being evaluated in clinical trials for the prevention GvHD post-HSC transplantation[410-412,514], implying that production of Treg according to current good manufacturing practices (cGMP)[515] is possible. It is foreseeable that Treg cellular therapy may be available for VCA transplantation in the future. As such, there is a need to evaluate human Treg therapy in the context of human skin transplantation.

In *section 1.6.2.1* we examined the experimental evidence for Treg therapy and the various populations of Treg that have been described together with their phenotypic markers. As discussed, human Treg for therapy are generally produced by isolation of cells from peripheral or umbilical cord blood for subsequent *ex vivo* expansion or direct use[312,411,412]. The ideal markers for the isolation of a pure population of nTreg are still not clearly defined. However, human $CD4^+$ Treg that express high levels of CD25 and low levels of CD127 appear to represent a population of potently suppressive cells with high expression levels of FoxP3, the transcription factor necessary for, and associated with, Treg function[357-359,516]. Protocols for the expansion of these cells *in vitro*, using stimulation with αCD3/αCD28 microbeads in the presence of rhIL-2 have been established both in our laboratory and by others[312,370,411,448,517]. The non-specific TCR stimulation in these protocols leads to the production of a polyclonally-reactive population of activated Treg. This activation status may be important for suppressive activity[518].

Previous work from our group has demonstrated that *in vivo* cellular therapy with *ex vivo*-expanded human $CD4^+CD25^+CD127^{lo}$ Treg effectively reduces intimal hyperplasia in a humanised mouse model of human vessel rejection[448]. These cells are therefore a good starting population to evaluate in the current humanised skin transplantation model. The majority of studies using *ex vivo*-expanded human Treg have used cells derived and expanded from the recipient ('autologous Treg'). However, some studies have also evaluated Treg that are derived from a 'third party', allogeneic to both donor and recipient ('non-autologous Treg')[411,519]. Non-autologous Treg offer distinct advantages. For example, they may be pre-expanded and cryopreserved for use 'off the shelf', or a particular population that is reactive against a specific HLA haplotype may be expanded well in advance of the transplant date.

In the first two chapters we developed a humanised mouse model of skin transplantation and demonstrated the cellular and histological characteristics of human skin rejection, defining parameters that may be examined and quantified in rejection. This model provides a translational *in vivo* system in which to safely assess the efficacy of novel human-specific therapies without direct patient participation.

In the current chapter we hypothesise that Treg expanded *ex vivo* from a population of $CD4^+CD25^+CD127^{lo}$ human cells and derived from the transplant recipient (i.e. autologous Treg) are able to extend human skin allograft survival in the humanised mouse model in the absence of any other immunosuppression. Firstly, we investigate the importance of expansion of Treg in this model, hypothesising that the

activation of Treg in the expansion process is critical to their activity. In skin grafts from Treg-treated mice, we hypothesise that the histological features of rejection will be diminished. Secondly, we examine mechanisms of immunoregulation that are operational, defining the tissues in which Treg may be active. Finally, we investigate and characterise the most effective Treg therapy for the prevention of human skin rejection, evaluating the efficacy of non-autologous Treg that are derived from a third party.

5.1.1 Chapter aims

In this chapter we aim to evaluate the efficacy of *ex vivo*-expanded naturally-occurring $CD4^{+}CD25^{+}CD127^{lo}$ human Treg, derived from either the recipient or from a third party, as an immunoregulatory therapy for the prevention of human skin graft rejection. We also aim to investigate the mechanisms by which Treg are protective *in vivo* and delineate a strategy for the use of Treg cellular therapy in clinical VCA transplantation.

5.2 Expanded human Treg maintain their phenotype and are suppressive *in vitro*

We hypothesised that human nTreg may be derived from PBMC on the basis of the markers $CD4^+CD25^+CD127^{lo}$ and that these Treg may be expanded *in vitro* to produce functional putative Treg that maintain their phenotype post-expansion. *Ex vivo*-expansion of human Treg was performed in collaboration with Dr Joanna Hester. Human $CD4^+CD25^+CD127^{lo}$ cells were sorted from $CD4^+$-enriched PBMC to a purity of over 94% as per established protocols in our laboratory[448] and subsequently expanded (up to 600-fold) *in vitro* over two 7-week culture rounds with rhIL-2 and αCD3/αCD28 microbeads (***Figure 5.1a***). Post-expansion, the majority of cells maintained a high expression of CD25 and low expression of CD127 (***Figure 5.1a***). Expanded cells also expressed the Treg master transcription marker FoxP3 and the Treg marker CD27 as well as CD62L, CCR7 or both (***Figure 5.1b***). The latter two markers have been previously demonstrated to be important for Treg function, allowing the homing of Treg to peripheral lymphoid tissues where they may suppress activated or proliferating lymphocytes[347,520]. CD62L is highly conserved between species[521] and is therefore relevant in the current humanised model.

We then performed an *in vitro* suppression assay of *ex vivo*-expanded Treg in order to confirm their functionality. Target PBMC were stimulated polyclonally with αCD3/αCD28 microbeads or allostimulated with irradiated allogeneic PBMC, to produce a proliferative response measured by ^{3}H-thymidine incorporation. For the allostimulation assay, $1x10^5$ PBMC were incubated with $1x10^5$ irradiated allogeneic PBMC. For the polyclonal stimulation assay, $2x10^4$ PBMC were incubated with $2x10^3$

αCD3/αCD28 microbeads. The titration of increasing numbers of *ex vivo*-expanded human Treg derived from the same donor as the target PBMC into the culture suppressed ^{3}H-thymidine incorporation of both polyclonally stimulated and allostimulated PBMC in a dose-dependent manner (***Figure 5.2a***). A crowding control, where twice the number of PBMC were cultured without Treg was also included to eliminate the possibility that Treg prevent the proliferation of PBMC by virtue of overcrowding of cells in the culture well (*data not shown*). These data indicate a dose-dependent suppression of PBMC proliferation by *ex vivo*-expanded autologous Treg.

A greater number of PBMC are likely to respond to stimulation with αCD3/αCD28 microbeads compared with an allostimulus and therefore prove more challenging to suppress. However, Treg will also be more efficacious when polyclonally activated with αCD3/αCD28 microbeads, explaining the greater suppression seen with Treg in the polyclonally-stimulated PBMC assay. In addition, allostimulation may activate other non-T cell leukocytes in the culture condition, whereas polyclonal stimulation is directed exclusively against T cells. Allostimulation may therefore lead to higher levels of proinflammatory cytokines in the culture conditions, reducing the efficacy of Treg-mediated suppression.

In the absence of Treg, there appeared to be lower proliferation levels of PBMC with polyclonal stimulation compared with allostimulation. However, the assay using polyclonally-stimulated PBMC was set up with a lower number of cells per well than the allostimulated PBMC assay ($2x10^4$ vs. $1x10^5$) and a relatively low bead to cell

ratio of 1:10, which may explain the low proliferation compared to alloantigen-stimulated PBMC. Nevertheless, we wondered whether the polyclonally-activated T cells were being exhausted in the 7-day culture period. However in an assay in which CFSE-labelled PBMC were stimulated in a similar manner to that in the ^{3}H-thymidine *in vitro* suppression test, using $2x10^{4}$ responders stimulated with $2x10^{3}$ αCD3/αCD28 microbeads, cells with a high CFSE concentration are still detectable even at day 7 ($CD4^{+}$ cells in ***Figure 5.2b***). Furthermore, even when using double the amount of responder cells, with $2x10^{4}$ CFSE-labelled and $2x10^{4}$ unlabelled PBMC stimulated similarly with $2x10^{3}$ αCD3/αCD28 microbeads, most of the cells remain positive for CFSE ($CD4^{+}$ cells in ***Figure 5.2c***). These data indicate that polyclonally-stimulated PBMC are not exhausted in the 7-day culture period and that crowding is not a cause of the reduced proliferation with the addition of Treg in the ^{3}H-thymidine assay.

5.3 *Ex vivo*-expanded human Treg prevent human skin allograft rejection in a dose-dependent manner

We hypothesised that *ex vivo*-expanded Treg would prevent human skin graft rejection in the standard humanised mouse model. BALB/c-Rag2$^{-/-}$cγ$^{-/-}$ mice received a human skin allograft and 5 weeks later an intraperitoneal injection of $5x10^{6}$ allogeneic PBMC alone or together with varying amounts of *ex vivo*-expanded Treg derived from the same donor as the PBMC (i.e. autologous Treg). Treg were given at doses of $5x10^{6}$ cells (1:1 ratio with PBMC), $1x10^{6}$ cells (5:1 ratio with PBMC) or $0.5x10^{6}$ cells (10:1 ratio with PBMC). Mice not achieving human leukocyte

chimerism levels of >1% in the spleen or >0.1% in the peripheral blood were excluded from all analyses. As expected, mice receiving PBMC alone rejected their skin allografts with a MST of 36.5 days, whereas Treg given at a 1:1 or 5:1 ratio promoted the long-term survival of the majority of skin grafts (MST>100 days for both 1:1 and 5:1 ratios, $p<0.0001$ and $p=0.0001$ respectively, ***Figures 5.3a and b***). Treg given at a 10:1 ratio promoted long-term survival in 2 out of 5 skin allografts but the overall MST was not significantly extended compared with PBMC alone (MST 40 days *cf.* 36.5 days for PBMC alone, $p=0.0876$, ***Figures 5.3a and b***). Skin grafts that survived with the use of Treg appeared normal with no macroscopic appearances of inflammation, and were soft and pliable (***Figure 5.3c***). We inferred from these data that *ex vivo*-expanded autologous Treg act to prevent PBMC-mediated destruction of human skin allografts *in vivo*.

5.4 Expansion or activation of human Treg is required to ensure their regulatory activity

We next asked whether the expansion process reduces the suppressive capability of Treg, for example by introducing non-Treg contaminants, and thus whether Treg pre-expansion would be more effective. In an *in vitro* ^{3}H-thymidine incorporation assay performed as described in *section 5.2*, PBMC stimulated with αCD3/αCD28 microbeads were incubated with either *ex vivo*-expanded or non-expanded (i.e. immediately post-flow sorting) $CD127^{lo}CD25^{+}CD4^{+}$ autologous Treg, at a ratio of 4 PBMC to 1 Treg (1:1/4 ratio). The percentage suppression of proliferation was similar for both types of Treg ($p=0.9888$, ***Figure 5.4a***).

We proceeded to determine whether there were any differences in the *in vivo* capability of *ex vivo*-expanded or non-expanded Treg to prevent human skin allograft rejection. As a dose of $1x10^6$ Treg in the previous assay was effective at preventing skin graft rejection in the majority of mice (***Figure 5.3***), we used this dose for the current assay. Mice received a human skin graft and 5 weeks later were reconstituted with $5x10^6$ allogeneic PBMC alone or together with $1x10^6$ *ex vivo*-expanded or non-expanded $CD127^{lo}CD25^+CD4^+$, derived from the same donor as the reconstituting PBMC (i.e. autologous Treg). Mice that did not achieve human leukocyte chimerism levels of >1% in the spleen were excluded from the analysis. As expected, reconstitution of mice with PBMC alone resulted in rejection of all the skin allografts with a MST of 34 days, whereas the addition of $1x10^6$ *ex vivo*-expanded Treg promoted the long-term survival of the majority of skin allografts (MST >100 days, $p<0.0001$, ***Figures 5.4b and c***). In contrast, the addition of non-expanded Treg did not significantly extend skin allograft survival time, although 2 out of 10 skin grafts survived long-term (MST=42.5, $p=0.0649$, ***Figures 5.4b and c***).

Enhanced *in vivo* regulation with expansion of mouse Treg has been reported previously[518]. We hypothesised that the enhanced suppressive qualities of Treg observed post-expansion were secondary to activation of Treg with αCD3/αCD28 microbeads. $CD127^{lo}CD25^+CD4^+$ human Treg were therefore flow sorted and polyclonally stimulated *in vitro* with αCD3/αCD28 microbeads for 12 hours and the pre- and post-stimulation phenotype assessed. We first confirmed that 12 hours of stimulation is sufficient to promote an activated Treg phenotype. Post-stimulation, the percentage of cells expressing Ki-67, a protein closely associated with cellular

proliferation, increased in 3 out of 4 assays (***Figure 5.5a*** and representative FACS plots in ***Figure 5.5g***), while there was also a significant increase in the percentage of cells expressing CD69, a marker of T cell activation (***Figure 5.5b*** and representative FACS plots in ***Figure 5.5g***).

We next assessed the pre- and post-stimulation expression of LAP, CD25 and FoxP3, all phenotypic markers that are associated with Treg (see *section 1.6.2*). Importantly, both FoxP3 and LAP are important for Treg function[260,365,366]. Post-stimulation, there was a significant increase in the percentage of cells expressing LAP (***Figure 5.5c*** and representative FACS plots in ***Figure 5.5g***), as well as an increase in the percentage of cells expressing FoxP3 (***Figure 5.5d*** and representative FACS plots in ***Figure 5.5g***). Furthermore, the median fluorescence intensity (MFI) of both CD25 and FoxP3 were significantly increased post-activation (***Figures 5.5e and f***).

We then asked whether the increase in expression of the Treg marker FoxP3 was restricted to proliferating ($Ki67^+$) or activated ($CD69^+$) Treg, and whether cells expressing an activated phenotype within pre-stimulated cells also have higher levels of FoxP3. Cells were gated by FACS on those expressing CD69 or Ki67 within each group, and the expression of FoxP3 in these cells compared with the expression in the total population. FoxP3 MFI was higher in proliferating and activated Treg compared with the overall population in both pre- and post-stimulation groups (***Figures 5.5h and i***). Moreover, $Ki67^+$ or $CD69^+$ cells in the post-stimulation group expressed higher levels of FoxP3 than their counterparts in the pre-stimulation group (***Figures 5.5h and i***), indicating that stimulation with αCD3/αCD28 microbeads

not only increases the numbers of activated or proliferating cells, but also enhances their suppressive phenotype. Finally, we asked whether the expression of the Treg function-associated molecule LAP is associated with enhanced FoxP3 expression, as has been demonstrated by others in the mouse[365]. LAP^+ cells did indeed express higher levels of FoxP3 compared with the total population for both pre- and post-stimulation groups (***Figure 5.5j***), indicating that this association is also true for human cells. In addition, LAP^+ cells post-stimulation expressed higher levels of FoxP3 than LAP^+ cells pre-stimulation, indicating that αCD3/αCD28 microbead stimulation enhances the FoxP3-associated suppressive phenotype of LAP^+ cells overall.

We next asked whether the *in vitro* stimulation of Treg enhanced their *in vivo* suppressive ability. BALB/c-$Rag2^{-/-}c\gamma^{-/-}$ mice received a human skin graft and 5 weeks later were reconstituted with $5x10^6$ allogeneic PBMC, $5x10^6$ allogeneic PBMC together with $1x10^6$ FACS-sorted $CD127^{lo}CD25^+CD4^+$ Treg which were sorted but not stimulated or expanded *in vitro* ('fresh sorted, unstimulated' Treg), or $5x10^6$ allogeneic PBMC with $1x10^6$ FACS-sorted $CD127^{lo}CD25^+CD4^+$ Treg that were stimulated *in vitro* with αCD3/αCD28 microbeads as above ('stimulated' Treg). Treg were derived from the same donor as the reconstituting PBMC (i.e. autologous Treg). Mice not achieving human leukocyte chimerism levels of >1% in the spleen were excluded from the analysis. Interestingly, only stimulated Treg promoted long-term skin allograft survival (MST>100, p=0.0011). By comparison, unstimulated Treg only extended survival modestly (MST 42.5 days *cf.* 23 days for PBMC alone, p=0.0003, ***Figures 5.6a and b***). Importantly, stimulated Treg significantly enhanced survival in comparison to unstimulated Treg (p=0.0180).

Together, these data show that activation of Treg with αCD3/αCD28 microbeads during the expansion process is at least partly responsible for enhancing their suppressive activity. Treg expansion is therefore important not only for producing large numbers of Treg for therapy, but also for promoting their regulatory activity. It is important to note that because these Treg have been expanded using polyclonal activation with αCD3/αCD28 microbeads they will be reactive against a range of alloantigens, and as such, are polyclonal in nature. Whether only a certain fraction of the Treg used are initially active *in vivo,* then leading to wider bystander suppression, or whether the majority are non-specifically suppressive due to their activated nature is not clear.

5.5 Therapy with *ex vivo*-expanded Treg is associated with a reduction in the number of circulating proliferating human leukocytes

We hypothesised that one of the mechanisms whereby *ex vivo*-expanded human Treg prevent human skin rejection is through reducing engraftment levels of PBMC in the mouse. We measured the number of human leukocytes present in the spleens of BALB/c-Rag2$^{-/-}$cγ$^{-/-}$ mice receiving a human skin graft and 5x10^6 allogeneic PBMC only (at the point of rejection) or 5x10^6 allogeneic PBMC with 5x10^6 *ex vivo*-expanded Treg derived from the same donor as the PBMC (at long-term survival), pooling data from the survival assays presented in *section 5.3*. Despite a large variation in the numbers of human leukocytes within each group, there was overall no significant difference in the number of engrafting cells between the groups (***Figure 5.7a***). Importantly, all but one of the mice receiving Treg achieved human

leukocyte chimerism levels of >10% in the spleen, a level at which skin rejection is normally guaranteed (*Chapter 3*).

However, we wondered whether this particular analysis conceals important differences given that multiple groups are being analysed at different time points. We therefore analysed the number and percentage chimerism of human leukocytes in spleens from skin-engrafted mice receiving $5x10^6$ allogeneic PBMC alone or together with $5x10^6$ *ex vivo*-expanded Treg (derived from the same donor as the PBMC) at 40 days post-adoptive cellular transfer, from a single *in vivo* assay. Again, there were no significant differences in either the number or percentage chimerism of human leukocytes at this single time point (***Figures 5.7b and c***). Importantly, in all mice receiving Treg, levels of human leukocyte chimerism at 40 days reached the threshold of >1% in the spleen and were therefore defined as adequately reconstituted.

Nevertheless, there appeared to be a trend in the spleen towards a reduction in leukocyte chimerism levels in mice receiving Treg and we therefore wondered whether any differences were present in the peripheral blood, a more sensitive marker for active immune responses. Both the number and percentage chimerism of human leukocytes were therefore measured serially in the peripheral blood of BALB/c-$Rag2^{-/-}c\gamma^{-/-}$ mice that received a human skin graft and 5 weeks later an injection of $5x10^6$ PBMC alone or $5x10^6$ PBMC together with $5x10^6$ *ex vivo*-expanded Treg derived from the PBMC donor (i.e. autologous Treg). Only mice that achieved human leukocyte chimerism levels of >1% in the spleen at the point of harvest were

included in the analysis. Although there was no significant difference in the number of human leukocytes engrafting in the peripheral blood between the two groups (p=0.4153, ***Figure 5.8a***), there did appear to be a trend towards an increase in human leukocyte numbers around the point at which most skin grafts are rejected in mice receiving PBMC alone (***Figure 3.9***). However, in mice receiving PBMC with Treg, human leukocyte numbers remained virtually flat throughout (***Figure 5.8a***). Additionally, there was a significant reduction in overall human leukocyte chimerism levels in mice receiving PBMC with *ex vivo*-expanded Treg compared with mice receiving PBMC alone (p=0.0118, ***Figure 5.8b***). This reduction is probably underestimated as mice receiving Treg are effectively receiving twice the number of human $CD45^+$ cells as those receiving PBMC alone. In a separate assay discussed later, similar data were obtained using $1x10^6$ Treg (i.e. a 5:1 ratio of PBMC to Treg, ***Figure 5.19c***), indicating that this is a mechanism that is relevant even at lower doses of Treg.

Next, we asked whether the reduction in human leukocyte chimerism levels with Treg was partly due to a reduction in the number of proliferating T cells. The number of $Ki67^+$ human $CD4^+$ and $CD8^+$ T cells was measured in the spleen and peripheral blood of BALB/c-$Rag2^{-/-}c\gamma^{-/-}$ mice receiving a human skin graft followed 5 weeks later by an injection of $5x10^6$ allogeneic PBMC alone or together with $5x10^6$ *ex vivo*-expanded Treg (derived from the same donor as the PBMC). $Ki67^+$ cells were measured in the two groups 40 days post-adoptive cellular transfer. Only mice that achieved human leukocyte chimerism levels of >1% in the spleen were included in the analysis. There was a significant reduction in the number of $Ki67^+$ T cells in both

the spleen and blood of mice receiving Treg compared with those receiving PBMC alone (***Figure 5.9***). Hence, Treg act partly by reducing the number of proliferating T cells *in vivo*.

We then looked to ascertain whether Treg act nonspecifically to reduce the proliferation and subsequent engraftment of all PBMC *in vivo*, or whether they act to suppress the proliferation of graft responding cells. We hypothesised that Treg would not reduce the number of human leukocytes or percentage human leukocyte chimerism in mice receiving Treg if no skin graft was present, as T cells are not activated by graft antigens. BALB/c-Rag2$^{-/-}$cγ$^{-/-}$ mice were therefore injected with 5x10^{6} PBMC alone, or 5x10^{6} PBMC with 5x10^{6} *ex vivo*-expanded Treg derived from the same donor as the PBMC (i.e. autologous Treg), in the absence of a skin allograft. Both the number and percentage chimerism of human leukocytes were monitored over time in the peripheral blood. Mice not achieving human leukocyte chimerism levels of >1% in the spleen at the point of harvest were excluded from the analysis. Here, there was no reduction in either the number of engrafting human leukocytes (p=0.0852, ***Figure 5.10a***), or the percentage human leukocyte chimerism (p=0.2926, ***Figure 5.10b***) in mice receiving PBMC with Treg compared with mice receiving PBMC alone.

These data confirm that Treg *in vivo* reduce chimerism levels only in the presence of a human skin allograft. This may be due to a need for Treg to be activated by the allorecognition of antigens on the skin graft before they may suppress the proliferation of PBMC. Importantly, once activated, suppression of proliferation may

be non-specific, engaging bystander suppressive mechanisms. This is illustrated by the observation that mice receiving a skin graft with PBMC and Treg have a low rate of XvHD development, whereas mice receiving PBMC with Treg and no skin graft have higher rates of XvHD development (*data not shown*). It is possible that once Treg are activated by the allograft, all effector responses may be suppressed, including human anti-mouse xenoresponses. This may account for the marked reduction in human leukocyte chimerism levels in mice receiving PBMC with Treg in the presence of a skin allograft.

Although only 10% of T cells are likely to respond to a specific transplant antigen, it appears that a greater percentage of cells are suppressed *in vivo*. This may be explained by bystander suppression, whereby activated Treg prevent the proliferation of many more than only the T cells that are responding to the allograft[264].

The use of Treg reduced both the total level of human leukocyte chimerism in the peripheral blood and the number of proliferating T cells. Importantly, in all these analyses, mice that did not achieve >1% human leukocyte chimerism in the spleen at the point of harvest were excluded. Therefore, although the levels of human leukocyte chimerism were reduced in mice receiving Treg compared with those receiving PBMC alone, chimerism levels in these Treg-treated mice (in which skin grafts are accepted) were still at levels considered adequately reconstituted as per established definitions. This implies that other mechanisms of suppression are

active in Treg-treated mice that prevent T cell-mediated destruction of human skin allografts.

5.6 *Ex vivo*-expanded Treg reduce human immunoglobulin production *in vivo*

As demonstrated, there is a reduction in human leukocyte chimerism levels in skin-transplanted mice treated with Treg, together with a reduction in the number of circulating proliferating T cells (***Figures 5.8b and 5.9***). The majority of this effect will be naturally directed against T cells, given that these cells are the principal engrafting cell type and the main effector cell type in the alloresponse against the human skin allograft (***Figure 3.12a*** and ***Figure 4.5***). However, humanised mice also produce significant amounts of human IgG and IgM (***Figure 4.9a***), despite low engraftment rates of B cells (***Figure 3.12a***). Due to the very low engraftment levels of B cells with PBMC alone, it is difficult to ascertain whether the addition of Treg reduces these levels to any degree. Although the human antibody produced in these humanised mice is not HLA-specific (***Figures 4.9b and c***), we nevertheless asked whether Treg have any effect on B cell activity. There are very few reports of Treg suppression of B cells[277] and this is therefore of interest. We hypothesised that if Treg exerted suppressive activity on B cell engraftment or B cell activity, this would result in a reduced concentration of human immunoglobulin in the serum of mice.

BALB/c-Rag2$^{-/-}$cγ$^{-/-}$ mice received a human skin allograft and 5 weeks later were reconstituted with 5x10^6 allogeneic PBMC alone or together with 5x10^6 *ex vivo*-expanded Treg derived from the same donor as the PBMC (i.e. autologous Treg at a 1:1 ratio with PBMC). We sacrificed mice 21 days post-adoptive transfer, i.e. at a

time point before rejection is fully complete but at which there are adequate levels of reconstitution (***Figure 3.11a***), in order to determine the immune status while the response against the allograft is still active. Human IgG and IgM serum concentrations were measured in both groups of mice. While there was no difference in the serum concentration of human IgM between the two groups (p=0.3112, ***Figure 5.11a right panel***), there was a significant reduction in the serum concentration of human IgG in mice receiving Treg (p=0.0381, ***Figure 5.11a left panel***).

We then asked whether this Treg-associated reduction in human immunoglobulin levels is sustained. To this end, human immunoglobulin levels were measured in mice receiving PBMC alone at the point of skin rejection and compared with immunoglobulin levels in mice receiving PBMC with Treg at the point of long-term survival (>100 days). Human IgG levels were significantly lower in mice receiving Treg compared with mice receiving PBMC alone (p=0.0079, ***Figure 5.11b left panel***), although human IgM levels were again not significantly different between the two groups (p=0.2348, ***Figure 5.11b right panel***). In mice receiving PBMC alone, both IgG and IgM levels were higher in mice at the point of rejection compared with levels at day 21 (***Figure 5.11b*** *cf.* ***Figure 5.11a***), indicating that production of human immunoglobulin continues to increase with time together with the increase in leukocyte reconstitution levels. These data indicate that Treg may act to suppress B cells, although it is likely that the effect is indirect via the suppression of T cells that provide B cell help for immunoglobulin production and class switching.

5.7 Therapy with *ex vivo*-expanded Treg preserves skin allograft microarchitecture and reduces the intragraft leukocytic infiltrate

To elucidate the mechanisms of suppression that are active we defined the histological changes associated with Treg therapy. We previously demonstrated the histological changes that occur with human skin allograft rejection in the humanised mouse model (*sections 4.3* and *4.4*). As discussed, these changes are consistent with defined changes that occur with human skin rejection in clinical VCA transplantation. With this in mind we asked whether the use of Treg preserves the microarchitecture of human skin allografts to reduce the microscopic signs of rejection.

BALB/c-Rag2$^{-/-}$cγ$^{-/-}$ mice received a human skin transplant and 5 weeks later were reconstituted with 5x10^6 allogeneic PBMC alone, or 5x10^6 allogeneic PBMC with 5x10^6 *ex vivo*-expanded Treg derived from the PBMC donor (i.e. autologous Treg). Skin grafts were harvested at day 40, a point at which skin destruction in mice receiving PBMC alone would be maximal, based on the defined MST of 35 days (***Figure 3.9b***). On the one hand, skin grafts from mice receiving PBMC alone displayed gross evidence of rejection histologically, with loss of the superficial layers of the epidermis, evidence of cellular apoptosis and heavy dermal cellular infiltrates with some junctional and epidermal infiltrates (representative photomicrograph, ***Figure 5.12a***). On the other hand, skin grafts from mice receiving Treg with PBMC were generally well preserved, with all layers of the epidermis maintained, no marked vacuolation of cells to indicate cellular apoptosis, and no junctional or epidermal cellular infiltrates (representative photomicrograph, ***Figure 5.12b***). However, we did note that some cellular infiltrates remained, principally around

dermal microvessels (red arrow, ***Figure 5.12b***). Human skin grafts from Treg-treated mice would be categorised under the Banff 2007 classification[434] as Grade I (mild) rejection due to the presence of mild perivascular infiltrates located only in the dermis. However such changes are not particularly specific and may be seen in a variety of other dermatological conditions[494]. Clinically, the histopathological diagnosis of rejection when it is at this stage is controversial, especially as the skin may look macroscopically normal[494].

The condition of the microvessels within skin is a sensitive indicator of damage[494,522]. Skin grafts in our current model were allowed a period of healing and therefore revascularisation. Both mouse and human microvessels develop within human skin transplants (***Figure 3.3***). This is an advantageous element of the model as it allows the assessment of skin as a vascularised transplant (as it would be in the context of a VCA), and also allows the opportunity to examine the degree of microvascular injury that takes place. We hypothesised that reconstitution of mice with $5x10^6$ PBMC that are allogeneic to the skin graft would result in the destruction of human microvessels, and that the addition of $5x10^6$ *ex vivo*-expanded Treg (derived from the same donor as the PBMC) would prevent this from taking place. Skin grafts from mice receiving PBMC alone or PBMC with Treg were harvested 21 days post-adoptive transfer of cells and stained by immunohistochemistry for human $CD31^+$ and mouse $CD31^+$ cells in order to visualise human or mouse vascular ECs. A further group of mice did not receive any cells to act as a control for normal vascularisation. Complete rings of human or mouse $CD31^+$ positive cells were enumerated in each skin graft. In mice receiving PBMC, there was a relative loss of human microvessels

compared with mice receiving no cells (p=0.0017), while mouse microvessels were spared any destruction by PBMC (***Figures 5.13a and b***). Destruction of human skin allograft microvessels is a central feature of skin rejection, and its reduction a key feature of successful immunosuppression or immunoregulation[447,457,458,476,522,523]. Encouragingly, human microvessels in skin grafts from mice receiving Treg were not destroyed (***Figures 5.13a and c***). This protection of human microvessels continued, whereby in long-term surviving skin grafts (i.e. at >100 days) from Treg-treated mice, there was an abundance of human microvessels (***Figure 5.13d***). In long-term surviving skin grafts from Treg-treated mice, mouse microvessels were also well preserved (***Figure 5.13e***). Together these data indicate that there is a destructive human alloresponse directed against human ECs and that treatment with Treg protects human ECs against this process. In addition, these data demonstrate that there is no significant human anti-mouse xenoresponse directed against mouse vascular ECs in mice receiving PBMC alone or together with Treg.

We noted previously that skin grafts from Treg-treated mice did not appear completely protected from leukocytic infiltration (***Figure 5.12b***). Nevertheless, we hypothesised that immunoregulation of skin grafts with Treg reduces human leukocytic infiltrates in comparison to skin grafts from mice receiving PBMC alone. BALB/c-Rag2$^{-/-}$cγ$^{-/-}$ mice received a human skin allograft and 5 weeks later were reconstituted with 5x10^6 allogeneic PBMC alone or together with 5x10^6 *ex vivo*-expanded Treg derived from the same donor as the PBMC (i.e. autologous Treg at a 1:1 ratio with PBMC). We sacrificed mice 21 days post-adoptive cellular transfer, a time point at which the immune response against the allograft is active and ongoing.

Skin grafts were analysed for the total number of human $CD45^+$, $CD4^+$ and $CD8^+$ cells in both groups of mice. There was no difference in the number of graft infiltrating human $CD45^+$ cells between mice receiving PBMC alone or PBMC with Treg (top panel, ***Figure 5.14a***). Neither was there a difference in the number of graft infiltrating human $CD4^+$ cells (middle panel, ***Figure 5.14a***). Notably however, there was a significant reduction in the number of graft infiltrating human $CD8^+$ cells (p=0.0122, bottom panel, ***Figure 5.14a***). We wondered whether this was a sustained effect, and therefore measured the number of graft infiltrating human $CD45^+$, $CD4^+$ and $CD8^+$ cells in skin grafts from mice at rejection (for PBMC alone) and long-term survival (for PBMC with Treg). Here again, there was no difference in the number of graft infiltrating $CD45^+$ or $CD4^+$ cells in mice receiving Treg, whereas a significant reduction in infiltrating $CD8^+$ cells was observed in Treg-treated mice (p=0.0280, ***Figure 5.14b***). As further confirmation that overall levels of infiltrating T cells were not altered, there was also no difference in human *CD3* mRNA levels between the two groups (p=0.4144, ***Figure 5.14c***).

The lack of a reduction in the total leukocytic infiltrate of skin allografts in Treg-treated mice is consistent with the observation that while human leukocytic chimerism levels are reduced in mice receiving a skin graft and Treg therapy (***Figure 5.8***), chimerism levels in mice receiving Treg still remain at >1% in the spleen (a level at which rejection is normally induced in mice receiving PBMC alone, ***Figure 5.7c***). While chimerism levels in Treg-treated mice are not low enough to cause an overall reduction in the number of skin infiltrating leukocytes, the lower levels of chimerism may reflect a specific suppression of proliferation of graft responding cells. Previous

studies examining the cellular infiltrate in skin allografts have revealed that only a small fraction are allospecific, and that the overall number of infiltrating leukocytes does not predict the rapidity of rejection[157,524,525]. However, the marked reduction in infiltrating human $CD8^+$ cells may reflect the importance of these cells in the destructive alloimmune response against skin and the possibility that regulation of $CD8^+$ cells may be sufficient to prevent rejection of the skin graft. Nevertheless, $CD4^+$ cells have been demonstrated to cause significant damage to human skin grafts alone[370,467], indicating that there is more to the immunoregulatory effect than simply a protection from the $CD8^+$ cellular infiltrate.

5.8 Treg home to the skin allograft-draining lymph node and the skin allograft to regulate alloresponses

Treg have been shown to migrate from the peripheral blood into the allograft and the draining lymph nodes to suppress T cell responses[482,526-528]. In these studies Treg attenuate the priming of T cells in the lymph node to prevent their migration to the allograft, a mechanism which may be taking place in the current model to prevent infiltration of skin allografts with $CD8^+$ cells. We hypothesised that $FoxP3^+$ cells would be detectable in higher numbers in the skin-draining axillary lymph node compared with the contralateral axillary lymph node in mice that receive PBMC with Treg compared with those that receive PBMC alone. BALB/c-$Rag2^{-/-}c\gamma^{-/-}$ mice received a human skin allograft and 5 weeks later were reconstituted with $5x10^6$ allogeneic PBMC alone or together with $5x10^6$ *ex vivo*-expanded Treg derived from the same donor as the PBMC. 21 days after injection of cells, mice were sacrificed

and the skin-draining and contralateral axillary lymph nodes analysed by FACS for the presence of $FoxP3^+$ cells. In both groups, the number of detectable $FoxP3^+$ cells as a proportion of total cells was insignificant. This was partly due to difficulties in staining for a relatively rare intracellular marker in the presence of a large number of nonhuman cells, as well as human $FoxP3^-$ cells.

We therefore asked whether we would be able to detect human $CD4^+$ cells in the same lymph nodes in a system where the only human $CD4^+$ cells present are Treg. Injections of Treg alone do not successfully engraft in BALB/c-$Rag2^{-/-}c\gamma^{-/-}$ mice, and previous assays have indicated that the presence of the non-$CD4^+$ components of PBMC are required to allow cellular engraftment of the $CD4^+$ component (*unpublished observations* and other studies[447]). We therefore injected mice that had received a human skin graft with $5x10^6$ allogeneic PBMC depleted of $CD4^+$ cells by magnetic bead separation (-$CD4^+$ group), or $5x10^6$ allogeneic PBMC depleted of $CD4^+$ cells mixed with $5x10^6$ *ex vivo*-expanded Treg from the same donor (+Treg group), in order to provide the PBMC components necessary for $CD4^+$ cellular engraftment. A further group received unmanipulated PBMC (PBMC control group). Human $CD4^+$ cells were enumerated in the skin-draining axillary and contralateral lymph nodes, as well as the para-aortic lymph nodes (to provide a further control site) 30 days later. Mice in the +Treg group displayed a higher number of $CD4^+$ cells in the skin-draining lymph node compared with the contralateral lymph node (p=0.0144, ***Figure 5.15***) or the skin-draining lymph node of mice in the –$CD4^+$ group (p=0.0062). There was no significant difference in the number of $CD4^+$ cells in the skin-draining lymph node between mice in the +Treg group and the PBMC control

group (p=0.0592), although here the $CD4^+$ cells are more likely to be effector T cells than Treg. The presence of a low number of $CD4^+$ cells in lymph nodes of the $–CD4^+$ group implies incomplete depletion of $CD4^+$ cells from the cellular preparations. As the great majority of $CD4^+$ cells present in the +Treg group are Treg, these data imply that Treg preferentially aggregate at the skin-draining lymph node, a site at which alloantigen may be present. This is consistent with the studies demonstrating that Treg exert suppressive effects in the allograft-draining lymph nodes[482,526,528].

Treg have also been shown to actively regulate responses within the allograft[482,527]. As Treg did not fully prevent infiltration of human leukocytes into the human skin graft, we asked whether Treg would be detectable in the skin grafts where they may act to suppress cells that had already infiltrated the allograft. We hypothesised that higher numbers of human $FoxP3^+$ cells would be present in skin allografts from Treg-treated mice compared with skin allografts from mice receiving PBMC alone. Human $FoxP3^+$ cells were stained by immunohistochemistry in skin grafts from mice harvested 21 days post-adoptive transfer of $5x10^6$ allogeneic PBMC with or without $5x10^6$ *ex vivo*-expanded Treg derived from the same donor as the PBMC. A significantly higher number of human $FoxP3^+$ cells were present in skin grafts of mice that received Treg compared with those that received PBMC alone (p=0.0372, ***Figure 5.16a***). Representative photomicrographs demonstrate a relative lack of $FoxP3^+$ cells in the skin grafts from mice receiving PBMC alone compared with those receiving PBMC with Treg (***Figure 5.16c***). To further confirm this finding, we analysed the same skin grafts for levels of human *FOXP3* mRNA by qPCR. Here there was a trend

for increased human *FOXP3* mRNA levels in mice that received Treg compared with those that received PBMC alone (*p*=0.0506, ***Figure 5.16b***).

It has previously been demonstrated that mature activated Treg preferentially migrate to skin by virtue of their expression of the skin homing receptor CCR4[363,364]. We therefore asked whether *ex vivo*-expanded Treg express CCR4 after stimulation, thereby facilitating their migration into the skin allografts. We cultured Treg without stimulation for 18 hours or with αCD3/αCD28 microbead stimulation for 18 or 48 hours in order to simulate their activation *in vivo*. While unstimulated Treg had a relatively low expression of CCR4, after stimulation for 48 hours approximately one third of cells expressed CCR4 (***Figure 5.16d***), indicating their ability to migrate to the human skin allograft.

We next analysed long-term surviving human skin allografts from Treg treated mice to ask whether human $FoxP3^+$ cells persist within these allografts to continuously regulate alloresponses locally. Immunohistochemical staining revealed the widespread presence of human $FoxP3^+$ cells in long-term surviving skin allografts (***Figure 5.16e***). These cells all stained positive for human $CD4^+$ using a double staining immunohistochemistry protocol (*data not shown*). In order to determine whether the putative Treg in these allografts are active in regulation, we retransplanted long-term surviving allografts from Treg-treated mice to a new set of mice that were then reconstituted with $5x10^6$ PBMC (***Figure 5.17a***). As a control to ensure that the immunogenicity of the graft was not compromised, another set of mice received skin grafts that were parked on mice not reconstituted with PBMC for

the same period of time as the grafts from Treg-treated mice. This group also received $5x10^6$ PBMC. While mice that received skin grafts that were parked on mice not receiving PBMC rejected the human skin retransplants, mice receiving the retransplanted skin grafts from the Treg-treated mice engrafted the skin long-term (p=0.0169, ***Figure 5.17b and c***). These data imply that in mice receiving human Treg, human skin allografts are infiltrated with functional human Treg that are active in regulation even in the event of a fresh alloresponse.

5.9 Autologous Treg are more effective than non-autologous Treg

The studies performed up to this point in this chapter have all utilised autologous Treg derived from the same donor as the reconstituting PBMC used to 'humanise' the BALB/c-Rag2$^{-/-}$cγ$^{-/-}$ mice. While this is clearly an effective therapy, there have been reports that non-autologous Treg, derived from a third party unrelated to either the donor or recipient, may also be effective[519,529-531]. The advantage of non-autologous Treg is that they may be prepared in advance in large numbers to cGMP standards, to then be used as an 'off the shelf' therapy. More importantly, non-autologous Treg may be expanded in advance against a range of alloantigens to provide a bank of Treg that are alloreactive against a variety of HLA haplotypes. Treg reactive against a specific donor HLA haplotype may then be selected for therapy from this bank. This is particularly relevant in light of recent work that has demonstrated that human Treg that are donor alloantigen-reactive are more potent inhibitors of skin allograft rejection compared with polyclonally-reactive Treg[370]. However, while expansion and cryopreservation of recipient-derived Treg pre-

transplantation may be possible with polyclonally-reactive Treg, producing large numbers of recipient-derived Treg that are reactive to donor alloantigen would be logistically difficult clinically given that donors and recipients are matched and transplants performed at short notice. In such a situation there would be a potentially detrimental delay between the time of transplantation and the first dose of Treg therapy whilst the Treg are produced. The studies in this thesis have utilised Treg therapy at the time of PBMC reconstitution, simulating a scenario where Treg may be given at a time of lymphopaenia post-induction immunosuppression therapy. Whether Treg would be effective after a delay when immune reconstitution is underway is not clear.

To address some of these issues we first asked whether non-autologous Treg derived from neither donor nor recipient would be effective at regulating alloresponses to a human skin graft with the same efficacy as recipient-derived autologous Treg. We first determined whether non-autologous Treg suppress PBMC proliferation *in vitro* to the same degree as autologous Treg. *Ex vivo*-expanded human Treg were titrated into cultures of CFSE-labelled PBMC responders stimulated with αCD3/αCD28 microbeads and derived from the same Treg donor (autologous responders) or derived from a different allogeneic donor (non-autologous responders). The percentage of non-divided cells (i.e. $CFSE^+$) was determined by FACS as a measure of the degree of suppression of responder proliferation. There was no difference between the levels of suppression of either autologous or non-autologous $CD4^+$ (***Figure 5.18a*** and representative histograms in ***Figure 5.18c***) or $CD8^+$ (***Figures 5.18b*** and representative histograms in ***Figure 5.18d***) responders.

To ensure that this finding was not specific to the donors used in this particular assay, we repeated the *in vitro* suppression assay across a range of random donors and their permutations. A median of 5 HLA mismatches across HLA-A, HLA-B and HLA-DR was ensured between the permutations of PBMC and Treg donors. Again, there was no significant difference between the levels of suppression of autologous or non-autologous $CD4^+$ (p=0.1862, ***Figure 5.18e***) or $CD8^+$ (p=0.3609, ***Figure 5.18f***) responders. However, it is important to note that the above *in vitro* suppression assays utilised αCD3/αCD28 microbeads to stimulate PBMC rather than allogeneic stimulation, and therefore may not provide a completely accurate reflection of the suppressive efficacy of Treg *in vivo*, where PBMC would be stimulated by alloantigens. Furthermore, in these *in vitro* assays Treg would also be stimulated by the αCD3/αCD28 microbeads, providing them with a strong stimulus for activation that may not be matched *in vivo*.

We next hypothesised that non-autologous Treg would be effective at preventing human skin allograft rejection *in vivo*. BALB/c-$Rag2^{-/-}c\gamma^{-/-}$ mice received a human skin transplant and 5 weeks later were reconstituted with $5x10^6$ allogeneic PBMC alone, $5x10^6$ allogeneic PBMC with $5x10^6$ *ex vivo*-expanded Treg (i.e. 1:1 ratio PBMC to Treg), or $5x10^6$ allogeneic PBMC with $1x10^6$ *ex vivo*-expanded Treg (i.e. 5:1 ratio PBMC to Treg). In both cases Treg were derived from a donor allogeneic to both the reconstituting PBMC and skin donors (non-autologous Treg). Mice not achieving human leukocyte chimerism levels of >1% in the spleen were deemed to have failed to reconstitute and excluded from the survival analysis. Interestingly, whilst both ratios of non-autologous Treg prolonged skin allograft survival (1:1 MST 81.5 days

p=0.0025; 5:1 MST 67 days *p*=0.0111 *cf.* PBMC alone MST 35 days, ***Figures 5.19a and b***), neither was as effective as autologous Treg, where long-term survival may be attained with both 1:1 and 5:1 ratios of PBMC to Treg (***Figures 5.3a and b***). A 1:1 ratio of PBMC to non-autologous Treg was required to achieve the same regulatory capability achieved using a 5:1 ratio of PBMC to autologous Treg.

In *section 5.5*, we demonstrated that one of the mechanisms whereby autologous Treg prevent human skin allograft rejection is through a reduction of the percentage human leukocyte chimerism *in vivo* (***Figure 5.8b***). We hypothesised that non-autologous Treg would fail to reduce levels of human leukocyte chimerism to the same degree as autologous Treg. BALB/c-Rag2$^{-/-}$cγ$^{-/-}$ mice received a human skin transplant and 5 weeks later were reconstituted with 5x10^6 allogeneic PBMC alone, 5x10^6 allogeneic PBMC with 1x10^6 *ex vivo*-expanded Treg derived from the PBMC donor (i.e. autologous Treg), or 5x10^6 allogeneic PBMC with 1x10^6 *ex vivo*-expanded Treg derived from neither the PBMC nor skin graft donor (non-autologous Treg). Levels of human leukocyte chimerism were then measured regularly in the peripheral blood. As expected, while autologous Treg significantly reduced peripheral blood human leukocyte chimerism levels (*p*=0.0420), non-autologous Treg did not (*p*=0.6322, ***Figure 5.19c***).

5.10 Non-autologous Treg do not survive as well *in vivo* as autologous Treg

Killing of allogeneic cells requires priming of alloresponding cells *in vivo*[532]. We therefore hypothesised that the discrepancy between *in vitro* and *in vivo* suppressive

activity of non-autologous Treg was secondary to their killing *in vivo* by allogeneic PBMC. To test this, we injected BALB/c-Rag2$^{-/-}$cγ$^{-/-}$ mice with 5x10^6 PBMC from one donor (PBMC A), 5x10^6 PBMC A with 5x10^6 CFSE-labelled Treg from the same donor (Treg A; i.e. autologous Treg), 5x10^6 PBMC from a second donor (PBMC B), or 5x10^6 PBMC B with 5x10^6 CFSE-labelled Treg A (i.e. non-autologous Treg). 7 days later, intraperitoneal lavage fluid was obtained and the number of CD4$^+$CFSE$^+$ cells (i.e. Treg) determined by FACS analysis. The number of CD4$^+$CFSE$^+$ cells was significantly higher in mice receiving autologous Treg compared with mice receiving non-autologous Treg (p=0.0383, ***Figure 5.20a***). Importantly, this was not due to a complete dividing out of CFSE$^+$ cells in non-autologous Treg, as very few divisions were visible in histograms or dot plots from these groups (right panel, ***Figure 5.20b***). Moreover, dividing Treg were detectable in autologous Treg groups (left panel, ***Figure 5.20b***). Overall there was a significantly higher percentage of non-divided Treg in mice receiving non-autologous Treg compared to those receiving autologous Treg (p<0.0001, ***Figures 5.20c and d***), but a much lower number of Treg overall (***Figure 5.20a***).

These data suggest that non-autologous Treg do not survive *in vivo* as well as autologous Treg, and have lower proliferation rates. The poor performance of non-autologous Treg *in vivo* in preventing human skin allograft rejection compared with autologous Treg may be explained by this finding. However, it is important to note that non-autologous Treg still partially extend human skin allograft survival *in vivo*, and therefore a small number may still survive and seed in the mouse to suppress alloresponses, albeit less efficiently than autologous Treg.

5.11 *Ex vivo*-expanded Treg are less effective when given two weeks after PBMC injection

Together, the data in this chapter imply that *ex vivo*-expanded autologous Treg are a more effective therapy at preventing human skin allograft rejection than non-autologous Treg. However, as previously discussed, donor-reactive Treg are likely to be more effective than polyclonally reactive Treg. If autologous Treg were to be used, there would be a delay between the time of donor and recipient matching and transplantation and the subsequent expansion of donor-reactive Treg using donor APC or APC loaded with donor alloantigens. Clinically, there would be a delay between depletional induction immunosuppression and the time at which donor-reactive Treg may be ready for use. This delay may be long enough that a relative recovery in the state of leukopaenia develops by the time Treg are ready for use.

We previously demonstrated that the human leukocytes become detectable at significant levels in BALB/c-Rag2$^{-/-}$cγ$^{-/-}$ mice two weeks post-human PBMC injection (***Figure 3.11a***). We aimed to simulate a clinical scenario where there is a resolution of leukopaenia post-depletional immunosuppression followed by subsequent use of *ex vivo*-expanded Treg therapy. To achieve this, we asked whether autologous Treg would still be effective in our model if injected two weeks after PBMC injection, with the knowledge that human leukocyte engraftment is underway at this point. BALB/c-Rag2$^{-/-}$cγ$^{-/-}$ mice received a human skin transplant and 5 weeks later were reconstituted with 5x10^6 allogeneic PBMC, 5x10^6 allogeneic PBMC together with 5x10^6 *ex vivo*-expanded Treg, or 5x10^6 allogeneic PBMC followed two weeks later with 5x10^6 *ex vivo*-expanded Treg. As expected, conventional Treg therapy resulted

in long-term skin allograft survival (MST >100 days *cf.* 40.5 days for PBMC only, *p*=0.0084, ***Figures 5.21a and b***). In contrast, in mice receiving delayed Treg, long-term skin allograft survival was not achieved (MST 70 days, *p*=0.2072 compared with PBMC alone, ***Figures 5.21a and b***). Together these data indicate that injection of *ex vivo*-expanded autologous Treg at the time of PBMC injection is the most effective therapy for the prevention of human skin allograft rejection in our model.

5.12 Discussion

In this chapter we show for the first time the ability of autologous *ex vivo*-expanded human Treg to promote long-term engraftment of human skin allografts in a clinically relevant model (***Figure 5.3***). This effect is dose-dependent and occurs in the absence of any adjunctive immunosuppression. These data are particularly significant given the recognised challenge of regulating immune responses to human skin allografts.

Over the past decade Treg have attracted increasing interest as an adjunctive cellular therapy and we are closer than ever to the first clinical trials of Treg in SOT. Data from this humanised model, together with *in vitro* mechanistic data, provide a case for the therapeutic translation of Treg to clinical VCA transplantation. While the efficacy of Treg here is evident, further work is required to determine the safety of such a therapy *in vivo*. In particular, it is necessary to determine whether the use of a polyclonally-reactive population of Treg such as that used in this study would be detrimental to immune responses directed against pathogens and mutated cells.

Virtually no cases of XvHD were observed in mice receiving Treg with long-term surviving skin allografts (*unpublished observations*), suggesting a broad and possibly non-specific suppression of immune responses. This broad suppression is also suggested by the suppression of human antibody production in Treg treated mice (***Figure 5.11***), although this may be secondary to reduced B cell help from suppressed T cells.

Nevertheless, the concern regarding widespread suppression of alloresponses using polyclonally-reactive Treg may be unfounded. In a mouse model of Treg-mediated suppression of cardiac allograft rejection developed in our laboratory, host antiviral responses remained intact[533]. Treg act physiologically to suppress only activated effector T cells and not a blanket suppression of all T cells[18]. Through bystander suppressive mechanisms, cells in the locality of the site of regulation will be suppressed. In our model, the activated cells present will be alloresponsive cells directed against the allograft and weakly xenoreactive cells directed against mouse antigens (including xenoreactive B cells, ***Figure 4.10***). Therefore both these populations may be suppressed. The lasting effect of regulation will arise from Treg that gain antigen-specificity and remain as 'memory' Treg (such as those that exist normally to prevent the activity of autoreactive T cells that have escaped thymic negative selection)[18]. Cells that are not activated effector cells at the time of infusion of Treg cellular therapy will not be subject to Treg suppression, either in the short or long term. In essence, polyclonally-reactive Treg may convert into donor-reactive Treg after infusion, as long as the only source of inflammation and activation of effector cells is the allograft.

In mice that received a skin graft, but not mice that did not receive a skin graft, a significant reduction in the percentage of human leukocyte chimerism in the peripheral blood was observed (***Figures 5.8-5.10***). This suggests improved suppression of proliferating cells in mice receiving skin grafts. Considering that a significant T cell response develops against the skin allograft, these data suggest that there is a specific suppression of only activated or alloresponding T cells. In mice without a skin allograft there is no alloresponse and therefore Treg may not suppress the proliferation of T cells to the same degree, explaining why human leukocyte chimerism levels are not reduced (***Figure 5.10***). An alternative explanation is the requirement for Treg to be exposed to alloantigens to ensure their activation. In a mouse model of cardiac transplant tolerance, the presence of the allograft itself as a source of donor alloantigen was found to be essential for maintaining T cell unresponsiveness *in vivo*[534]. Here, the presence of the allograft may be necessary for the renewal of Treg throughout the life of the allograft through the process of infectious tolerance[535].

Introducing a known pathogen into Treg-treated mice with long-term surviving human skin allografts and then monitoring the efficacy of its clearance would help to assess whether other immune responses remain intact in Treg-treated mice. Furthermore, in Treg-treated mice that have engrafted a human skin transplant long term, monitoring the survival of a second human skin graft from an allogeneic donor applied to the same mouse would help to assess whether donor-specific immunoregulation has developed. These assays would help determine whether true tolerance has developed.

Donor alloantigen-reactive Treg are theoretically safer for *in vivo* use[536], however methods for their production in large numbers have not yet been optimised. Moreover, the current methods for the production of antigen-reactive Treg, for example by culture with allogeneic stimulators[371,372] or retroviral vector transduction of Treg with genes that encode for TCRs with known antigen specificities[373], may not produce Treg that are phenotypically and functionally activated to the same degree as Treg expanded in the presence of strong stimulation with αCD3/αCD28 microbeads. Given that activation of Treg is critical for their *in vivo* functionality (***Figure 5.6***), and that this is a significant advantage of the polyclonal expansion process (***Figure 5.4***), a concern would be that Treg expanded using donor allostimulation would not as effective as Treg expanded using polyclonal stimulation.

Nevertheless, a recent study using Treg expanded using donor APC stimulators found a modest improvement in the histological features of rejection of human skin allografts compared with polyclonally-stimulated Treg[370]. Donor-reactive Treg may indeed be more suppressive on a cell-by-cell basis compared with polyclonal Treg. However, whether it is absolutely necessary to use such cells is debatable, given that similar results may be achieved with higher numbers of polyclonally-reactive Treg that are more easily expanded *in vitro* to produce large numbers. The use of recipient-derived donor-reactive Treg would necessitate a delay between receipt of the allograft and infusion of Treg therapy while Treg are expanded using donor alloantigen (assuming the donor is not previously arranged, which would be the case for all VCA transplants but not for some SOT living donor transplants). This delay may reduce the efficacy of Treg (***Figure 5.21***), therefore negating any benefit of

using donor-reactive Treg. In contrast, recipient-derived polyclonally-reactive Treg may be expanded using αCD3/αCD28 microbeads at any time before transplantation and cryopreserved for use at the optimum time point.

Treg have been shown to prevent lymphopaenia-induced proliferation of T cells[537,538]. The improved efficacy of Treg given early may be related to the need for Treg to be present early at a time of lymphopaenia, at which point they are still able to suppress this proliferation process that ultimately results in the expansion of alloreactive effector T cells. Alternatively, the effectiveness of Treg given early may be related to the simple fact that Treg are more effective when given at higher ratios of Treg to PBMC (***Figure 5.3***). Two weeks post-PBMC injection, a higher number of effector cells would be present, effectively increasing the PBMC to Treg ratio. It would be interesting to evaluate whether delayed Treg therapy becomes effective when larger numbers of Treg are infused.

Expansion and cryopreservation of a variety of non-autologous Treg against a wide range of HLA types, which may then be selected according to donor HLA haplotype, may circumvent the problem of having to inject Treg early. However these Treg are again less effective than recipient-derived Treg in our model (***Figure 5.19***) due to their killing by alloreactive host cells (***Figure 5.20***). Killing of allogeneic Treg is consistent with observations in the literature. For example, in a clinical study where Brunstein and colleagues examined third-party UCB-derived Treg for the prevention of GvHD after clinical HSC transplantation, a reduction over time in detectable Treg

was observed[411]. This reduction was more rapid after the second infusion of Treg, suggesting a sensitisation of the alloresponse against allogeneic Treg *in vivo*.

Another explanation for the relatively poor efficacy of non-autologous Treg in preventing skin graft rejection may stem from the requirement of Treg to recognise the same HLA-peptide complex targeted by recipient effector T cells[539,540]. It is possible that Treg may need to be self-restricted in the same manner as the effector cells they regulate in order to be effective. Finally, it is important to keep in mind that Treg expanded against donor antigen will theoretically only be active via the direct allorecognition pathway. Evidence indicates that Treg need to be both directly and indirectly alloreactive in order to be suppressive in the long-term[353].

There are few studies in the literature that evaluate the efficacy of human Treg derived from a third party. In the Brunstein et al. study, Treg were derived from UCB and were therefore significantly different in phenotype from the population of Treg used in our study[411]. Studies directly comparing the efficacy of autologous and non-autologous Treg are also few. In one study of xenotransplantation of pig pancreatic tissue into mice, mouse third-party derived and recipient-derived Treg were said to be similar in efficacy, although a direct comparison was not shown[531]. In a more relevant study of non-human primate Treg, expanded third-party derived and recipient-derived Treg were found to suppress proliferation of responder cells stimulated with alloantigen to equal degrees *in vitro*[541]. Our study is the first to clearly demonstrate the reduced efficacy of non-autologous (third-party derived) Treg compared with autologous (recipient-derived) Treg in the prevention of human

skin rejection. While the use of non-autologous Treg may not be advantageous in its current form, their use must be kept as an option for a select group of patients in whom expansion of functional autologous Treg may not be possible, such as those with autoimmune disease secondary to functionally defective Treg.

In our study, both non-autologous and autologous Treg displayed an equal degree of suppressive ability *in vitro* (***Figure 5.18***). However, it is important to note that cells in the assay were stimulated with αCD3/αCD28 microbeads, which would also stimulate Treg efficiently, therefore improving their potency. This *in vitro* assay could therefore be improved by using allogeneic stimulators instead of αCD3/αCD28 microbeads for stimulation. Nevertheless, an important point to note is that *in vitro* and *in vivo* observations do not always correspond. While *in vitro* recipient-derived and third party-derived Treg were equally effective at suppressing responder cell proliferation, *in vivo* third party-derived Treg were not as effective as recipient-derived Treg at preventing skin rejection (***Figure 5.19*** *cf.* ***Figure 5.3***). Treg may employ dissimilar suppressive mechanisms *in vivo* and *in vitro*, in part explaining this discrepancy[542]. More importantly, allogeneic Treg may be killed *in vivo* (***Figure 5.20***), whereas *in vitro* this may not take place due to the lack of appropriate priming signals. Another explanation may be that *in vitro* the majority of responding cells will not be of memory phenotype, whereas *in vivo* the majority of engrafting effector T cells gain the memory cell marker CD45RO (***Figure 3.12c***). Such cells may be more difficult to suppress[146]. Ultimately, these findings highlight the importance of evaluating cellular therapies such as Treg within a clinically relevant humanised system *in vivo*.

Human *ex vivo*-expanded Treg in our study expressed low levels of CD127, high levels of CD27, as well as high levels of CCR7, CD62L, and after stimulation, moderate levels of CCR4 (***Figures 5.1 and 5.16***). The low expression of CD127 and high expression of CD27 is indicative of a highly suppressive subpopulation of Treg that primarily act in the allograft and draining lymph node[357,358,448]. This is confirmed further by the expression of CD62L and CCR7 which are peripheral lymphoid tissue homing receptors[311,347,520]. The majority of Treg in our study also expressed CD45RO, with only around 20% expressing CD45RA instead (*unpublished data,* Dr J Hester). $CD45RO^+$ Treg express high levels of CLA and CCR4 and therefore preferentially migrate to skin through the ligation of CCL17[363,364,543]. In the current study we found that human Treg express significant levels of CCR4 after stimulation (***Figure 5.16***). This expression of both lymphoid and skin homing receptors in the Treg used in our study fits in with their detection in both the skin allograft-draining lymph node and the skin allograft itself (***Figures 5.15*** and ***5.16***). The expression of these receptors is important for their function[347,395,520]: Treg act in the graft draining lymph nodes to prevent the priming of effector T cells and within the allograft itself to suppress cells directly[482].

FoxP3 may be expressed transiently on activated $CD4^+$ T cells[544] and this poses a problem when using FoxP3 for the detection of Treg, as we did in skin grafts (***Figure 5.16***). However, the higher number of $FoxP3^+$ cells in skin grafts from mice receiving Treg compared with those receiving PBMC alone indicates that at least some of these cells are likely to be true Treg, as a higher number of activated effector cells

(which may express FoxP3) would be expected to be seen in mice receiving PBMC only.

As further evidence, skin grafts which are retransplanted from primary recipients that had received Treg therapy survive long-term on new mice that receive PBMC (***Figure 5.17***), indicating that a regulatory population exists within the skin graft that is capable of suppressing a new population of effector cells. These data suggest that the prevention of rejection in our model is an active process that operates beyond the draining lymph node. In a mouse model where Treg-dependent skin allograft tolerance was induced, retransplanted skin allografts were shown to contain Treg that recolonised the new host and prevented nontolerant lymphocytes from rejecting fresh skin allografts[527]. Further work is required to determine whether the Treg within the allograft in our model may be detected in the new mouse host. In addition, it would be interesting to evaluate whether such Treg are able to prevent the rejection of a fresh skin allograft on the same mouse and if so whether the phenomenon is donor-specific, implying the development of donor-specific tolerance.

The majority of engrafting PBMC in our model gain phenotypic markers of memory T cells. While there is some concern that Treg are unable to suppress memory T cells[124], data from our study indicate that this is not necessarily the case. In a recent mouse study, $CD8^+$ memory T cell-mediated skin graft rejection could be regulated as long as granulocytes were depleted[341]. $CD8^+$ memory T cells rapidly recruit granulocytes to the allograft, which then cause significant damage. In the current

study, there is no engraftment of human granulocytes in the mouse. Moreover, mouse granulocytes were found not to be significant in mediating damage to the allograft (***Figure 4.7***). Hence, if granulocytes are the 'barrier' to memory T cell regulation in skin, this barrier does not exist in our model. A reduction in the human skin graft cellular infiltrate is a good indicator of a reduction in alloimmune injury[457,458]. We found a significant reduction in the infiltration of regulated human skin grafts with $CD8^+$ cells but not $CD4^+$ cells (***Figure 5.14***). However, any reduction in the $CD4^+$ graft infiltrate may be underestimated, as in mice receiving Treg, many of these cells are $FoxP3^+$ and thus putative Treg, not effector cells (***Figure 5.16***). Moreover, mice receiving Treg are receiving a larger number of $CD4^+$ cells than those receiving PBMC alone, given that Treg are $CD4^+$. The observation that intragraft $CD4^+$ cell numbers are similar in both groups does not take this confounding factor into account.

The reduction in graft infiltrating $CD8^+$ cells may be an important mechanism by which Treg prevent skin graft rejection. $CD8^+$ cells are critical to mouse skin rejection[341,482] and in human skin rejection there is a slight predominance of graft infiltrating $CD8^+$ cells over graft infiltrating $CD4^+$ cells[505]. This suggests the relative importance of $CD8^+$ cells in human skin rejection. In accordance with this, we have observed a higher proportion of human $CD8^+$ compared with $CD4^+$ cells in the peripheral blood of mice that are rejecting a human skin allograft (***Figure 3.12***). Moreover, we have observed that $CD8^+$ cells are the predominant population to enter the epidermis (***Figure 4.5c***), where an important element of graft destruction takes place. In the Banff 2007 classification of skin rejection, infiltration of and

damage to the epidermis results in a classification of Grade III/IV (severe) rejection[434].

However, acute allograft rejection may still occur in the complete absence of $CD8^+$ T cells[125,545,546]. Moreover, in a humanised model of skin rejection in which mice were reconstituted with $CD4^+$ T cells alone, skin damage was still observed (although not complete skin destruction)[370]. In this particular study, Treg therapy reduced skin graft $CD4^+$-mediated alloimmune injury, indicating that Treg may also suppress $CD4^+$ cells. We have been unable to engraft single $CD4^+$ or $CD8^+$ T cell populations in BALB/c-$Rag2^{-/-}c\gamma^{-/-}$ mice in order to address the respective impact each population has on the rejection process. However, Pober and colleagues have shown in a humanised SCID mouse model that elimination of human $CD8^+$ T cells from the inoculum does not alter the pattern of injury, although the $CD4^+$ cells that proliferate in the mouse become perforin positive, thus undergoing abnormal differentiation in order to compensate for the lack of $CD8^+$ cells[447]. The role of $CD4^+$ T cells in human skin rejection in the presence of $CD8^+$ T cells thus requires further investigation.

In our model, Treg may suppress $CD4^+$ cells through different mechanisms than those employed to block the infiltration of $CD8^+$ cells into the allograft. We noted a significant reduction in the levels of human leukocyte chimerism and number of proliferating human T cells in mice receiving Treg (***Figures 5.8 and 5.9***). While this may partly explain the reduction in the infiltration of human skin grafts with $CD8^+$ cells, it also indicates a widespread suppression of T cells, especially as the effect was not restricted to only $CD8^+$ T cells but also extended to the suppression of $CD4^+$ T cell

proliferation (***Figure 5.9***). Clearly however, there are other mechanisms active given that $CD4^+$ infiltration of skin grafts was not reduced to the same degree as $CD8^+$ cell infiltration. The expression of LAP on Treg in our study (***Figure 5.5***) suggests that these cells may be active through the production of suppressive soluble factors, in contrast with LAP^- Treg that are only active through cell-contact dependent mechanisms[365,367]. In particular, LAP^+ Treg express surface TGFβ and produce soluble TGFβ, both of which suppress the proliferation of effector cells or prevent their activation[365,547]. Assays where TGFβ or LAP are blocked *in vivo* would assist in the elucidation of the mechanisms at play and their importance in regulating the immune responses to skin in our model.

An important characteristic of long-term surviving Treg-treated human skin allografts is the relative protection of their microvessels (***Figure 5.13***). In *Chapter 3* we demonstrated that human skin grafts revascularise successfully with human microvasculature pervading the skin graft and even the native mouse tissues. The state of the microvasculature of skin is a highly sensitive marker for rejection, and various studies have used it as a quantitative marker for the degree of skin allograft protection attained when evaluating a novel therapy[370,457,458]. Significant damage to skin microvessels will result in necrosis of the skin allograft, especially if the vessels are not replaced with functional vessels that supply the skin. Their condition is therefore critical and their destruction would signify imminent loss of the skin graft. In a study from our laboratory using a humanised mouse model of vessel transplant rejection, human ECs within the vessel allograft were replaced with mouse ECs[448]. This was followed by intimal hyperplasia of these vessels. In the current study, we

show that injection of PBMC alone mediates the loss of human ECs and that this effect is reversed with the use of Treg (***Figure 5.13***). Importantly, PBMC did not mediate any significant damage to mouse microvessels. This indicates a lack of a xenoresponse against mouse vessels in the same time frame as the alloresponse against human vessels, suggesting that the xenoresponse that develops is not as potent as the human alloresponse. As discussed in *Chapter 4*, ECs may act as the primary APCs in the allorecognition process given the lack of human host DCs and the relative unimportance of donor passenger leukocytes in mediating graft loss (***Figure 4.2***). The alloresponse therefore appears to begin and end with the ECs and the protection of these pivotal cells by Treg is significant.

In this chapter we have provided valuable data for the efficacy of Treg in the prevention of human skin rejection in a clinically relevant translational model. Together, these data indicate that polyclonally-reactive Treg are most effective when they are expanded (***Figure 5.4***) or activated (***Figure 5.6***), derived from the recipient (***Figures 5.3*** and ***5.19***), given at the same time as PBMC inoculation (or at a time of lymphopaenia) (***Figure 5.21***), and given at ratios of 5:1 PBMC to Treg or above (***Figure 5.3***). Although a 5:1 ratio of PBMC to Treg may on face value appear to be a large number of necessary Treg, if given at a time of host lymphopaenia, this would translate to a relatively low number of Treg. Extending these data to clinical VCA transplantation, the most effective Treg therapy would therefore be an *ex vivo*-expanded population of Treg derived from the VCA recipient and given together or shortly after induction immunosuppression, at a time of relative lymphopaenia.

5.13 Figures and legends

Figure 5.1. Sorting and expansion strategy for human Treg and post-expansion phenotype.

(a) Schematic representation and representative FACS plots of the human Treg sorting and expansion protocol. Initial FACS plot is gated on live human $CD4^+$ cells. $CD127^{lo}CD25^+CD4^+$ cells were flow-sorted to a high purity and subsequently expanded *in vitro* with rhIL-2 and αCD3/αCD28 microbeads. Representative FACS plots of cells pre-sort, post-sort, and post-expansion are shown. Post-sorting and expansion, the majority of cells (89.3% in the FACS plot shown) maintained the expression $CD127^{lo}CD25^+$. **(b)** Representative FACS plots of human Treg post-expansion. Cells expressed high levels of FoxP3, CD25, CD62L, CCR7, and CD27, as well as low levels of CD127. FACS plots shown are representative of n=7 independent assays.

Figure 5.2 PBMC are suppressed *in vitro* by *ex vivo*-expanded Treg in a dose-dependent manner.

(a) *In vitro* suppression assay of human *ex vivo*-expanded $CD127^{lo}CD25^{+}CD4^{+}$ human Treg. PBMC were stimulated *in vitro* with αCD3/αCD28 microbeads (*top panel*) or irradiated allogeneic PBMC (*bottom panel*) and cultured in the presence of *ex vivo*-expanded Treg for 7 days. ^{3}H-thymidine was added for the last 16 hours of culture (n=4 independent assays for polyclonally-stimulated PBMC and n=6 independent assays for allostimulated PBMC). A 2:0 ratio of PBMC to Treg crowding control is included together with a 0:1 Treg only control. CPM: counts per minute. **(b)** Representative FACS plots from a 7-day culture of $2x10^{4}$ CFSE-labelled PBMC stimulated with $2x10^{3}$ αCD3/αCD28 microbeads. Cells are gated on live human $CD3^{+}$ cells and then further gated into $CD4^{+}$ and $CD8^{+}$ cells. **(c)** Representative FACS plots from a 7-day culture of $2x10^{4}$ CFSE-labelled and $2x10^{4}$ unlabelled PBMC stimulated with $2x10^{3}$ αCD3/αCD28 microbeads. Cells are gated on live human $CD3^{+}$ cells and then further gated into $CD4^{+}$ and $CD8^{+}$ cells. FACS plots are representative of n=4 independent assays.

Figure 5.3 *Ex vivo*-expanded human Treg prevent *in vivo* human skin allograft rejection.

BALB/c-Rag2$^{-/-}$cγ$^{-/-}$ mice received a human skin transplant and 5 weeks later were injected with 5x10^6 allogeneic PBMC (n=22 mice) or 5x10^6 allogeneic PBMC together with *ex vivo*-expanded CD127^{lo}CD25$^+$CD4$^+$ human Treg derived from the PBMC donor (i.e. autologous Treg). Treg were given at 5x10^6 cells (n=12 mice), 1x10^6 cells (n=13 mice), or 0.5x10^6 Treg cells (n=5 mice). **(a) and (b)** Human skin graft survival. The MST was calculated for each group. Statistically significant prolongation of survival compared to PBMC alone was achieved with 5x10^6 Treg (p=<0.0001) and 1x10^6 Treg (p=0.0001), but not 0.5x10^6 Treg (p=0.0876). Data are pooled from n=6 separate survival assays using different skin and PBMC donor combination for each. The median HLA mismatch across the 6 assays was 6.5. **(c)** Representative photographs of human skin grafts from mice receiving 5x10^6 PBMC together with 5x10^6 Treg. The right panel shows the pliability of the graft when pinched.

Figure 5.4. *In vitro* expansion of human Treg improves their *in vivo* efficacy.

(a) *In vitro* ^{3}H-thymidine incorporation suppression assay of polyclonally-stimulated PBMC. PBMC incubated with αCD3/αCD28 microbeads and autologous *ex vivo*-expanded or non-expanded $CD127^{lo}CD25^{+}CD4^{+}$ human Treg at a ratio of 1:1/4 PBMC to Treg. Percentage suppression of proliferation is shown relative to the proliferation of PBMC in the absence of Treg (1:0 ratio of PBMC to Treg). Data are represented as mean ±SD, NS: p=0.9888. **(b) and (c)** BALB/c-$Rag2^{-/-}c\gamma^{-/-}$ mice received a human skin transplant and 5 weeks later were injected with $5x10^{6}$ allogeneic PBMC (n=24 mice) or $5x10^{6}$ allogeneic PBMC with either $1x10^{6}$ *ex vivo*-expanded $CD127^{lo}CD25^{+}CD4^{+}$ human Treg (n=15 mice) or $1x10^{6}$ flow-sorted but non-expanded $CD127^{lo}CD25^{+}CD4^{+}$ human Treg (n=10 mice). Data are pooled from n=7 separate survival assays using a different skin and PBMC donor combination for each. Long-term survival (MST >100) was only achieved using *ex vivo*-expanded human Treg (p<0.0001).

Figure 5.5. Polyclonally-stimulated human Treg display an activated and suppressive phenotype.

$CD127^{lo}CD25^{+}CD4^{+}$ human Treg were flow-sorted and subsequently stimulated *in vitro* with αCD3/αCD28 microbeads for 12 hours (at a ratio of 1 bead to 10 cells). Treg were assessed before stimulation and after *in vitro* stimulation with αCD3/αCD28 microbeads for **(a)** the percentage of cells expressing Ki67, **(b)** the percentage of cells expressing CD69, **(c)** the percentage of cells expressing LAP, **(d)** the percentage of cells expressing FoxP3, **(e)** the median fluorescence intensity (MFI) of CD25 and **(f)** the MFI of FoxP3. Data are shown from n=4 separate PBMC donors pre- and post-stimulation, with one data point per PBMC donor. ****:$p<0.0001$; **:$p<0.01$; *:$p<0.05$. **(g)** Representative FACS plots with arrows indicating increases in respective cellular markers post-stimulation. FACS plots are representative of n=4 independent assays.

FoxP3 MFI was determined in cells pre-stimulation and post-stimulation, and levels gated on total cells or cells that were positive within pre-stimulation and post-stimulation groups for: **(h)** CD69, **(i)** Ki67 or **(j)** LAP. Data are shown from n=4 separate PBMC donors pre- and post-stimulation, with one data point per PBMC donor and calculated means.

Figure 5.6. Stimulated Treg are more effective than unstimulated Treg *in vivo*.

(a) and (b) BALB/c-Rag2$^{-/-}$cγ$^{-/-}$ mice received a human skin transplant and 5 weeks later were injected with 5x10^6 allogeneic PBMC (n=13 mice) or 5x10^6 allogeneic PBMC with either 1x10^6 FACS-sorted CD127^{lo}CD25$^+$CD4$^+$ human Treg derived from the PBMC donor (i.e. autologous Treg) and stimulated *in vitro* for 12 hours with αCD3/αCD28 microbeads (stimulated Treg, n=4 mice) or 1x10^6 flow-sorted CD127^{lo}CD25$^+$CD4$^+$ autologous human Treg that are not stimulated *in vitro* (fresh sorted, unstimulated Treg, n=10 mice). Data are pooled from n=8 separate survival assays using a different skin and PBMC donor combination for each assay. Long-term survival (MST >100) was only achieved using *in vitro* stimulated human Treg (*p*=0.0011).

Figure 5.7. Effect of *ex vivo*-expanded human Treg therapy on human leukocyte reconstitution levels in BALB/c-Rag2$^{-/-}$cγ$^{-/-}$ mouse spleens.

BALB/c-Rag2$^{-/-}$cγ$^{-/-}$ mice received a human skin graft and 5 weeks later were injected with 5x10^6 allogeneic PBMC or 5x10^6 allogeneic PBMC with 5x10^6 *ex vivo*-expanded CD127^{lo}CD25$^+$CD4$^+$ human Treg derived from the PBMC donor (i.e. autologous Treg). **(a)** At the point of skin graft rejection (for PBMC only, n=10 mice) or long-term survival (for PBMC with Treg, n=7 mice), spleens from mice were analysed for the total number of live human 7AAD$^-$CD45$^+$ cells present (huCD45$^+$). Data are pooled from n=3 separate assays using a different skin and PBMC donor combination for each and represented as mean ±SD.

In a separate assay, BALB/c-Rag2$^{-/-}$cγ$^{-/-}$ mice received a human skin graft and 5 weeks later were injected with 5x10^6 allogeneic PBMC (n=4 mice) or 5x10^6 allogeneic PBMC with 5x10^6 *ex vivo*-expanded CD127^{lo}CD25$^+$CD4$^+$ Treg derived from the PBMC donor (i.e. autologous Treg, n=4 mice). Mice were sacrificed 40 days after cellular transfer and spleens analysed for **(b)** the total number of live human 7AAD$^-$CD45$^+$ (huCD45$^+$) and **(c)** the percentage of live human 7AAD$^-$CD45$^+$ cells as a proportion of total live mononuclear cells (%huCD45$^+$). Data are represented as mean ±SD from a single skin and PBMC donor combination.

Figure 5.8. Effect of *ex vivo*-expanded human Treg therapy on human leukocyte reconstitution levels in the peripheral blood of BALB/c-Rag2$^{-/-}$cγ$^{-/-}$ mice transplanted with human skin allografts.

BALB/c-Rag2$^{-/-}$cγ$^{-/-}$ mice received a human skin graft and 5 weeks later were injected with 5x10^6 allogeneic PBMC (n=12 mice) or 5x10^6 allogeneic PBMC with 5x10^6 *ex vivo*-expanded CD127^{lo}CD25$^+$CD4$^+$ human Treg derived from the PBMC donor (i.e. autologous Treg, n=12 mice) and the peripheral blood analysed weekly by FACS for **(a)** the number of live human 7AAD$^-$CD45$^+$ cells (huCD45$^+$) per 100µl blood and **(b)** the percentage of live human 7AAD$^-$CD45$^+$ cells as a proportion of total live mononuclear cells (%huCD45$^+$). *:*p*=0.0118, two-way ANOVA. Data are represented as mean ±SD and are pooled from n=5 separate assays using a different skin and PBMC donor combination for each assay.

Figure 5.9. BALB/c-Rag2$^{-/-}$cγ$^{-/-}$ mice receiving *ex vivo*-expanded human Treg therapy demonstrate reduced numbers of circulating proliferating lymphocytes.

BALB/c-Rag2$^{-/-}$cγ$^{-/-}$ mice received a human skin graft and 5 weeks later were injected with 5x10^6 allogeneic PBMC (n=4 mice) or 5x10^6 allogeneic PBMC with 5x10^6 *ex vivo*-expanded CD127^{lo}CD25$^+$CD4$^+$ human Treg derived from the PBMC donor (i.e. autologous Treg, n=4 mice). 40 days post-adoptive cellular transfer, mice were sacrificed and peripheral blood and spleens analysed for the presence of human Ki67$^+$ cells. Cells were gated on live human 7AAD$^-$CD45$^+$ cells and then further gated on human CD3$^+$, CD3$^+$CD4$^+$ or CD3$^+$CD8$^+$ cells. Data are represented as mean ±SD and derived from a single *in vivo* assay. Statistical significance was determined between PBMC only and PBMC + Treg groups: *:p<0.05; **:p<0.01.

Figure 5.10. Effect of *ex vivo*-expanded human Treg therapy on human leukocyte reconstitution levels in the peripheral blood of BALB/c-Rag2$^{-/-}$cγ$^{-/-}$ mice without a human skin allograft.

BALB/c-Rag2$^{-/-}$cγ$^{-/-}$ mice were injected with 5x10^6 PBMC alone (n=4 mice) or 5x10^6 PBMC with 5x10^6 *ex vivo*-expanded CD127^{lo}CD25$^+$CD4$^+$ human Treg derived from the PBMC donor (i.e. autologous Treg, n=5 mice). The peripheral blood was analysed weekly by FACS for **(a)** the number of live human 7AAD$^-$CD45$^+$ cells (huCD45$^+$) per 100µl blood and **(b)** the percentage of live human 7AAD$^-$CD45$^+$ cells as a proportion of the total live mononuclear cell count (%huCD45$^+$). Mice did not receive a skin graft. Data are represented as mean ±SD and are obtained from a single *in vivo* assay using one PBMC donor.

Figure 5.11. BALB/c-Rag2$^{-/-}$cγ$^{-/-}$ mice receiving Treg therapy display reduced levels of serum human immunoglobulin.

BALB/c-Rag2$^{-/-}$cγ$^{-/-}$ mice received a human skin graft and 5 weeks later were injected with 5x10^6 allogeneic PBMC (n=13 mice) or 5x10^6 allogeneic PBMC with 5x10^6 *ex vivo*-expanded CD127^{lo}CD25$^+$CD4$^+$ human Treg derived from the PBMC donor (i.e. autologous Treg, n=8 mice). **(a)** 21 days post-adoptive transfer, n=4 mice from each group were sacrificed and serum levels of human IgG and IgM were determined by ELISA. **(b)** The remaining mice (PBMC n=9, PBMC + Treg n=4) were sacrificed at the point of skin graft rejection (for the PBMC group) or long-term survival (LTS, for the PBMC + Treg group) and serum levels of human IgG and IgM determined by ELISA. Mice not achieving human leukocyte chimerism levels of >1% in the spleen were excluded from the analysis in (b). Data are represented as mean ±SD and pooled from n=3 separate *in vivo* assays using a different skin and PBMC donor combination for each assay. *:p=0.0381; **:p=0.0079.

Figure 5.12. Human skin allograft microarchitecture is preserved in Treg-treated humanised BALB/c-Rag2$^{-/-}$cγ$^{-/-}$ mice.

BALB/c-Rag2$^{-/-}$cγ$^{-/-}$ mice received a human skin graft and 5 weeks later were injected with 5x10^6 allogeneic PBMC (n=4 mice) or 5x10^6 allogeneic PBMC with 5x10^6 *ex vivo*-expanded CD127^{lo}CD25$^+$CD4$^+$ human Treg derived from the PBMC donor (i.e. autologous Treg, n=4 mice). Representative photomicrographs of human skin sections harvested 40 days post adoptive cellular transfer and stained with H&E are shown from **(a)** a mouse receiving PBMC only and **(b)** a mouse receiving PBMC with Treg. The green arrow indicates loss of the superficial layers of the epidermis (stratum corneum and stratum lucidum) in mice not receiving Treg compared to preservation of the respective layers in mice receiving Treg. The white arrow indicates cells undergoing vacuolation. The red arrows indicate cellular infiltrates and aggregates. The histology shown is representative of 8 stained sections from each of n=4 mice for each experimental group.

Figure 5.13. Human microvessels in human skin allografts are preserved in Treg-treated humanised BALB/c-Rag2$^{-/-}$cγ$^{-/-}$ mice.

BALB/c-Rag2$^{-/-}$cγ$^{-/-}$ mice received a human skin graft and 5 weeks later were injected with 5x10^6 allogeneic PBMC (n=3 mice) or 5x10^6 allogeneic PBMC with 5x10^6 *ex vivo*-expanded CD127^{lo}CD25$^+$CD4$^+$ human Treg derived from the PBMC donor (i.e. autologous Treg, n=3 mice). A further group did not receive any cells (RPMI-1640 medium only, n=2 mice). **(a)** 21 days post-adoptive cellular transfer, skin grafts were harvested and analysed by immunohistochemistry for the number of complete cellular rings staining positive for either human CD31 or mouse CD31 within the dermis and epidermis. Complete rings were counted in the entirety of 3 separate sections (i.e. in triplicate) per skin sample. Data are represented as mean values of the average of these triplicate values ±SD from a single *in vivo* assay using one PBMC donor and one skin donor. **:p<0.005, ****:p<0.0001, NS: not significant.

Representative photomicrographs are shown of human skin sections harvested 21 days post adoptive cellular transfer and stained by immunohistochemistry to visualise human CD31$^+$ or mouse CD31$^+$ cells in **(b)** mice receiving 5x10^6 PBMC only and **(c)** mice receiving 5x10^6 PBMC with 5x10^6 *ex vivo*-expanded Treg. Sections are counterstained with haematoxylin. The histology shown is representative of 6 stained sections for each type of stain for each of n=3 mice for each group.

Representative photomicrographs are shown of human skin sections from mice receiving PBMC with Treg, harvested >100 days post adoptive cellular transfer and stained by immunohistochemistry for **(d)** human CD31$^+$ cells and **(e)** mouse CD31$^+$ cells. Sections are counterstained with haematoxylin. Multiple complete human and mouse CD31$^+$ rings are visible. Photomicrographs are representative of 6 sections from each of n=4 mice.

Figure 5.14. Infiltration of human skin allografts with human $CD8^+$ cells is reduced in humanised BALB/c-$Rag2^{-/-}c\gamma^{-/-}$ mice receiving Treg therapy.

BALB/c-$Rag2^{-/-}c\gamma^{-/-}$ mice received a human skin graft and 5 weeks later were injected with $5x10^6$ allogeneic PBMC or $5x10^6$ allogeneic PBMC with $5x10^6$ *ex vivo*-expanded $CD127^{lo}CD25^+CD4^+$ human Treg derived from the PBMC donor (i.e. autologous Treg). **(a)** 21 days post-adoptive cellular transfer, skin grafts were harvested from mice receiving PBMC (n=4 mice) or mice receiving PBMC with Treg (n=3 mice) and analysed by immunohistochemistry for the number of human $CD45^+$ ($huCD45^+$), $CD4^+$ ($huCD4^+$) or $CD8^+$ ($huCD8^+$) cells present. **(b)** At the point of rejection (for the PBMC only group, n=4 mice) or long-term survival (LTS, for the PBMC + Treg group, n=5 mice), skin grafts were harvested and analysed by immunohistochemistry for the number of $huCD45^+$, $huCD4^+$ or $huCD8^+$ cells present. The number of positive cells was quantified in 3 random fields at 400X magnification for each of 4 separate sections for each skin graft and antigen, and the mean of these counts taken for each data point. Data are represented as the mean of these values ±SD. *:$p<0.05$. **(c)** At the same time points as (b), human skin grafts were analysed for the level of human *CD3* mRNA normalised to *HPRT* (mRNA/*HPRT*) by qPCR (n=5 mice for PBMC only and n=4 mice for PBMC with Treg). Data are represented as the measured data points and calculated mean for each group, $p=0.4058$.

Figure 5.15. Human Treg home to the skin allograft-draining lymph node.

BALB/c-Rag2$^{-/-}$cγ$^{-/-}$ mice received a human skin graft and 3 days later were injected with 5x10^6 allogeneic PBMC depleted of CD4$^+$ cells (-CD4$^+$ group, n=3 mice) or 5x10^6 allogeneic PBMC depleted of CD4$^+$ cells with 5x10^6 *ex vivo*-expanded CD127^{lo}CD25$^+$CD4$^+$ human Treg (+Treg group, n=3 mice). CD4$^+$ cells were depleted from PBMC by magnetic bead separation to a purity of >98%. A further control group received 5x10^6 unmanipulated allogeneic PBMC alone (n=3 mice). 21 days post-adoptive cellular transfer, mice were sacrificed and the axillary skin-draining and contralateral lymph nodes harvested, as well as the para-aortic lymph nodes for the –CD4$^+$ and +Treg groups. For the unmanipulated PBMC group, only the skin-draining axillary lymph nodes were harvested. The number of live human 7AAD$^-$ CD45$^+$CD4$^+$ (huCD4$^+$) cells was determined in each lymph node for each group. Data are represented as the measured data points and calculated mean values. **:p=0.0062, *:p=0.0144.

Figure 5.16. Human FoxP3$^+$ cells accumulate in human skin allografts of Treg-treated humanised BALB/c-Rag2$^{-/-}$cγ$^{-/-}$ mice.

BALB/c-Rag2$^{-/-}$cγ$^{-/-}$ mice received a human skin graft and 5 weeks later were injected with 5x10^6 allogeneic PBMC or 5x10^6 allogeneic PBMC with 5x10^6 *ex vivo*-expanded CD127^{lo}CD25$^+$CD4$^+$ derived from the PBMC donor (i.e. autologous Treg). **(a)** 21 days later, skin grafts from mice receiving PBMC only (n=5 mice) and mice receiving PBMC with Treg (n=5 mice) were analysed by immunohistochemistry for the number of intragraft human FoxP3$^+$ (huFoxP3$^+$) cells present. Also shown is the number of huFoxP3$^+$ cells in a human skin sample pre-transplantation (n=2 samples). The number of positive cells was quantified in 3 random fields at 400X magnification for each of 4 separate sections for each skin graft and the mean taken for each data point. Data are represented the mean of these mean values ±SD, *:*p*=0.0372. **(b)** At the same time point, skin grafts from mice receiving PBMC only (n=3 mice) and mice receiving PBMC with Treg (n=3 mice) were analysed by qPCR for levels of *FOXP3* mRNA relative to the housekeeping gene *HPRT*. Also shown are data from one skin graft pre-transplantation. Data are represented as measured values and calculated means. **(c)** Representative photomicrographs of skin grafts from mice receiving PBMC alone or PBMC with Treg harvested 21 days after injection of cells and stained by immunohistochemistry for human FoxP3$^+$ cells (indicated with arrow) and counterstained with haematoxylin. The histology shown is representative of 6 stained sections from each of n=5 mice for each group. **(d)** 5x10^3 *ex vivo*-expanded human Treg were analysed by FACS for the percentage expressing human CCR4 without stimulation (0h) and after 18 hours or 48 hours of stimulation. Unstimulated cells were cultured for 18 hours with only 200U/ml rhIL-2. Stimulated cells were cultured with αCD3/αCD28 microbeads at a 1:1 ratio and 200U/ml rhIL-2. Data are represented as mean ±SD from triplicate wells. **(e)** Representative photomicrograph of a human skin graft from a mouse receiving PBMC and Treg at >100 days post-adoptive cellular transfer (i.e. long-term survival), stained by immunohistochemistry for human FoxP3$^+$ cells (indicated with arrow) and counterstained with haematoxylin. The histology shown is representative of 6 stained sections from each of n=4 mice.

Figure 5.17. Human Treg present within skin grafts from Treg-treated humanised BALB/c-Rag2$^{-/-}$cγ$^{-/-}$ mice actively regulate responses against the skin allograft.

(a) Schematic representation. BALB/c-Rag2$^{-/-}$cγ$^{-/-}$ mice received a human skin graft and 5 weeks later were injected with 5x10^6 allogeneic PBMC all, 5x10^6 allogeneic PBMC with 5x10^6 *ex vivo*-expanded CD127^{lo}CD25$^+$CD4$^+$ derived from the PBMC donor (i.e. autologous Treg), or no cells. All mice receiving PBMC alone rejected their skin allografts. Mice not receiving cells or mice receiving PBMC together with Treg engrafted the human skin allograft long-term. Long-term surviving skin grafts from these mice were subsequently re-transplanted onto new BALB/c-Rag2$^{-/-}$cγ$^{-/-}$ mice and allowed to heal for 5 weeks. Mice receiving skin from Treg-treated mice (i.e. 'Treg-treated allografts', n=3 mice) or mice receiving skin from mice that did not receive cells (i.e. 'control allografts', n=5 mice) then received an injection of 5x10^6 PBMC from the same donor as that used in the primary group of mice. Mice not achieving human leukocyte chimerism levels of >1% in the spleen were excluded from the analysis. **(b) and (c)** Survival analysis of 'Treg-treated allografts' and 'control allografts' on mice reconstituted with PBMC. The MST was calculated for each group. Allografts from Treg-treated mice survived long-term (MST >100 days) whereas control allografts rejected with a MST of 41 days (p=0.0169).

Figure 5.18. *Ex vivo*-expanded human Treg suppress the proliferation of autologous and non-autologous PBMC responders to similar levels *in vitro*.

In vitro suppression assay of *ex vivo*-expanded $CD127^{lo}CD25^{+}CD4^{+}$ human Treg against PBMC responders derived from the same Treg donor (autologous responders) or allogeneic PBMC derived from a different donor (non-autologous responders). CFSE-labelled PBMC were cultured alone, with αCD3/αCD28 microbeads (at a ratio of 1 bead per 5 cells), or with αCD3/αCD28 microbeads in the presence of varying amounts of *ex vivo*-expanded Treg (at ratios of 1:2, 1:4 and 1:8 Treg to PBMC). After 72 hours of culture, cells were analysed by FACS for the percentage of $CFSE^{+}$ cells (i.e. non-divided cells). Cells are gated on live human $7AAD^{-}CD3^{+}$ cells and then further gated into **(a)** human $CD4^{+}$ and **(b)** human $CD8^{+}$ cells. Shown are data from one autologous PBMC responder and one non-autologous PBMC responder, with n=3 repeats per donor per culture condition. Calculated means are shown for each culture condition. Also shown are representative FACS histograms from this culture, gated on human **(c)** $CD4^{+}$ and **(d)** $CD8^{+}$ cells.

The *in vitro* suppression CFSE limited dilution assay was repeated across n=6 separate Treg donors (labelled A to F) and permutations for three pairs of these donors (A and B; C and D; E and F). The percentage suppression for **(e)** $CD4^{+}$ cells and **(f)** $CD8^{+}$ cells was calculated relative to αCD3/αCD28 microbead-stimulated PBMC without Treg. Data are represented as mean ±SD with triplicate wells per donor combination.

Figure 5.19. *Ex vivo*-expanded human Treg are less effective at suppressing allogeneic PBMC responders than autologous PBMC responders *in vivo*.

BALB/c-Rag2$^{-/-}$cγ$^{-/-}$ mice received a human skin transplant and 5 weeks later were injected with 5x10^6 allogeneic PBMC (n=9 mice) or 5x10^6 allogeneic PBMC with either 5x10^6 (n=6 mice) or 1x10^6 (n=8 mice) *ex vivo*-expanded human Treg derived from a third party donor and allogeneic to the skin and PBMC donors (non-autologous Treg). **(a) and (b)** Survival data. The MST was calculated for each group. Data are pooled from n=3 separate survival assays using a different skin and PBMC donor combination for each assay. **(c)** The peripheral blood of mice receiving a human skin graft and 5x10^6 allogeneic PBMC only (n=9 mice), 5x10^6 PBMC with 1x10^6 Treg derived from the PBMC donor (i.e. autologous Treg, n=5 mice) or 5x10^6 PBMC with 1x10^6 Treg derived from a third party PBMC donor ('non-autologous Treg' n=8 mice) was analysed weekly by FACS for the percentage of live human 7AAD$^-$CD45$^+$ cells as a proportion of total live mononuclear cells (%huCD45$^+$ cells). Data are represented as mean ±SD and are pooled from n=3 separate assays using a different skin and PBMC donor combination for each assay. *:*p*=0.0420, two-way ANOVA.

Figure 5.20. *Ex vivo*-expanded human Treg do not suppress the proliferation of autologous and allogeneic PBMC responders to similar levels *in vivo*.

In vivo suppression assay of *ex vivo*-expanded $CD127^{lo}CD25^{+}CD4^{+}$ human Treg against PBMC responders derived from the same Treg donor (autologous responders) or PBMC derived from an allogeneic donor (non-autologous responders). PBMC from two different donors (A and B) were injected intraperitoneally into BALB/c-$Rag2^{-/-}c\gamma^{-/-}$ mice with or without Treg derived from donor A. Groups were: $5x10^6$ PBMC A alone (n=4 mice), $5x10^6$ PBMC B alone (n=4 mice), $5x10^6$ PBMC A with $5x10^6$ Treg A (n=5 mice), and $5x10^6$ PBMC B with $5x10^6$ Treg A (n=4 mice). All Treg were CFSE labelled. **(a)** 7 days later, intraperitoneal lavage fluid was obtained and the number of live human $7AAD^{-}CD45^{+}CD4^{+}CFSE^{+}$ cells determined by FACS analysis. Data are represented as individual data points with calculated means. *:$p<0.0383$. **(b)** Representative FACS plots and histograms from the assay described. **(c)** The percentage of non-divided live human $7AAD^{-}$ $CD45^{+}CD4^{+}CFSE^{+}$ cells in the groups receiving CFSE-labelled Treg was determined using gates shown in the representative histograms in **(d)**. ****:$p<0.0001$.

Figure 5.21. *Ex vivo*-expanded human Treg are more effective if given at the same time as PBMC than two weeks after PBMC injection.

BALB/c-Rag2$^{-/-}$cγ$^{-/-}$ mice received a human skin graft and 5 weeks later were injected with 5x10^6 allogeneic PBMC (n=4 mice), 5x10^6 allogeneic PBMC with 5x10^6 *ex vivo*-expanded Treg (n=4 mice) or 5x10^6 allogeneic PBMC followed two weeks later by and injection of 5x10^6 *ex vivo*-expanded Treg (n=4 mice). All Treg were derived from the same PBMC donor as reconstituting PBMC (i.e. autologous Treg). **(a) and (b)** The survival time for each skin graft was measured from the time of PBMC injection. The MST was calculated for each group. Data shown are representative of one assay using a single PBMC donor and skin donor.

CHAPTER 6: RESULTS SUMMARY AND GENERAL DISCUSSION

6.1 Introduction

Over the past decade, VCA transplantation has emerged as an effective reconstructive option for some of the most complex traumatic injuries. The reconstructive techniques developed in the First and Second World Wars gave soldiers who would normally have been confined to lives on the edges of society a new hope for social reintegration. In the same manner, VCA transplantation now provides patients with normally unreconstructable defects a route for attaining a normalised appearance. However, VCA transplantation moves beyond aesthetic improvements to also reconstruct structures to a functional standard not realised by conventional techniques. Limb transplants allow a return to normal unassisted life and face transplants allow normal breathing, eating, smelling and speaking. For such patients the benefits of transplantation outweigh the risks of immunosuppression.

However, for the vast majority of patients with the 'average' congenital, traumatic, or post-surgical defect, immunosuppression is not an option. The current results attained using conventional autologous reconstructive techniques for these patients are excellent. However, they do not replace 'like with like' in the same manner as a VCA transplant. Furthermore, these techniques result in the morbidity of a donor site from which tissue is removed for the reconstruction. If the need for immunosuppression could be reduced or even eliminated, a larger proportion of

patients would be able to benefit from the results attained with VCA transplantation, thus revolutionising the field of reconstructive surgery.

In recent years, various therapies have been investigated in an effort to achieve donor-specific tolerance in transplantation. Techniques for harnessing central tolerance by induction of mixed chimerism have been a particular focus in experimental VCA transplantation, but have yielded disappointing results in terms of prolonging survival of the skin component of the VCA, particularly in large animal transplantation models. These techniques may yet prove successful, as they have in SOT.

Peripheral immunoregulation methods based on Treg cellular therapy have also drawn increasing interest recently. In general, these techniques have centred on the use of Treg as an adjunctive cellular therapy, although some work has also investigated the use of Treg-facilitating immunosuppression *in vivo*. A wealth of information now exists on the properties of mouse Treg. However, as discussed in *Chapter 1*, human Treg are functionally and phenotypically dissimilar to mouse Treg and data from mouse studies are not easily extrapolated to the human. Human Treg as a cellular therapy may be derived from *ex vivo*-expansion of nTreg, induction from naïve $CD4^+$ precursors using a variety of cytokines and small molecules, or transduction of naïve $CD4^+$ cells with appropriate viral vectors. Such Treg may be derived either from the host (autologous Treg) or from a third, allogeneic, party (non-autologous Treg). Although few studies have directly compared the efficacy of these two different populations of Treg, data from these studies indicate that non-

autologous Treg are as effective as autologous Treg[531,541]. Non-autologous Treg are advantageous as they may be expanded at any time and cryopreserved for future use as an 'off the shelf' therapy.

Despite the majority of human studies of Treg for the prevention of GvHD being based on *in vitro* assays, Phase 0 and Phase I clinical trials are currently ongoing for the evaluation of non-autologous Treg cellular therapy in GvHD post-HSC engraftment for patients with haematological malignancies. In these studies, $CD4^{+}CD25^{hi}$ or $CD4^{+}CD25^{+}CD127^{lo}$ Treg are generally used 'as is' after isolation of large numbers by leukapheresis, or isolation in smaller numbers and expansion *in vitro*. Another clinical trial currently recruiting patients will evaluate the use of *ex vivo*-expanded autologous human $CD4^{+}CD25^{+}CD127^{lo}$ Treg for the treatment of type 1 diabetes[548].

In terms of Treg in SOT, there is a good evidence-base of *in vitro* studies, as well as a few *in vivo* translational studies in humanised mouse systems. Although it has become clear that multiple populations of Treg exist, the $CD4^{+}CD25^{+}CD127^{lo}$ population has shown particular promise. However, as with mixed chimerism techniques, it is not clear whether Treg would be effective in VCA transplantation, and in particular at preventing skin rejection. Furthermore, there are no ongoing clinical trials for human Treg in SOT or VCA transplantation, although the Phase 0/I 'ONE' Study is currently gearing up for the evaluation of $CD4^{+}CD25^{+}CD127^{lo}$ Treg in renal transplantation[514,549]. In contrast to the treatment of severe GvHD in HSC transplant recipients, there is a particularly high risk in the evaluation of a novel

cellular therapy such as Treg in SOT or VCA transplant patients, in whom graft survival overall is excellent. With this in mind, and with the knowledge that skin is a particularly challenging tissue in which to suppress rejection, there is a need to evaluate Treg efficacy in a preclinical system before its introduction to clinical VCA transplantation. Furthermore, because of the infancy of the field of VCA transplantation, there is limited data on the alloimmune characteristics of human skin rejection. An experimental model in which human skin rejection is emulated is therefore of particular value.

In this thesis we developed a humanised mouse model of human skin rejection, in which the peripheral immune and histological characteristics of rejecting human skin were examined. This model provided a translational platform in which to evaluate the ability of *ex vivo*-expanded human $CD4^{+}CD25^{+}CD127^{lo}$ Treg cellular therapy to delay or prevent the rejection of human skin allografts.

6.2 Summary of experimental results

6.2.1 Chapter 3

In *Chapter 3* we developed a reliable model of human skin allograft rejection. This is the first reported model in which complete alloimmune-dependent human skin destruction is achieved.

The most efficient route for the reconstitution of human leukocytes using PBMC in the in the BALB/c-$Rag2^{-/-}c\gamma^{-/-}$ mouse was through the intraperitoneal route (***Figure***

3.1). Human skin grafts transplanted onto these mice revascularised appropriately with the emergence of both mouse and human microvasculature (***Figures 3.2 and 3.3***). Three days after transplantation, the injection of $5x10^6$ PBMC allogeneic to the human skin grafts reliably resulted in their destruction (***Figures 3.4 and 3.5***). However, injection of autologous PBMC also resulted in graft destruction, indicating that this may not be a true alloresponse (***Figure 3.6***). We found that allowing skin grafts to heal for 5 weeks before introduction of PBMC ensured that only PBMC allogeneic to the skin graft induce its destruction, resulting also in the preferential aggregation of human cells in the allograft-draining lymph node (***Figure 3.8***). The presumed reduction in inflammation after healing also resulted in marginally longer survival times for allografts that were allowed to heal for 5 weeks compared with those that were not allowed to heal (***Figure 3.9***). In all cases mice that achieved human leukocyte chimerism levels of >1% in the spleen reliably lost their skin allograft (***Figures 3.9 and 3.11***). All *in vivo* assays from this point onwards were performed using the 'healed in' model (***Figure 3.7***).

A sensitivity to the degree of HLA mismatch was not observed, with similar MSTs achieved in assays where there were between 4 and 8 total mismatches across HLA-A, B, DR and DQ (***Figure 3.10***). In mice receiving a human skin graft and allogeneic PBMC, human leukocytes were not detectable in the peripheral blood in significant numbers until week 2 post-inoculation, then increasing steadily until the time at which most skin grafts were lost (***Figure 3.11a***). Human leukocytes engrafted throughout the peripheral lymphoid tissues of the mouse, although numbers of detectable human cells varied according to the PBMC donor used (***Figures 3.11b-d***).

The variation in cell numbers by PBMC donor used did not have a significant bearing on the MST of skin grafts (***Figure 3.11e***). Mice engrafted mainly human T cells, with an increasing proportion of $CD8^+$ T cells compared with $CD4^+$ T cells over time, up to the point at which most skin grafts were rejected (***Figure 3.12***). These cells gained a memory phenotype post-engraftment (***Figure 3.12c***). No significant engraftment of DCs or monocytes was detected.

These data indicate that the most reliable human skin rejection model in the BALB/c-$Rag2^{-/-}c\gamma^{-/-}$ mouse requires $5x10^6$ PBMC injected 5 weeks after human skin graft transplantation. Having developed this model, in the next chapter we proceeded to characterise in more depth the histological profile of rejecting skin and the elements of alloresponse that develop.

6.2.2 Chapter 4

In this chapter we examined in further detail the characteristics of the alloresponse against the human skin transplant and the histological features of skin rejection.

We first explored the importance of donor-derived passenger leukocytes in the alloresponse. Human skin grafts contained significant numbers of leukocytes (***Figure 4.1a***). These cells were detected in BALB/c-$Rag2^{-/-}c\gamma^{-/-}$ mice that did not receive an adoptive transfer of human PBMC, but did not achieve chimerism levels that were significant in comparison with mice that received PBMC inoculations (***Figure 4.1b***). Nevertheless, a sizeable number of leukocytes derived from the skin graft survived,

even in the presence of allogeneic PBMC inoculations (***Figure 4.2***). However, skin allografts that were depleted of these passenger leukocytes were rejected at similar rates to unmanipulated skin allografts (***Figure 4.2***) indicating that they are not significant in the alloresponse in this model. We suggest that the main source of HLA for allorecognition is on the ECs and keratinocytes of the skin graft itself (***Figure 4.3***).

Consistent with Grade III/IV Banff skin rejection, rejecting allogeneic skin grafts in our model displayed microarchitectural changes that were consistent with those seen in clinical skin transplantation, including dyskeratosis of the stratum spinosum, perivascular infiltrates, vacuolation of cells and junctional inflammation (***Figure 4.4***). Infiltrating cells were all $CD4^+$ and $CD8^+$ T cells in equal proportions (***Figure 4.5***). A mouse granulocytic infiltrate was apparent in mice inoculated with PBMC (***Figure 4.6***) but was not significant in the rejection response (***Figure 4.7***). In NSG mice, this mouse granulocytic infiltrate appeared to be detrimental to human skin grafts (***Figure 4.8***), implying that BALB/c-$Rag2^{-/-}c\gamma^{-/-}$ mice are better hosts for modeling human skin rejection.

Despite low levels of B cell engraftment, PBMC-engrafted BALB/c-$Rag2^{-/-}c\gamma^{-/-}$ mice produced significant amounts of human IgG and IgM that was not skin donor-specific (***Figure 4.9***). At least some of this antibody was xenoreactive against mouse antigens (***Figure 4.10***).

In the second part of this chapter we explored HSC engraftment as a method for the improvement of B cell reconstitution in BALB/c-Rag2$^{-/-}$cγ$^{-/-}$ mice. HSC-engrafted mice harboured levels of human leukocytes at similar levels to PBMC-engrafted mice (***Figures 4.11 and 4.13***). Human leukocyte development in HSC-engrafted mice was improved by the presence of a human skin allograft (***Figure 4.13***). In contrast to PBMC-engrafted mice, B cell reconstitution levels were high (***Figure 4.15***). T cells also developed in HSC-engrafted mice, although their appearance was late and overall lower than the levels achieved in PBMC-engrafted mice (***Figure 4.14*** *cf.* ***Figure 3.12***). Despite high levels of B cell reconstitution in HSC-engrafted mice, immunoglobulin levels were low until the late emergence of T cells (***Figure 4.16***). The reconstitution of T cells and production of human immunoglobulin was improved with the inoculation of human MNCs derived from the UCB unit from which HSCs were obtained (***Figures 4.14-4.16***). Nevertheless, the functionality of both T and B cells in this model is in doubt as no skin donor-specific antibody was produced (***Figure 4.17***), and skin grafts were not rejected in a reliable fashion (***Figure 4.18***). However this model may act as a platform for further development, as there was a more complete spectrum of human leukocyte development together with the emergence of peripheral blood monocytes, high numbers of B cells, and infiltration of skin grafts with T cells, B cells and macrophages (***Figures 4.14-4.18***).

We selected the standard model using skin that is allowed to heal for 5 weeks before inoculation of 5x10^6 allogeneic PBMC for the assays detailed in the following chapter. This model provided the most reliable time course for skin rejection and

displayed histological and cellular features of rejection that are concordant with clinical observations of skin rejection.

6.2.3 Chapter 5

In this chapter we evaluated the efficacy of *ex vivo*-expanded human $CD4^+CD25^+CD127^{lo}$ Treg in the prevention of human skin rejection and the mechanisms by which Treg protect human skin.

$CD4^+CD25^+CD127^{lo}$ Treg that were FACS-sorted and *in vitro* expanded with αCD3/αCD28 microbeads and rhIL-2 maintained Treg-associated phenotypic markers (***Figure 5.1***) and were suppressive *in vitro* against both polyclonally-stimulated and allostimulated PBMC responders (***Figure 5.2***). Inoculation of autologous Treg (i.e. derived from the same donor used to reconstitute mice with PBMC) resulted in dose-dependent prolongation of human skin allograft survival, with ratios of 1:1 and 5:1 PBMC to Treg promoting long-term skin engraftment (***Figure 5.3***). Expanded Treg were more efficacious at preventing skin rejection that non-expanded Treg (***Figure 5.4***). Treg that were not expanded but stimulated with αCD3/αCD28 microbeads for 12 hours post-sorting displayed an improved suppressive phenotype (***Figure 5.5***) and prevented human skin graft rejection with a similar efficacy as expanded Treg (***Figure 5.6***), indicating that it is the activation of cells during the expansion process that improves their suppressive capabilities.

Mice receiving human skin allografts and PBMC that were treated with Treg displayed a reduced level of human leukocyte chimerism in the peripheral blood (***Figure 5.8***) with reduced proliferation of human $CD4^+$ and $CD8^+$ T cells (***Figure 5.9***). This effect was not apparent in mice that did not receive a skin allograft (***Figure 5.10***), suggesting that there is either a specific suppression of cells that are responding to the allograft, or that Treg require the presence of donor alloantigen to ensure their activity. Despite a lack of human donor-specific antibody production, there was a reduction in the serum concentration of both human IgG and IgM in Treg-treated mice (***Figure 5.11***). The microarchitecture of skin allografts from Treg-treated mice was preserved (***Figure 5.12***), and intragraft human microvessels were protected (***Figure 5.13***). In Treg-treated mice, a reduction in the infiltration of human skin allografts with human $CD8^+$ cells was observed, although overall human leukocyte infiltration levels were unchanged (***Figure 5.14***). In mice receiving Treg therapy, Treg were detectable in the skin allograft draining lymph node (***Figure 5.15***). Moreover, a greater number of human $FoxP3^+$ cells were present within skin allografts from Treg-treated mice compared with allografts from mice not receiving Treg (***Figure 5.16***). These human $FoxP3^+$ cells persisted in long-term surviving human skin allografts (***Figure 5.16***). When long-term surviving skin grafts from Treg-treated mice were retransplanted onto new mice that were then reconstituted with PBMC, these skin retransplants survived long-term (***Figure 5.17***). This indicated that Treg within the long-term surviving allografts are capable of continuing to regulate effector immune responses.

We next evaluated the efficacy of non-autologous *ex vivo*-expanded $CD4^+CD25^+CD127^{lo}$ Treg in preventing human skin allograft rejection. Non-autologous Treg were as effective as autologous Treg at suppressing PBMC responders (***Figure 5.18***). However *in vivo*, non-autologous Treg were not as effective as autologous Treg at preventing human skin rejection, with autologous Treg at a 5:1 ratio of PBMC to Treg being as effective as non-autologous Treg at a 1:1 ratio (***Figure 5.19*** *cf.* ***Figure 5.3***). The discrepancy between *in vitro* and *in vivo* effectiveness was due to poor survival of the non-autologous Treg *in vivo* (***Figure 5.20***).

Together these data indicate that human Treg are most effective at preventing human skin rejection if they are expanded or activated, derived from the recipient (autologous), and given early at a ratio of at least 5:1 PBMC to Treg. Treg migrate to the graft draining lymph node and graft itself to prevent rejection. The mechanisms of skin allograft protection included a reduction in proliferating T cells in the blood, a reduction of the $CD8^+$ intragraft infiltrate and a protection of human $CD31^+$ skin ECs.

Figure 6.1 is a schematic summarising the humanised mouse model of skin transplantation developed together with the characteristics and features of skin rejection and the effects of immunoregulation with *ex vivo*-expanded autologous human Treg.

6.3 Discussion

The data in this thesis have two principal implications. Firstly, clinical human skin rejection may be successfully emulated in the laboratory. Secondly, a foundation has been provided for the translation of *ex vivo*-expanded human Treg cellular therapy to clinical VCA transplantation.

Human skin rejection has always posed a unique challenge to the transplantation immunologist. Methods to study the process in the laboratory are therefore instrumental in furthering our understanding. The characteristics of skin rejection in our study are in accordance with what has been observed clinically. This implies that the pathology may be studied in detail on a large scale in an environment that does not pose any risk to patients, and importantly, that the findings will have clinical relevance.

Although the model developed is limited to human T cell responses, these responses are of particular interest clinically as there is very little evidence of B cell-mediated alloimmunity in VCA transplantation[6,12,495]. Nevertheless there is clearly a need to improve the range of immune responses in the model and to incorporate human innate immune responses. This may be achieved with improved humanisation with HSC progenitors. Development of the model to ensure a wider spectrum of human leukocyte reconstitution will ensure that data obtained are more readily translatable to the clinic.

The field of humanised mice is rapidly evolving, and therefore the precise model used in each study needs to be taken into consideration when evaluating the experimental data obtained. The model will vary according to the immunodeficient mouse strain, the number and type of human cells used to reconstitute the mouse, and the method of transplantation. While NSG mice may be useful for models of GvHD, they are poor models for human skin allografting considering the detrimental mouse innate response that develops against human skin. Human leukocytes developing in humanised mice will also need to be assessed for their functionality. Clearly, HSC mice produce large numbers of human B cells but this is not particularly relevant if no donor-specific antibody response is mounted. Furthermore, there is an association between the number of circulating human leukocytes present and the initiation and maintenance of vigorous allograft rejection. Models that allow the most efficient engraftment of cells must be therefore used. We have also demonstrated that controls using autologous human leukocytes are critical to ensure that a true alloresponse develops against the transplanted human tissue, not a non-specific immune-mediated destruction. Finally, the type of tissue used and its state of vascularisation is important. Human neonatal skin allografts lose a proportion of their human ECs[447] and human foetal skin ECs do not express HLA Class II[459]. Both of these characteristics would dampen down the alloimmune response generated. Cadaveric tissue may also behave differently depending on the amount of time it is ischaemic before transplantation, as ischaemia would impact the ensuing IRI-associated and cell death-induced inflammatory response.

The finding that donor-derived passenger leukocytes do not play as much of a role in the generation of the immune response against skin as previously thought is of particular interest. This is despite the knowledge that a large number of APCs are present in skin and that these cells migrate out of the graft post-transplantation[64,550]. It is conceivable that there are differences between the mechanisms of rejection of renal and skin allografts, explaining the finding that rat renal allografts depleted of these cells do not reject acutely[73,74], whereas skin grafts depleted of passenger leukocytes in our model reject with the same tempo as those that are not depleted. These differences may come down to the central role that skin ECs play in the alloresponse. No other tissue contains ECs that are able to activate and induce the migration of memory T cells to the same degree[172]. Because the majority of engrafting cells in immunodeficient mice gain a memory phenotype through spontaneous and homeostatic proliferation in a lymphopaenic environment[472,474,486], such cells would not require priming via APCs for initiation of rejection. These memory T cells would be able to recognise alloantigens directly on human skin ECs to mediate their destruction[551].

Further experimental evidence supports this hypothesis. Human neonatal skin ECs and keratinocytes express no HLA Class II and only weak HLA Class I, whereas foetal skin cells express both[459]. In a study comparing the rejection tempo of human neonatal and foetal skin in a humanised SCID model, prolonged survival of human foetal skin compared to neonatal skin was observed[459], highlighting the importance of HLA molecules expressed on the skin in mediating the alloresponse.

Moreover, there is mounting evidence demonstrating that only memory T cells are able to induce skin graft rejection. In a study presented by Barbara Fazekas de St. Groth at the TTS Congress 2010[552], mouse 5C.CR transgenic $CD4^+$ T cells specific for IA^S which maintain their naïve phenotype after adoptive transfer were not able to reject a skin graft from a B10.S donor (expressing IA^S), whereas primed 5C.CR effector memory cells were capable of inducing skin rejection.

These data extend to human cells. In a humanised mouse skin transplantation model by Shiao et al. where mice were engrafted with either $CD45RA^+$ naïve T cells or $CD45RO^+$ memory T cells, only the memory T cells induced a vigorous alloimmune response and caused significant skin damage[478]. In this study, a large number of cells was injected ($1.5x10^8$), which may mean that these cells are not subject to lymphopaenia-induced proliferation and activation to the same degree as in other models, maintaining the naïve phenotype of injected cells. In addition, the time-scale of assays was short with skin grafts being analysed at 15 days. In our study we found that human leukocyte engraftment levels are low at this point, indicating that only a small degree of human leukocyte proliferation has taken place. Cells in the Shiao et al. study would therefore be at an early stage of proliferation and activation, explaining the maintenance of a naïve phenotype.

Nevertheless, it is important to keep in mind that no host-type DCs engraft in our model, therefore reducing the effectiveness of the naïve alloresponse. Furthermore, in immunocompetent animal models, or where the allograft is a SOT in which ECs are less relevant, naïve T cells may instead come to the forefront of the alloresponse.

Indeed, in such models, secondary lymphoid tissue is required in order to ensure priming of alloresponding cells by donor antigen[61]. However in these mouse studies, mice are generally kept in specific pathogen-free conditions and therefore memory T cells primed through heterologous immunity may not be present in high numbers. In contrast, in humans memory T cells primed through heterologous immunity or prior exposure to antigen are normally present and are known to be detrimental to the allograft[146]. While it may be argued that the state of lymphopaenia that is conducive to memory T cell generation in our model is not replicated clinically, in VCA recipients receiving induction immunosuppression a state of lymphopaenia develops that may potentially promote the expansion of memory T cells.

Together with our study, these data suggest that memory T cells primed through heterologous immunity that develop in lymphopaenic hosts may mediate the bulk of the damage to skin allografts through their direct allorecognition of antigens on ECs.

It is clear that the alloresponse to skin is different to that of other tissues. This is at least in part due to the role ECs play. The loss of human ECs during rejection both in our model and other studies is therefore significant. EC loss is likely to be a late manifestation of rejection, signalling the end of the acute phase of the immune response and leading to devascularisation of the allograft (particularly if host vessels do not develop to replace the lost donor vessels). In CAD, ECs may play a different role whereby they are replaced with host-type ECs which process alloantigen to provide a pathway for indirect allorecognition by host T cells[553].

The degree of loss of donor-type ECs is a sensitive marker for the damage caused by the alloresponse, and therefore the protection of human ECs in our model with *ex vivo*-expanded $CD4^+CD25^+CD127^{lo}$ Treg therapy is significant. The use of Treg therapy also maintained the macroscopic and microscopic appearances of the skin allografts and reduced the Banff grading of skin rejection from III/IV to 0/I. Together with the reduction in circulating proliferating leukocytes, skin-infiltrating $CD8^+$ cells and serum immunoglobulin levels, these findings demonstrate the efficacy of Treg at suppressing the effector response to protect the allografts from damage. Further work is required to understand the importance of the reduction in human immunoglobulin levels. In particular it would be interesting to know whether this is a direct effect as previously reported[554], or whether it is secondary to reduced B cell help from suppressed $CD4^+$ Th2 cells.

The importance of the prevention of $CD8^+$ T cell infiltration into regulated skin grafts requires further investigation. It is likely that the suppressive mechanisms employed by Treg at suppressing $CD4^+$ and $CD8^+$ T cells differ, given that only $CD8^+$ T cells were prevented from infiltrating the skin graft. The mechanisms whereby Treg suppress $CD8^+$ T cells are poorly understood compared with the mechanisms employed against $CD4^+$ T cells. However, recent evidence indicates that Treg limit $CD8^+$ T cell differentiation by competing for leukocytotrophic IL-2[555]. Although ECs may effectively activate memory T cells, they do not promote their subsequent differentiation into specialised $CD4^+$ Th subtypes. They do, however, promote the differentiation of $CD8^+$ T cells into EC-specific CTLs which may cause significant damage[556,557]. Moreover, a predominance in infiltrating $CD8^+$ T cells is seen clinically

in skin transplantation, and a higher level of circulating $CD8^+$ T cells compared with $CD4^+$ T cells was detected in our model. Given that $CD8^+$ T cells may effect the early destruction of skin through activation and subsequent differentiation by EC signals, their early control may be especially important in preventing skin rejection. Clearly, once skin grafts are infiltrated with $CD8^+$ T cells, the rejection process is underway and potentially irreversible.

Certain qualities of Treg are necessary for their efficacy in our model. Importantly, Treg must be able to survive in the host. There is therefore a requirement for the cells to be autologous, or possibly at least haplotype matched to the recipient. Non-autologous Treg may be effective only in the short term until they are killed by allogeneic host leukocytes. This point may be less relevant for Treg used in GvHD prevention post-HSC transplantation, where they may only need to be active for a short period of time after infusion. Treg also need to be activated or expanded in order to maximise their functional properties. Apart from upregulating certain functional molecules such as LAP and leading to higher levels of function-associated FoxP3 expression, activation may improve the ability of Treg to survive *in vivo*. Loss of CD3, CD28 and IL-2R stimulation leads to the inactivity of Treg and the eventual inactivation of cell survival signals through the Bcl family of anti-apoptotic proteins. It is therefore interesting to know whether methods for the transduction of anti-apoptotic molecules would be sufficient to ensure Treg activity *in vivo* in transplantation[558,559].

It is unclear how long the original Treg used for therapy would need to survive to ensure long-term allograft survival. While infectious tolerance mechanisms may guarantee a self-replenishing population of Treg to suppress anti-graft alloimmune responses[535,560], there may be a need for regular 'topping up' of Treg throughout the life of the transplant. Alternatively, Treg may be used as a 'rescue therapy' to treat a rejection episode, in which case their longevity may not be as critical. However, further work is required to evaluate whether Treg would be effective at the reversal of an immune response that is already active and destructive. The reduced effectiveness of delayed Treg in our model suggests that they may be less successful at this task.

Contamination of Treg preparations by other cell populations that could be pathogenic is a concern in Treg cellular therapy. However, the detrimental effects of Treg themselves must also be taken into account. As discussed in *Chapter 1*, there is increasing evidence that Treg may convert into pathogenic effector cells, especially in lymphopaenic conditions[306]. This aspect will need further clarification particularly given the lymphopaenia that develops post-immunosuppression. As discussed in *Chapter 5*, the suppressive effects of Treg that are not directed against graft alloresponding cells also require further clarification. While alloantigen-reactive Treg may circumvent this issue, the effects of bystander suppression of effector T cells in the locality of the allograft will need to be addressed. Treg may need to be genetically manipulated to incorporate a suicide-switch to eliminate all injected Treg should any adverse effects develop.

Whether donor antigen-reactive Treg are necessary is debatable. In a recent humanised mouse model of human skin rejection, $CD4^+$-mediated damage of allografted skin was reduced more effectively with the use of alloantigen-expanded human Treg compared with polyclonally-expanded human Treg[370]. While this is an interesting finding, given the importance of $CD8^+$ cells in the alloresponse against skin and the finding in our study that graft infiltrating $CD8^+$ T cells are reduced with Treg therapy, the conclusions of this study are limited. Furthermore, as discussed in *Chapter 5*, there is an argument that antigen-reactive or even antigen-specific Treg are unnecessary. Polyclonally-reactive Treg may be produced in higher numbers than antigen-reactive Treg, and therefore given in higher numbers to circumvent the higher efficacy of antigen-reactive Treg. It is also possible that polyclonally-reactive Treg, if given at the correct time post-transplantation, would regulate only the effector cells that are activated at the time, thus specifically regulating alloresponding effector T cells.

While purity is important to ensure that there are no pathogenic contaminants in the population to be used for therapy, an increase in purity comes at the expense of total Treg cell numbers that may be obtained. Some markers, such as LAP may indeed signify a more potent population of Treg, but this does not necessarily mean that LAP^- cells are not able to regulate through different mechanisms. A pragmatic view therefore needs to be taken, with a certain balance accepted between the degree of purity and number of cells obtained.

Numerous phenotypic markers have been described for the identification of human Treg. What is not clear is whether these markers identify purer populations of Treg, or whether they identify subpopulations of Treg. For example, nTreg may express CD45RO or CD45RA, making them memory or naïve in phenotype[361,363,561]. These two populations of Treg have dissimilar qualities in terms of their capacity for proliferation and suppression, and are present at different levels in adult and umbilical cord blood. However while some may argue that $CD45RA^+$ are more potent suppressors due to their tendency to proliferate and suppress for longer periods of time, $CD45RO^+$ Treg are more efficient at migrating to a skin allograft and peripheral lymphoid tissue by virtue of their higher expression of CD62L, CCR4 and CLA[195,363,364,526]. We therefore propose that distinct subpopulations of Treg will be effective for particular conditions. For example, $CD45RO^+$ Treg may be more effective in skin transplantation, and $CD45RA^+$ more effective in solid organ transplantation. It is therefore important that each subpopulation of Treg be tested *in vivo* against human targets for the condition of interest. For example, Treg that are effective against skin transplant rejection may not be effective against renal transplant rejection. Furthermore, human Treg employ different mechanisms of suppression *in vitro* and *in vivo*, and as such will need to be assessed in relevant *in vivo* models for a true reflection of their clinical value. Our data demonstrating the conflicting results from *in vitro* and *in vivo* studies highlight this point.

Cellular therapy with Treg is a promising prospect for VCA and solid organ transplantation[514,562,563]. Treg are powerful regulators of allograft rejection and

harnessing their suppressive capabilities may be the key to reducing morbidity and mortality post-transplantation.

6.4 Future directions

We have clearly demonstrated the efficacy of human Treg therapy for the prevention of skin rejection. While this is the main obstacle in VCA transplantation, the other tissues within the VCA need to be taken into consideration. Evidence suggests that these tissues are less immunogenic and that as an overall unit a VCA is less immunogenic than skin alone. It is therefore arguable that a therapy that is active against the rejection of skin would by extension be active against the rejection of the other components of a VCA, although this would require confirmation. Further work will also be required to determine the stability of Treg *in vivo*, in order to ensure that they do not become pathogenic after engraftment.

We are now closer than ever to the first clinical trials of Treg in conventional SOT[514]. These trials are planning to evaluate Treg as a supplementary therapy in conjunction with immunosuppressive drug therapy. When considering this however, it is important to keep in mind the excellent short-term graft survival rates achieved with conventional immunosuppression. The beneficial effects of Treg therapy in the majority of SOT cases are envisaged to be in the long-term. To evaluate Treg therapy in the short-term, trials will need to be performed in situations where acute rejection rates are high and conventional immunosuppression is risky. The clinical trials in GvHD prevention highlight this point. Here, studies were performed as

limited Phase 0/I Clinical Trials with primary outcome measures evaluating the safety and feasibility of Treg, and secondary outcome measures evaluating improvement in disease[411,412]. In these studies, there was a good chance of detecting an improvement in disease given the high rates of GvHD development and poor outcomes with conventional treatment. In the clinical trials of Treg in SOT that are currently being designed, primary outcome measures of safety and feasibility may potentially provide useful data. However given the excellent short-term graft survival rates achieved with conventional immunosuppression, a beneficial effect of Treg therapy on this secondary outcome measure is unlikely to be detected, at least in the short-term.

VCA transplantation therefore presents an ideal opportunity in which to evaluate Treg therapy. Acute rejection rates are incredibly high with over 85% of patients experiencing at least one episode in the 1st year[6]. Immunosuppression is also risky given that most patients are otherwise healthy and the transplant is not life saving. There is therefore an argument for evaluating Treg therapy in these patients in a Phase 0 Clinical Trial. As candidates for VCA transplantation are currently few, expansion and cryopreservation of Treg from these patients is feasible. In the treatment group, Treg cellular therapy may be given in the first instance together with conventional immunosuppression and both primary and secondary outcome measures evaluated. The monitoring of biomarkers of tolerance in these patients may then provide guidance as to whether any patients would be amenable to controlled withdrawal of immunosuppression[379,380,564,565]. Although the attainment of tolerance is an ideal solution, whether this can be achieved in each and every

transplant recipient is unknown. For the majority of patients, reducing immunosuppression to a minimum level would markedly reduce the complications of long-term drug therapy.

The humanised mouse model of skin transplantation developed in this thesis provides a valuable system for the investigation of the alloresponse against human skin and the evaluation of other regulatory therapies that are on the horizon. Together with further work assessing the safety and stability of Treg *in vivo*, the data in this thesis provide the pre-clinical evidence base for a future Phase 0 Clinical Trial of *ex vivo*-expanded human Treg in VCA transplantation.

6.5 Figures and legends

Figure 6.1. Summary of human skin allograft rejection and immunoregulation with *ex vivo*-expanded Treg in the humanised mouse model.

BALB/c-Rag2$^{-/-}$cγ$^{-/-}$ mice transplanted with a human skin graft followed 5 weeks later by an intraperitoneal injection of 5x10^{6} allogeneic PBMC reject the skin allograft with a MST of 35 days. Treatment of humanised mice with *ex vivo*-expanded autologous CD4^{+}CD25^{+}CD127^{lo} Treg at ratios of 5:1 PBMC to Treg and above promotes long-term survival of the skin allograft.

PUBLICATIONS

Papers

2011 Issa F, Chandrasekharan D, Wood KJ. **Regulatory T cells in chronic allograft injury**. *Curr Opin Immunol.* 10.1016/j.coi.2011.06.005

2010 Issa F, Hester J, Goto R, Nadig SN, Goodacre TE, Wood KJ. ***Ex vivo-expanded* human regulatory T cells prevent the rejection of skin allografts in a humanised mouse model**. *Transplantation*. 2010. 90(12): 1321-1327.

2010 Issa F & Wood KJ. **CD4+ regulatory T cells in solid organ transplantation**. *Curr Opin Org Transplant.* 2010. 15(6): 757-764.

2010 Issa F, Wieckiewicz J, Goto R, Goodacre T, Wood KJ. **Regulatory T cell therapy prolongs human skin allograft survival in a humanised mouse model**. *Transplantation*. 2010. 90(2S): 5.

2010 Issa F, Schiopu A, Wood KJ. **Role of T cells in transplant rejection and regulation**. *Expert Rev Clin Immunol.* 2010. 6(1): 155-169.

Book Chapters

2011 Issa F, Goto R, Wood KJ. **Principles of Immunology**. *Organ Transplantation: A Clinical Guide*. Ed. Klein, Lewis & Madsen. Cambridge University Press, 2011. ISBN 9780521197533.

Abstracts

2011 Issa F, Hester J, Goto R, Goodacre T, Wood KJ. **Regulatory T cell-induced prevention of human skin allograft rejection is dependent on the source of regulatory T cells.** *10th Meeting of the International Hand and Composite Tissue Allotransplantation Society, Atlanta, USA*

2011 Issa F, Hester J, Goto R, Goodacre T, Wood KJ. **Induction of long-term human skin allograft survival by human regulatory T cell monotherapy**. *British Transplantation Society Annual Congress, Bournemouth*

2010 Issa F, Wieckiewicz J, Goto R, Nadig SN, Wood KJ. **Regulatory T cells prolong skin allograft survival in a humanised mouse model**. *XXIII International Congress of the Transplantation Society, Vancouver, Canada*

REFERENCES

1. Transplant Activity in the UK, Activity Report 2009/2011. *NHS Blood and Transplant* (2011).
2. Morris, P.J., Johnson, R.J., Fuggle, S.V., Belger, M.A. & Briggs, J.D. Analysis of factors that affect outcome of primary cadaveric renal transplantation in the UK. HLA Task Force of the Kidney Advisory Group of the United Kingdom Transplant Support Service Authority (UKTSSA). *Lancet* **354**, 1147-1152 (1999).
3. Taylor, A.L., Watson, C.J. & Bradley, J.A. Immunosuppressive agents in solid organ transplantation: Mechanisms of action and therapeutic efficacy. *Crit Rev Oncol Hematol* **56**, 23-46 (2005).
4. Tobin, G.R.*, et al.* The history of human composite tissue allotransplantation. *Transplant Proc* **41**, 466-471 (2009).
5. Wu, S., Xu, H., Ravindra, K. & Ildstad, S.T. Composite tissue allotransplantation: past, present and future-the history and expanding applications of CTA as a new frontier in transplantation. *Transplant Proc* **41**, 463-465 (2009).
6. Petruzzo, P.*, et al.* The International Registry on Hand and Composite Tissue Transplantation. *Transplantation* **90**, 1590-1594 (2010).
7. Swearingen, B.*, et al.* Science of composite tissue allotransplantation. *Transplantation* **86**, 627-635 (2008).
8. Kanitakis, J.*, et al.* Clinicopathologic monitoring of the skin and oral mucosa of the first human face allograft: Report on the first eight months. *Transplantation* **82**, 1610-1615 (2006).
9. Kanitakis, J.*, et al.* Clinicopathologic features of graft rejection of the first human hand allograft. *Transplantation* **76**, 688-693 (2003).
10. Lanzetta, M.*, et al.* Second report (1998-2006) of the International Registry of Hand and Composite Tissue Transplantation. *Transpl Immunol* **18**, 1-6 (2007).
11. Lanzetta, M.*, et al.* The International Registry on Hand and Composite Tissue Transplantation. *Transplantation* **79**, 1210-1214 (2005).
12. Petruzzo, P.*, et al.* Long-term follow-up in composite tissue allotransplantation: in-depth study of five (hand and face) recipients. *Am J Transplant* **11**, 808-816 (2011).
13. Petruzzo, P.*, et al.* The international registry on hand and composite tissue transplantation. *Transplantation* **86**, 487-492 (2008).
14. Petruzzo, P.*, et al.* First human double hand transplantation: efficacy of a conventional immunosuppressive protocol. *Clin Transplant* **17**, 455-460 (2003).
15. Humar, A.*, et al.* Immunologic factors: the major risk for decreased long-term renal allograft survival. *Transplantation* **68**, 1842-1846 (1999).
16. Billingham, R.E., Brent, L. & Medawar, P.B. Actively acquired tolerance of foreign cells. *Nature* **172**, 603-606 (1953).
17. Van Parijs, L. & Abbas, A.K. Homeostasis and self-tolerance in the immune system: turning lymphocytes off. *Science* **280**, 243-248 (1998).

18. Sakaguchi, S. Naturally arising CD4+ regulatory t cells for immunologic self-tolerance and negative control of immune responses. *Annu Rev Immunol* **22**, 531-562 (2004).
19. Wood, K.J. & Sakaguchi, S. Regulatory T cells in transplantation tolerance. *Nat Rev Immunol* **3**, 199-210 (2003).
20. Ellis, H. Two pioneers of plastic surgery: Sir Harold Delf Gillies and Sir Archibald McIndoe. *Br J Hosp Med (Lond)* **71**, 698 (2010).
21. Carrel, A. Landmark article, Nov 14, 1908: Results of the transplantation of blood vessels, organs and limbs. By Alexis Carrel. *JAMA* **250**, 944-953 (1983).
22. SKIN homografts in clinical practice. *Br Med J* **2**, 1073-1074 (1951).
23. Gibson, T. & Medawar, P.B. The fate of skin homografts in man. *J Anat* **77**, 299-310 294 (1943).
24. Medawar, P.B. The behaviour and fate of skin autografts and skin homografts in rabbits: A report to the War Wounds Committee of the Medical Research Council. *J Anat* **78**, 176-199 (1944).
25. Medawar, P.B. A second study of the behaviour and fate of skin homografts in rabbits; a report to the War Wounds Committee of the Medical Research Council. *J Anat* **79**, 157-176 (1945).
26. Murray, J.E., Tilney, N.L. & Wilson, R.E. Renal transplantation: a twenty-five year experience. *Ann Surg* **184**, 565-573 (1976).
27. Calne, R.Y. Inhibition of the rejection of renal homografts in dogs by purine analogues. *Transplant Bull* **28**, 65-81 (1961).
28. Murray, J.E., Merrill, J.P., Harrison, J.H., Wilson, R.E. & Dammin, G.J. Prolonged survival of human-kidney homografts by immunosuppressive drug therapy. *N Engl J Med* **268**, 1315-1323 (1963).
29. Wright, P. Ronald Malt. *Lancet* **360**, 1521 (2002).
30. Gilbert, R. Transplant is successful with a cadaver forearm. *Med Trib Med News* **5**, 20-22 (1964).
31. Gilbert, R. Hand transplanted from cadaver is reamputated. *Med Trib Med News* **5**, 23-25 (1964).
32. Ekberg, H*., et al.* Calcineurin inhibitor minimization in the Symphony study: observational results 3 years after transplantation. *Am J Transplant* **9**, 1876-1885 (2009).
33. Dubernard, J.M*., et al.* Human hand allograft: report on first 6 months. *Lancet* **353**, 1315-1320 (1999).
34. Devauchelle, B*., et al.* First human face allograft: early report. *Lancet* **368**, 203-209 (2006).
35. Dubernard, J.M*., et al.* Outcomes 18 months after the first human partial face transplantation. *N Engl J Med* **357**, 2451-2460 (2007).
36. Selvaggi, G*., et al.* Abdominal wall transplantation: surgical and immunologic aspects. *Transplant Proc* **41**, 521-522 (2009).
37. Kirschner, M.H., Brauns, L., Gonschorek, O., Buhren, V. & Hofmann, G.O. Vascularised knee joint transplantation in man: the first two years experience. *Eur J Surg* **166**, 320-327 (2000).
38. Diefenbeck, M*., et al.* Outcome of allogeneic vascularized knee transplants. *Transpl Int* **20**, 410-418 (2007).
39. AFP. Transplant patient's joy on seeing new legs. *Associated Press* (2011).

40. Birchall, M. & Macchiarini, P. Airway transplantation: a debate worth having? *Transplantation* **85**, 1075-1080 (2008).
41. Meier-Kriesche, H.U.*, et al.* Increased impact of acute rejection on chronic allograft failure in recent era. *Transplantation* **70**, 1098-1100 (2000).
42. Lite, J. Chinese face-transplant recipient has died. *Scientific American* **Dec 22**(2008).
43. Comeau, E. Brigham and Women's performs face transplant on woman mauled by chimp. *White Coat News* (2011).
44. Khouri, R.K.*, et al.* A prospective study of microvascular free-flap surgery and outcome. *Plast Reconstr Surg* **102**, 711-721 (1998).
45. Pucci, A.M., Forbes, R.D. & Billingham, M.E. Pathologic features in long-term cardiac allografts. *J Heart Transplant* **9**, 339-345 (1990).
46. www.ihctas.org.
47. Baumeister, S.*, et al.* Risks of allogeneic hand transplantation. *Microsurgery* **24**, 98-103 (2004).
48. Marcen, R. Immunosuppressive drugs in kidney transplantation: impact on patient survival, and incidence of cardiovascular disease, malignancy and infection. *Drugs* **69**, 2227-2243 (2009).
49. Brouha, P.*, et al.* Risk acceptance in composite-tissue allotransplantation reconstructive procedures. *Microsurgery* **26**, 144-149; discussion 149-150 (2006).
50. Barker, J.H.*, et al.* Investigation of risk acceptance in facial transplantation. *Plast Reconstr Surg* **118**, 663-670 (2006).
51. Vasilic, D.*, et al.* Plastic surgeon's risk acceptance in facial transplantation. *Plast Reconstr Surg* **121**, 41e-48e (2008).
52. Rygaard, J. Immunobiology of the mouse mutant "Nude". Preliminary investigations. *Acta Pathol Microbiol Scand* **77**, 761-762 (1969).
53. Miller, J.F.A.P. Effect of neonatal thymectomy on the immunological responsiveness of the mouse. *Proc R Soc Lond B Biol Sci* **156**, 415-428 (1962).
54. Nelson, P.J. & Krensky, A.M. Chemokines, chemokine receptors, and allograft rejection. *Immunity* **14**, 377-386 (2001).
55. Lu, C.Y., Penfield, J.G., Kielar, M.L., Vazquez, M.A. & Jeyarajah, D.R. Hypothesis: is renal allograft rejection initiated by the response to injury sustained during the transplant process? . *Kidney Int.* **55**, 2157-2168 (1999).
56. Bharat, A.*, et al.* Early posttransplant inflammation promotes the development of alloimmunity and chronic lung allograft rejection. *Transplantation* **83**, 150-158 (2007).
57. Hancock, W.W., Gao, W., Faia, K.L. & Csizmadia, V. Chemokines and their receptors in allograft rejection. *Curr Opin Immunol* **12**, 511-516 (2000).
58. El-Sawy, T., Fahmy, N.M. & Fairchild, R.L. Chemokines: directing leukocyte infiltration into allografts. . *Curr Opin Immunol* **14**, 562-568 (2002).
59. Carvalho-Gaspar, M., Billing, J.S., Spriewald, B.M. & Wood, K.J. Chemokine gene expression during allograft rejection: comparison of two quantitative PCR techniques. *J Immunol Methods* **301**, 41-52 (2005).
60. Larsen, C.P., Morris, P.J. & Austyn, J.M. Migration of dendritic leukocytes from cardiac allografts into host spleens. A novel pathway for initiation of rejection. *J Exp Med* **171**, 307-314 (1990).

61. Lakkis, F.G., Arakelov, A., Konieczny, B.T. & Inoue, Y. Immunologic 'ignorance' of vascularized organ transplants in the absence of secondary lymphoid tissue. *Nat Med* **6**, 686-688 (2000).
62. Lechler, R., Ng, W.F. & Steinman, R.M. Dendritic cells in transplantations: friend or foe? *Immunity* **14**, 357-368 (2001).
63. Talmage, D.W., Dart, G., Radovich, J. & Lafferty, K.J. Activation of transplant immunity: effect of donor leukocytes on thyroid allograft rejection. *Science* **191**, 385-388 (1976).
64. Larsen, C.P.*, et al.* Migration and maturation of Langerhans cells in skin transplants and explants. *J Exp Med* **172**, 1483-1493 (1990).
65. Peugh, W.N., Superina, R.A., Wood, K.J. & Morris, P.J. The role of H-2 and non-H-2 antigens and genes in the rejection of murine cardiac allografts. *Immunogenetics* **23**, 30-37 (1986).
66. Goulmy, E. Minor histocompatibility antigens: from transplantation problems to therapy of cancer. *Hum Immunol* **67**, 433-438 (2006).
67. Gokmen, M.R., Lombardi, G. & Lechler, R.I. The importance of the indirect pathway of allorecognition in clinical transplantation. *Curr Opin Immunol* **20**(2008).
68. Shoskes, D.A. & Wood, K.J. Indirect presentation of MHC antigens in transplantation. *Immunol Today* **15**, 32-38 (1994).
69. Hernandez-Fuentes, M.P., Baker, R.J. & Lechler, R.I. The alloresponse. *Rev Immunogenet* **1**, 282-296 (1999).
70. Baker, R.J., Hernandez-Fuentes, M.P., Brookes, P.A., Chaudhry, A.N. & Lechler, R. Comparison of the direct and indirect pathways of allorecognition in chronic allograft failure. *Transplant Proc* **33**, 449 (2001).
71. Pietra, B.A., Wiseman, A., Bolwerk, A., Rizeq, M. & Gill, R.G. T cell-mediated cardiac allograft rejection requires donor but not host MHC class II. *J Clin Invest* **106**, 1003-1010 (2000).
72. Trivedi, H. Immunobiology of rejection and adaptation. *Trans Proceed* **39**, 647-652 (2007).
73. Lechler, R.I. & Batchelor, J.R. Immunogenicity of retransplanted rat kidney allografts. Effect of inducing chimerism in the first recipient and quantitative studies on immunosuppression of the second recipient. *J Exp Med* **156**, 1835-1841 (1982).
74. Lechler, R.I. & Batchelor, J.R. Restoration of immunogenicity to passenger cell-depleted kidney allografts by the addition of donor strain dendritic cells. *J Exp Med* **155**, 31-41 (1982).
75. Baker, R.J.*, et al.* Loss of direct and mainenance of indirect alloresponses in renal allograft recipients: implications for the pathogenesis of chronic allograft nephropathy. *J Immunol*, 7199-7206 (2001).
76. Auchincloss, H.J.*, et al.* The role of "indirect" recognition in initiating rejection of skin grafts from major histocompatibility complex class II-deficient mice. *Proc Natl Acad Sci USA* **90**, 3373-3377 (1993).
77. Fluck, N., Witzke, O., Morris, P.J. & Wood, K.J. Indirect allorecognition is involved in both acute and chronic allograft rejection. . *Transplant Proc* **31**, 842-843 (1999).

78. Dalchau, R., Fangmann, J. & Fabre, J.W. Allorecognition of isolated, denatured chains of class I and class II major histocompatibility complex molecules. Evidence for an important role for indirect allorecognition in transplantation. *Eur J Immunol* **22**, 669-677 (1992).
79. Vella, J.P.*, et al.* Indirect allorecognition of major histocompatibility complex allopeptides in human renal transplant recipients with chronic graft dysfunction. *Transplantation* **64**, 795-800 (1997).
80. Heeger, P.S. T cell allorecognition and transplant rejection: a summary and update. *Am J Transplant* **3**, 525-533 (2003).
81. Herrera, O.B.*, et al.* A novel pathway of alloantigen presentation by dendritic cells. *J Immunol* **173**, 4828-4837 (2004).
82. Morelli, A.E.*, et al.* Endocytosis, intracellular sorting, and processing of exosomes by dendritic cells. *Blood* **104**, 3257-3266 (2004).
83. Game, D.S., Rogers, R.J. & Lechler, R.I. Acquisition of HLA-DR and costimulatory molecules by T cells from allogeneic antigen presenting cells. *Am J Transplant* **5**, 1614-1625 (2005).
84. Le Moine, A., Goldman, M. & Abramowicz, D. Multiple pathways to allograft rejection. *Transplantation* **73**, 1373-1381 (2002).
85. Barbara, J.A.*, et al.* Islet allograft rejection can be mediated by CD4+, alloantigen experienced, direct pathway T cells of TH1 and TH2 cytokine phenotype. *Transplantation* **70**, 1641-1649 (2000).
86. Chadha, R., Heidt, S., Jones, N.D. & Wood, K.J. Th17: contributors to allograft rejection and a barrier to the induction of transplantation tolerance? *Transplantation* **91**, 939-945 (2011).
87. Heidt, S., Segundo, D.S., Chadha, R. & Wood, K.J. The impact of Th17 cells on transplant rejection and the induction of tolerance. *Curr Opin Organ Transplant* **15**, 456-461 (2010).
88. O'Connell, P.J.*, et al.* Unmodified pancreatic islet allograft rejection results in the preferential expression of certain T cell activation transcripts. *J Immunol* **150**, 1093-1104 (1993).
89. Dallman, M.J., Larsen, C.P. & Morris, P.J. Cytokine gene transcription in vascularised organ grafts: analysis using semiquantitative polymerase chain reaction. *J Exp Med* **174**, 493-496 (1991).
90. Hauser, I.A.*, et al.* Prediction of acute renal allograft rejection by urinary monokine induced by IFN-gamma (MIG). *J Am Soc Nephrol* **16**, 1849-1858 (2005).
91. Halloran, P.F.*, et al.* IFN-gamma alters the pathology of graft rejection: protection from early necrosis. *J Immunol* **166**, 7022-7081 (2001).
92. Miura, M., El-Sawy, T. & Fairchild, R.L. Neutrophils mediate parenchymal tissue necrosis and accelerate the rejection of complete major histocompatibility complex-disparate cardiac allografts in the absence of interferon-gamma. *Am J Pathol* **162**, 509-519 (2003).
93. Sadeghi, M.*, et al.* Evidence for IFN-gamma up-and IL-4 downregulation late posttransplant in patients with good kidney graft outcome. *Clin Transplant* **21**, 449-459 (2007).

94. Sawitzki, B.*, et al.* IFN-gamma production by alloantigen-reactive regulatory T cells is important for their regulatory function in vivo. *J Exp Med* **201**, 1925-1935 (2005).
95. Harrington, L.E.*, et al.* Interleukin 17-producing CD4+ effector T cells develop via a lineage distinct from the T helper type 1 and 2 lineages. *Nat Immunol* **6**, 1123-1132 (2005).
96. Famulski, K.S., Sis, B., Billesberger, L. & Halloran, P.F. Interferon-gamma and donor MHC class I control alternative macrophage activation and activin expression in rejecting kidney allografts: a shift in the Th1-Th2 paradigm. *Am J Transplant* **8**, 547-556 (2008).
97. Feng, G.*, et al.* Exogenous IFN-gamma ex vivo shapes the alloreactive T-cell repertoire by inhibition of Th17 responses and generation of functional Foxp3 regulatory T cells. *Eur J Immunol* **38**, 2512-2527 (2008).
98. Yuan, X.*, et al.* A novel role of CD4 Th17 cells in mediating cardiac allograft rejection and vasculopathy. *J Exp Med* **205**(2008).
99. Chan, S.Y., DeBruyne, L.A., Goodman, R.E., Eichwald, E.J. & Bishop, D.K. In vivo depletion of CD8+ T cells results in Th2 cytokine production and alternate mechanisms of allograft rejection. *Transplantation* **59**, 1155-1161 (1995).
100. Krams, S.M.*, et al.* Cytokine and T cell receptor gene expression at the site of allograft rejection. *Transplantation* **53**, 151-156 (1992).
101. Martinez, O.M.*, et al.* Evidence for a nonclassical pathway of graft rejection involving interleukin 5 and eosinophils. *Transplantation* **55**, 909-918 (1993).
102. Martinez, O.M.*, et al.* IL-2 and IL-5 gene expression in response to alloantigen in liver allograft recipients and in vitro. *Transplantation* **55**, 1159-1166 (1993).
103. VanBuskirk, A.M., Wakely, M.E. & Orosz, C.G. Transfusion of polarized TH2-like cell populations into SCID mouse cardiac allograft recipients results in acute allograft rejection. *Transplantation* **62**, 229-238 (1996).
104. Barbara, J.A.*, et al.* Islet allograft rejection can be mediated by CD4+, alloantigen experienced, direct pathway T cells of TH1 and TH2 cytokine phenotype. *Transplantation* **70**, 1641-1649 (70).
105. Veldhoen, M.*, et al.* Transforming growth factor-beta 'reprograms' the differentiation of T helper 2 cells and promotes an interleukin 9-producing subset. *Nat Immunol* **9**, 1341-1346 (2008).
106. Dardalhon, V.*, et al.* IL-4 inhibits TGF-beta-induced Foxp3+ T cells and, together with TGF-beta, generates IL-9+ IL10+ Foxp3(-) effector T cells. *Nat Immunol* **9**, 1347-1355 (2008).
107. Soroosh, P. & Doherty, T.A. Th9 and allergic disease. *Immunology* **127**, 450-458 (2009).
108. Mills, K.H.G. Induction, function and regulation of IL-17 producing T cells. *EJI* **38**, 2636-2649 (2008).
109. Chen, H.*, et al.* A pathogenic role of IL-17 at the early stage of corneal allograft rejection. *Transpl Immunol* **21**, 155-161 (2009).
110. Loong, C.C., Hsieh, H.G., Lui, W.Y., Chen, A. & Lin, C.Y. Evidence for the early involvement of interleukin 17 in human and experimental renal allograft rejection. *J Pathol* **197**(2002).

111. Van Kooten, C.*, et al.* Interleukin-17 activates human renal epithelial cells in vitro and is expressed during renal allograft rejection. *J Am Soc Nephrol* **9**, 1526-1534 (1998).
112. Vanaudenaerde, B.M.*, et al.* The role of interleukin-17 during acute rejection after lung transplantation. *Eur Respir J* **27**, 779-787 (2006).
113. Rao, D.A.*, et al.* Interleukin (IL)-1 promotes allogeneic T cell intimal infiltration and IL-17 production in a model of human artery rejection. *J Exp Med* **205**, 3145-3158 (2008).
114. Antonysamy, M.A.*, et al.* Evidence for a role of IL-17 in organ allograft rejection: IL-17 promotes the functional differentiation of dendritic cell progenitors. *J Immunol* **162**, 577-584 (1999).
115. Antonysamy, M.A.*, et al.* Evidence for a role of IL-17 in alloimmunity: A novel IL-17 antagonist promotes heart graft survival. *Transplant Proc* **31**, 93 (1999).
116. Afzali, B., Lombardi, G., Lechler, R.I. & Lord, G.M. The role of T helper 17 (Th17) and regulatory T cells (Treg) in human organ transplantation and autoimmune disease. *Clin Exp Immunol* **148**, 32-46 (2007).
117. Cornell, L.D., Smith, R.N. & Colvin, R.B. Kidney transplantation: mechanisms of rejection and acceptance. *Annu Rev Pathol Mech Dis* **3**, 189-220 (2008).
118. Robertson, H., Wheeler, J., Kirby, J.A. & Morley, A.R. Renal allograft rejection: in situ demonstration of cytotoxic intratubular cells. *Transplantation* **61**, 1546-1549 (1996).
119. Einecke, G.*, et al.* Tubulitis and epithelial cell alterations in mouse kidney transplant rejection are independent of CD103, perforin or granzymes A/B. *Am J Transplant* **6**, 2109-2120 (2006).
120. Hoffmann, S.C.*, et al.* Functionally significant renal allograft rejection is defined by transcriptional criteria. *Am J Transplant* **5**, 573-581 (2005).
121. Desvaux, D.*, et al.* Molecular diagnosis of renal-allograft rejection: correlation with histolopathologic evaluation and antirejection-therapy resistance. *78* (2004).
122. Sarwal, M.*, et al.* Molecular heterogeneity in acute renal allograft rejection identified by DNA microarray profiling. *N Engl J Med* **349**, 125-138 (2003).
123. Surquin, M.*, et al.* Skin graft rejection elicited by beta 2-microglobulin as a minor transplantation antigen involved multiple effector pathways: role of Fas-Fas ligand interactions and Th2-dependent graft eosinophil infiltrates. *J Immunol* **500-506**(2002).
124. Yang, J.*, et al.* Allograft rejection mediated by memory T cells is resistant to regulation. *Proc Natl Acad Sci U S A* **104**, 19954-19959 (2007).
125. Walsh, C.M.*, et al.* Cell-mediated cytotoxicity results from, but may not be critical for, primary allograft rejection. *J Immunol* **156**, 1436-1441 (1996).
126. Koyama, I.*, et al.* Depletion of CD8 memory T cells for induction of tolerance of a previously transplanted kidney allograft. *Am J Transplant* **7**, 1055-1061 (2007).
127. Chang, A.T. & Platt, J.L. The role of antibodies in transplantation. *Transplant Rev* (2009).
128. Mauiyyedi, S. & Colvin, R. Humoral rejection in kidney transplantation: new concepts in diagnosis and treatment. *Curr Opin Nephrol Hypertens* **11**, 609-618 (2002).

129. George, J.F*., et al.* Utility of postransplantation panel-reactive antibody measurements for the prediction of rejection frequency and survival of heart transplant recipients. *J Heart Lung Transplant* **14**, 856-864 (1995).
130. Smith, J.D., Danskine, A.J. & Rose, M.L. Specificity of lymphcytotoxic antibodies formed after cardiac transplantation and correlation with rejection episodes. *Transplantation* **53**, 1358-1362 (1992).
131. McKenna, R.M., Takemoto, S.K. & Terasaki, P.I. Anti-HLA antibodies after solid organ transplantation. *Transplantation* **69**, 319-326 (2000).
132. Terasaki, P.I. & Ozawa, M. Predictive value of HLA antibodies and serum creatinine in chronic rejection: results of a 2-year prospective trial. *Transplantation* **80**, 1194-1197 (2005).
133. Terasaki, P.I. Humoral theory of transplantation. *Am J Transplant* **3**, 665-673 (2003).
134. Mauiyyedi, S*., et al.* Chronic humoral rejection: identification of antibody-mediated chronic renal allograft rejection by C4d deposits in peritubular capillaries. *J Am Soc Nephrol* **12**, 574-582 (2001).
135. McKenna, R.M., Takemoto, S.K. & Terasaki, P.I. Anti-HLA antibodies after solid organ transplantation. *Transplantation* **69**, 319-326 (2000).
136. Rodriguez, E.R*., et al.* Antibody-mediated rejection in human cardiac allografts: evaluation of immunoglobulins and complement activation products C4d and C3d as markers. *Am J Transplant* **5**, 2778-2785 (2005).
137. Smith, R.N*., et al.* C4d deposition in cardiac allografts correlates with alloantibody. *J Heart Lung Transplant* **24**, 1202-1210 (2005).
138. Valujskikh, A. Memory T cells in allograft rejection. *Adv Exp Med Biol* **601**, 247-256 (2007).
139. Bingaman, A.W. & Farber, D.L. Memory T cells in transplantation: generation, function, and potential role in rejection. *Am J Transplant* **2004**, 846-852 (2004).
140. Oldstone, M.B. Molecular mimicry and autoimmune disease. *Cell* **50**, 819-820 (1987).
141. Tough, D.F., Borrow, P. & Sprent, J. Induction of bystander T cell proliferation by viruses and type I interferon in vivo. *Science* **272**(1996).
142. Wu, Z*., et al.* Homeostatic proliferation is a barrier to transplantation tolerance. *Nat Med* **10**, 87-92 (2004).
143. Surh, C.D. & Sprent, J. Homeostasis of naive and memory T cells. *Immunity* **29**, 848-862 (2008).
144. Trzonkowski, P., Zilvetti, M., Friend, P. & Wood, K.J. Recipient memory-like lymphocytes remain unresponsive to graft antigens after CAMPATH-1H induction with reduced maintenance immunosuppression. *Transplantation* **82**, 1342-1351 (2006).
145. Pearl, J.P*., et al.* Immunocompetent T-cells with a memory-like phenotype are the dominant cell type following antibody-mediated T-cell depletion. *Am J Transplant* **5**, 465-474 (2005).
146. Brook, M.O., Wood, K.J. & Jones, N.D. The impact of memory T cells on rejection and the induction of tolerance. *Transplantation* **82**, 1-9 (2006).

147. Augustine, J.J*., et al.* Pre-transplant IFN-gamma ELISPOTs are associated with post-transplant renal function in African American renal transplant recipients. *Am J Transplant* **5**, 1971-1975 (2005).
148. Carroll, M.C. & Prodeus, A.P. Linkages of innate and adaptive immunity. *Curr Opin Immunol* **10**, 36-40 (1998).
149. Brown, E.J. Complement receptors, adhesion, and phagocytosis. *Infect Agents Dis* **1**, 63-70 (1992).
150. Thieblemont, N*., et al.* Triggering of complement receptors CR1 (CD35) and CR3 (CD11b/CD18) induces nuclear translocation of NF-kappa B (p50/p65) in human monocytes and enhances viral replication in HIV-infected monocytic cells. *J Immunol* **155**, 4861-4867 (1995).
151. Jacquier-Sarlin, M.R., Gabert, F.M., Villiers, M.B. & Colomb, M.G. Modulation of antigen processing and presentation by covalently linked complement C3b fragment. *Immunology* **84**, 164-170 (1995).
152. Muller-Eberhard, H.J. The membrane attack complex of complement. *Annu Rev Immunol* **4**, 503-528 (1986).
153. Barao, I. & Murphy, W.J. The immunobiology of natural killer cells and bone marrow allograft rejection. *Biol Blood Marrow Transplant* **9**, 727-741 (2003).
154. Yu, G., Xu, X., Vu, M.D., Kilpatrick, E.D. & Li, X.C. NK cells promote transplant tolerance by killing donor antigen-presenting cells. *J Exp Med* **203**, 1851-1858 (2006).
155. Sheil, A.G., Moseley, R.V. & Murray, J.E. Differential Skin and Renal Homograft Survival in Dogs on Immunosuppressive Therapy. *Surg Forum* **15**, 166-168 (1964).
156. Lee, W.P*., et al.* Relative antigenicity of components of a vascularised limb allograft. *Plast Reconstr Surg* **87**, 401-411 (1991).
157. Jones, N.D., Morris, P.J. & Wood, K.J. Differential susceptibility of heart, skin and islet allografts to T cell-mediated rejection. *J Immunol* **166**, 2824-2830 (2001).
158. Buttemeyer, R., Jones, N.F., Min, Z. & Rao, U. Rejection of the component tissues of limb allografts in rats immunosuppressed with FK-506 and cyclosporine. *Plast Reconstr Surg* **97**, 139-148; discussion 149-151 (1996).
159. Zamfirescu, D.G*., et al.* Sentinel skin allograft-a reliable marker for monitoring of composite tissue transplant rejection. *Transplant Proc* **41**, 503-508 (2009).
160. Perloff, L.J. & Barker, C.F. The immediately vascularized skin allograft. *Transplantation* **28**, 125-130 (1979).
161. Mathes, D.W*., et al.* Split tolerance to a composite tissue allograft in a swine model. *Transplantation* **75**, 25-31 (2003).
162. Fuchimoto, Y*., et al.* Skin-specific alloantigens in miniature swine. *Transplantation* **72**, 122-126 (2001).
163. Hettiaratchy, S*., et al.* Tolerance to composite tissue allografts across a major histocompatibility barrier in miniature swine. *Transplantation* **77**, 514-521 (2004).
164. Barker, C.F. & Billingham, R.E. The role of afferent lymphatics in the rejection of skin homografts. *J Exp Med* **128**, 197-221 (1968).
165. Austyn, J.M. & Larsen, C.P. Migration patterns of dendritic leukocytes. Implications for transplantation. *Transplantation* **49**, 1-7 (1990).

166. Larsen, C.P., Austyn, J.M. & Morris, P.J. The role of graft-derived dendritic leukocytes in the rejection of vascularized organ allografts. Recent findings on the migration and function of dendritic leukocytes after transplantation. *Ann Surg* **212**, 308-315; discussion 316-307 (1990).
167. Larsen, C.P., Morris, P.J. & Austyn, J.M. Donor dendritic leukocytes migrate from cardiac allografts into recipients' spleens. *Transplant Proc* **22**, 1943-1944 (1990).
168. Larsen, C.P., Morris, P.J. & Austyn, J.M. Migration of dendritic leukocytes from cardiac allografts into host spleens. A novel pathway for initiation of rejection. *J Exp Med* **171**, 307-314 (1990).
169. Horner, B.M.*, et al.* In vivo observations of cell trafficking in allotransplanted vascularized skin flaps and conventional skin grafts. *J Plast Reconstr Aesthet Surg* **63**, 711-719 (2010).
170. Nasir, S., Bozkurt, M., Krokowicz, L., Klimczak, A. & Siemionow, M. Correlation of chimerism with graft size and revascularization in vascularized and nonvascularized skin allografts. *Ann Plast Surg* **62**, 430-438 (2009).
171. Cines, D.B.*, et al.* Endothelial cells in physiology and in the pathophysiology of vascular disorders. *Blood* **91**, 3527-3561 (1998).
172. Pober, J.S., Kluger, M.S. & Schechner, J.S. Human endothelial cell presentation of antigen and the homing of memory/effector T cells to skin. *Ann N Y Acad Sci* **941**, 12-25 (2001).
173. Pober, J.S., Orosz, C.G., Rose, M.L. & Savage, C.O. Can graft endothelial cells initiate a host anti-graft immune response? *Transplantation* **61**, 343-349 (1996).
174. Epperson, D.E. & Pober, J.S. Antigen-presenting function of human endothelial cells. Direct activation of resting CD8 T cells. *J Immunol* **153**, 5402-5412 (1994).
175. Karmann, K., Hughes, C.C., Fanslow, W.C. & Pober, J.S. Endothelial cells augment the expression of CD40 ligand on newly activated human CD4+ T cells through a CD2/LFA-3 signaling pathway. *Eur J Immunol* **26**, 610-617 (1996).
176. Karmann, K., Hughes, C.C., Schechner, J., Fanslow, W.C. & Pober, J.S. CD40 on human endothelial cells: inducibility by cytokines and functional regulation of adhesion molecule expression. *Proc Natl Acad Sci U S A* **92**, 4342-4346 (1995).
177. Rosenberg, A.S. & Singer, A. Cellular basis of skin allograft rejection: an in vivo model of immune-mediated tissue destruction. *Annu Rev Immunol* **10**, 333-358 (1992).
178. Pober, J.S. & Cotran, R.S. Cytokines and endothelial cell biology. *Physiol Rev* **70**, 427-451 (1990).
179. Sprague, A.H. & Khalil, R.A. Inflammatory cytokines in vascular dysfunction and vascular disease. *Biochem Pharmacol* **78**, 539-552 (2009).
180. Stenderup, K.*, et al.* Resolution of Psoriasis by a Leukocyte-Targeting Bacterial Protein in a Humanized Mouse Model. *J Invest Dermatol* (2011).
181. He, C.*, et al.* Effects of T cell frequency and graft size on transplant outcome in mice. *J Immunol* **172**, 240-247 (2004).
182. Poggio, E.D.*, et al.* Donor kidney volume and outcomes following live donor kidney transplantation. *Am J Transplant* **6**, 616-624 (2006).

183. Boyse, E.A. & Old, L.J. Loss of skin allograft tolerance by chimeras. *Transplantation* **6**, 619 (1968).
184. Silverman, M.S. & Chin, P.H. Differences in the rejection of skin transplants and blood cells of donor marrow origin by radiation-induced chimeras. *Ann N Y Acad Sci* **99**, 542-549 (1962).
185. Steinmuller, D. Tissue-specific and tissue-restricted histocompatibility antigens. *Immunology Today* **5**, 234-240 (1984).
186. Steinmuller, D. The enigma of skin allograft rejection. *Transplantation Reviews* **12**, 42-57 (1998).
187. Petit, F*., et al.* Prolongation of skin allograft survival after neonatal injection of donor bone marrow and epidermal cells. *Plast Reconstr Surg* **113**, 270-276 (2004).
188. Jackman, S.H., De Pirro, E.S. & Goldberg, E.H. Immunohistochemical identification of Skn antigens in mouse epidermis. *J Invest Dermatol* **93**, 46-49 (1989).
189. Rees, D., Carey, F. & Goldberg, E.H. Skn antigens: identification of a 95-kilodalton protein in mouse neural tissue. *Reg Immunol* **5**, 94-99 (1993).
190. Scheid, M., Boyse, E.A., Carswell, E.A. & Old, L.J. Serologically demonstrable alloantigens of mouse epidermal cells. *J Exp Med* **135**, 938-955 (1972).
191. Boyse, E.A., Carswell, E.A., Scheid, M.P. & Old, L.J. Tolerance of Sk-incompatible skin grafts. *Nature* **244**, 441-442 (1973).
192. Steinmuller, D. Skin allograft rejection by stable hematopoietic chimeras that accept organ allografts sill is an enigma. *Transplantation* **72**, 8-9 (2001).
193. Steinmuller, D., Wakely, E. & Landas, S.K. Evidence that epidermal alloantigen Epa-1 is an immunogen for murine heart as well as skin allograft rejection. *Transplantation* **51**, 459-463 (1991).
194. Zhang, Z*., et al.* Pattern of liver, kidney, heart, and intestine allograft rejection in different mouse strain combinations. *Transplantation* **62**, 1267-1272 (1996).
195. Clark, R.A*., et al.* The vast majority of CLA+ T cells are resident in normal skin. *J Immunol* **176**, 4431-4439 (2006).
196. Galkowska, H. Dendritic cells as regulators of immune reactivity: implications for skin transplantation. *Ann Transplant* **9**, 5-10 (2004).
197. Black, A.P*., et al.* Human keratinocyte induction of rapid effector function in antigen-specific memory CD4+ and CD8+ T cells. *Eur J Immunol* **37**, 1485-1493 (2007).
198. Illigens, B.M*., et al.* The relative contribution of direct and indirect antigen recognition pathways to the alloresponse and graft rejection depends upon the nature of the transplant. *Hum Immunol* **63**, 912-925 (2002).
199. Mestas, J. & Hughes, C.C.W. Of mice and not men: differences between mouse and human immunology. *J Immunol* **172**, 2731-2738 (2004).
200. Mestas, J. & Hughes, C.C. Endothelial cell costimulation of T cell activation through CD58-CD2 interactions involves lipid raft aggregation. *J Immunol* **167**, 4378-4385 (2001).
201. Murphy, L.L., Mazanet, M.M., Taylor, A.C., Mestas, J. & Hughes, C.C. Single-cell analysis of costimulation by B cells, endothelial cells, and fibroblasts

demonstrates heterogeneity in responses of CD4(+) memory T cells. *Cell Immunol* **194**, 150-161 (1999).
202. Bianchi, M.E. DAMPs, PAMPs and alarmins: all we need to know about danger. *J Leukoc Biol* **81**, 1-5 (2007).
203. Oppenheim, J.J., Tewary, P., de la Rosa, G. & Yang, D. Alarmins initiate host defense. *Adv Exp Med Biol* **601**, 185-194 (2007).
204. Scaffidi, P., Misteli, T. & Bianchi, M.E. Release of chromatin protein HMGB1 by necrotic cells triggers inflammation. *Nature* **418**, 191-195 (2002).
205. Schmitt, E., Gehrmann, M., Brunet, M., Multhoff, G. & Garrido, C. Intracellular and extracellular functions of heat shock proteins: repercussions in cancer therapy. *J Leukoc Biol* **81**, 15-27 (2007).
206. Foell, D., Wittkowski, H., Vogl, T. & Roth, J. S100 proteins expressed in phagocytes: a novel group of damage-associated molecular pattern molecules. *J Leukoc Biol* **81**, 28-37 (2007).
207. Werman, A*., et al.* The precursor form of IL-1alpha is an intracrine proinflammatory activator of transcription. *Proc Natl Acad Sci U S A* **101**, 2434-2439 (2004).
208. Shi, Y., Evans, J.E. & Rock, K.L. Molecular identification of a danger signal that alerts the immune system to dying cells. *Nature* **425**, 516-521 (2003).
209. Moussion, C., Ortega, N. & Girard, J.P. The IL-1-like cytokine IL-33 is constitutively expressed in the nucleus of endothelial cells and epithelial cells in vivo: a novel 'alarmin'? *PLoS One* **3**, e3331 (2008).
210. Liew, F.Y., Pitman, N.I. & McInnes, I.B. Disease-associated functions of IL-33: the new kid in the IL-1 family. *Nat Rev Immunol* **10**, 103-110 (2010).
211. Hueber, A.J*., et al.* IL-33 induces skin inflammation with mast cell and neutrophil activation. *Eur J Immunol* **41**, 2229-2237 (2011).
212. Nestle, F.O., Di Meglio, P., Qin, J.-Z. & Nickoloff, B.J. Skin immune sentinels in health and disease. *Nat Rev Immunol* **9**, 679-691 (2009).
213. Hvid, M*., et al.* IL-25 in atopic dermatitis: a possible link between inflammation and skin barrier dysfunction? *J Invest Dermatol* **131**, 150-157 (2011).
214. Angkasekwinai, P., Chang, S.H., Thapa, M., Watarai, H. & Dong, C. Regulation of IL-9 expression by IL-25 signaling. *Nat Immunol* **11**, 250-256 (2010).
215. Saenz, S.A., Taylor, B.C. & Artis, D. Welcome to the neighborhood: epithelial cell-derived cytokines license innate and adaptive immune responses at mucosal sites. *Immunol Rev* **226**, 172-190 (2008).
216. Wang, Y.H*., et al.* IL-25 augments type 2 immune responses by enhancing the expansion and functions of TSLP-DC-activated Th2 memory cells. *J Exp Med* **204**, 1837-1847 (2007).
217. Buhler, L.H*., et al.* Induction of kidney allograft tolerance after transient lymphohematopoietic chimerism in patients with multiple myeloma and end-stage renal disease. *Transplantation* **74**, 1405-1409 (2002).
218. Fudaba, Y*., et al.* Myeloma responses and tolerance following combined kidney and nonmyeloablative marrow transplantation: in vivo and in vitro analyses. *Am J Transplant* **6**, 2121-2133 (2006).
219. Spitzer, T.R*., et al.* Long-term follow-up of recipients of combined human leukocyte antigen-matched bone marrow and kidney transplantation for

multiple myeloma with end-stage renal disease. *Transplantation* **91**, 672-676 (2011).
220. Kawai, T., Cosimi, A.B. & Sachs, D.H. Preclinical and clinical studies on the induction of renal allograft tolerance through transient mixed chimerism. *Curr Opin Organ Transplant* **16**, 366-371 (2011).
221. Kawai, T.*, et al.* HLA-mismatched renal transplantation without maintenance immunosuppression. *N Engl J Med* **358**, 353-361 (2008).
222. LoCascio, S.A.*, et al.* Mixed chimerism, lymphocyte recovery, and evidence for early donor-specific unresponsiveness in patients receiving combined kidney and bone marrow transplantation to induce tolerance. *Transplantation* **90**, 1607-1615 (2010).
223. Butler, P.E., Lee, W.P., van de Water, A.P. & Randolph, M.A. Neonatal induction of tolerance to skeletal tissue allografts without immunosuppression. *Plast Reconstr Surg* **105**, 2424-2430; discussion 2431-2422 (2000).
224. Cober, S.R., Randolph, M.A. & Lee, W.P. Skin allograft survival following intrathymic injection of donor bone marrow. *J Surg Res* **85**, 204-208 (1999).
225. Mathes, D.W.*, et al.* Long-term acceptance of renal allografts following prenatal inoculation with adult bone marrow. *Transplantation* **80**, 1300-1308 (2005).
226. Jonker, M.*, et al.* Immunomodulation by intrathymic injection of donor leukocytes in rhesus monkeys. *Transplantation* **72**, 1432-1436 (2001).
227. Cobbold, S.P., Martin, G., Qin, S. & Waldmann, H. Monoclonal antibodies to promote marrow engraftment and tissue graft tolerance. *Nature* **323**, 164-166 (1986).
228. Yunusov, M.Y.*, et al.* Partial donor-specific tolerance to delayed skin grafts after rejection of hematopoietic cell graft. *Transplantation* **82**, 629-637 (2006).
229. Tillson, M.*, et al.* Hematopoietic chimerism induces renal and skin allograft tolerance in DLA-identical dogs. *Exp Hematol* **34**, 1759-1770 (2006).
230. Bozulic, L.D., Wen, Y., Xu, H. & Ildstad, S.T. Evidence that FoxP3+ regulatory T cells may play a role in promoting long-term acceptance of composite tissue allotransplants. *Transplantation* **91**, 908-915 (2011).
231. Pan, H.*, et al.* Rapamycin, mycophenolate mofetil, methylprednisolone, and cytotoxic T-lymphocyte-associated antigen 4 immunoglobulin-based conditioning regimen to induce partial tolerance to hind limb allografts without cytoreductive conditioning. *Transplant Proc* **40**, 1714-1721 (2008).
232. Foster, R.D., Pham, S., Li, S. & Aitouche, A. Long-term acceptance of composite tissue allografts through mixed chimerism and CD28 blockade. *Transplantation* **76**, 988-994 (2003).
233. Qin, S.X.*, et al.* Induction of tolerance in peripheral T cells with monoclonal antibodies. *Eur J Immunol* **20**, 2737-2745 (1990).
234. Wekerle, T.*, et al.* Allogeneic bone marrow transplantation with co-stimulatory blockade induces macrochimerism and tolerance without cytoreductive host treatment. *Nat Med* **6**, 464-469 (2000).
235. Wekerle, T.*, et al.* Anti-CD154 or CTLA4Ig obviates the need for thymic irradiation in a non-myeloablative conditioning regimen for the induction of

mixed hematopoietic chimerism and tolerance. *Transplantation* **68**, 1348-1355 (1999).
236. Durham, M.M.*, et al.* Cutting edge: administration of anti-CD40 ligand and donor bone marrow leads to hemopoietic chimerism and donor-specific tolerance without cytoreductive conditioning. *J Immunol* **165**, 1-4 (2000).
237. Seung, E., Mordes, J.P., Rossini, A.A. & Greiner, D.L. Hematopoietic chimerism and central tolerance created by peripheral-tolerance induction without myeloablative conditioning. *J Clin Invest* **112**, 795-808 (2003).
238. Hequet, O.*, et al.* Allogeneic donor bone marrow cells recovery and infusion after allogeneic face transplantation from the same donor. *Bone Marrow Transplant* **41**, 1059-1061 (2008).
239. UPMC. UPMC completes third successful bilateral hand transplant. *UPMC Press Release* (2010).
240. Siemionow, M. & Klimczak, A. Immunodepletive anti-alpha/beta-TCR antibody in transplantation of composite tissue allografts: Cleveland Clinic research experience. *Immunotherapy* **1**, 585-598 (2009).
241. Siemionow, M., Oke, R., Ozer, K., Izycki, D. & Prajapati, R. Induction of donor-specific tolerance in rat hind-limb allografts under antilymphocyte serum and cyclosporine A protocol. *J Hand Surg Am* **27**, 1095-1103 (2002).
242. Siemionow, M.*, et al.* Induction of tolerance in composite-tissue allografts. *Transplantation* **74**, 1211-1217 (2002).
243. Siemionow, M.Z., Izycki, D.M. & Zielinski, M. Donor-specific tolerance in fully major histocompatibility major histocompatibility complex-mismatched limb allograft transplants under an anti-alphabeta T-cell receptor monoclonal antibody and cyclosporine A protocol. *Transplantation* **76**, 1662-1668 (2003).
244. Ozer, K., Izycki, D., Zielinski, M. & Siemionow, M. Development of donor-specific chimerism and tolerance in composite tissue allografts under alphabeta-T-cell receptor monoclonal antibody and cyclosporine a treatment protocols. *Microsurgery* **24**, 248-254 (2004).
245. Ozer, K.*, et al.* Induction of tolerance to hind limb allografts in rats receiving cyclosporine A and antilymphocyte serum: effect of duration of the treatment. *Transplantation* **75**, 31-36 (2003).
246. Quatra, F.*, et al.* Induction of tolerance to composite tissue allograft in a rat model. *Microsurgery* **26**, 573-578 (2006).
247. Siemionow, M., Zielinski, M., Ozmen, S. & Izycki, D. Intraosseus transplantation of donor-derived hematopoietic stem and progenitor cells induces donor-specific chimerism and extends composite tissue allograft survival. *Transplant Proc* **37**, 2303-2308 (2005).
248. Siemionow, M. New minimal immunosuppression strategies for composite tissue allograft transplantation: the cleveland clinic experience. *J Am Acad Orthop Surg* **19 Suppl 1**, S38-39 (2011).
249. Nasir, S., Bozkurt, M., Klimczak, A. & Siemionow, M. Large antigenic skin load in total abdominal wall transplants permits chimerism induction. *Ann Plast Surg* **61**, 572-579 (2008).
250. Demir, Y., Ozmen, S., Klimczak, A., Mukherjee, A.L. & Siemionow, M. Tolerance induction in composite facial allograft transplantation in the rat model. *Plast Reconstr Surg* **114**, 1790-1801 (2004).

251. Kulahci, Y., Klimczak, A., Madajka, M., Altuntas, S. & Siemionow, M. Long-term survival of composite hemiface/mandible/tongue allografts correlates with multilineage chimerism development in the lymphoid and myeloid compartments of recipients. *Transplantation* **90**, 843-852 (2010).
252. Li, Z*., et al.* CD8+ T-Cell depletion and rapamycin synergize with combined coreceptor/stimulation blockade to induce robust limb allograft tolerance in mice. *Am J Transplant* **8**, 2527-2536 (2008).
253. Mathes, D.W*., et al.* Recipient bone marrow engraftment in donor tissue after long-term tolerance to a composite tissue allograft. *Transplantation* **73**, 1880-1885 (2002).
254. Lanzetta, M*., et al.* Human hand transplantation: what have we learned? *Transplant Proc* **36**, 664-668 (2004).
255. Granger, D.K*., et al.* Lack of donor hyporesponsiveness and donor chimerism after clinical transplantation of the hand. *Transplantation* **74**, 1624-1630 (2002).
256. Li, Z*., et al.* Donor T-cell development in host thymus after heterotopic limb transplantation in mice. *Transplantation* **83**, 815-818 (2007).
257. Wood, K.J. Passenger leukocytes and microchimerism: what role in tolerance induction? *Transplantation* **75**, 17S-20S (2003).
258. Brunkow, M.E*., et al.* Disruption of a new forkhead/winged-helix protein, scurfin, results in the fatal lymphoproliferative disorder of the scurfy mouse. *Nat Genet* **27**, 68-73 (2001).
259. Bennett, C.L*., et al.* The immune dysregulation, polyendocrinopathy, enteropathy, X-linked syndrome (IPEX) is caused by mutations of FOXP3. *Nat Genet* **27**, 20-21 (2001).
260. Josefowicz, S.Z. & Rudensky, A. Control of regulatory T cell lineage commitment and maintenance. *Immunity* **30**, 616-625 (2009).
261. Hori, S., Nomura, T. & Sakaguchi, S. Control of regulatory T cell development by the transcription factor Foxp3. *Science (New York, N.Y* **299**, 1057-1061 (2003).
262. Karim, M., Kingsley, C.I., Bushell, A.R., Sawitzki, B.S. & Wood, K.J. Alloantigen-induced CD25+CD4+ regulatory T cells can develop in vivo from CD25-CD4+ precursors in a thymus-independent process. *J Immunol* **172**, 923-928 (2004).
263. Kingsley, C.I., Karim, M., Bushell, A.R. & Wood, K.J. CD25+CD4+ regulatory T cells prevent graft rejection: CTLA-4- and IL-10-dependent immunoregulation of alloresponses. *J Immunol* **168**, 1080-1086 (2002).
264. Karim, M., Feng, G., Wood, K.J. & Bushell, A.R. CD25+CD4+ regulatory T cells generated by exposure to a model protein antigen prevent allograft rejection: antigen-specific reactivation in vivo is critical for bystander regulation. *Blood* **105**, 4871-4877 (2005).
265. Vukmanovic-Stejic, M*., et al.* The kinetics of CD4+Foxp3+ T cell accumulation during a human cutaneous antigen-specific memory response in vivo. *J Clin Invest* **118**, 3639-3650 (2008).
266. Roncarolo, M.G*., et al.* Interleukin-10-secreting type 1 regulatory T cells in rodents and humans. *Immunol Rev* **212**, 28-50 (2006).
267. Kemper, C*., et al.* Activation of human CD4+ cells with CD3 and CD46 induces a T-regulatory cell 1 phenotype. *Nature* **421**, 388-392 (2003).

268. Pillai, V., Ortega, S.B., Wang, C.K. & Karandikar, N.J. Transient regulatory T-cells: a state attained by all activated human T-cells. *Clin Immunol* **123**, 18-29 (2007).
269. Wang, J., Ioan-Facsinay, A., van der Voort, E.I., Huizinga, T.W. & Toes, R.E. Transient expression of FOXP3 in human activated nonregulatory CD4+ T cells. *Eur J Immunol* **37**, 129-138 (2007).
270. Lal, G. & Bromberg, J.S. Epigenetic mechanisms of regulation of Foxp3 expression. *Blood* **114**, 3727-3735 (2009).
271. Lal, G.*, et al.* Epigenetic regulation of Foxp3 expression in regulatory T cells by DNA methylation. *J Immunol* **182**, 259-273 (2009).
272. Wieczorek, G.*, et al.* Quantitative DNA methylation analysis of FOXP3 as a new method for counting regulatory T cells in peripheral blood and solid tissue. *Cancer research* **69**, 599-608 (2009).
273. Thornton, A.M.*, et al.* Expression of Helios, an Ikaros transcription factor family member, differentiates thymic-derived from peripherally induced Foxp3+ T regulatory cells. *J Immunol* **184**, 3433-3441 (2010).
274. Shevach, E.M. Mechanisms of foxp3+ T regulatory cell-mediated suppression. *Immunity* **30**, 636-645 (2009).
275. Broere, F.*, et al.* Oral or nasal antigen induces regulatory T cells that suppress arthritis and proliferation of arthritogenic T cells in joint draining lymph nodes. *J Immunol* **181**, 899-906 (2008).
276. Wang, L.*, et al.* Post-immune UV irradiation induces Tr1-like regulatory T cells that suppress humoral immune responses. *Int Immunol* **20**, 57-70 (2008).
277. Ludwig-Portugall, I., Hamilton-Williams, E.E., Gottschalk, C. & Kurts, C. Cutting edge: CD25+ regulatory T cells prevent expansion and induce apoptosis of B cells specific for tissue autoantigens. *J Immunol* **181**, 4447-4451 (2008).
278. Vignali, D.A., Collison, L.W. & Workman, C.J. How regulatory T cells work. *Nat Rev Immunol* **8**, 523-532 (2008).
279. Gondek, D.C., Lu, L.F., Quezada, S.A., Sakaguchi, S. & Noelle, R.J. Cutting edge: contact-mediated suppression by CD4+CD25+ regulatory cells involves a granzyme B-dependent, perforin-independent mechanism. *J Immunol* **174**, 1783-1786 (2005).
280. Grossman, W.J.*, et al.* Human T regulatory cells can use the perforin pathway to cause autologous target cell death. *Immunity* **21**, 589-601 (2004).
281. Garin, M.I.*, et al.* Galectin-1: a key effector of regulation mediated by CD4+CD25+ T cells. *Blood* **109**, 2058-2065 (2007).
282. Hara, M.*, et al.* IL-10 is required for regulatory T cells to mediate tolerance to alloantigens in vivo. *J Immunol* **166**, 3789-3796 (2001).
283. Collison, L.W.*, et al.* The inhibitory cytokine IL-35 contributes to regulatory T-cell function. *Nature* **450**, 566-569 (2007).
284. Tang, Q.*, et al.* Distinct roles of CTLA-4 and TGF-beta in CD4+CD25+ regulatory T cell function. *Eur J Immunol* **34**, 2996-3005 (2004).
285. Thornton, A.M. & Shevach, E.M. CD4+CD25+ immunoregulatory T cells suppress polyclonal T cell activation in vitro by inhibiting interleukin 2 production. *J Exp Med* **188**, 287-296 (1998).

286. Pandiyan, P., Zheng, L., Ishihara, S., Reed, J. & Lenardo, M.J. CD4+CD25+Foxp3+ regulatory T cells induce cytokine deprivation-mediated apoptosis of effector CD4+ T cells. *Nat Immunol* **8**, 1353-1362 (2007).
287. Wing, K.*, et al.* CTLA-4 control over Foxp3+ regulatory T cell function. *Science* **322**, 271-275 (2008).
288. Mellor, A.L. & Munn, D.H. IDO expression by dendritic cells: tolerance and tryptophan catabolism. *Nat Rev Immunol* **4**, 762-774 (2004).
289. Liang, B.*, et al.* Regulatory T cells inhibit dendritic cells by lymphocyte activation gene-3 engagement of MHC class II. *J Immunol* **180**, 5916-5926 (2008).
290. Shalev, I.*, et al.* Targeted deletion of fgl2 leads to impaired regulatory T cell activity and development of autoimmune glomerulonephritis. *J Immunol* **180**, 249-260 (2008).
291. Borsellino, G.*, et al.* Expression of ectonucleotidase CD39 by Foxp3+ Treg cells: hydrolysis of extracellular ATP and immune suppression. *Blood* **110**, 1225-1232 (2007).
292. Bushell, A. & Wood, K. GITR ligation blocks allograft protection by induced CD25+CD4+ regulatory T cells without enhancing effector T-cell function. *Am J Transplant* **7**, 759-768 (2007).
293. Kim, J.I.*, et al.* Blockade of GITR-GITRL interaction maintains Treg function to prolong allograft survival. *Eur J Immunol* **40**, 1369-1374 (2010).
294. Kitamura, N.*, et al.* OX40 costimulation can abrogate Foxp3+ regulatory T cell-mediated suppression of antitumor immunity. *Int J Cancer* **125**, 630-638 (2009).
295. Gri, G.*, et al.* CD4+CD25+ regulatory T cells suppress mast cell degranulation and allergic responses through OX40-OX40L interaction. *Immunity* **29**, 771-781 (2008).
296. Piconese, S.*, et al.* Mast cells counteract regulatory T-cell suppression through interleukin-6 and OX40/OX40L axis toward Th17-cell differentiation. *Blood* **114**, 2639-2648 (2009).
297. Griseri, T., Asquith, M., Thompson, C. & Powrie, F. OX40 is required for regulatory T cell-mediated control of colitis. *J Exp Med* **207**, 699-709 (2010).
298. Ruby, C.E.*, et al.* Cutting Edge: OX40 agonists can drive regulatory T cell expansion if the cytokine milieu is right. *J Immunol* **183**, 4853-4857 (2009).
299. Zhou, X.*, et al.* Instability of the transcription factor Foxp3 leads to the generation of pathogenic memory T cells in vivo. *Nat Immunol* **10**, 1000-1007 (2009).
300. Yang, X.O.*, et al.* Molecular antagonism and plasticity of regulatory and inflammatory T cell programs. *Immunity* **29**, 44-56 (2008).
301. Komatsu, N.*, et al.* Heterogeneity of natural Foxp3+ T cells: a committed regulatory T-cell lineage and an uncommitted minor population retaining plasticity. *Proc Natl Acad Sci U S A* **106**, 1903-1908 (2009).
302. Voo, K.S.*, et al.* Identification of IL-17-producing FOXP3+ regulatory T cells in humans. *Proc Natl Acad Sci U S A* **106**, 4793-4798 (2009).
303. Ayyoub, M.*, et al.* Human memory FOXP3+ Tregs secrete IL-17 ex vivo and constitutively express the T(H)17 lineage-specific transcription factor RORgamma t. *Proc Natl Acad Sci U S A* **106**, 8635-8640 (2009).

304. Bovenschen, H.J*., et al.* Foxp3+ Regulatory T Cells of Psoriasis Patients Easily Differentiate into IL-17A-Producing Cells and Are Found in Lesional Skin. *J Invest Dermatol* (2011).
305. Zhang, L., Yang, X.Q., Cheng, J., Hui, R.S. & Gao, T.W. Increased Th17 cells are accompanied by FoxP3(+) Treg cell accumulation and correlated with psoriasis disease severity. *Clin Immunol* **135**, 108-117 (2010).
306. Duarte, J.H., Zelenay, S., Bergman, M.-L., Martins, A.C. & Demengeot, J. Natural Treg cells spontaneously differentiate into pathogenic helper cells in lymphopaenic conditions. *Eur J Immunol* **39**, 948-955 (2009).
307. Kingsley, C.I., Nadig, S.N. & Wood, K.J. Transplantation tolerance: lessons from experimental rodent models. *Transpl Int* **20**, 828-841 (2007).
308. Bushell, A., Karim, M., Kingsley, C.I. & Wood, K. Pretransplant blood transfusion without additional immunotherapy generates CD25+CD4+ regulatory T cells: a potential explanation for the blood-transfusion effect. *Transplantation* **76**, 449-455 (2003).
309. Boyman, O., Kovar, M., Rubinstein, M.P., Surh, C.D. & Sprent, J. Selective stimulation of T cell subsets with antibody-cytokine immune complexes. *Science* **311**, 1924-1927 (2006).
310. Feng, G*., et al.* Exogenous IFN-gamma ex vivo shapes the alloreactive T-cell repertoire by inhibition of Th17 responses and generation of functional Foxp3+ regulatory T cells. *Eur J Immunol* **38**, 2512-2527 (2008).
311. Feng, G., Wood, K.J. & Bushell, A. Interferon-gamma conditioning ex vivo generates CD25+CD62L+Foxp3+ regulatory T cells that prevent allograft rejection: potential avenues for cellular therapy. *Transplantation* **86**, 578-589 (2008).
312. Hoffmann, P., Eder, R., Kunz-Schughart, L.A., Andreesen, R. & Edinger, M. Large-scale in vitro expansion of polyclonal human CD4(+)CD25high regulatory T cells. *Blood* **104**, 895-903 (2004).
313. Levings, M.K., Sangregorio, R. & Roncarolo, M.G. Human cd25(+)cd4(+) t regulatory cells suppress naive and memory T cell proliferation and can be expanded in vitro without loss of function. *J Exp Med* **193**, 1295-1302 (2001).
314. Battaglia, M*., et al.* Rapamycin promotes expansion of functional CD4+CD25+FOXP3+ regulatory T cells of both healthy subjects and type 1 diabetic patients. *J Immunol* **177**, 8338-8347 (2006).
315. Fantini, M.C., Dominitzki, S., Rizzo, A., Neurath, M.F. & Becker, C. In vitro generation of CD4+ CD25+ regulatory cells from murine naive T cells. *Nat Protoc* **2**, 1789-1794 (2007).
316. Sun, C.M*., et al.* Small intestine lamina propria dendritic cells promote de novo generation of Foxp3 T reg cells via retinoic acid. *J Exp Med* **204**, 1775-1785 (2007).
317. Chen, W*., et al.* Conversion of peripheral CD4+CD25- naive T cells to CD4+CD25+ regulatory T cells by TGF-beta induction of transcription factor Foxp3. *J Exp Med* **198**, 1875-1886 (2003).
318. Yamazaki, S*., et al.* Direct expansion of functional CD25+ CD4+ regulatory T cells by antigen-processing dendritic cells. *J Exp Med* **198**, 235-247 (2003).
319. Walker, M.R*., et al.* Induction of FoxP3 and acquisition of T regulatory activity by stimulated human CD4+CD25- T cells. *J Clin Invest* **112**, 1437-1443 (2003).

320. Rao, P.E., Petrone, A.L. & Ponath, P.D. Differentiation and expansion of T cells with regulatory function from human peripheral lymphocytes by stimulation in the presence of TGF-{beta}. *J Immunol* **174**, 1446-1455 (2005).
321. Zheng, S.G., Gray, J.D., Ohtsuka, K., Yamagiwa, S. & Horwitz, D.A. Generation ex vivo of TGF-beta-producing regulatory T cells from CD4+CD25- precursors. *J Immunol* **169**, 4183-4189 (2002).
322. Ocklenburg, F.*, et al.* UBD, a downstream element of FOXP3, allows the identification of LGALS3, a new marker of human regulatory T cells. *Lab Invest* **86**, 724-737 (2006).
323. Allan, S.E.*, et al.* Generation of potent and stable human CD4+ T regulatory cells by activation-independent expression of FOXP3. *Mol Ther* **16**, 194-202 (2008).
324. Yagi, H.*, et al.* Crucial role of FOXP3 in the development and function of human CD25+CD4+ regulatory T cells. *Int Immunol* **16**, 1643-1656 (2004).
325. Battaglia, M., Stabilini, A. & Roncarolo, M.G. Rapamycin selectively expands CD4+CD25+FoxP3+ regulatory T cells. *Blood* **105**, 4743-4748 (2005).
326. Feng, G.*, et al.* Functional regulatory T cells produced by inhibiting cyclic nucleotide phosphodiesterase type 3 prevent allograft rejection. *Sci Transl Med* **3**, 83ra40 (2011).
327. Collison, L.W.*, et al.* IL-35-mediated induction of a potent regulatory T cell population. *Nat Immunol* **11**, 1093-1101 (2010).
328. Seyerl, M.*, et al.* Human rhinoviruses induce IL-35-producing Treg via induction of B7-H1 (CD274) and sialoadhesin (CD169) on DC. *Eur J Immunol* **40**, 321-329 (2010).
329. Long, E. & Wood, K.J. Regulatory T cells in transplantation: transferring mouse studies to the clinic. *Transplantation* **88**, 1050-1056 (2009).
330. Francis, R.S.*, et al.* Induction of transplantation tolerance converts potential effector T cells into graft-protective regulatory T cells. *Eur J Immunol* **41**, 726-738 (2011).
331. Warnecke, G., Bushell, A., Nadig, S.N. & Wood, K.J. Regulation of transplant arteriosclerosis by CD25+CD4+ T cells generated to alloantigen in vivo. *Transplantation* **83**, 1459-1465 (2007).
332. Bushell, A., Morris, P.J. & Wood, K.J. Transplantation tolerance induced by antigen pretreatment and depleting anti-CD4 antibody depends on CD4+ T cell regulation during the induction phase of the response. *Eur J Immunol* **25**, 2643-2649 (1995).
333. Bushell, A., Morris, P.J. & Wood, K.J. Induction of operational tolerance by random blood transfusion combined with anti-CD4 antibody therapy. A protocol with significant clinical potential. *Transplantation* **58**, 133-139 (1994).
334. Saitovitch, D., Bushell, A., Mabbs, D.W., Morris, P.J. & Wood, K.J. Kinetics of induction of transplantation tolerance with a nondepleting anti-Cd4 monoclonal antibody and donor-specific transfusion before transplantation. A critical period of time is required for development of immunological unresponsiveness. *Transplantation* **61**, 1642-1647 (1996).

335. Saitovitch, D., Bushell, A., Morris, P.J. & Wood, K.J. Modulation of the CD4 molecule is a major event in the induction of transplantation tolerance with anti-CD4 monoclonal antibodies. *Transplant Proc* **29**, 1159 (1997).
336. Saitovitch, D., Bushell, A.R., Morris, P.J. & Wood, K.J. Induction of transplantation tolerance using a nondepleting anti-CD4 MAb and donor-specific transfusion before transplantation: evidence that a critical period of time is required for the development of immunological unresponsiveness. *Transplant Proc* **27**, 117-118 (1995).
337. Wood, K.J*., et al.* Mechanism of induction of transplantation tolerance using donor antigen and anti-CD4 monoclonal antibody. *Transplant Proc* **23**, 133-134 (1991).
338. Kingsley, C.I., Karim, M., Bushell, A.R. & Wood, K.J. CD25+CD4+ regulatory T cells prevent graft rejection: CTLA-4 and IL-10 dependent immunoregulation of alloresponses. *J Immunol* **168**, 1080-1086 (2002).
339. Golshayan, D*., et al.* In vitro-expanded donor alloantigen-specific CD4+CD25+ regulatory T cells promote experimental transplantation tolerance. *Blood* **109**, 827-835 (2007).
340. van Maurik, A., Herber, M., Wood, K.J. & Jones, N.D. Cutting edge: CD4+CD25+ alloantigen-specific immunoregulatory cells that can prevent CD8+ T cell-mediated graft rejection: implications for anti-CD154 immunotherapy. *J Immunol* **169**, 5401-5404 (2002).
341. Jones, N.D., Brook, M.O., Carvalho-Gaspar, M., Luo, S. & Wood, K.J. Regulatory T cells can prevent memory CD8+ T-cell-mediated rejection following polymorphonuclear cell depletion. *Eur J Immunol* **40**, 3107-3116 (2010).
342. Long, E.T., Baker, S., Oliveira, V., Sawitzki, B. & Wood, K.J. Alpha-1,2-mannosidase and hence N-glycosylation are required for regulatory T cell migration and allograft tolerance in mice. *PLoS One* **5**, e8894 (2010).
343. Graca, L*., et al.* Both CD4(+)CD25(+) and CD4(+)CD25(-) regulatory cells mediate dominant transplantation tolerance. *J Immunol* **168**, 5558-5565 (2002).
344. Yamaguchi, T*., et al.* Control of immune responses by antigen-specific regulatory T cells expressing the folate receptor. *Immunity* **27**, 145-159 (2007).
345. Webster, K.E*., et al.* In vivo expansion of T reg cells with IL-2-mAb complexes: induction of resistance to EAE and long-term acceptance of islet allografts without immunosuppression. *J Exp Med* **206**, 751-760 (2009).
346. Adeegbe, D*., et al.* In vivo induction of myeloid suppressor cells and CD4+Foxp3+ T regulatory cells prolongs skin allograft survival in mice. *Cell Transplant* (2010).
347. Oliveira, V*., et al.* Anti-CD4-mediated selection of Treg in vitro - in vitro suppression does not predict in vivo capacity to prevent graft rejection. *Eur J Immunol* **38**, 1677-1688 (2008).
348. Yamazaki, S*., et al.* Effective expansion of alloantigen-specific Foxp3+ CD25+ CD4+ regulatory T cells by dendritic cells during the mixed leukocyte reaction. *Proc Natl Acad Sci U S A* **103**, 2758-2763 (2006).

349. Tang, Q*., et al.* In vitro-expanded antigen-specific regulatory T cells suppress autoimmune diabetes. *J Exp Med* **199**, 1455-1465 (2004).
350. Park, Y.H*., et al.* Effect of in vitroexpanded CD4(+)CD25(+)Foxp3(+) regulatory T cell therapy combined with lymphodepletion in murine skin allotransplantation. *Clin Immunol* **135**, 43-54 (2010).
351. Warnecke, G*., et al.* CD4+ Regulatory T Cells Generated in Vitro with IFN-{gamma} and Allogeneic APC Inhibit Transplant Arteriosclerosis. *Am J Pathol* **177**, 464-472 (2010).
352. Wei, B., Baker, S., Wieckiewicz, J. & Wood, K.J. IFN-gamma Triggered STAT1-PKB/AKT Signalling Pathway Influences the Function of Alloantigen Reactive Regulatory T Cells. *Am J Transplant* (2009).
353. Joffre, O*., et al.* Prevention of acute and chronic allograft rejection with CD4+CD25+Foxp3+ regulatory T lymphocytes. *Nat Med* **14**, 88-92 (2008).
354. Tsang, J.Y*., et al.* Conferring indirect allospecificity on CD4+CD25+ Tregs by TCR gene transfer favors transplantation tolerance in mice. *J Clin Invest* **118**, 3619-3628 (2008).
355. Issa, F., Schiopu, A. & Wood, K.J. Role of T cells in graft rejection and transplantation tolerance. *Exp Rev Clin Immunol* **6**, 155-169 (2010).
356. Wang, R., Wan, Q., Kozhaya, L., Fujii, H. & Unutmaz, D. Identification of a regulatory T cell specific cell surface molecule that mediates suppressive signals and induces Foxp3 expression. *PLoS One* **3**, e2705 (2008).
357. Liu, W*., et al.* CD127 expression inversely correlates with FoxP3 and suppressive function of human CD4+ T reg cells. *J Exp Med* **203**, 1701-1711 (2006).
358. Seddiki, N*., et al.* Expression of interleukin (IL)-2 and IL-7 receptors discriminates between human regulatory and activated T cells. *J Exp Med* **203**, 1693-1700 (2006).
359. Putnam, A.L*., et al.* Expansion of human regulatory T-cells from patients with type 1 diabetes. *Diabetes* **58**, 652-662 (2009).
360. Kleinewietfeld, M*., et al.* CD49d provides access to "untouched" human Foxp3+ Treg free of contaminating effector cells. *Blood* **113**, 827-836 (2009).
361. Miyara, M*., et al.* Functional delineation and differentiation dynamics of human CD4+ T cells expressing the FoxP3 transcription factor. *Immunity* **30**, 899-911 (2009).
362. Riley, J.L., June, C.H. & Blazar, B.R. Human T regulatory cell therapy: take a billion or so and call me in the morning. *Immunity* **30**, 656-665 (2009).
363. Booth, N.J*., et al.* Different proliferative potential and migratory characteristics of human CD4+ regulatory T cells that express either CD45RA or CD45RO. *J Immunol* **184**, 4317-4326 (2010).
364. Hirahara, K*., et al.* The majority of human peripheral blood CD4+CD25highFoxp3+ regulatory T cells bear functional skin-homing receptors. *J Immunol* **177**, 4488-4494 (2006).
365. Chen, M.L., Yan, B.S., Bando, Y., Kuchroo, V.K. & Weiner, H.L. Latency-associated peptide identifies a novel CD4+CD25+ regulatory T cell subset with TGFbeta-mediated function and enhanced suppression of experimental autoimmune encephalomyelitis. *J Immunol* **180**, 7327-7337 (2008).

366. Ali, N.A*., et al.* Latency associated peptide has in vitro and in vivo immune effects independent of TGF-beta1. *PLoS One* **3**, e1914 (2008).
367. Tran, D.Q*., et al.* Selective expression of latency-associated peptide (LAP) and IL-1 receptor type I/II (CD121a/CD121b) on activated human FOXP3+ regulatory T cells allows for their purification from expansion cultures. *Blood* **113**, 5125-5133 (2009).
368. Trzonkowski, P*., et al.* First-in-man clinical results of the treatment of patients with graft versus host disease with human ex vivo expanded CD4+CD25+CD127- T regulatory cells. *Clinical immunology (Orlando, Fla* **133**, 22-26 (2009).
369. Sagoo, P., Lombardi, G. & Lechler, R.I. Regulatory T cells as therapeutic cells. *Curr Opin Organ Transplant* **13**, 645-653 (2008).
370. Sagoo, P*., et al.* Human regulatory T cells with alloantigen specificity are more potent inhibitors of alloimmune skin graft damage than polyclonal regulatory T cells. *Sci Transl Med* **3**, 83ra42 (2011).
371. Peters, J.H., Hilbrands, L.B., Koenen, H.J. & Joosten, I. Ex vivo generation of human alloantigen-specific regulatory T cells from CD4(pos)CD25(high) T cells for immunotherapy. *PloS one* **3**, e2233 (2008).
372. Masteller, E.L*., et al.* Expansion of functional endogenous antigen-specific CD4+CD25+ regulatory T cells from nonobese diabetic mice. *J Immunol* **175**, 3053-3059 (2005).
373. Jiang, S*., et al.* Generation and expansion of human CD4+ CD25+ regulatory T cells with indirect allospecificity: Potential reagents to promote donor-specific transplantation tolerance. *Transplantation* **82**, 1738-1743 (2006).
374. Lerut, J. & Sanchez-Fueyo, A. An appraisal of tolerance in liver transplantation. *Am J Transplant* **6**, 1774-1780 (2006).
375. Orlando, G*., et al.* Clinical operational tolerance after renal transplantation: current status and future challenges. *Ann Surg* **252**, 915-928 (2010).
376. Koshiba, T*., et al.* Clinical, immunological, and pathological aspects of operational tolerance after pediatric living-donor liver transplantation. *Transpl Immunol* **17**, 94-97 (2007).
377. Li, Y*., et al.* Analyses of peripheral blood mononuclear cells in operational tolerance after pediatric living donor liver transplantation. *Am J Transplant* **4**, 2118-2125 (2004).
378. Li, Y*., et al.* The presence of Foxp3 expressing T cells within grafts of tolerance human liver transplant recipients. *Transplantation* **86**, 1837-1843 (2008).
379. Martinez-Llordella, M*., et al.* Multiparameter immune profiling of operational tolerance in liver transplantation. *Am J Transplant* **7**, 309-319 (2007).
380. Sagoo, P*., et al.* Development of a cross-platform biomarker signature to detect renal transplant tolerance in humans. *J Clin Invest* **120**, 1848-1861 (2010).
381. Moraes-Vieira, P.M*., et al.* Differential monocyte STAT6 activation and CD4(+)CD25(+)Foxp3(+) T cells in kidney operational tolerance transplanted individuals. *Hum Immunol* **71**, 442-450 (2010).
382. Dijke, I.E*., et al.* Intragraft FOXP3 mRNA expression reflects antidonor immune reactivity in cardiac allograft patients. *Transplantation* **83**, 1477-1484 (2007).

383. Bunnag, S*., et al.* FOXP3 expression in human kidney transplant biopsies is associated with rejection and time post transplant but not with favorable outcomes. *Am J Transplant* **8**, 1423-1433 (2008).
384. Muthukumar, T*., et al.* Messenger RNA for FOXP3 in the urine of renal-allograft recipients. *N Engl J Med* **353**, 2342-2351 (2005).
385. Carroll, R.P*., et al.* Immune phenotype predicts risk for posttransplantation squamous cell carcinoma. *J Am Soc Nephrol* **21**, 713-722 (2010).
386. Wekerle, T. T-regulatory cells-what relationship with immunosuppressive agents? *Transplant Proc* **40**, S13-16 (2008).
387. Vogtenhuber, C*., et al.* Constitutively active Stat5b in CD4+ T-cells inhibits graft-versus-host disease (GVHD) lethality associated with increased regulatory T-cell (Treg) potency and decreased T effector cell (Teff) responses. *Blood* (2010).
388. Burchill, M.A., Yang, J., Vogtenhuber, C., Blazar, B.R. & Farrar, M.A. IL-2 receptor beta-dependent STAT5 activation is required for the development of Foxp3+ regulatory T cells. *J Immunol* **178**, 280-290 (2007).
389. Delgoffe, G.M*., et al.* The mTOR kinase differentially regulates effector and regulatory T cell lineage commitment. *Immunity* **30**, 832-844 (2009).
390. Zeiser, R*., et al.* Differential impact of mammalian target of rapamycin inhibition on CD4+CD25+Foxp3+ regulatory T cells compared with conventional CD4+ T cells. *Blood* **111**, 453-462 (2008).
391. Battaglia, M*., et al.* Rapamycin and interleukin-10 treatment induces T regulatory type 1 cells that mediate antigen-specific transplantation tolerance. *Diabetes* **55**, 40-49 (2006).
392. Gao, W*., et al.* Contrasting effects of cyclosporine and rapamycin in de novo generation of alloantigen-specific regulatory T cells. *Am J Transplant* **7**, 1722-1732 (2007).
393. Hendrikx, T.K*., et al.* Monotherapy rapamycin allows an increase of CD4 CD25 FoxP3 T cells in renal recipients. *Transpl Int* **22**, 884-891 (2009).
394. Li, J., Zhang, K., Ye, P., Wang, S. & Xia, J. CCR5 blockade in combination with rapamycin prolongs cardiac allograft survival in mice. *Clin Exp Immunol* **157**, 437-445 (2009).
395. Lange, C.M*., et al.* Increased frequency of regulatory T cells and selection of highly potent CD62L+ cells during treatment of human lung transplant recipients with rapamycin. *Transpl Int* **23**, 266-276 (2010).
396. Raimondi, G*., et al.* Mammalian target of rapamycin inhibition and alloantigen-specific regulatory T cells synergize to promote long-term graft survival in immunocompetent recipients. *J Immunol* **184**, 624-636 (2010).
397. Horibe, E.K*., et al.* Rapamycin-conditioned, alloantigen-pulsed dendritic cells promote indefinite survival of vascularized skin allografts in association with T regulatory cell expansion. *Transpl Immunol* **18**, 307-318 (2008).
398. Wang, Z*., et al.* Low-dose of tacrolimus favors the induction of functional CD4(+)CD25(+)FoxP3(+) regulatory T cells in solid-organ transplantation. *Int Immunopharmacol* **9**, 564-569 (2009).
399. Kogina, K*., et al.* Tacrolimus differentially regulates the proliferation of conventional and regulatory CD4(+) T cells. *Mol Cells* **28**, 125-130 (2009).

400. D'Addio, F*., et al.* A novel clinically relevant approach to tip the balance toward regulation in stringent transplant model. *Transplantation* **90**, 260-269 (2010).
401. Stary, G*., et al.* Glucocorticosteroids modify Langerhans cells to produce TGF-beta and expand regulatory T cells. *J Immunol* **186**, 103-112 (2011).
402. Bloom, D.D*., et al.* CD4+ CD25+ FOXP3+ regulatory T cells increase de novo in kidney transplant patients after immunodepletion with Campath-1H. *Am J Transplant* **8**, 793-802 (2008).
403. Trzonkowski, P*., et al.* Homeostatic repopulation by CD28-CD8+ T cells in alemtuzumab-depleted kidney transplant recipients treated with reduced immunosuppression. *Am J Transplant* **8**, 338-347 (2008).
404. Bluestone, J.A*., et al.* The effect of costimulatory and interleukin 2 receptor blockade on regulatory T cells in renal transplantation. *Am J Transplant* **8**, 2086-2096 (2008).
405. Presser, D*., et al.* Differential kinetics of effector and regulatory T cells in patients on calcineurin inhibitor-based drug regimens. *Kidney Int* **76**, 557-566 (2009).
406. Ma, A*., et al.* Combined therapy of CD4(+)CD25(+) regulatory T cells with low-dose sirolimus, but not calcineurin inhibitors, preserves suppressive function of regulatory T cells and prolongs allograft survival in mice. *Int Immunopharmacol* **9**, 553-563 (2009).
407. Vlad, G*., et al.* Anti-CD25 treatment and FOXP3-positive regulatory T cells in heart transplantation. *Transpl Immunol* **18**, 13-21 (2007).
408. Caproni, M*., et al.* The effects of tacrolimus ointment on regulatory T lymphocytes in atopic dermatitis. *J Clin Immunol* **26**, 370-375 (2006).
409. Poirier, N*., et al.* Inducing CTLA-4-dependent immune regulation by selective CD28 blockade promotes regulatory T cells in organ transplantation. *Sci Transl Med* **2**, 17ra10 (2010).
410. Trzonkowski, P*., et al.* First-in-man clinical results of the treatment of patients with graft versus host disease with human ex vivo expanded CD4+CD25+CD127- T regulatory cells. *Clin Immunol* **133**, 22-26 (2009).
411. Brunstein, C.G*., et al.* Infusion of ex vivo expanded T regulatory cells in adults transplanted with umbilical cord blood: safety profile and detection kinetics. *Blood* **117**, 1061-1070 (2011).
412. Di Ianni, M*., et al.* Tregs prevent GVHD and promote immune reconstitution in HLA-haploidentical transplantation. *Blood* **117**, 3921-3928 (2011).
413. Roncarolo, M.G. & Battaglia, M. Regulatory T-cell immunotherapy for tolerance to self antigens and alloantigens in humans. *Nat Rev Immunol* **7**, 585-598 (2007).
414. Allan, S.E*., et al.* CD4+ T-regulatory cells: toward therapy for human diseases. *Immunol Rev* **223**, 391-421 (2008).
415. Kuo, Y.R*., et al.* Mesenchymal stem cells prolong composite tissue allotransplant survival in a swine model. *Transplantation* **87**, 1769-1777 (2009).
416. Eljaafari, A*., et al.* Isolation of regulatory T cells in the skin of a human hand-allograft, up to six years posttransplantation. *Transplantation* **82**, 1764-1768 (2006).

417. Achauer, B.M.*, et al.* Long-term skin allograft survival after short-term cyclosporin treatment in a patient with massive burns. *Lancet* **1**, 14-15 (1986).
418. Woodruff, M.F. & Lennox, B. Reciprocal skin grafts in a pair of twins showing blood chimaerism. *Lancet* **2**, 476-478 (1959).
419. Kenter, M.J. & Cohen, A.F. Establishing risk of human experimentation with drugs: lessons from TGN1412. *Lancet* **368**, 1387-1391 (2006).
420. Suntharalingam, G.*, et al.* Cytokine storm in a phase 1 trial of the anti-CD28 monoclonal antibody TGN1412. *N Engl J Med* **355**, 1018-1028 (2006).
421. Houser, S.L., Benjamin, L.C., Wain, J.C., Madsen, J.C. & Allan, J.S. Constitutive expression of major histocompatibility complex class II antigens in pulmonary epithelium and endothelium varies among different species. *Transplantation* **77**, 605-607 (2004).
422. Choo, J.K.*, et al.* Species differences in the expression of major histocompatibility complex class II antigens on coronary artery endothelium: implications for cell-mediated xenoreactivity. *Transplantation* **64**, 1315-1322 (1997).
423. Taams, L.S., van Eden, W. & Wauben, M.H. Antigen presentation by T cells versus professional antigen-presenting cells (APC): differential consequences for T cell activation and subsequent T cell-APC interactions. *Eur J Immunol* **29**, 1543-1550 (1999).
424. Denton, M.D., Geehan, C.S., Alexander, S.I., Sayegh, M.H. & Briscoe, D.M. Endothelial cells modify the costimulatory capacity of transmigrating leukocytes and promote CD28-mediated CD4(+) T cell alloactivation. *J Exp Med* **190**, 555-566 (1999).
425. Barnaba, V., Watts, C., de Boer, M., Lane, P. & Lanzavecchia, A. Professional presentation of antigen by activated human T cells. *Eur J Immunol* **24**, 71-75 (1994).
426. Ma, W. & Pober, J.S. Human endothelial cells effectively costimulate cytokine production by, but not differentiation of, naive CD4+ T cells. *J Immunol* **161**, 2158-2167 (1998).
427. Ensminger, S.M.*, et al.* Mouse endothelial CD40 expression does not play a role during the development of transplant arteriosclerosis. *Endothelium* **10**, 111-117 (2003).
428. Elbe, A., Foster, C.A. & Stingl, G. T-cell receptor alpha beta and gamma delta T cells in rat and human skin--are they equivalent? *Semin Immunol* **8**, 341-349 (1996).
429. Pena-Cruz, V., Ito, S., Dascher, C.C., Brenner, M.B. & Sugita, M. Epidermal Langerhans cells efficiently mediate CD1a-dependent presentation of microbial lipid antigens to T cells. *J Invest Dermatol* **121**, 517-521 (2003).
430. Hunger, R.E.*, et al.* Langerhans cells utilize CD1a and langerin to efficiently present nonpeptide antigens to T cells. *J Clin Invest* **113**, 701-708 (2004).
431. Mizumoto, N. & Takashima, A. CD1a and langerin: acting as more than Langerhans cell markers. *J Clin Invest* **113**, 658-660 (2004).
432. Kobayashi, C.*, et al.* GM-CSF-Independent CD1a Expression in Epidermal Langerhans Cells: Evidence from Human CD1A Genome-Transgenic Mice. *J Invest Dermatol* **132**, 241-244 (2012).

433. Shortman, K. & Liu, Y.J. Mouse and human dendritic cell subtypes. *Nat Rev Immunol* **2**, 151-161 (2002).
434. Cendales, L.C.*, et al.* The Banff 2007 working classification of skin-containing composite tissue allograft pathology. *Am J Transplant* **8**, 1396-1400 (2008).
435. Porter, R.M. Mouse models for human hair loss disorders. *J Anat* **202**, 125-131 (2003).
436. Treuting, P.M. & Dintziz, S.M. Comparative Anatomy and Histology: A Mouse and Human Atlas. (2012).
437. Wong, V.W., Sorkin, M., Glotzbach, J.P., Longaker, M.T. & Gurtner, G.C. Surgical approaches to create murine models of human wound healing. *J Biomed Biotechnol* **2011**, 969618 (2011).
438. Shultz, L.D., Ishikawa, F. & Greiner, D.L. Humanized mice in translational biomedical research. *Nat Rev Immunol* **7**, 118-130 (2007).
439. Bosma, G.C., Custer, R.P. & Bosma, M.J. A severe combined immunodeficiency mutation in the mouse. *Nature* **301**, 527-530 (1983).
440. Mombaerts, P.*, et al.* RAG-1 deficient mice have no mature B and T lymphocytes. *Cell* **68**, 869-877 (1992).
441. Shinkai, Y.*, et al.* RAG-2-deficient mice lack mature lymphocytes owing to inability to initiate V(D)J rearrangement. *Cell* **68**, 855-867 (1992).
442. Shultz, L.D.*, et al.* Multiple defects in innate and adaptive immunologic function in NOD/LtSz-scid mice. *J Immunol* **154**, 180-191 (1995).
443. DiSanto, J.P., Muller, W., Guy-Grand, D., Fischer, A. & Rajewsky, K. Lymphoid development in mice with a targeted deletion of the interleukin 2 receptor gamma-chain. *Proc Natl Acad Sci U S A* **92**, 377-381 (1995).
444. Cao, X.*, et al.* Defective lymphoid development in mice lacking expression of the common cytokine receptor gamma chain. *Immunity* **2**, 223-238 (1995).
445. Sugamura, K.*, et al.* The interleukin-2 receptor gamma chain: its role in the multiple cytokine receptor complexes and T cell development in XSCID. *Annu Rev Immunol* **14**, 179-205 (1996).
446. Shibata, S.*, et al.* SCID-bg mice as xenograft recipients. *Lab Anim* **31**, 163-168 (1997).
447. Pober, J.S.*, et al.* Immunopathology of human T cell responses to skin, artery and endothelial cell grafts in the human peripheral blood lymphocyte/severe combined immunodeficient mouse. *Springer Semin Immunopathol* **25**, 167-180 (2003).
448. Nadig, S.N.*, et al.* In vivo prevention of transplant arteriosclerosis by ex vivo-expanded human regulatory T cells. *Nat Med* **16**, 809-813 (2010).
449. Marcheix, B.*, et al.* Multiple human mesenteric arterial grafts from the same donor to study human chronic vascular rejection in humanized SCID/beige mice. *J Heart Lung Transplant* **25**, 675-682 (2006).
450. Yacoub-Youssef, H.*, et al.* Use of human mesenteric arteries to study chronic vascular rejection in SCID/beige mice reconstituted with human spleen cells. *Transplant Proc* **37**, 75-76 (2005).
451. Brehm, M.A.*, et al.* Human immune system development and rejection of human islet allografts in spontaneously diabetic NOD-Rag1null IL2rgammanull Ins2Akita mice. *Diabetes* **59**, 2265-2270 (2010).

452. King, M., Pearson, T., Rossini, A.A., Shultz, L.D. & Greiner, D.L. Humanized mice for the study of type 1 diabetes and beta cell function. *Ann N Y Acad Sci* **1150**, 46-53 (2008).
453. King, M.*, et al.* Development of new-generation HU-PBMC-NOD/SCID mice to study human islet alloreactivity. *Ann N Y Acad Sci* **1103**, 90-93 (2007).
454. King, M.*, et al.* A new Hu-PBL model for the study of human islet alloreactivity based on NOD-scid mice bearing a targeted mutation in the IL-2 receptor gamma chain gene. *Clin Immunol* **126**, 303-314 (2008).
455. Racki, W.J.*, et al.* NOD-scid IL2rgamma(null) mouse model of human skin transplantation and allograft rejection. *Transplantation* **89**, 527-536 (2010).
456. Coates, P.T., Krishnan, R., Kireta, S., Johnston, J. & Russ, G.R. Human myeloid dendritic cells transduced with an adenoviral interleukin-10 gene construct inhibit human skin graft rejection in humanized NOD-scid chimeric mice. *Gene Ther* **8**, 1224-1233 (2001).
457. Snanoudj, R.*, et al.* A role for CD2 antibodies (BTI-322 and its humanized form) in the in vivo elimination of human T lymphocytes infiltrating an allogeneic human skin graft in SCID mice: an Fcgamma receptor-related mechanism involving co-injected human NK cells. *Transplantation* **78**, 50-58 (2004).
458. Shiao, S.L.*, et al.* Immunomodulatory properties of FK734, a humanized anti-CD28 monoclonal antibody with agonistic and antagonistic activities. *Transplantation* **83**, 304-313 (2007).
459. Erdag, G. & Morgan, J.R. Survival of fetal skin grafts is prolonged on the human peripheral blood lymphocyte reconstituted-severe combined immunodeficient mouse/skin allograft model. *Transplantation* **73**, 519-528 (2002).
460. Tary-Lehmann, M., Saxon, A. & Lehmann, P.V. The human immune system in hu-PBL-SCID mice. *Immunol Today* **16**, 529-533 (1995).
461. Feng, G., Chan, T., Wood, K.J. & Bushell, A. Donor reactive regulatory T cells. *Curr Opin Organ Transplant* **14**, 432-438 (2009).
462. Roncador, G.*, et al.* Analysis of FOXP3 protein expression in human CD4+CD25+ regulatory T cells at the single-cell level. *Eur J Immunol* **35**, 1681-1691 (2005).
463. Lim, H.W., Broxmeyer, H.E. & Kim, C.H. Regulation of trafficking receptor expression in human forkhead box P3+ regulatory T cells. *J Immunol* **177**, 840-851 (2006).
464. Carvalho-Gaspar, M., Billing, J.S., Spriewald, B.M. & Wood, K.J. Chemokine gene expression during allograft rejection: comparison of two quantitative PCR techniques. *J Immunol Methods* **301**, 41-52 (2005).
465. Livak, K.J. & Schmittgen, T.D. Analysis of relative gene expression data using real-time quantitative PCR and the 2(-Delta Delta C(T)) Method. *Methods* **25**, 402-408 (2001).
466. Boehncke, W.-H. & Schon, M.P. Animal models of psoriasis. *Clin Dermatol* **25**, 596-605 (2007).
467. Turgeon, N.A.*, et al.* Alloimmune injury and rejection of human skin grafts on human peripheral blood lymphocyte-reconstituted non-obese diabetic severe

combined immunodeficient beta2-microglobulin-null mice. *Exp Biol Med (Maywood)* **228**, 1096-1104 (2003).
468. Lepus, C.M.*, et al.* Comparison of human fetal liver, umbilical cord blood, and adults blood hematopoietic stem cell engraftment in NOD-scid/gammac-/-, Balb/c-Rag1-/- gammac-/-, and C.B-17-scid/bg immunodeficient mice. *Hum Immunol* **70**, 790-802 (2009).
469. Wang, Y.*, et al.* Interferon-gamma plays a nonredundant role in mediating T cell-dependent outward vascular remodeling of allogeneic human coronary arteries. *FASEB J* **18**, 606 (2004).
470. Baccala, R. & Theofilopoulos, A.N. The new paradigm of T-cell homeostatic proliferation-induced autoimmunity. *Trend Immunol* **26**, 5-8 (2005).
471. Kieper, W.C. & Jameson, S.C. Homeostatic expansion and phenotypic conversion of naive T cells in response to self peptide/MHC ligands. *Proc Natl Acad Sci U S A* **96**, 13306-13311 (1999).
472. Min, B., Yamane, H., Hu-Li, J. & Paul, W.E. Spontaneous and homeostatic proliferation of CD4 T cells are regulated by different mechanisms. *J Immunol* **174**, 6039-6044 (2005).
473. Krupica, T., Fry, T.J. & Mackall, C.L. Autoimmunity during lymphopaenia: A two-hit model. *Clin Immunol* **120**, 121-128 (2006).
474. Le Campion, A.*, et al.* Lymphopenia-induced spontaneous T-cell proliferation as a cofactor for autoimmune disease development. *Blood* **114**, 1784-1793 (2009).
475. Matzinger, P. The Danger Model: A Renewed Sense of Self. *Science* **296**, 301-305 (2002).
476. Kirkiles-Smith, N.C.*, et al.* Development of a humanised mouse model to study the role of macrophages in allograft injury. *Transplantation* **87**, 189-197 (2009).
477. Bingaman, A.W.*, et al.* Vigorous allograft rejection in the absence of danger. *J Immunol* **164**, 3065-3071 (2000).
478. Shiao, S.L., McNiff, J.M. & Pober, J.S. Memory T cells and their costimulators in human allograft injury. *J Immunol* **175**, 4886-4896 (2005).
479. Doxiadis, I.I.N.*, et al.* Simpler and equitable allocation of kidneys from postmortem donors primarily based on full HLA-DR compatibility. *Transplantation* **83**, 1207-1213 (2007).
480. Opelz, G. & Wujciak, T. The influence of HLA compatibility on graft survival after heart transplantation. *NEJM* **330**, 816-819 (1994).
481. Schulman, L.L.*, et al.* Mismatches at the HLA-DR and HLA-B loci are risk factors for acute rejection after lung transplantation. *Am J Resp CCM* **157**, 1833-1837 (1998).
482. Carvalho-Gaspar, M.*, et al.* Location and time-dependent control of rejection by regulatory T cells culminates in a failure to generate memory T cells. *J Immunol* **180**, 6640-6648 (2008).
483. Tary-Lehmann, M. & Saxon, A. Human mature T cells that are anergic in vivo prevail in SCID mice reconstituted with human peripheral blood. *J Exp Med* **175**, 503-516 (1992).

484. Tary-Lehmann, M., Lehmann, P.V., Schoos, D., Roncarolo, M.G. & Saxon, A. Anti-SCID mouse reactivity shapes the human CD4+ T cell repertoire in hu-PBMC-SCID chimeras. *J Exp Med* **180**, 1817-1827 (1994).
485. Hoffman-Fezer, G., Gall, C., Zengerle, U., Kranz, B. & Thierfelder, S. Immunohistology and immunocytology of human T-cell chimerism and graft-versus-host disease in SCID mice. *Blood* **81**, 3440-3448 (1993).
486. Goldrath, A.W., Bogatzki, L.Y. & Bevan, M.J. Naive T cells transiently acquire a memory-like phenotype during homeostasis-driven proliferation. *J Exp Med* **192**, 557-564 (2000).
487. Petzelbauer, P., Schechner, J. & Pober, J.S. Endothelium. In: Fitzpatrick TB, Eisen AZ, Wolff K, et al. (eds) Dermatology in general medicine. 6th edn. McGraw-Hill, New York., 216-230 (2003).
488. Morita, K*., et al.* Early chemokine cascades in murine cardiac grafts regulate T cell recruitment and progression of acute allograft rejection. *J Immunol* **167**, 2979-2984 (2001).
489. Petzelbauer, P., Groger, M., Kunstfeld, R., Petzelbauer, E. & Wolff, K. Human delayed-type hypersensitivity reaction in a SCID mouse engrafted with human T cells and autologous skin. *J Invest Dermatol* **107**, 576-581 (1996).
490. Khoruts, A. & Fraser, J.M. A causal link between lymphopenia and autoimmunity. *Immunol Lett* **98**, 23-31 (2005).
491. Schulze-Koops, H. Lymphopenia and autoimmune diseases. *Arthritis Res Ther* **6**, 178-180 (2004).
492. Fahy, O*., et al.* Chemokine-induced cutaneous inflammatory cell infiltration in a model of Hu-PBMC-SCID mice grafted with human skin. *Am J Pathol* **158**, 1053-1063 (2001).
493. Hanto, D.W., Widmer, M.B. & Simmons, R.L. Mediation of cellular recruitment in vivo by functionally distinct T cell clones. *Transplantation* **42**, 168-171 (1986).
494. Kanitakis, J. The challenge of dermatopathological diagnosis of composite tissue allograft rejection: a review. *J Cutan Pathol* **35**, 738-744 (2008).
495. Kanitakis, J*., et al.* Absence of c4d deposition in human composite tissue (hands and face) allograft biopsies: an immunoperoxidase study. *Transplantation* **84**, 265-267 (2007).
496. NHS. Immunoglobulin reference ranges. *CMFT NHS UK* (Accessed Aug 2011).
497. Pei, R., Lee, J., Chen, T., Rojo, S. & Terasaki, P.I. Flow cytometric detection of HLA antibodies using a spectrum of microbeads. *Hum Immunol* **60**, 1293-1302 (1999).
498. Lan, P., Tonomura, N., Shimizu, A., Wang, S. & Yang, Y.G. Reconstitution of a functional human immune system in immunodeficient mice through combined human fetal thymus/liver and CD34+ cell transplantation. *Blood* **108**, 487-492 (2006).
499. Bhatia, M., Wang, J.C., Kapp, U., Bonnet, D. & Dick, J.E. Purification of primitive human hematopoietic cells capable of repopulating immune-deficient mice. *Proc Natl Acad Sci U S A* **94**, 5320-5325 (1997).
500. Krause, D.S., Fackler, M.J., Civin, C.I. & May, W.S. CD34: structure, biology, and clinical utility. *Blood* **87**, 1-13 (1996).

501. Brehm, M.A., *et al.* Parameters for establishing humanized mouse models to study human immunity: analysis of human hematopoietic stem cell engraftment in three immunodeficient strains of mice bearing the IL2rgamma(null) mutation. *Clin Immunol* **135**, 84-98 (2010).
502. Watanabe, Y., *et al.* The analysis of the functions of human B and T cells in humanized NOD/shi-scid/gammac(null) (NOG) mice (hu-HSC NOG mice). *Int Immunol* **21**, 843-858 (2009).
503. Liu, C., *et al.* Progenitor cell dose determines the pace and completeness of engraftment in a xenograft model for cord blood transplantation. *Blood* **116**, 5518-5527 (2010).
504. Zell, T., Kivens, W.J., Kellermann, S.A. & Shimizu, Y. Regulation of integrin function by T cell activation: points of convergence and divergence. *Immunol Res* **20**, 127-145 (1999).
505. Bhan, A.K., Mihm, M.C., Jr. & Dvorak, H.F. T cell subsets in allograft rejection. In situ characterization of T cell subsets in human skin allografts by the use of monoclonal antibodies. *J Immunol* **129**, 1578-1583 (1982).
506. Shultz, L.D., Ishikawa, F. & Greiner, D.L. Humanized mice in translational biomedical research. *Nat Rev Immunol* **7**, 118-130 (2007).
507. Schall, T.J., Simpson, N.J. & Mak, J.Y. Molecular cloning and expression of the murine RANTES cytokine: structural and functional conservation between mouse and man. *Eur J Immunol* **22**, 1477-1481 (1992).
508. Murray, A.G., *et al.* Dermal microvascular injury in the human peripheral blood lymphocyte reconstituted-severe combined immunodeficient (HuPBL-SCID) mouse/skin allograft model is T cell mediated and inhibited by a combination of cyclosporine and rapamycin. *Am J Pathol* **153**, 627-638 (1998).
509. Shultz, L.D., *et al.* Human lymphoid and myeloid cell development in NOD/LtSz-scid IL2R gamma null mice engrafted with mobilized human hemopoietic stem cells. *J Immunol* **174**, 6477-6489 (2005).
510. Wege, A.K., Melkus, M.W., Denton, P.W., Estes, J.D. & Garcia, J.V. Functional and phenotypic characterization of the humanized BLT mouse model. *Curr Top Microbiol Immunol* **324**, 149-165 (2008).
511. Shultz, L.D., *et al.* Generation of functional human T-cell subsets with HLA-restricted immune responses in HLA class I expressing NOD/SCID/IL2r{gamma}null humanized mice. *Proc Natl Acad Sci U S A* **107**, 13022-13027 (2010).
512. Pomahac, B. & Aflaki, P. Composite tissue transplantation: a new era in transplantation surgery. *Eplasty* **10**(2010).
513. Ravindra, K.V., Wu, S., McKinney, M., Xu, H. & Ildstad, S.T. Composite tissue allotransplantation: current challenges. *Transplant Proc* **41**, 3519-3528 (2009).
514. McMurchy, A.N., Bushell, A., Levings, M.K. & Wood, K.J. Moving to tolerance: Clinical application of T regulatory cells. *Semin Immunol* (2011).
515. MHRA. Good Manufacturing Practice: Guidance and legislation. *http://www.mhra.gov.uk/Howweregulate/Medicines/Inspectionandstandards/GoodManufacturingPractice/Guidanceandlegislation/index.htm* (2011).

516. Nadig, S.N.*, et al.* In vivo prevention of transplant arteriosclerosis by ex vivo-expanded human regulatory T cells. *Nat Med* **16**, 809-813 (2010).
517. Godfrey, W.R.*, et al.* In vitro-expanded human CD4(+)CD25(+) T-regulatory cells can markedly inhibit allogeneic dendritic cell-stimulated MLR cultures. *Blood* **104**, 453-461 (2004).
518. Chai, J.G.*, et al.* In vitro expansion improves in vivo regulation by CD4+CD25+ regulatory T cells. *J Immunol* **180**, 858-869 (2008).
519. Steiner, D., Brunicki, N., Blazar, B.R., Bachar-Lustig, E. & Reisner, Y. Tolerance induction by third-party "off-the-shelf" CD4+CD25+ Treg cells. *Exp Hematol* **34**, 66-71 (2006).
520. Ermann, J.*, et al.* Only the CD62L+ subpopulation of CD4+CD25+ regulatory T cells protects from lethal acute GVHD. *Blood* **105**, 2220-2226 (2005).
521. Jutila, M.A., Watts, G., Walcheck, B. & Kansas, G.S. Characterization of a functionally important and evolutionarily well-conserved epitope mapped to the short consensus repeats of E-selectin and L-selectin. *J Exp Med* **175**, 1565-1573 (1992).
522. Dvorak, H.F., Mihm, M.C., Jr., Dvorak, A.M., Barnes, B.A. & Galli, S.J. The microvasculature is the critical target of the immune response in vascularized skin allograft rejection. *J Invest Dermatol* **74**, 280-284 (1980).
523. Murray, A.G.*, et al.* Human T-cell-mediated destruction of allogeneic dermal microvessels in a severe combined immunodeficient mouse. *Proc Natl Acad Sci U S A* **91**, 9146-9150 (1994).
524. Mayer, T.G., Bhan, A.K. & Winn, H.J. Immunohistochemical analyses of skin graft rejection in mice. Kinetics of lymphocyte infiltration in grafts of limited immunogenetic disparity. *Transplantation* **46**, 890-899 (1988).
525. Ascher, N.L., Hoffman, R., Chen, S. & Simmons, R.L. Specific and nonspecific infiltration of sponge matrix allografts by specifically sensitized cytotoxic lymphocytes. *Cell Immunol* **52**, 38-47 (1980).
526. Zhang, N.*, et al.* Regulatory T cells sequentially migrate from inflamed tissues to draining lymph nodes to suppress the alloimmune response. *Immunity* **30**, 458-469 (2009).
527. Graca, L., Cobbold, S.P. & Waldmann, H. Identification of regulatory T cells in tolerated allografts. *J Exp Med* **195**, 1641-1646 (2002).
528. Tang, Q.*, et al.* Visualizing regulatory T cell control of autoimmune responses in nonobese diabetic mice. *Nat Immunol* **7**, 83-92 (2006).
529. Hanash, A.M. & Levy, R.B. Donor CD4+CD25+ T cells promote engraftment and tolerance following MHC-mismatched hematopoietic cell transplantation. *Blood* **105**, 1828-1836 (2005).
530. Adeegbe, D., Bayer, A.L., Levy, R.B. & Malek, T.R. Cutting edge: allogeneic CD4+CD25+Foxp3+ T regulatory cells suppress autoimmunity while establishing transplantation tolerance. *J Immunol* **176**, 7149-7153 (2006).
531. Tchorsh-Yutsis, D.*, et al.* Embryonic pig pancreatic tissue for the treatment of diabetes: potential role of immune suppression with "off-the-shelf" third-party regulatory T cells. *Transplantation* **91**, 398-405 (2011).
532. Bevan, M.J. Cross-priming. *Nat Immunol* **7**, 363-365 (2006).

533. Bushell, A., Jones, E., Gallimore, A. & Wood, K. The generation of CD25+ CD4+ regulatory T cells that prevent allograft rejection does not compromise immunity to a viral pathogen. *J Immunol* **174**, 3290-3297 (2005).
534. Hamano, K., Rawsthorne, M.A., Bushell, A.R., Morris, P.J. & Wood, K.J. Evidence that the continued presence of the organ graft and not peripheral donor microchimerism is essential for maintenance of tolerance to alloantigen in vivo in anti-CD4 treated recipients. *Transplantation* **62**, 856-860 (1996).
535. Qin, S.*, et al.* "Infectious" transplantation tolerance. *Science* **259**, 974-977 (1993).
536. Gaidot, A.*, et al.* Immune reconstitution is preserved in hematopoietic stem cell transplantation coadministered with regulatory T cells for GVHD prevention. *Blood* **117**, 2975-2983 (2011).
537. Sojka, D.K., Hughson, A. & Fowell, D.J. CTLA-4 is required by CD4+CD25+ Treg to control CD4+ T-cell lymphopenia-induced proliferation. *Eur J Immunol* **39**, 1544-1551 (2009).
538. Winstead, C.J., Fraser, J.M. & Khoruts, A. Regulatory CD4+CD25+Foxp3+ T cells selectively inhibit the spontaneous form of lymphopenia-induced proliferation of naive T cells. *J Immunol* **180**, 7305-7317 (2008).
539. Taylor, P.A., Lees, C.J. & Blazar, B.R. The infusion of ex vivo activated and expanded CD4(+)CD25(+) immune regulatory cells inhibits graft-versus-host disease lethality. *Blood* **99**, 3493-3499 (2002).
540. Shevach, E.M., McHugh, R.S., Piccirillo, C.A. & Thornton, A.M. Control of T-cell activation by CD4+ CD25+ suppressor T cells. *Immunol Rev* **182**, 58-67 (2001).
541. Anderson, A.*, et al.* Expanded nonhuman primate tregs exhibit a unique gene expression signature and potently downregulate alloimmune responses. *Am J Transplant* **8**, 2252-2264 (2008).
542. Bluestone, J.A. & Tang, Q. How do CD4+CD25+ regulatory T cells control autoimmunity? *Curr Opin Immunol* **17**, 638-642 (2005).
543. Gilet, J.*, et al.* Role of CCL17 in the generation of cutaneous inflammatory reactions in Hu-PBMC-SCID mice grafted with human skin. *J Invest Dermatol* **129**, 879-890 (2009).
544. Wang, J., Ioan-Facsinay, A., van der Voort, E.I., Huizinga, T.W. & Toes, R.E. Transient expression of FOXP3 in human activated nonregulatory CD4+ T cells. *Eur J Immunol* **2007**, 1 (2007).
545. VanBuskirk, A.M., Wakely, M.E. & Orosz, C.G. Acute rejection of cardiac allografts by noncytolytic CD4(+) T cell populations. *Transplantation* **62**, 300-302 (1996).
546. Schulz, M.*, et al.* Acute rejection of vasular heart allografts by perforin-deficient mice. *Eur J Immunol* **25**, 474-479 (1995).
547. Oida, T., Xu, L., Weiner, H.L., Kitani, A. & Strober, W. TGF-beta-mediated suppression by CD4+CD25+ T cells is facilitated by CTLA-4 signaling. *J Immunol* **177**, 2331-2339 (2006).
548. Bluestone, J. & Gitelman, S.E. T1DM Immunotherapy Using CD4+CD127lo/-CD25+ Polyclonal Tregs, http://clinicaltrials.gov/ct2/show/NCT01210664. (2011).
549. http://www.onestudy.org/. The ONE Study. (2011).

550. Celli, S., Albert, M.L. & Bousso, P. Visualizing the innate and adaptive immune responses underlying allograft rejection by two-photon microscopy. *Nat Med* **17**, 744-749 (2011).
551. Shiao, S.L.*, et al.* Human effector memory CD4+ T cells directly recognize allogeneic endothelial cells in vitro and in vivo. *J Immunol* **179**, 4397-4404 (2007).
552. http://www.tts.org. The Transplantation Society Congress, Vancouver. (2010).
553. Kapessidou, Y.*, et al.* The replacement of graft endothelium by recipient-type cells conditions allograft rejection mediated by indirect pathway CD4(+) T cells. *Transplantation* **81**, 726-735 (2006).
554. Lim, H.W., Hillsamer, P., Banham, A.H. & Kim, C.H. Cutting edge: direct suppression of B cells by CD4+ CD25+ regulatory T cells. *J Immunol* **175**, 4180-4183 (2005).
555. McNally, A., Hill, G.R., Sparwasser, T., Thomas, R. & Steptoe, R.J. CD4+CD25+ regulatory T cells control CD8+ T-cell effector differentiation by modulating IL-2 homeostasis. *Proc Natl Acad Sci U S A* **108**, 7529-7534 (2011).
556. Biedermann, B.C. & Pober, J.S. Human endothelial cells induce and regulate cytolytic T cell differentiation. *J Immunol* **161**, 4679-4687 (1998).
557. Biedermann, B.C. & Pober, J.S. Human vascular endothelial cells favor clonal expansion of unusual alloreactive CTL. *J Immunol* **162**, 7022-7030 (1999).
558. Bluestone, J.A. & Hebrok, M. Safer, longer-lasting regulatory T cells with beta-catenin. *Nat Med* **14**, 118-119 (2008).
559. Ding, Y., Shen, S., Lino, A.C., Curotto de Lafaille, M.A. & Lafaille, J.J. Beta-catenin stabilization extends regulatory T cell survival and induces anergy in nonregulatory T cells. *Nat Med* **14**, 162-169 (2008).
560. Jonuleit, H.*, et al.* Infectious tolerance: human CD25(+) regulatory T cells convey suppressor activity to conventional CD4(+) T helper cells. *J Exp Med* **196**, 255-260 (2002).
561. Hoffmann, P.*, et al.* Only the CD45RA+ subpopulation of CD4+CD25high T cells gives rise to homogeneous regulatory T-cell lines upon in vitro expansion. *Blood* **108**, 4260-4267 (2006).
562. Wood, K.J., Bushell, A. & Jones, N.D. Immunologic unresponsiveness to alloantigen in vivo: a role for regulatory T cells. *Immunol Rev* **241**, 119-132 (2011).
563. Wood, K.J. Regulatory T cells in transplantation. *Transplant Proc* **43**, 2135-2136 (2011).
564. Heidt, S.*, et al.* Peripheral blood sampling for the detection of allograft rejection: biomarker identification and validation. *Transplantation* **92**, 1-9 (2011).
565. Martinez-Llordella, M.*, et al.* Using transcriptional profiling to develop a diagnostic test of operational tolerance in liver transplant recipients. *J Clin Invest* **118**, 2845-2857 (2008).